ID : ASEE 004

1st International Conference on Advances in Civil Engineering 2012 (ICACE 2012)

12 –14 December 2012

CUET, Chittagong, Bangladesh

OPTIMIZATION OF CONTINUOUS POST-TENSIONED I-GIRDER BRIDGE SYSTEM

S. KABIR[1], S. RANA[2] & R. AHSAN[3]

[1]*Environment & Infrastructure Management Solution, Dhaka-1215, Bangladesh*
shamim.buet@ymail.com
[2]*Bangladesh University of Engineering & Technology, Dhaka-1000, Bangladesh*
shohel.ce@gmail.com
[3]*Bangladesh University of Engineering & Technology, Dhaka-1000, Bangladesh*
raquibahsan@gmail.com

ABSTRACT

In this paper, cost optimization approach of a continuous post-tensioned PC I-girder bridge system is presented. The objective is to minimize the total cost of superstructure of I-girder bridge in the design process. Design constraints for the optimization are considered according to AASTHO LRFD 2007 Specification. An optimization algorithm called Evolutionary Operation (EVOP) is used, in order to identify the global minimum. The paper shows the comparison between an existing design and the cost optimum design. The cost optimum design of a girder bridge with continous deck is found to be 40% cost effective than the existing design. Optimum girder depth increases with increase in cost of steels. The cost of bridge increases with the increase in girder span and girder spacing is higher in smaller span than larger span.

Keywords: Prestressed Concrete, I-girder, Optimization, EVOP,Continous deck**.**

INTRODUCTION

Usually, in the design process of a prestressed concrete I girder bridge system, the engineers follow an iterative method. At the initial stage a standard I-beam geometry and girder spacing is selected, for a given deck width, span length (L) and AASHTO loading, using knowledge acquired from past bridge projects, design charts, or design guidelines. Then, the deck is designed based on the girder spacing. If the initial design is not satisfactory, the process is repeated for modified girder spacing. The traditional design procedure does not consider the overall cost of the structure explicitly. For a structure made of two or more different materials; minimum weight has no meaning with respect to optimization. Optimization has to be formulated as minimum cost. Over the last thirty years many researchers have comprehensively used optimization algorithm for solving structural problems especially in prestressed concrete structure such as Gahtani et al**.** (1993), Lounis and Cohn (1993) , Han et al. (1995)**,** S.Barakat et al. **(**2003**),** Fereig (1985). However, none of these studies use optimization algorithm EVOP except S.Rana(2010)**.** In the present study a cost optimum design approach of a two span continuous (continuity is made using conventional deck reinforcement) PC I-girder bridge system is presented (Figure-1).

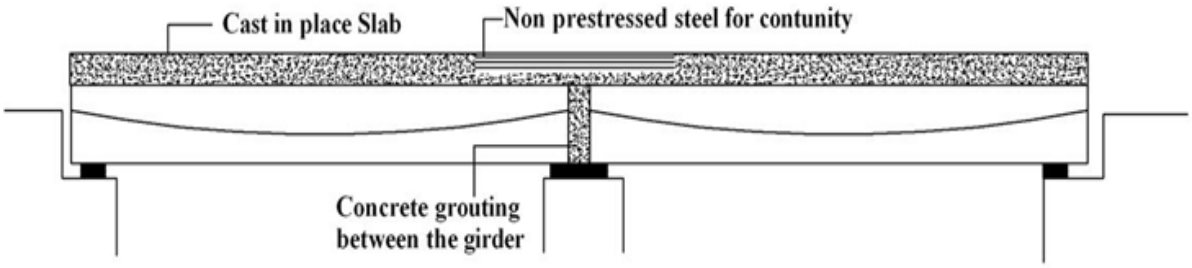

Figure 1: Continuity using conventional deck reinforcement in slab.

OBJECTIVE FUNCTION

In order to determine the minimum cost of the entire girder of the bridge structure, it is necessary to consider all of the design variables simultaneously, regardless of whether they are discrete or continuous. The total cost function per span is defined according to the following relationship:

$T=A+B+C+D$ (1)

where, A = Cost of girder concrete; B = Cost of deck concrete; C = Cost of prestressing steel; D = Cost of non prestressing steel.

Cost of individual components is as follows:

$A = (UP_{GC}*V_{GC}+UP_{GF}*SA_G)*N_G$ (2)

$B = (UP_{DC}*V_{DC}+UP_{DF}(S-W_{TF}))* N_G$ (3)

$C = (UP_{PS}*W_{PS}+2UP_{ANC}* T_N +UP_{SH}*T_N*L)*N_G$ (4)

$D = U_{POS}(W_{OS}+W_{OSG})*N_G$ (5)

where UP_{GC},UP_{DC},UP_{PS} and U_{POS} are the unit prices including materials, labor fabrication, and installation of precast girder concrete, deck concrete, prestressing steel, and ordinary steel, respectively. $UP_{GF,}$ $UP_{DF,}$ $UP_{ANC,}$$UP_{SH}$ are the unit prices of girder formwork, deck formwork, anchorage set, and metal sheath for duct. The unit cost is taken from RHD cost schedule 2006.

IMPLICIT CONSTRAINTS

A total 51 implicit constraints are considered according to the ***AASHTO LRFD 2007*** specifications which are categorized into eight groups:

i) Flexural working stress constraints
ii) Flexural ultimate strength constraints
iii) Shear constraints (ultimate strength)
iv) Ductility constraints
v) Deflection constraint
vi) Lateral stability constraint
vii) Tendons eccentricity constraint and
viii) Deck slab design constraint

DESIGN VARIABLES AND EXPLICIT CONSTRAINTS

The explicit constraints are defined as :

$$L_L \leq X \leq U_L \quad (6)$$

where X = Design variable,
L_L = Lower limit of the design variable,
U_L = Upper limit of the design variable.

Explicit constraints for girder spacing: Lower and upper limit of girder spacing is such that number of girder in the Bridge can vary from 1 to 10.

Explicit constraints for top flange: The lower limit of top flange width is assumed as 300 mm from lateral stability and bearing consideration and upper limit equal to girder spacing. Similarly the lower and upper limits of explicit constraints of other design variables are shown in **Table 1.**

Table1: Design variables with explicit constraints

Design variables	**Explicit constraints**
Girder spacing(S_G) (m)	$BW/10 \leq S_G \leq BW$
Girder depth(D_G) (mm)	$1000 \leq D_G \leq 3500$
Top flange width(W_T) (mm)	$300 \leq W_T \leq S_G$
Top flange thickness(T_T) (mm)	$75 \leq T_T \leq 300$
Top flange transition thickness(T_{TFT}) (mm)	$50 \leq T_{TFT} \leq 300$
Bottom flange width(W_B) (mm)	$300 \leq W_B \leq S_G$
Bottom flange thickness(T_B)(mm)	$a \leq T_B \leq 600$
web width(Ww) (mm)	$b \leq Ww \leq 300$
Number of strand in a tendon (S_N)	$1 \leq S_N \leq 27$
Number of tendon in a girder(T_N)	$1 \leq T_N \leq 20$
Lower most tendon position at the end from bottom(Z)(mm)	$AM \leq Z \leq 1000$
initial stage prestress(β)	$1\% \leq \beta \leq 100\%$
slab thickness(t) (mm)	$175 \leq t \leq 300$
Slab main reinforcement ratio, ρ(%)	$\rho\ min \leq \rho \leq \rho max$
reinforcement ratio used in negative moment section.ρneg (%)	$\rho min \leq \rho neg \leq \rho max$

where **BW**=Bridge width, **a**=clear cover+ duct dia, **b**= clear cover+ duct dia+web rebar, **AM**= anchorage minimum vertical edge distance.

CONTINUITY

Several methods are available to make the bridge continous. In this paper the optimization of continuous prestressed Bridge structure is performed considering Conventional Deck Reinforcement.

MATERIAL PROPERTY AND DESIGN DATA

Material properties	Ultimate strength of prestressing steel ,fpu=1861 Mpa;
	Yield strength of reinforcing steel, fy=410 Mpa;
	Girder concrete strength, fc=40Mpa;
	Deck concrete strength , fcdeck=25 Mpa;
Bridge design data	Girder Length= 50m (L=48.8m)
	Bridge width, Bw= 12.0m (3 lane)
	Live load= HS20-44
	No. of diaphram = 4; diaphram width=250mm;
	Curb height=600mm; Curb width=450mm;
	Wearing coarse=50mm;
	7 wire low-relaxation strand; Freyssinet anchorage system.

OPTIMIZATION PROBLEM FORMULATIONS AND LINKING WITH EVOP:

The following flowchart diagram (Figure-2) represents the total optimum problem formulation and how this problem is linked with EVOP algorithm**.**

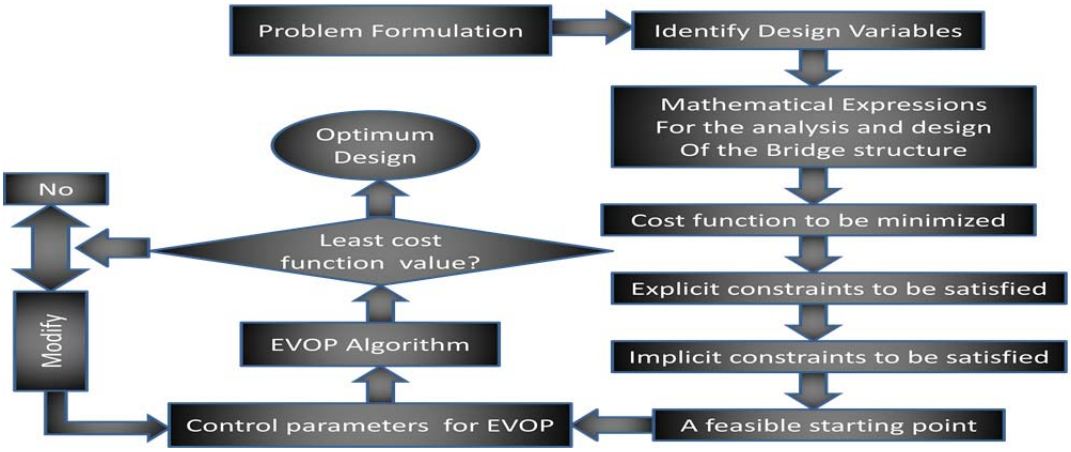

Figure 2: Problem formulation and linking with EVOP**.**

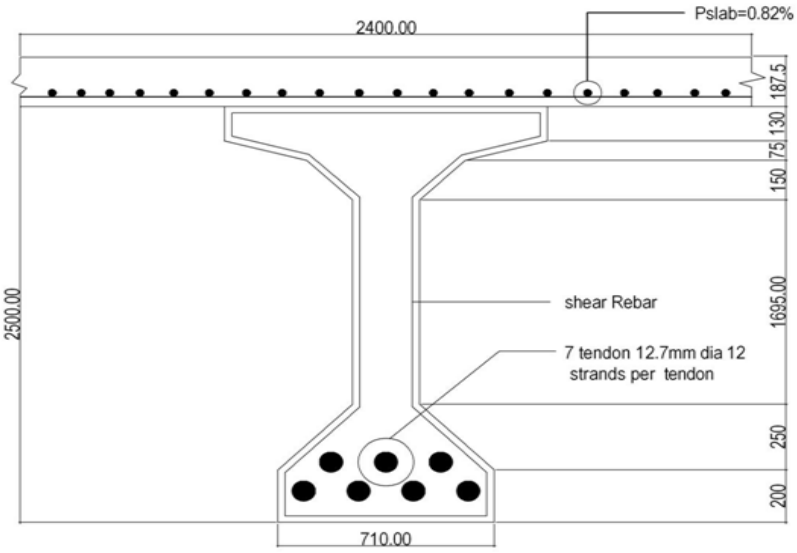

Figure 3: The Existing Design.

RESULTS COMPARISON

The proposed optimization method is applied to a practical project and variation between existing design (Figure-3) and cost optimum design (Figure-4) is identified. In this paper it is shown that the cost optimum design (as continuous) is 40% cost effective than the existing design.

In existing design the tendon profile considered as fixed (Figure 5) but in optimum design tendon profile is considered as variable (Fig 6) because the capacity depends on tendons configuration on girder. The tendon profile in existing simply supported design and in continuous design are shown in the following figures.

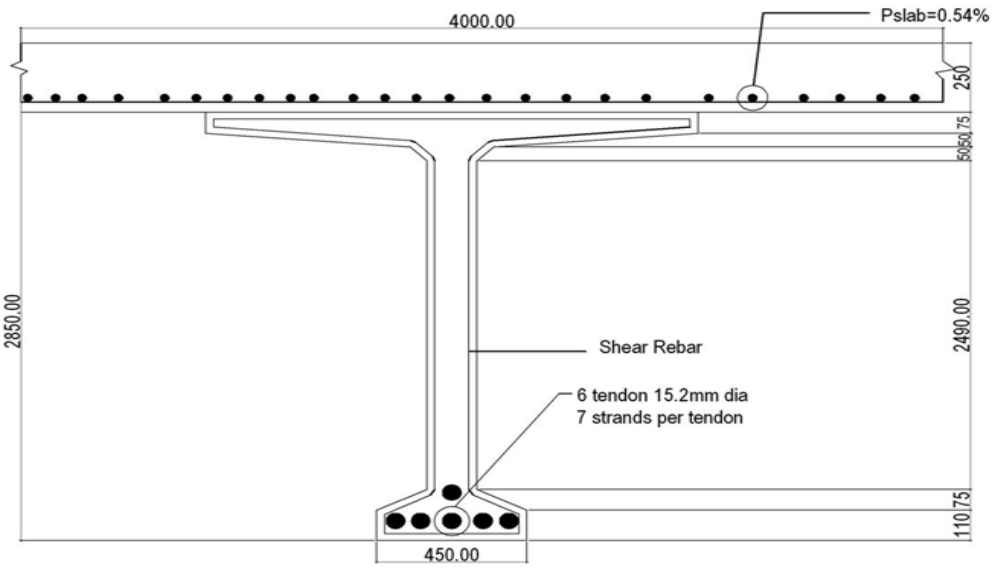

Figure 4: Optimum Design as continuous.

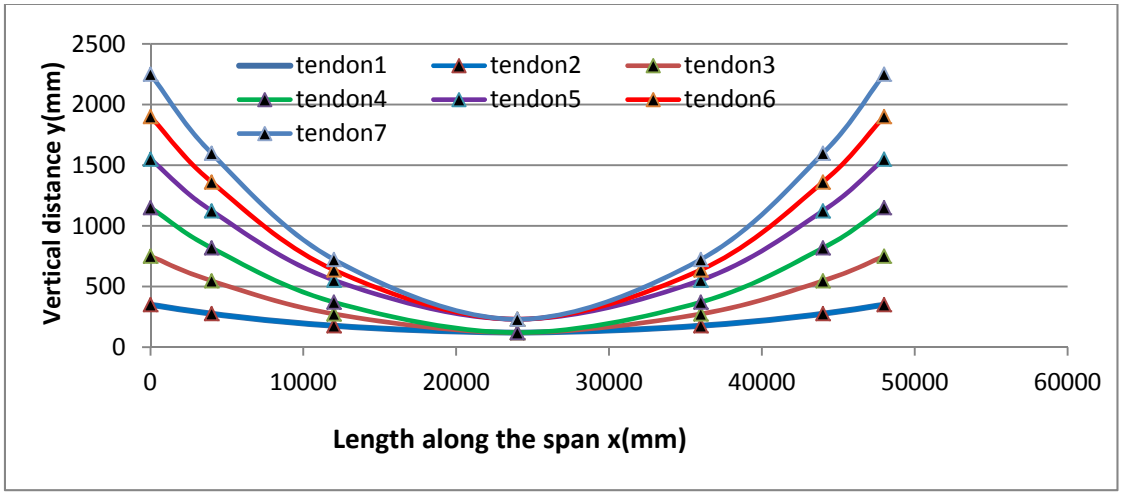

Figure 5: Tendon profile in Existing Design

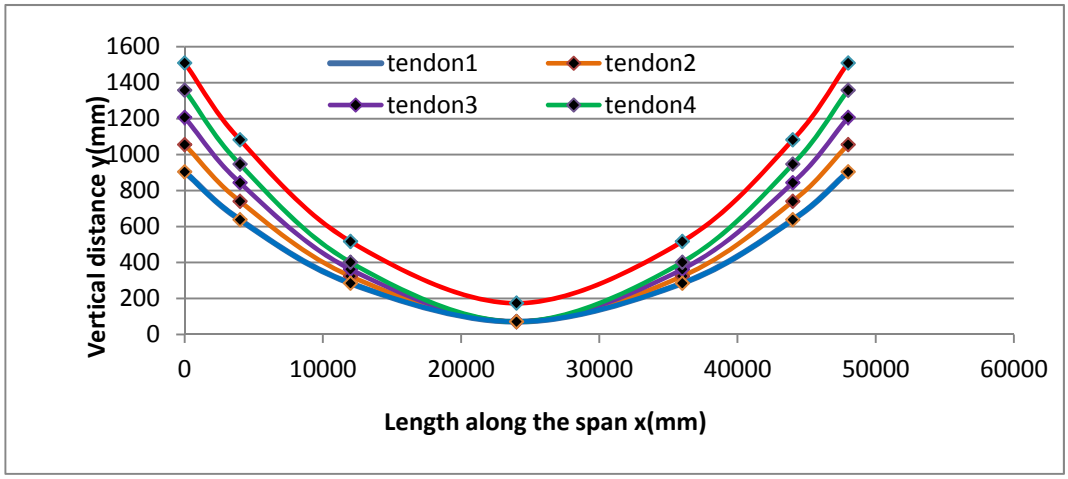

Figure 6: Tendon profile in optimum Design (continuous).

CONCLUSIONS AND RECOMMENDATIONS

The cost optimum design as a girder bridge with continuous deck is 40% cost effective than existing simply supported design. Optimum girder depth increases with increase in cost of steels. The cost of bridge increases with the increase in girder span and girder spacing is higher in smaller span than larger span. In future high strength concrete can be applied to the present optimization problem and it may yield higher optimum result. Partial prestressing can also be applied to the present optimization problem for both simply supported and continuous support conditions. Life cycle maintenance cost can be considered for the present problem.

REFERENCES

AASTHO "American Association of State Highway and Transportation Officials."Standard Specifications for Highway Bridges, Washington, DC, 2007.

Ghani,S. N. "A versatile algorithm for optimization of a nonlinear non differentiable constrained objective function."UKEA Harwell Report number R13714, ISBN 0-7058-1566-8, HMSO Publication Centre, PO Box 276, London, SW85DT, 1989.

Ghani, S. N. (1995). "Performance of global optimization algorithm EVOP for nonlinear non-differentiable constrained objective functions", Proceedings of IEEE international Conference on Evolutionary Computation, (IEEE ICEC'95), Vol 1, The University of Western Australia, Perth, Western Australia, pp. 320 — 325, November 29, 1995 to December 1, 1995.

Goble, G. G. and Lapay, W.S. "Optimum design of prestressed beams." ACI Journal, vol. 68(9) pp.712-718, 1971.

Han, S.H., Adamu, A. and Karihaloo, B.L. "Application of DCOC to optimum prcstrcssed concrete beam design." Engineering optimization, vol. 25(3), pp. 179-200, 1995.

Kirsch.U."Optimum design of prestressed beams." Computers and Structures, vol.2 (4), pp. 573-583. 1972.

Lounis, Z. and Cohn. M.Z. "Optimization of precast prestressed concrete bridge girder systems." PCI Journal, vol. 38(4). pp.60-78, 1993.

Rana, S. Ahsan, R. & Ghani, S.N. " Design of prestressed concrete I-girder bridge superstructure using optimization algorithm.", IABSE-JSCE Joint Conference on Advances in Bridge Engineering-II, Dhaka, Bangladesh, ISBN: 978-984-33-1893-0, 2010.

ID : ASEE 007

1st International Conference on Advances in Civil Engineering 2012 (ICACE 2012)
12 –14 December 2012
CUET, Chittagong, Bangladesh

EFFECTS OF CURVATURE AND BOTTOM BRACINGS ON FREE VIBRATION CHARACTERISTICS OF TWO-SPAN HORIZONTALLY CURVED TWIN I-GIRDER BRIDGES

M. R. AWALL[1*] & T. HAYASHIKAWA[2]

[1] *Department of Civil Engineering, Rajshahi University of Engineering & Technology, Rajshahi, Bangladesh, <robi95@gmail.com>*
[2] *Faculty of Engineering, Hokkaido University, Sapporo, Japan, <toshiroh@eng.hokudai.ac.jp>*
**Corresponding Author*

ABSTRACT

Horizontally curved bridges have become an important component in modern highway systems as a viable option at complicated interchanges or river crossings. This bridge type has very small torsional stiffness so it can be easy to vibrate under external dynamic loads. In this study, the effects of radius of curvatures and bottom bracings on free vibration characteristics of two-span horizontally curved twin I-girder bridge are extensively studied. To this end, elaborate three-dimensional finite element models of original bridge with considering super-elevation are developed by using commercially available ANSYS code. In this study, not only to learn about the free vibration characteristics of horizontally curved two-span twin I-girder bridges but also to improve these characteristics by using bottom bracings. For this, the same cross sectional properties but several radiuses of bridges are considered to take into account the effects of curvature. Five types of bottom bracings are designed to investigate their effects on the free vibration characteristics of studied bridges with different curvatures. The numerical results show that the curvature has a significant effect on natural frequencies and mode shapes. In curved bridges, bending and torsional mode shapes are always coupled. Torsional frequencies increase significantly after providing bottom bracings, and the increasing rate depends on bottom bracing types and their locations of installation. It is found that the performances of several bottom bracing systems are effective in improving the torsional stiffness of the two-span horizontally curved twin I-girder bridges.

Keywords: Two-span curved twin I-girder bridge, Curvature, Bottom bracing, Finite Element model, Natural frequency, Torsional stiffness

INTRODUCTION

Twin I-girder steel bridges are one of the most popular bridge types for short and medium span highway bridges in Japan (Kim et al., 2004), because of their numerous beneficial merits such as design, fabrication, and the low cost for maintenance and construction (Montens et al., 2003). Although possessing numerous beneficial merits, this type of bridges has often failed to attract practicing design engineers simply due to the lack of information on their complex behaviors (Culver 1967; Linzell et al., 2004). In addition, contrary to the straight bridges, very limited documentation on those behaviors of horizontally curved twin I-girder bridges has been made available. However, these I-girders have very little torsional stiffness and are stable only when connected to other girders using

transverse members (Linzell et al., 2004). Therefore, they can be vulnerable to vibrate by many kinds of dynamic loadings when their spans become longer.

The free vibration frequencies of a simple-span curved beam were derived by Culver (1967) with respect to analytical solutions of the equations of motion. Chaudhuri and Shore (1977) and Yoon et al. (2005) analyzed the free vibration of horizontally curved I-girder bridges using finite element (FE) method. Mathematical model for free vibration analysis of a circularly curved Timoshenko beam was presented by Wu and Chiang (2004). In their study the element stiffness matrix was derived from the force-displacement equations and the element consistent mass matrix was derived from the kinetic energy equations. Another FE formulation was presented by Duan (2008) for the nonlinear free vibration of thin-walled curved beams with non-symmetric open across section and the kinetic and potential energies were derived by the virtual principle.

When a curved bridge is subjected to aerodynamic forces or an eccentrically running vehicle, it is usually vibrates both vertically and torsionally (Linzell et al., 2004). These unexpected vibrations cause fatigue damage in bridge members especially at connections due to stress concentration and sometimes lead to brittle fracture of the bridge. An effective method to mitigate these vibrations in bridge members is changing of its natural frequencies. Generally lateral bracing can be used to transfer lateral loads both during construction and while in-service. Also, it increases the torsional resistance in curved bridges. Davidson et al. (1995) used FE method to model the horizontally curved bridges connected by cross-frames. The effects of a number of parameters on behavior of the curved girder system were established and compared to these parameters in straight girder systems. Maneetes and Linzell (2003) investigated the effects of cross-frame and lateral bracing of free vibration response of a single-span, non-composite, curved multi I-girder bridge by both experimental and FE analysis. These parametric studies provided influential parameters affecting dynamic response of the system. However, very little documentation has been found on the study of free vibration characteristics of two-span curved I-girder bridges and effects of different lateral, sway and cross bracing systems. Also most of studies used analytical formulation, simple elements or not enough number of curvatures to have a clear look on dynamic response of curved I-girder bridges. In such a case, it is difficult to get an overall understanding about free vibration characteristics and its improvement of the curved I-girder bridges.

In this study, a series of horizontally curved two-span twin I-girder composite bridges with varying of radius are investigated in detail by using three-dimensional (3-D) FE method. Five different types of bottom bracings and curvatures are studied to clarify its effects on free vibration characteristic of two-span curved bridges. These investigations are not only to enhance the understanding about free vibration characteristics but also to find out the methods improving these characteristics of the bridge.

FINITE ELEMENT MODEL

The original bridge chosen in this study is a two span horizontally curved, composite steel twin I-girder one whose each span length is 50 m and total length of the bridge is 100 m. Several radii of bridge measured from the origin of the circular arc to the centerline of the bridge deck are considered to take into account the effects of curvature. Thus, length of the two main girders varies in accordance with the chance of bridge's curvature; whereas, the total mass of the bridge remain unchanged. The two main I-girders are 3 m deep and spaced transversely at 6 m. These main structural members are tied together by a reinforced concrete slab which acts compositely with the girders and transverse steel members. The transverse members are radial cross-beams which are spaced equally along the span. 3% super-elevation is considered throughout the study. Studied bridge layout, cross-section and basic geometric properties are presented in Fig. 1, Fig. 2 and Table 1 respectively.

In this study, the original bridge model is the one without any additional bottom bracings, which is referred as M0 model throughout the paper. The FE models of original bridge model and five different types of devised bottom bracing models are shown in Fig. 3. Model M1 is the V-shaped diagonal bottom bracing system using I-section members of 0.5 m depth. Model M2, M3 and M4 are the X-shaped bottom bracings using T-section steel members of the same dimension as model M1, while

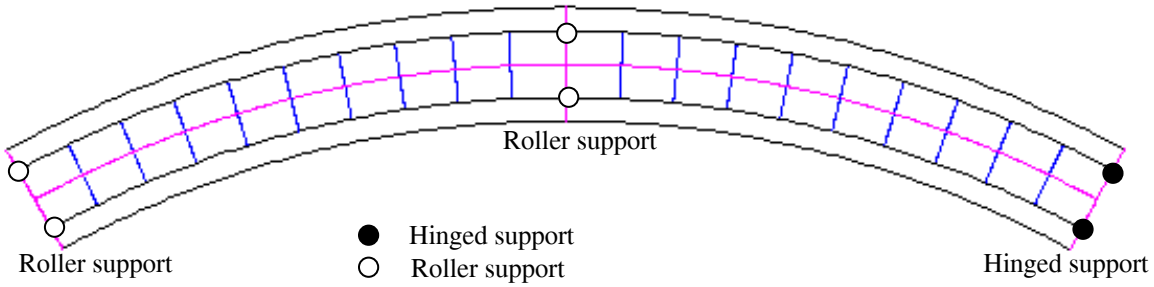

Fig. 1 Layout of studied bridge

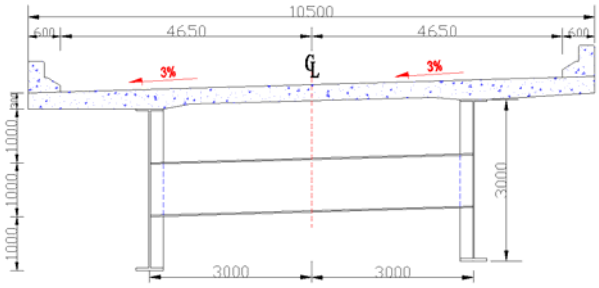

Fig. 2 Cross-section of studied bridge (mm)

Table 1 Geometric properties of studied bridge

Span number	2
Each span length [m]	50
Deck width × thickness [m]	10.5 × 0.3
Dimensions of main girders [mm]	WEB 3000 × 30 Upper FLG 500 × 40 Lower FLG 500 × 50
Dimensions of intermediate cross-beams [mm]	WEB 1000 × 16 FLG 300 × 25
Dimensions of end cross-beams [mm]	WEB 3000 × 16 FLG 300 × 25
Dimensions of bottom bracings [mm]	WEB 500 × 16 FLG 300 × 25

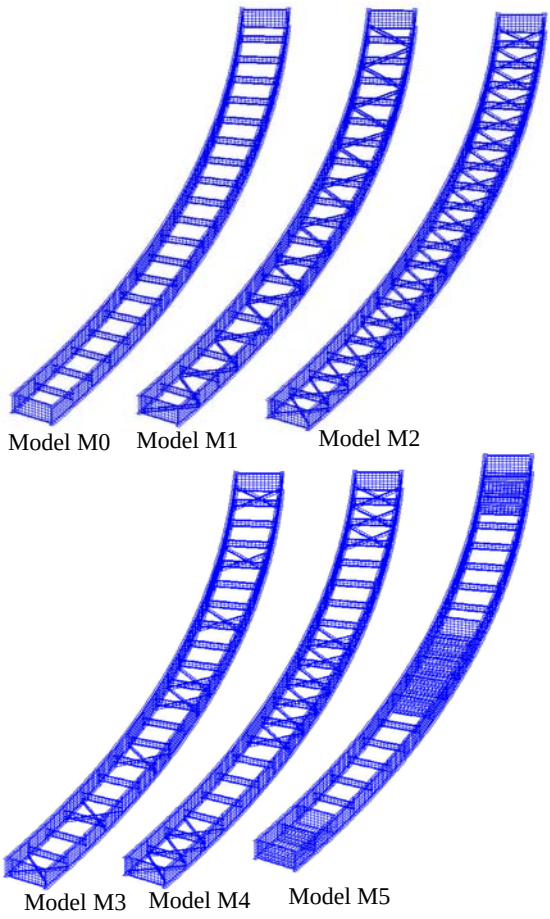

Fig. 3 FE models of studied bridges

braced bays are different for each model. In these X-shaped models one T-section steel member is allocated at the lower part, while the other inverted T-section steel member is allocated just at the upper part of the first member and the touching portion of the two members are rigidly jointed. Model M5 is the bottom plate bracing system, which has 20.0 mm thick steel plates in the plane of bottom flanges along with the full height intermediate diaphragms. There are totally four end-bays braced by bottom plates, two of which are equally located at each end of this model. Hexagonal 8-node solid elements are used for the 3-D modeling of the concrete deck and all steel members are modeled by considering quadrilateral 4-node shell elements. All the elements and boundary conditions are defined based on cylindrical coordinate system, whose origin is the centre of bridge's curvature. Lumped mass method is used for mass matrix formulation; and the numerical approach for solving natural frequencies and associated mode shape is Block Lanczos method.

ANALYTICAL RESULTS AND DISCUSSIONS

An overall understanding of natural vibration analysis as well as knowledge of the natural frequencies and mode shapes is important for all types of dynamic analysis. This study concentrate on improving natural frequencies and corresponding mode shapes with the varying of bridge curvatures (namely R = 100 m, 200 m, 400 m and 800 m) by providing five different types of bottom bracing systems.

Mode shapes

Five mode shapes of different types of studied bridge models of 200 m radius of curvatures are shown in Fig. 4. All the mode shapes in curved models are coupled of bending and torsion vibrations. The higher of curvature, the larger of coupling effects can be seen. However, based on the primary difference in vibrations of the two main girders, these mode shapes can be classified. In the vertical-related modes, the two main girders vibrate in the same directions and the magnitude of the outside main girder's vibrations is always larger than that of the inside one and vice versa in the torsion-related modes.

In the original bridge model, regardless of curvature first vertical (V1), first torsional-horizontal (TH1), first torsional (T1), second vertical (V2) and second torsional (T2) modes are related to first, second, third, fourth and fifth mode, respectively. However, in bottom bracing models, the first vertical mode is always related to the first mode and remaining modes order are changed according to the bottom bracing patterns. In the M1, M2 and M4 models, second vertical mode is observed before the first torsional mode. That means by providing the bottom bracing systems torsional stiffness increased considerably. In the M5 model, first and second vertical modes are obtained at first and second mode respectively but, first torsional mode, first torsional-horizontal mode and second torsional mode are obtained at 11th, 12th and 16th modes. Between these modes some local vibration modes of the bottom plate are observed. Also local vibration modes combined with global bridge vibration are observed in bottom bracing of M1 model.

Natural frequencies

Natural frequencies of the first five modes with varying of curvatures are graphically presented in Fig. 5. From the figure, it is easy to realize that

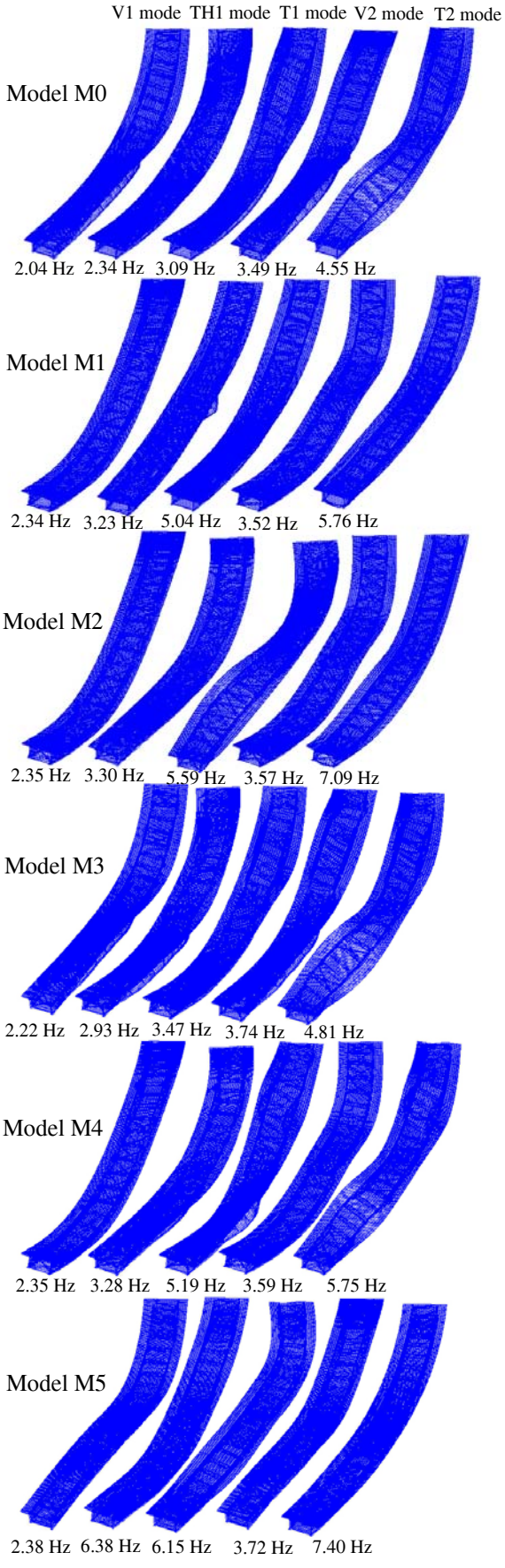

Fig. 4 Mode shapes of different types of models

the curvature has significant effects on the natural frequencies of the studied models. It is noted that the boundary conditions, the length of centerline, the girder spacing, the number of cross frames, and the geometric properties of all models are unchanged. So the changes of the natural frequencies are mainly caused by different models' curvatures. Frequencies of the vertical-related modes and torsional-horizontal mode decrease, those of the torsion-related one tend to increase with the increase curvatures. Increasing of curvature means shortening the length of the inside main girder and lengthening that of the outside one. In connection with the primary difference in vibration between torsional and vertical modes as aforementioned, the changes of frequencies could be understood.

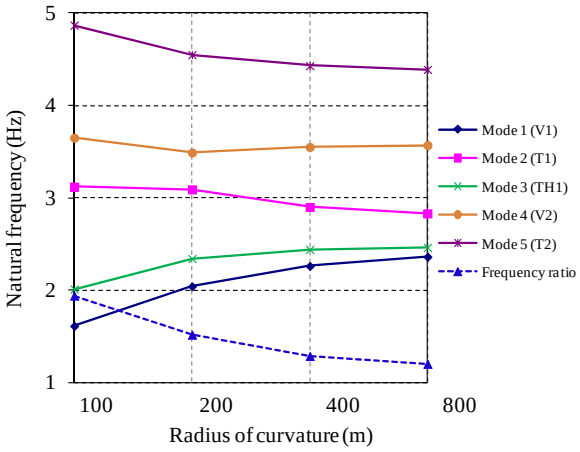

Fig. 5 Natural frequency with different radii of curvatures of original model

The effect of bottom bracings on natural frequencies of studied bridge models are typically represented in Fig. 6. The calculated result shows that the natural frequencies are increasing compared to the original model by providing different bottom bracing systems. Among them the bottom bracing configurations have great effect on torsional modes of studied bridges. Moreover, the bottom bracings also enhance vertical bending rigidity of curved bridges. In addition, frequencies are influenced considerably by both the bottom bracing types, the number and location of the braced bays. For all bracing models, frequencies related to vertical mode increased compared with the original model and the increasing rate is higher for small radii of curvatures as shown in Fig. 6a. From the calculated results it can be seen that M5 model performance is better to increase natural frequencies of all modes. But, this model produces local vibrations of bottom plates that causes fatigue damage in bridge members and sometimes lead to brittle fracture of the bridge. However, inspection and repair of fatigue damage is extremely difficult of this type of end bays box system especially when the fatigue damage occur at inside intermediate diaphragm. The second and third highest natural frequencies of all modes are observed in M2 and M4 model, respectively and this type of X-shaped bottom bracing system is much stiffer than others and dose not produces any local vibration.

To confirm the effect of different bottom bracing models with various radii of curvatures on the performance of the system, the frequency ratios (f_{T1}/f_{V1}) of these models, which are the ratios between the natural frequency of the first torsional (f_{T1}) and that of the first vertical modes (f_{V1}), are depicted in Fig. 7. From this figure, it can be seen that original bridge frequency ratios of all studied curvatures are small, the torsional and vertical vibration of these bridges could occur concurrently by external dynamic load. By providing bottom bracing systems, the frequency ratios are increasing compared to the original model and its increasing rate depends on bracing patterns. It can be seen that M5 model gives higher frequency ratios but, this model produces local vibration of the plate and the worst performance of M3 model. It can be assured the better performance contributed by the larger torsional

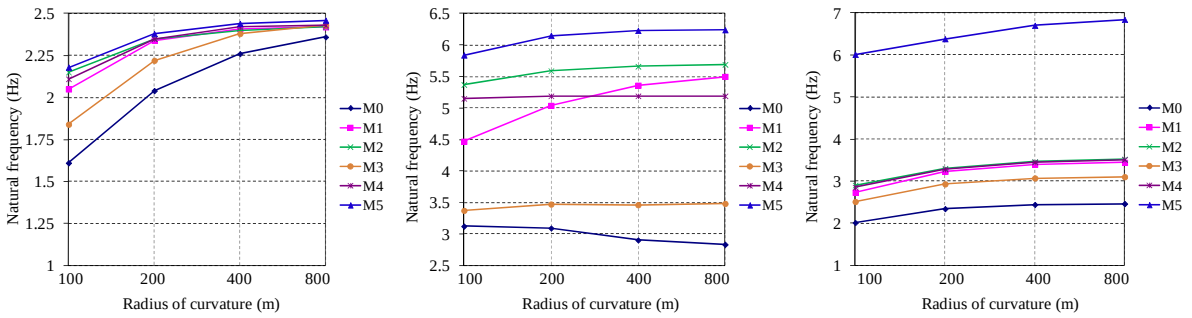

(a) First vertical mode (b) First torsional mode (c) First torsional-horizontal mode

Fig. 6 Natural frequencies of different modes of different models with radii of curvatures

stiffness of bottom bracing configurations of M2 model, which dose not produces any local vibrations. For small radii of curvature M4 model performance is better than the M1 model. However, using too many bottom-bracings becomes impractical when considering the cost effectiveness. Consequently, the M4 model can be suitable ones to increase the torsional stiffness of the studied bridges.

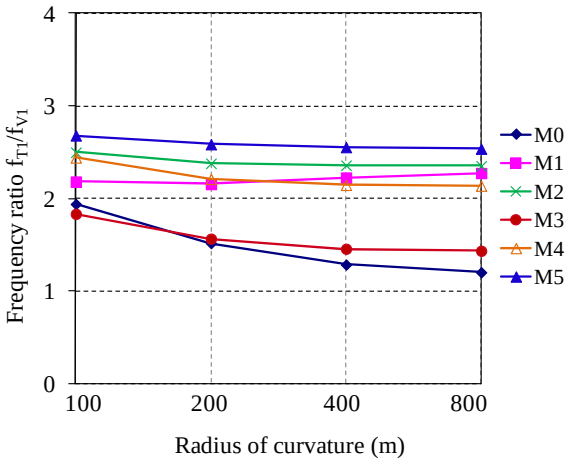

Fig. 7 Frequency ratios of different types of models

CONCLUSIONS

The present study has been investigated the effect of curvature and bottom bracing configurations on natural vibration characteristics of curved two-span twin I-girder bridges by using 3-D FE method of ANSYS. Based on the results, the followings conclusions are summarized.

All the mode shapes are coupled of bending and torsion vibrations. Curvature has significant effects on the natural frequencies of the studied models; the natural frequency of vertical modes tends to decrease, whereas, that of the torsional modes increases with the increase of curvature. By providing different types of bottom bracings cause changing not only in the natural frequencies but also in the associated mode shapes and mode shape type order of the studied models. Torsional frequencies increase significantly after providing bottom bracings, and the increasing rate depends on bottom bracing types and their locations of installation. Results indicate that M5 model produce higher torsional stiffness, however, this model has limitation to use because of its local vibrations may cause fatigue failure, inspection, repair problem and shorter service life. It can be confirmed that M2 model gives better performance contributed by the larger torsional stiffness, also M4 model is suitable one to considering the cost-performance effectiveness.

REFERENCES

Kim, CW; Kawatani, M and Hwang, WS. 2004. Reduction of traffic-induced vibration of two-girder steel bridge seated on elastomeric bearing. *Engineering Structures*, 26: 2185-2195.

Montens, M; Vollery, JC and Park, JH. 2003. Advantages of twin I beams composite solutions for highway and railway bridges. *Steel Structure*, 3(1): 65-72.

Linzell, D; Hall, D and White, D. 2004. Historical perspective on horizontally curved I girder bridge design in the United States. *Journal of Bridge Engineering*, 9(3): 218-229.

Culver, CG. 1967. Natural frequencies of horizontally curved beams. *Journal of Structural Engineering*, ASCE, 93(2): 189-203.

Chaudhuri, SK and Shore, S. 1977. Dynamic analysis of horizontally curved I girder bridges. *Journal of Structural Engineering*, ASCE, 103(8): 1589-1604.

Yoon, KY; Kang, YJ; Choi, YJ and Park, NH. 2005. Free vibration analysis of horizontally curved steel I-girder bridges. *Thin-Walled Structures*, 43: 679-699.

Wu, JS and Chiang, LK. 2004. Free vibration of a circularly curved Timoshenko beam normal to its initial plane using finite curved beam elements. *Computers and Structures*, 82: 2525-2540.

Duan, H. 2008. Nonlinear free vibration analysis of asymmetric thin-walled circularly curved beams with open cross section. *Thin-Walled Structures*, 46: 1107-1112.

Davidson, JS; Keller, MA and Yoo, CH. 1995. Cross-frame spacing and parametric effects in horizontally curved I-girder bridges. *Journal of Structural Engineering*, ASCE, 122(9): 1089-1096.

Maneetes, H and Linzell, DG. 2003. Cross-frame and lateral bracing influence on curved steel bridge vibration response. *Journal of Constructional Steel Research*, 59: 1101-1117.

ID: ASEE 012

1st International Conference on Advances in Civil Engineering 2012 (ICACE 2012)
12 –14 December 2012
CUET, Chittagong, Bangladesh

COMPARATIVE STUDY OF REINFORCED CONCRETE BUILDINGS WITH DIFFERENT SLAB SYSTEMS UNDER LATERAL LOADS

M. ARIFUJJAMAN[1*], B. AMIN[1], M. J. ANOWER[1] & A. I. RAJIB[2]

[1]*Research Engineer, Housing and Building Research Institute, Dhaka, 1216, Bangladesh.*
<islam.badol@yahoo.com >
[2]*Research Fellow, Housing & Building Research Institute, Dhaka, 1216, Bangladesh*
**Corresponding Author*

ABSTRACT

In Bangladesh, different types of floor system, such as edge supported slabs (One way, two way), column supported slabs (Flat slab, flat plate slab), ribbed slabs, waffle slabs etc. are commonly employed in reinforced concrete building structures. This study was undertaken to carryout inelastic pushover analysis of buildings with different slab systems using ETABS software. The analytical results obtain from buildings having edge supported slabs compared with the same having column supported slabs and also to conduct a parametric study on the lateral strength of buildings with different parameters. Total 18 nos. reinforced concrete buildings of different numbers of stories with two different slab systems 1) Edge supported slabs; 2) Column supported slabs are designed as model buildings using ETABS for the study. All the models are designed following Bangladesh National Building Code (BNBC-1993). The models are designed for gravity loads at first step. The responses of the models are verified for lateral loads in the subsequent steps according to the code UBC-97.

Keywords: inelastic, pushover, parametric, lateral loads

INTRODUCTION

The use of inelastic static analysis in earthquake engineering is traced to the work of Gulkan and Sozen (1974) or earlier, where a single degree of freedom system is derived to represent the multi-degree of freedom structure via an equivalent or 'substitute' structure. The load-displacement curve of this substitute to the real structure is evaluated by either finite element analysis or hand calculation to obtain the initial and post-yield stiffness, the yield strength and the ultimate strength. Simplified inelastic analysis procedures for multi-degree of freedom systems have also been proposed by Saiidi and Sozen (1981) and Fajfar and Fischinger (1988).There are several publications that review the advantages and disadvantages of pushover analysis, with varying degree of success. They all, however, utilize global response parameters, namely top displacement versus base shear. Lawson et al. (1994) discuss in some detail the range of applicability, the expected realism for various structural systems and highlight the difficulties encountered. The latter study is both conceptual and applied, rendering it specifically valuable. In the course of describing recent trends in seismic design, Krawinkler (1995) discusses pushover analysis as a prelude to capacity spectrum applications. The author mentions a contentious point, which is that 'in most cases the normalized displacement profile at a first estimate of the target displacement level is utilized for these (defining the shape vector) purpose. Attempts at improving the procedure have been made, with varying degree of rigor and

success. The simplest and most pragmatic of which is the work of Sasaki et al. (1998). This comprises running several pushover analyses under forcing vectors representing the various modes deemed to be excited in the dynamic response. The pros and cons of the procedure were also discussed by Krawinkler and Seneviranta (1998). They concluded that not all analysis of the same structure under a set of district earthquake records are predicted by pushover analysis, a rather obvious conclusion that did not require inelastic dynamic analysis to prove.

MATERIALS AND METHODS

In order to conduct a parametric study of the lateral resistance of eight, ten and twelve storied buildings having two different types of slabs:

1. Flat plate slab
2. Beam slab

Three model buildings are adopted in this study. The buildings have three length/ breath ratios: 1, 1.5, 2.0 all the buildings are designed using Bangladesh National Building code (BNBC-1993).It is worthy to mention that the buildings are designed for gravity loads at first step, and subsequently verified for lateral loads using UBC'97.The materials, loading and the designed sections of different basic components are described in the following sections.

MATERIALS PROPERTIES

Basic materials used in designing the model buildings are concrete and reinforcing steel and. To carry out designing the buildings, the materials parameters are selected first on the basis are availability in construction industry. The selected materials parameters are listed below:

Table 1 Materials properties

Materials	Properties	
Concrete	Compressive Strength of Concrete, f'_c=24 Mpa	Modulus of elasticity of Concrete, $E_c=4700\sqrt{f'_c}$ Mpa
Reinforcing Steel	Yield stress of reinforcing steel, f_y = 413 Mpa	Modulus of elasticity of reinforcing steel, $E_s = 200X10^2$ Mpa

ANALYTICAL INVESTIGATION

Pushover Analysis

Pushover analysis is a static, nonlinear procedure using simplified nonlinear technique to estimate seismic structural deformations. It is an incremental static analysis used to determine the force-displacement relationship, or the capacity curve, for a structure or structural element. The analysis involves applying horizontal loads, in a prescribed pattern, to the structure incrementally, i.e. pushing the structure and plotting the total applied shear force and associated lateral displacement at each increment, until the structure or collapse condition.

RESULTS

By pushover analysis variation of displacement with base reaction for different slab system and different parameter of buildings are given below:

Table 2 Analysis of Eight Storied Building

Plan Dimension	Beam supported slab		Flat plate slab without edge beam		% of resistance higher than flat plate slab	Average Of Percentage
	Lateral resistance (KN)	Displacement (mm)	Lateral resistance (KN)	Displacement (mm)		
18.3mx18.3m	467.57	45	363.03	45	28.80	25.5
18.3mx27.45m	600.15	45	480.92	45	24.80	
18.3mx36.6m	739.09	45	600.15	45	23.10	

Table 3 Analysis of Ten Storied Building

Plan Dimension	Beam supported slab		Flat plate slab without edge beam		% of resistance higher than flat plate slab	Average Of Percentage
	Lateral resistance (KN)	Displacement (mm)	Lateral resistance (KN)	Displacement (mm)		
18.3mx18.3m	462.06	45	353.68	45	30.64	27.5
18.3mx27.45m	598.19	45	469.22	45	27.48	
18.3mx36.6m	730.37	45	587.07	45	24.40	

Table 4 Analysis of Twelve Stored Building

Plan Dimension	Beam supported slab		Flat plate slab without edge beam		% of resistance higher than flat plate slab	Average Of Percentage
	Lateral resistance (KN)	Displacement (mm)	Lateral resistance (KN)	Displacement (mm)		
18.3mx18.3m	456.54	45	344.38	45	32.50	29.5
18.3mx27.45m	596.15	45	457.52	45	30.30	
18.3mx36.6m	721.65	45	574.04	45	25.70	

Graphical representations for different types of slab system where base reaction is varied for different story, i.e. Eight, Ten & Twelve

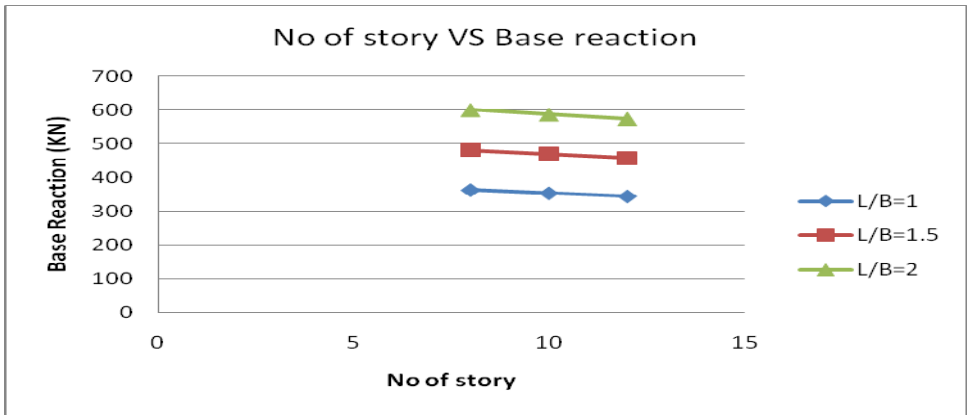

Fig. 1 No. of story VS Base reaction for flat plate slab

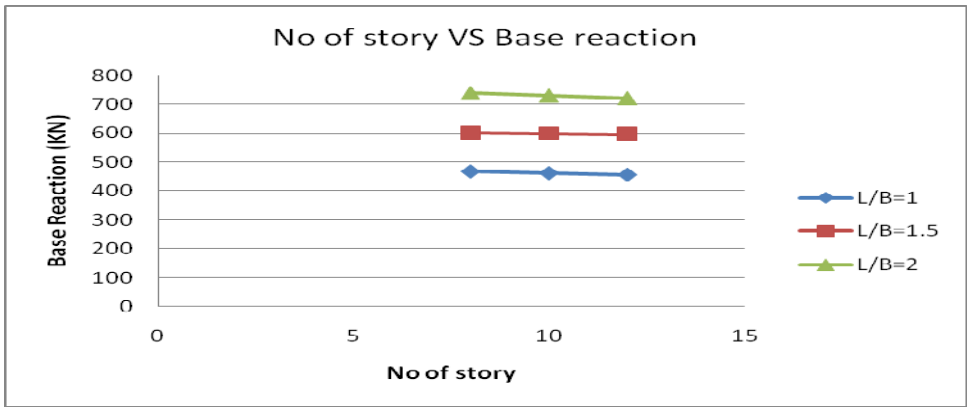

Fig.2. No. of story VS Base reaction for beam supported slab

Graphical representations for different types of slab system where base reaction is varied for different L/B Ratio, i.e.1, 1.5, 2.0

Eight Storied Building

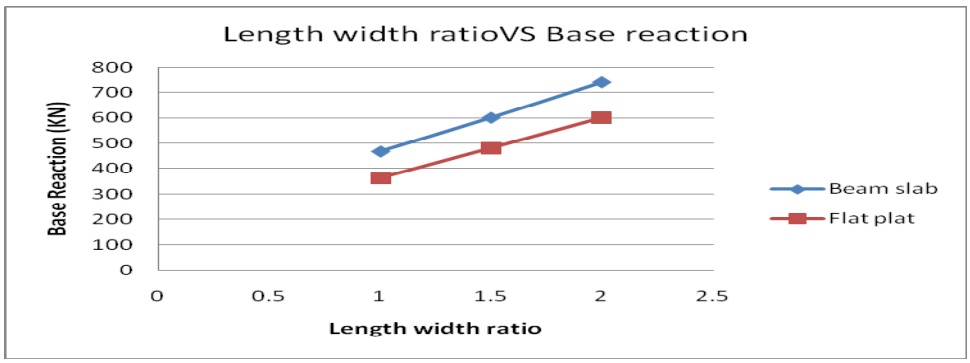

Fig.3. Length width ratio VS Base reaction curve for flat plate slab and beam supported sla

Ten Storied Building

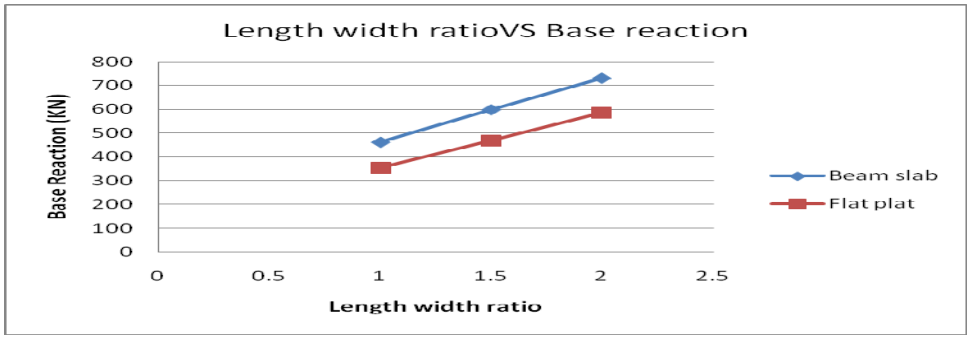

Fig.4. Length width ratio VS Base reaction curve for flat plate slab and beam supported slab

Twelve Storied Building

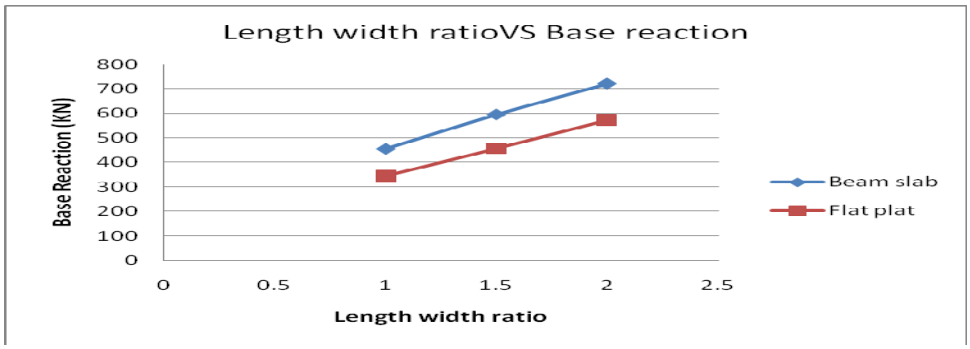

Fig.5. Length width ratio VS Base reaction curve for flat plate slab and beam supported slab

DISCUSSION

Lateral strength of eighteen reinforced concrete buildings with two different slab systems (1) beam supported slab; (2) flat plate slab

1. Base reaction is increased when L/B is increased.
2. When L/B is 1, 1.5, 2.0 then lateral load resistance capacities at beam supported slab is higher than the flat plate slab.
3. When the storey height is increase the base reaction is decrease.
4. For plan size 18.3mx18.3m, beam supported slab has 28.8% (For 8-storied), 24.8 % (For 10 storied) and 23.1% (For 12- storied) higher strength than that of the buildings with flat plate slabs.
5. For plan size 18.3mx27.45m, beam supported slab has 30.64% (For 8- storied), 27.48% (For 10- storied) and 24.4% (For 12- storied) higher strength than that of the buildings with flat plate slabs.
6. For plan size 18.3mx36.6m, beam supported slab has 32.56% (For 8- storied), 30.30% (For 10- storied) and 25.7% (For 12- storied) higher strength than that of the buildings with flat plate slabs

CONCLUSION

An analytical study on the lateral strength several storied buildings with two different slab systems (1) beam supported slab; (2) flat plate slab is carried out.
The buildings are designed for gravity loads at first steps and subsequently verified for lateral loads. The conditions drawn in the study are as follows:

1. It is found that the buildings with beam supported slabs have higher lateral strength than with flat plate slab.
2. It is found that the lateral strength is decreased when the storey height is increased in both cases of two different slab systems.
3. Differences in lateral strengths are obtained for different length width ratio of the buildings.

ACKNOLEDGEMENT

All praise to our Allah, our creator, our sustainers, to whom we all have to return. We bear the witness that there is none worthy of worship except Allah and we also bear the witness that Muhammad (Peace be upon him) is Allah's slave and messenger. Thanks to the member of my research partners for their valuable advice and encouragement.

REFERENCES

ATC, 1996,Seismic Evaluation and Retrofit of Concrete Buildings, Volume 1,ATC-40 report, Applied Technology Council , Redwood city ,California.
Bangladesh National Building Code (BNBC) 1993.
Building Seismic Safety Council .NEHRP Guidelines for the Seismic Rehabilitation of Buildings, FEMA-273.FederalEmergency Management Agency, Washington, DC, 20058
Chopra AK, Goel,RK.Amodal pushover analysis procedure for estimating seismic demands for buildings , Earthquake Engineering & Structural Dynamics 561-582(doi:10.1002/eqe.144,2002;31.
ETABS ,Integrated Design and analysis software for Building System, Computer and Structure Inc, Berkley, California,UAS,Version9.0,2000.
Fijfar P, Gaspersic P. The N2 method for seismic damage analysis of RC buildings Earthquake Engineering & Structural Dynamics 1996; 25:31-46
Fijfar, P. and Fischinger, M.(1988)N2-method for Nonlinear Seismic Analysis of Regular Structures, Procedings of the Ninth World Conference on Earthquake Engineering (Tokyo-Kyoto,Japan1988), Vol.5pp.111-116.
FEMA, 1997, NEHRP Guidelines for the Seismic Rehabilitation of Buildings, Developed by Buildings Seismic Safety Council for the Federal Emergency Management Agency(Report No.FEMA273),Washington,D.C.
Gupta A, Krawinkler H. Estimation of seismic drift demands for frame structures.
Earthquake Engineering & Structural Dynamics 2000;29:1287-1305.
Kim, S.and D'Amore,E (1999) pushover analysis procedures in earthquake engineering, Earthquake Spectra, Vol.15,No.3,Aaugust,pp.417-434.
Krawinkler H, Seneviratna GDPK. Pros and cons of a pushover analysis of seismic performance evaluation. Engineering Structures 1998;20(4-6):452-464.
Krawinkler H.(1995) New trends in seismic design methodology proceedings 10th ECEE, The Netherlands, Rotterdam,pp.821-830.
Krawinkler H, Seneviratna, G. D.(1998) Pros and cons of pushover analysis of seismic performance evaluation, Engineering Structures, Vol.20,No .4-6,pp.452-462.

ID: ASEE 014

1st International Conference on Advances in Civil Engineering 2012 (ICACE 2012)
12 –14 December 2012
CUET, Chittagong, Bangladesh

ANALYSIS AND DESIGN OF GRID FLOOR BY USING VISUAL BASIC SOFTWARE

AMIRUL ISLAM RAJIB[1*], M. Arifujjaman[2], B. Amin[2] & M. J. Anower[2]

[1]*Research Fellow, Housing & Building Research Institute, Dhaka, 1216, Bangladesh,*
< rajibamirul@gmail.com >
[2]*Research Engineer, Housing & Building Research Institute, Dhaka, 1216, Bangladesh*

**Corresponding Author*

ABSTRACT

Grid floor systems are normally in use for architectural reasons for large rooms such as auditoriums, theatre halls, show rooms of shops where column free space is often the main prerequisite. Grid floors have greater stiffness and in addition to pleasing look when viewed from bottom. The design of grid floor by hand calculation is much time-consuming.
The main goal of the research was to develop a computer programming for the analysis and design of grid floor by using Visual Basic software. In the analysis and design of two methods, namely, approximate method and plate theory method two programmes were developed. A typical structure was under consideration to design by both methods and a comparative study was established to show the variation in reinforcements. In the study, it was exhibited that approximate method is more economic than plate theory method. However, it might be mentioned that, where twisting moment is to develop for a structure of high-rise and very long span, plate theory method should be used for the design of grid floor.
Moreover, the analysis and design of grid floor with the help of computer programming is easier and require less time. The benefit of the computer programming is that, it may be error free or significantly less error calculation.

Keywords: Grid Floor, Computer Programming, Twisting Moment

INTRODUCTION

Grid flooring is such kinds of flooring where the open spaces or column free spaces is the major prerequisite. These flooring are normally adopted for artistic reasons for large accommodations such as auditoriums, theatre halls, showrooms of shops etc. Now a day's construction of auditoriums, theatre halls, showrooms of shops are significantly increases. The main benefit of the grid flooring is that grid floors have greater stiffness and in addition to pleasing appearance when viewed from bottom. The design of grid floor by hand calculation is much time consuming. By developing a programme, using Visual Basic software is more convenient for design the grid floor.
To achieve the desired goal, the main objectives of this study are as follow:

1. To design the grid floor based on approximate method by using visual basic software.
2. To design the grid floor based on plate theory method by using visual basic software.
3. To analyse the variation between these two methods.

METHODOLOGY:

Grid or coffered floor systems consisting of beams spaced at regular intervals in perpendicular directions, monolithic with a slab.
Basic rules for design of grid floor:
The rules are based on practical considerations [1].

(i) Thickness of top slab: The minimum thickness of top slab should not be less then 5 cm (or 2 in) or $1/12^{th}$ of the clear distances between the ribs, whichever is greater. The thickness of the top slab should be made sufficient to provide adequate compressive area. It normally varies from 5 cm to 9 cm.

(ii) Depth of rib: The combined depth of ribs and the top slab is determined in the manner as the depth of a solid slab. Thus, the depth of a rib depends on the loading condition and the span. Generally, the combined depth of rib and top slab should not exceed more then 3.5 times the breath of the rib.

(iii) Breadth of rib: The width of the rib depends upon the magnitude of shearing force. It normally varies between 6 cm to 12 cm.

(iv) Spacing between ribs: The spacing between two adjacent ribs should not exceed 12 times the thickness of top slab.

(v) Reinforcement in slab: Because of restriction of small span, the top slab is normally not designed. The slab is primarily reinforced for temperature and shrinkage stresses. The percentage of steel in the slab should in no case be less than 0.15% of the gross cross-sectional area of concrete. The reinforcement may be provided in the form of welded wire mesh or 6mm Ø bars spaced equally both ways. For thin slab, the maximum c/c spacing of the 6 mm Ø bars may be restricted to 25 cm.

Analysis of grid floor:

Approximate Method: Consider a grid floor shown in Fig.1 in which the spacing's of the ribs are a_1 and b_1 in the x and y directions respectively.

Let q = total load per unit area
q_1 and q_2 = the loads shared in the x and y directions
a = shorter dimension of grid
b = longer dimension of grid

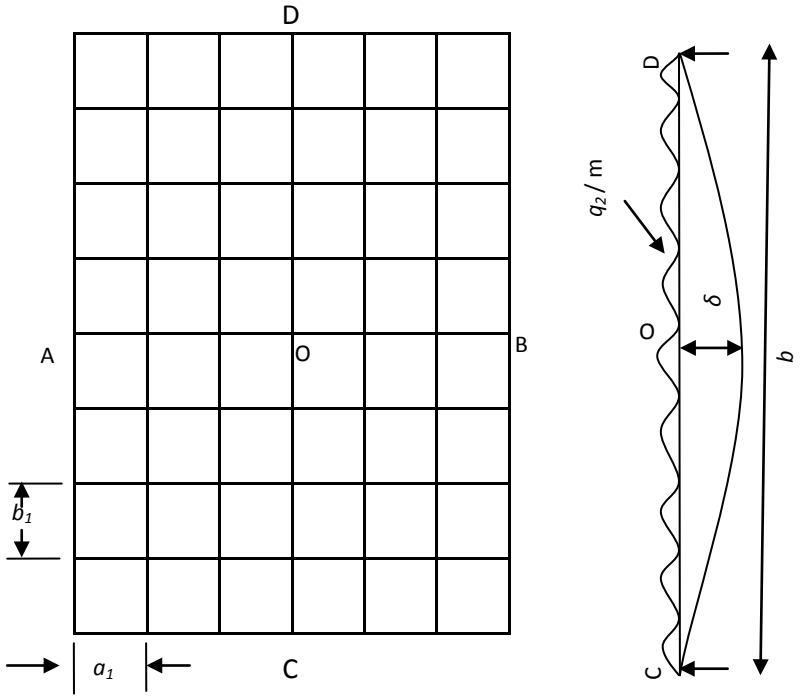

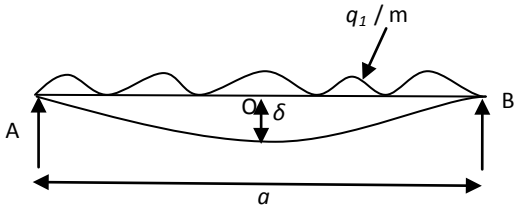

Fig.1 Deflections of Ribbed Slab

The deflections of the ribs AB and CD at the joint O must be the same and by equating the deflections, we have:

$$\delta = \left(\frac{5q_1 a^4}{384\ EI}\right) = \left(\frac{5q_2 b^4}{384\ EI}\right) \quad (1)$$

$$q_1 a^4 = q_2 b^4 \quad (2)$$

Also

$$q = q_1 + q_2 \quad (3)$$

Solving Eqs. (1) And (2), we have

$$q_1 = q\left(\frac{b^4}{a^4+b^4}\right) \text{ and } q_2 = q\left(\frac{a^4}{a^4+b^4}\right) \quad (4)$$

The bending moments for the central ribs are given by:

$$M_{AB} = \left(\frac{q_1 b_1 a^2}{8}\right) \qquad M_{BD} = \left(\frac{q_2 a_1 b^2}{8}\right) \quad (5)$$

The bending moments in the other ribs can also be determined in direct proportion to their distances from the center. The ribs are designed as flanged sections to resist moments and shears. However, the approximate methods do not yield the twisting moments in the beams.

Plate Theory Method:

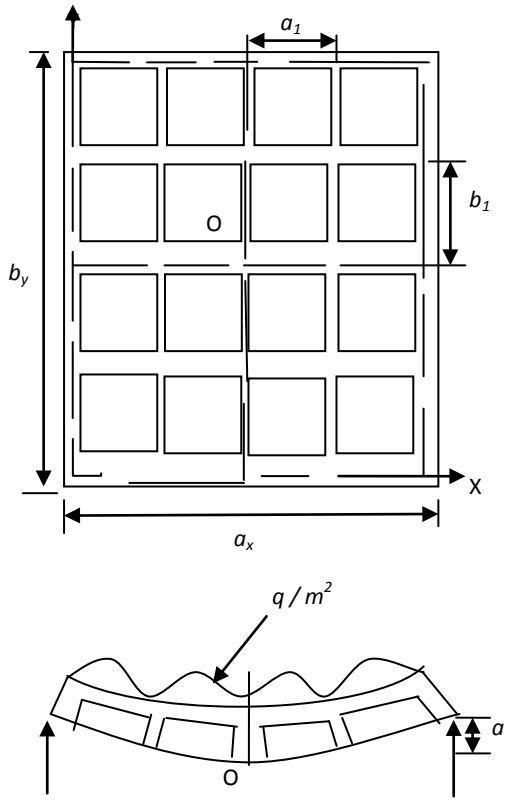

Fig.2 Deflection Characteristics of Grid Floor

The vertical deflection '*a*' at the point of the grid shown in Fig.2 is expressed as:

$$a = \frac{16}{\pi^6}\left[\frac{\sin\left(\frac{\pi x}{a_x}\right)\sin\left(\frac{\pi y}{b_y}\right)}{\frac{D_x}{a_x^4}+\frac{2H}{a_x^2 b_y^2}+\frac{D_y}{b_y^4}}\right] \quad (6)$$

Where q = total uniformly distributed load per unit area

a_x, b_y = length of plate in x and y directions respectively

D_x, D_y = flexural rigidity per unit length of plate along x and Y direction

C_x, C_y = torsional rigidity per unit length of plate along x and Y direction.

If a_1 and b_1 are the spacing's of the ribs in x and y directions respectively, then we have the relations:

$$D_x = (EI_1 / b_1) \qquad D_y = (EI_2 / a_1) \quad (7)$$

$$C_x = (C_1 / b_1) \qquad C_y = (C_2 / a_1) \quad (8)$$

Where EI_1, EI_2, C_1 and C_2 are the flexural and torsional rigidities of the effective section in x and y directions. The moments and shears are computed using the following expressions:

$$M_x = - D_x \left(\frac{\partial^2 a}{\partial x^2}\right) \qquad M_y = - D_y \left(\frac{\partial^2 a}{\partial y^2}\right) \quad (9)$$

$$T_{xy} = - \frac{C_1}{b_1}\left(\frac{\partial^2 a}{\partial x.\partial y}\right) \qquad T_{xy} = - \frac{C_2}{a_1}\left(\frac{\partial^2 a}{\partial x.\partial y}\right) \quad (10)$$

$$Q_x = - \frac{\partial}{\partial x}\left[D_X\left(\frac{\partial^2 a}{\partial x^2}\right) + \frac{C_2}{a_1}\left(\frac{\partial^2 a}{\partial x.\partial y}\right)\right] \quad (11)$$

$$Q_y = - \frac{\partial}{\partial y}\left[D_y\left(\frac{\partial^2 a}{\partial y^2}\right) + \frac{C_1}{b_1}\left(\frac{\partial^2 a}{\partial x.\partial y}\right)\right] \quad (12)$$

Maximum bending moments develop at centre of span while maximum torsional moments are generated at the corners of the grid and maximum shear forces develop at mid points of longer side supports.

If the size of the beam is same, then

$$C_1 = C_2 = k_1 G (2a)^3 . 2b = k_1 \left[\frac{E}{2(1+\mu)}\right](2a)^3 . 2b \quad (13)$$

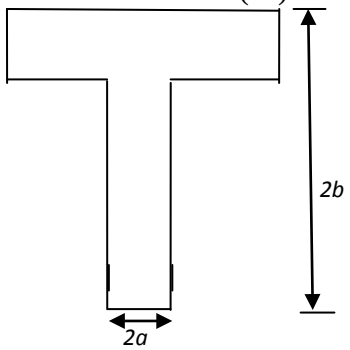

Fig.3 Section of Rib

The value of k_1 obtained from table in Timoshenko theory of elasticity [2].

$$I = C. b_w D_3 \quad (14)$$

b_w = width of web

The value of consistant C obtained from Reynolds R. C. designer handbook [3]. The modified modulus of elasticity

$$E_{cc} = \frac{E_c}{1+\theta} \quad (15)$$

θ = Creep coefficient

According to IS: the long term deflection should not exceed $\left(\frac{span}{250}\right)$

Analysis & Design by Software:

The following data were used to design the grid floor, which is shown in Fig.4

i. The properties of concrete (f'_c)
ii. The properties of steel (f_y)
iii. Density of concrete (lb/ ft^3)
iv. Size of the grid in X-direction (ft)
v. Size of the grid in Y-direction (ft)
vi. Spacing of rib in X-direction (ft)
vii. Spacing of rib in Y-direction (ft)
viii. Live load (lb/ft^2)
ix. Thickness of slab (in.)
x. Width of rib (in.)

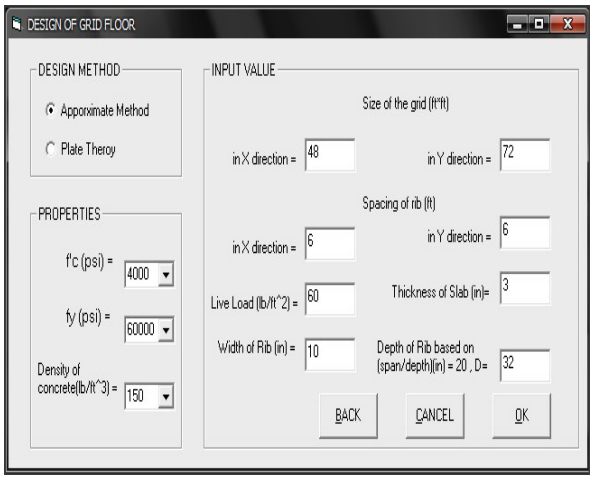

Fig.4 Input Value Window

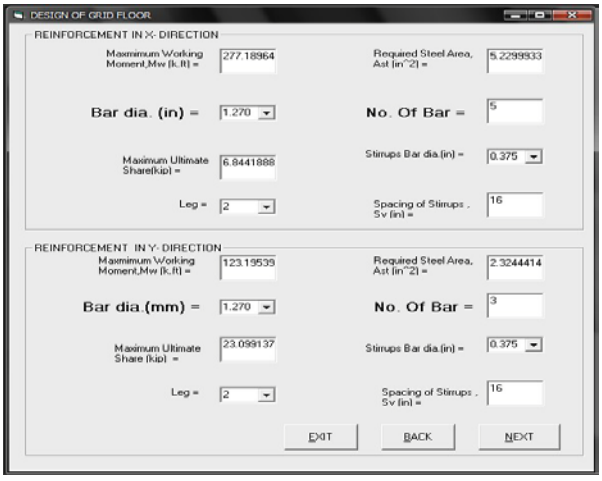

Fig.5 Reinforcement Calculation Window

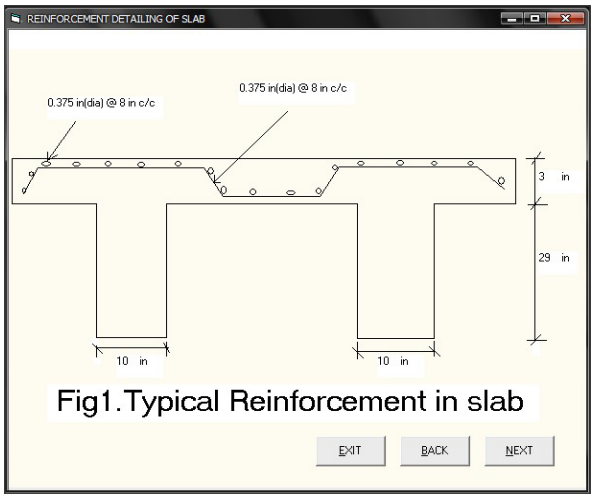

Fig.6 Typical Reinforcement in Slab

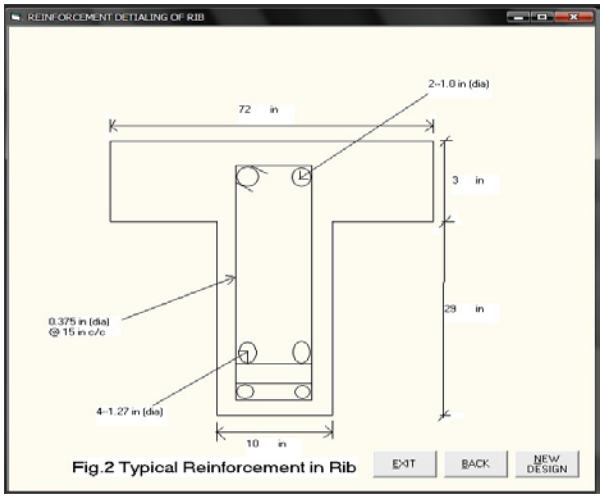

Fig7. Typical Reinforcement in Rib

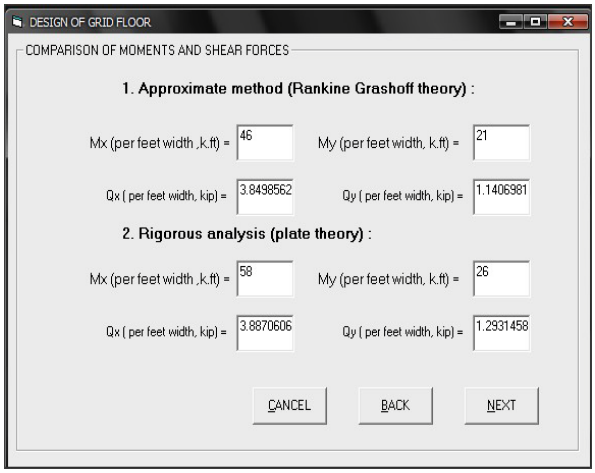

Fig.8 Comparison of Moments and Shear Forces

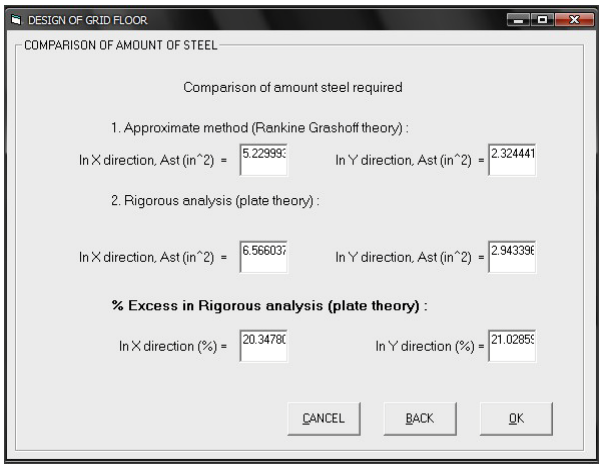

Fig.9 Comparison of Amount of Steels

RESULTS:

The results obtained in this study are as follows:

Table.1 Comparison of Moments, Shear Forces & Amount of Steels

Method	M_x (kip.ft)	M_y (kip.ft)	Q_x (kip)	Q_y (kip)	As (in.) (*X* direction)	As (in.) (*Y* direction)
Approximate Method	46	21	3.85	1.15	5.23	2.32
Plate Theory Method	58	26	3.88	1.30	6.56	2.95
% Increase at plate theory method with respect to approximate method	20.6	19.2	0.8	11.5	20.3	21.3

From this study it was found that, for a typical grid floor, plate theory method gives a higher value for moments (about 20%), shear forces (about 6%) & amount of steels (about 20%) comparison with the approximate method.

CONCLUSIONS:

For a typical grid floor design with the same data it was found that, approximate method requires less amount of steel comparison with the plate theory method.
Therefore, it was concluded that, approximate method is economical for grid floor design comparison with the plate theory method. However, it might be mentioned that, where twisting moment is to develop for a structure of high-rise and very long span plate theory method should be used for the design of grid floor.

REFERENCES:

[1] Raju Krishna. N (1986) "*Advanced Reinforced Concrete Design"*, CBS Publishers,4596/1-A,11 Darya Ganj, New Delhi.

[2] Timoshenko. S & Goodier. J (1970) "*Theory of Elasticity"*, Mcgraw-hill international edition.

[3] Reynolds. C & Steedman. J (1988) "*Reinforced Concrete Designer's Handbook.10th edition*", 11 New Fetter Lane, London.

ID : ASEE 015

1st International Conference on Advances in Civil Engineering 2012 (ICACE 2012)
12 –14 December 2012
CUET, Chittagong, Bangladesh

EFFECT OF TYRE DUST ON THE STRENGTH OF CONCRETE

B. AMIN[1*], M. Arifujjaman[1], A. I. Rajib[2] & M. J. Anower[1]

[1]*Research Engineer, Housing & Building Research Institute, Dhaka, 1216, Bangladesh, baminhbri@gmail.com*
[2]*Research Fellow, Housing & Building Research Institute, Dhaka, 1216, Bangladesh, rajibce06@yahoo.com*
**Corresponding Author*

ABSTRACT

Due to progressive increase of vehicles, the numbers of used tyre are going to be one of the environmental problems. For its reuse, researches have been developed. The use of tyres' rubber in the concrete may be a possible form of its application, aiming to recycling of this material. Concrete cylinders of 4 inch diameter & 8 inch height were prepared using 3% and 7% tyre dust by volume of concrete. Compressive and tensile strength of the cylinders were determined for standard curing period of 7 days and 28 days. Total 73 cylinders were tested for strength out of which 6 cylinders were tested for plain concrete and 12 cylinders were tested for tensile strength and rest were tested for compressive strength. Experimental results indicate that the higher volume of tyre dust produce a progressive reduction of compressive strength but improves tensile strength.

Keywords: Dust, Recycling, Compressive Strength, Tensile Strength

INTRODUCTION

The disposal of waste tyres is becoming a waste management problem in the world as well as Dhaka city. It is estimated that 37 millions car and truck tyres are being discarded annually and this number is set to increase, in line with the growth in road traffic and car ownership, by a further 39% by 2011 and 63% by 2021 (Martin, 2001). At present, it is estimated that 11% of post-consumer tyres are exported, 62% are refused, recycled or sent to energy recovery and 72% are landfill (shredded tyre), stockpiled (whole tyre) or bumped in illegal tyre dumps. Landfill has been one of the most convenient ways of disposal of waste tyres. As rubber's tyres are extremely durable and not naturally biodegradable, they will remain in landfill with very little degradation in landfill over time, presenting a continuing environmental hazard. However, landfill is no longer viable option due to the implementation of European legislation, which currently bans the disposal of tyre in landfill sites. There is, therefore, an urgent need to identify alternative solutions. This promotes recycling ahead of disposal and energy recovery. One of the largest potential recycling routes is in construction, but usage of waste tyres in civil engineering is currently very low. This is due to lack of high volume of applications and products involving recycled tyres. After the imposition of the landfill ban, there is a strong possibility of an increase in stockpile and dumping waste tyres, whether legally or illegally. However, tyres stockpiles are a considerable environmental and fire hazard. Uncontrolled combustion of tyre tends to release significant amount of unburned hydrocarbons and noxious emissions into the atmosphere. The melting tyres also produce large quantity of oil, which cause contamination of soil and ground water.

To find out a way to use tyres' rubber in concrete as a result of which the tensile strength get increased. Despite this aim there is another goal that is to know the strength behaviour of rubber matrix and to choose the better one. Consequently to reduce the growing environmental problem caused by the refused tyres. From the glow of the test result may the invisible mystery be unlocked. The test result may unfasten numbers of doors of investigation to the forthcoming researchers. The objectives of the projects are

1. To determine the compressive strength of selected numbers of rubberized concrete cylinders
2. To determine the tensile strength of selected numbers of rubberized concrete cylinders

MATERIALS AND METHODS

CEMENT:

For the purpose of the research work the Ordinary Portland Cement has been used in entire laboratory works as it used in wide range for construction project at present. For using in construction works OPC is manufactured as finely powered substance, usually grey or brownish grey composite largely of artificial crystalline materials, the most important which are Calcium and Aluminum silica etc. Substantial portion of OPC should passes through #200 sieves. The specific gravity ranges from 3.16 to 8.12, bulk unit weight is 90 lb/cft.

SAND:

Natural sands are disintegrated, weathered work out particles of natural rocks and are of various grades and depending on the amount the intensity of disintegration. Sand plays an important role as an engineering material. In concrete it is generally added as fine aggregate. To determine the physical properties, these may be subjected to mainly four tests-

- Sieve analysis or fines modulus test.
- Unit weight test.
- Specific gravity test.
- Absorption test.

COURSE AGGREGATE:

Aggregate should be clean, strong, durable and of suitable site and should not have any disturbing materials such as dust, dirt, inorganic impurities, florid etc. In choosing aggregate for using in particular concrete attention should be paid to three general requirements, such as below-

a) Economy of matrix.
b) Potential strength of hardened mass.
c) Probable durability of concrete structure.

For rubber mixed concrete cylinder following parameters have used:

A) In case of compressive strength test-
    a) Aggregate size 0.5" down grade
    b) Unit weight (bulk) 1130 kg/m^3
    c) Specific gravity of stone chips=2.54
B) In case of tensile strength test-
    a) Aggregate size 0.75" down grade
    b) Unit weight (bulk) 1100 kg/m^3
    c) Specific gravity of stone chips=2.12

WATER:

Water is an important ingredient of concrete as it actively participates in chemical reaction with cement. Since it helps to form the strength giving cement gel, the quality and quantity of water required to be looked into very carefully. In practice, very often great control on properties of cement and aggregate is exercised, but the control on the quantity of water is neglected. Since the quality of water affects the strength, it is necessary to go into the purity and quality of water.

The various requirements that have to meet by the by the water to be used for construction work-

- ✓ Water should not content sufficient amount of substance that may cause wound in concrete such as silt, oil acid, alkaline, salt of alkaline organic matter and sewage.
- ✓ Water should not contain chloride ion more than 200 ppm.
- ✓ Water should be drinkable.

The following guidelines should be taken into consideration regarding the quality of water-

- ✓ To neutralize 100 ml sample of water using phenolphthalein as an indicator, it should not require more than 5 ml of 0.02 normal NaOH.
- ✓ To neutralize 100 ml sample of water using mixed indicator, it should not require more than 25 ml of 0.02 normal H_2SO_4.

Table-01: Permissible limit for solids as per **IS 456 of 2000**

Material	Maximum Permissible Limit
Organic	200 mg/l
Inorganic	3000 mg/l
Sulphate (as SO_3)	400 mg/l

TYRE DUST:

Properties of rubber mixed concrete are affected by many factors such as

- ✓ Size of rubber used.
- ✓ Rubber surface.
- ✓ Finness of dust used.
- ✓ Fraction of tyre dust used.
- ✓ Matrix property.
- ✓ Mix design.
- ✓ Mixing method.
- ✓ Casting technique.
- ✓ Curing method.

For the experiment it was considered that all the tyre dust must be passed through #4 sieve.

METHODOLOGY

Procedure of Sampling and Use in Laboratory-

- ✓ Initially tyre dust was collected from a tyre recycling factory.
- ✓ In concrete laboratory the dust was cleaned by sieving.
- ✓ Then it was mixed with concrete matrix by various percentages of volume of the components of the mixed composition.
- ✓ Only the amount of tyre dust was varied.
- ✓ Then 61 rubber mixed concrete cylinders were prepared for 0%, 3%, 5% and 7% of tyre dust by volume of concrete, for various ages of curing and various tests.
- ✓ 18 nos. were tested for tensile strength and 12 nos. were tested as plain concrete cylinders out of 58 cylinders.
- ✓ Then test were performed for determining the strength of each cylinder.
- ✓ Finally all the tests data were summarized.

Test program-

The following tests were carried out to evaluate the strength properties of rubberized concrete.

1. Compressive Strength Test.
2. Tensile Strength Test.

Compressive Strength Test: - The compressive strength of concrete specimens was determined after 7 days and 28 days of standard curing. A Universal Testing Machine (UTM) was used to determine the maximum compressive loads carried by various cylinders. The load was applied at a rate of 14 N/mm^2 per minute in accordance with the BS 1881-116:1983 test method.

$$\sigma = F/A$$

Where, σ = Compressive strength, N/mm^2
F= maximum applied load, N
A= cross sectional area of cylinder, mm^2

Tensile Strength Test: - The splitting tensile strength test was determined after 7 days of standard curing period. The tests were carried out by splitting the cylinders in the machine used for compressive strength in accordance with BS 1881-117:1983. The testing machine was fitted with extra bearing bar to distribute the load along the full length of the cylinders. Hardboard strips, 15 mm wide and 4 mm thick was inserted between the cylinder and the testing machine top and bottom bearing surface. From the maximum applied load at failure the splitting tensile strength was calculated as follow.

$$\sigma = \frac{2F}{\pi dl}$$

Where, σ = Compressive strength, N/mm^2
F= maximum applied load, N
l= Length of cylinder, mm
d= Diameter of cylinder, mm

RESULT:

Table-02: Experimental Result

Compressive strength after 7 days						
Amount of tyre dust by volume of concrete	**Sample no.**	**Age (day)**	**Compressive load (N)**	**Compressive strength (N/mm^2)**	**Average compressive strength (N/mm^2)**	**Decrease of strength compared to plain concrete**
0%	1	07	20412	2.52	2.70	-
	2		21772	2.69		
	3		23587	2.91		
3%	1		12701	1.57	1.64	32%
	2		11340	1.40		
	3		15876	1.96		
7%	1		6804	0.84	0.90	55%
	2		4990	0.62		
	3		9979	1.23		
Compressive strength after 28 days						
0%	1	28	27216	3.36	3.30	-
	2		24948	3.08		
	3		28123	3.47		
3%	1		22680	2.80	2.42	27%
	2		15876	1.96		
	3		20412	2.52		
7%	1		18144	2.24	2.00	40%
	2		13608	1.68		
	3		16783	2.07		

Tensile strength after 7 days						
0%	1	07	2722	0.34	0.37	-
	2		3039	0.37		
	3		3311	0.41		
3%	1		3719	0.46	0.42	14%
	2		3583	0.44		
	3		2994	0.37		
7%	1		4853	0.60	0.52	39%
	2		4445	0.55		
	3		3266	0.40		

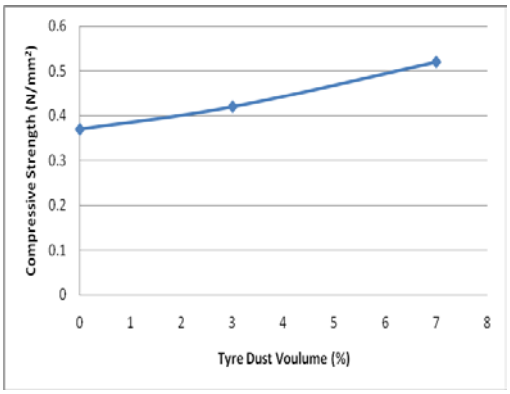

Fig.-01: Tensile Strength of Concrete after 7 days

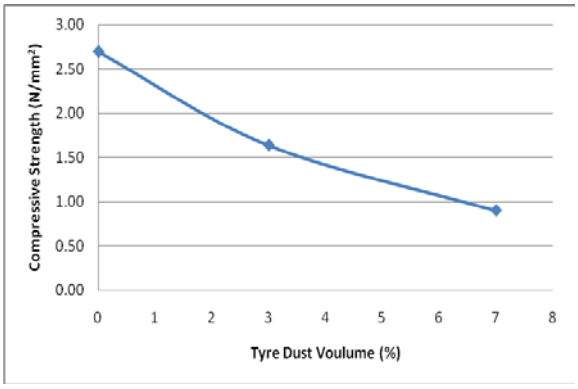

Fig.-02: Compressive Strength of Concrete after 7 days

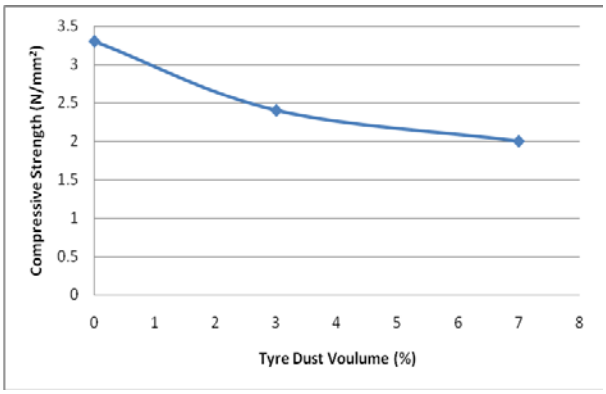

Fig.-03: Compressive Strength of Concrete after 28 days

DISCUSSION

Total 73 nos. rubberized concrete cylinders were prepared using 0%, 3% and 7% tyre dust by volume of concrete. Among which 15 cylinders were prepared for plain concrete i.e. using 0% of tyre dust by volume.

Compressive Strength-

From the test result of tyre dust mixed concrete it was found that the reduction of compressive strength in concrete increased with the increase of the tyre dust volume content. It was observed that the percentage decrease of compressive strength for 3% and 7% tyre dust mixed concrete were 32% and 55% for standard curing period of 7days and 27% and 40% for curing period of 28 days respectively. Thus from the above context, it is evident that there is a decrease in compressive strength with the increase of dust percentage. This strength reduction can be predicted primarily due to the more softness of rubber than the surrounding cement paste. Secondly the bonding between the rubber and the cement paste is highly seems to be week, so that the soft rubber aggregate may be viewed as voids in the concrete mix and voids have not a significant role in the resistance to applied external loading. It has been recognized that, in general, the strength of concrete depends greatly on density, size and hardness of the aggregate.

Tensile Strength-

From the test result of tyre dust mixed with concret it was found that the tensile strength increased with the increase of volume of tyre dust content. It was observed that the percentage increase of tensile strength for 3% and 7% tyre dust mixed concrete were 14% and 39% for curing period of 7 days respectively regarding the plain concrete. Thus from above context, it is evident that there is an increase in tensile strength with the increase of dust percentage.

CONCLUSION

The following conclusion are drawn from the experimental investigation-

1) The compressive strength of concrete with the mix proportion 1:2:4 and w/c=0.4 for curing period of 7 days was found to be 2.70 N/mm^2, whereas the 7 days compressive strength of concrete using 3% and 7% of tyre dust were 1.64 N/mm^2 and 0.90 N/mm^2 respectively.
2) The tensile strength of concrete with the mix proportion 1:2:4 and w/c=0.4 for curing period of 7 days was found to be 0.37 N/mm2, whereas the 7 days tensile strength of concrete using 3% and 7% of tyre dust were 0.42 N/mm^2 and 0.52 N/mm^2 respectively.
3) For the tyre dust mixed with concrete the compressive strength of concrete decrease with the increase of tyre dust percentage by volume of concrete, on the other hand the tensile strength of rubberized concrete increase with the increase of tyre dust percentage by volume of concrete.

REFERENCES

1. Siddique R, Naik TR. Properties of concrete containing scrap-tyre rubber – an overview. Waste Manage 2004;24(5):563–9.
2. Herna´ndez-Olivares F, Barluenga G, Bollati M, Witoszek B. Static and dynamic behaviour of recycled tyre rubber-filled concrete. Cement Concr Res 2002;32(10):1587–96.
3. Herna´ndez-Olivares F, Barluenga G. High strength concrete modified with solid particles recycled from elastomeric materials. In: Ko¨nig G, Dehn F, Faust T, editors. Proceedings of the 6th international symposium on high strength/high performance, Leipzig, Germany, 2002. p. 1067–77.
4. Herna´ndez-Olivares F, Barluenga G. Fire performance of recycled rubber-filled high-strength concrete. Cement Concr Res 2004;34(1):109–17.
5. Westergaard HM. Stresses in concrete pavements computed by theoretical analysis, public roads, US Department of Agriculture, Bureau of Public Roads 1926;7(2).
6. American Association of State Highway and Transportation Officials (AASHTO). guide for design of pavement structures. Edition 1993.
7. Ramsamooj DV, Lin GS, Ramadan J. Stresses at joints and cracks in highway and airport pavements. Eng Fract Mech 1998;60(5–6): 507–18.

8. Bollati MR, Talero R, Rodrı´guez M, Witoszek B, Herna´ndez F. Porous high performance concrete for road traffic. In: Dhir RK, Henderson NA, editors. Concrete for infrastructure and utilities.London: E&FN Spon; 1996. p. 589–99.
9. Pindado MA, Aguado A, Josa A. Fatigue behaviour of polymermodified porous concretes. Cement Concr Res 1999;29(7):1077–86.
10. Lee MK, Barr BIG. An overview of the fatigue behaviour of plain and fiber reinforced concrete. Cement Concr Compos 2004;26(4): 299–305.
11. Balaguru PN, Shah SP. Fiber-reinforced cement composites. New York: MacGraw-Hill; 1992.
12. Young WC. Roark's formulas for stress and strain [Rev. ed. of: Raymond J. Roark. Formulas for stress and strain, 5th ed., 1975]. 6th ed. New York: McGraw-Hill; 1989. pp. 473–474 (Table 26).
13. Hahn J. Vigas continuas, po´ rticos, placas y vigas flotantes sobre terreno ela´stico, Gustavo Gili Si.A., Barcelona, Spain, 1982 (in Spanish, from: J. Hahn, ''Durchlauftra¨ger, Rahmen, Platte und Balken auf elastischer Bettung'', Werner-Verlag, Du¨ sseldorf, Germany, 13th ed., 1981 in German).
14. Waddell WH, Evans LR. Use of nonblack fillers in tire compounds. Rubber Chem Technol 1996;69(3):377–423.

ID : ASEE 017

1st International Conference on Advances in Civil Engineering 2012 (ICACE 2012)
12 –14 December 2012
CUET, Chittagong, Bangladesh

VARIATION OF COMPRESSIVE STRENGTH VALUE BETWEEN FRESH FINE AGGREGATE CONCRETE AND OLD FINE AGGREGATE CONCRETE

MD. ASSADUZZAMAN[1*], MD. N. ISLAM[1], M. H. RASHID[2] & MD. M. HOSSAIN[2]

[1]Department of Civil Engineering, America Bangladesh University (ABU), Dhaka, Bangladesh*
asad_kuet06@yahoo.com
[1]Trust Alliance Technology Ltd, Dhaka-1212, Bangladesh
nazrulnasad@gmail.com,
[2]Department of Civil Engineering, Khulna University of Engineering &Technology (KUET), Khulna, Bangladesh
hafin02@yahoo.com,drmonjur@yahoo.com

ABSTRACT

Increasing shortage of natural aggregates for concrete in the construction field leads to a search for aggregates from new sources. This paper examines the use of crushed concrete fines produced from demolished concrete waste as fine aggregate in concrete. Tests were carried out to study the properties of recycled fine aggregate and compared their properties corresponding to Fresh fine aggregates. Natural fine aggregate in concrete was replaced with 10%, 20%, 30% of crushed brick and stone aggregates demolished concrete waste. For strength characteristics, the results showed a gradual decrease in compressive strength, as the percentage of recycled fine aggregate used in the specimens increased. Fresh cement in concrete was replaced with 10%, 20%, 30% of crushed brick and stone dust. For strength characteristics, the results showed a gradual decrease in compressive strength, as the percentage of crushed brick and stone dust used in the specimens increased. Fresh cement in concrete was replaced with 5%, 10%, and 15% of crushed Lime dust. For strength characteristics, the results showed a gradual decrease in compressive and tensile strength, as the percentage of Lime dust used in the specimens increased. It has been found that the detrimental effects of using crushed concrete fines and dust in concrete can be mitigated by a partial replacement of crushed concrete fines and dust.

Key-words: Aggregate; Compressive strength; Demolished concrete; Fresh cement

INTRODUCTION

Recycling of demolition and construction materials is not a recent strategy, It was known in the first few years after the second world war. In this period, the mineral materials, especially the bricks, were processed to be used in concrete production and the research works on the use of the bricks as concrete aggregates rapidly increased. Due to the interest in keeping the environment clean and to reserve the natural aggregates, the concentration on the recycling technology started at the end of the seventeenth years of the last century and continued until now. Waste arising from construction and demolition constitutes is one of the largest waste streams in the world large proportion of potentially useful material disposed of as landfill. In recent years, research and study on the utilization of this waste material is going on. The environmental and economic implications of this waste are no longer considered sustainable and as a result, the construction industry is experiencing more pressure than ever before to overcome this practice. On the other hand, in recent years the wisdom of continued wholesale extraction and use of aggregates from natural resources has been questioned at an international level. This is mainly because of the depletion of quality primary aggregates and greater

awareness of environmental protection. About 4.5 billion tons concrete consumed a year in the world. In every year approximately 50 million tons of concrete are discarded in the Europe, 60 million in USA, 20 million in Japan. Recycling concrete is becoming an increasingly popular way to utilize aggregates left behind when structures are demolished. In the past, this rubble was disposed of in landfills, but with more attention being paid to environmental concerns, concrete recycling allows reuse of the rubble while also keeping construction costs down. When structures made of concrete are demolished or renovated, concrete recycling is an increasingly common method of utilizing the rubble. Recycling has a number of benefits that have made it a more attractive option in this age of greater environmental awareness, more environmental laws, and the desire to keep construction costs down. There are also other economic and engineering benefits. Economic Factors: For demolition contractors landfill space is scarce, especially in urban areas. Some landfills may not accept construction materials and disposal of old concrete and masonry is costly. Furthermore, the cost and transport distances of fresh aggregates could continue to increase as sources grow scarce. With recycled aggregates there is potential for cost savings in hauling.

Chen, H.J., Yen, T. and Chen, K.H. (2003), conducted a study on "The Use of Building Rubbles in Concrete and Mortar". The main components of building rubble collected from demolished structures are waste concrete, brick and tile. A series of experiments using recycled aggregates of various compositions from building rubble were conducted. The test results (the slump test, air content, unit weight, and setting time) showed that building rubble can be transformed into useful recycled aggregate through proper processing. When the recycled aggregate was washed, the negative effects of absorption capacity on the recycled concrete were greatly reduced. This effect is especially meaningful for flexural strength.

Dosho, Y. (2007), conducted a study on "Development of a Sustainable Concrete Waste Recycling System". The generation of huge amounts of construction waste was anticipated due to the demolition of older structures such as power station built more than 30 years ago. On the other hand, the reuse of construction waste is highly essential from the view point of Life Cycle Assessment and effective recycling of construction resources. In order to promote the reuse of construction waste, it is necessary to achieve three basic concepts (1) assurance of safety and quality, (2) decrease of environmental impact, (3) increase of cost effectiveness of construction..Result of this study showed that recycle aggregate concrete using the aggregate replacing method can acquire sufficient quality as structural concrete and precast concrete products through material design based on the value of relative quality method.

Chen, H.J., Yen, T. and Chen, K.H. (2007), conducted a study on "Use of building rubbles as recycled aggregates". The application of building rubble collected from damaged and demolished structures is an important issue in every country. After crushing and screening, this material could serve as recycled aggregate in concrete. A series of experiments using recycled aggregate of various compositions from building rubble was conducted. The test results showed that the building rubble could be transformed into useful recycled aggregate through proper processing. Using unwashed recycled aggregate in concrete will affect its strength.

Sagawa, Y., Matsushita, H. and Kawabata, Y. (2007), conducted a study on "Development of a Sustainable Concrete Waste Recycling System". In this study, the strength and the carbonation speed of the mortar incorporating recycled fine aggregate were examined. Strength and carbonation speed could be evaluated by total water-cement ratio, which was obtained by summation of water content and total water absorbed in aggregate. Pore volume between 50nm and 2μm in new cement matrix phase was porous and loose when recycled fine aggregate with high water absorption was used in mortar. Performance of mortar incorporating recycled fine aggregate correlated closely with pore volume between 50nm and 2μm in new cement matrix phase. It was suggested that water included in recycled aggregate moved to new cement matrix phase during cement hydration.

Tempest, H., Cavallies, T., Gergely, J. and Weggel, D. (2010), conducted a study on "Construction and Demolition Waste used as Recycled Aggregates in Concrete". The use of crushed construction and demolition waste as a recycled aggregate in the production of new concrete has been successfully demonstrated by researchers as well as by practitioners in the field. In expanding urban areas, the intensive construction of new infrastructure, as well as rehabilitation and retrofitting of existing infrastructure, opens many potential markets for recycled aggregate concrete produced in various grades, including non-structural landscaping, pavements and even structural applications. The goal of

this study was to show that use of recycled aggregates in concrete is both economically viable and technically feasible.

Kumutha, R. and Vijai, K. (2010), conducted a study on "Strength of Concrete Incorporating Aggregate Recycled from Demolition Waste". The properties of concrete containing recycled aggregates were investigated. Recycled aggregates consist of either crushed concrete or crushed bricks from the demolition wastes available locally. Laboratory trials were conducted to investigate the possibility of using recycled aggregates as the replacement of natural coarse aggregates or fine aggregates in concrete. A series of tests were carried out to determine the density, compressive strength, split tensile strength, flexural strength and modulus of elasticity of concrete with and without recycled aggregates. Natural coarse aggregates in concrete was replaced with 0%, 20%, 40%, 60%, 80% and 100% of crushed concrete aggregates. Natural fine aggregate in concrete was replaced with 0%, 20%, 40%, 60%, 80% and 100% of crushed brick aggregates. For strength characteristics, the results showed a gradual decrease in compressive strength, split tensile strength, flexural strength and modulus of elasticity as the percentage of recycled aggregate used in the specimens increased.

Parekh D. N. and Dr. Modhera C. D. (2011), conducted a study on "Assessment of Recycled Aggregate Concrete". Use of recycled aggregate in concrete can be useful for environmental protection and economical terms. Recycled aggregates are the materials for the future. The application of recycled aggregate has been started in many construction projects in many European, American and Asian countries. This paper reports the basic properties of recycled fine aggregate and recycled course aggregate. It also compares these properties with natural aggregates. Basic concrete properties like compressive strength, flexural strength, workability etc were also explained for different combinations of recycled aggregate with natural aggregate. However, further work is needed to gradually develop the much wanted knowledge base and the necessary tools for the industry to be able to use these resources routinely and with confidence. Significant steps are being taken to improve the quality of RA and new standards are easing its use in higher value applications.

The main objectives of this study are given below:

(i) To compare the properties of fine aggregate obtained from demolished concrete made of brick and stone; and the dust obtained from demolished lime concrete.
(ii) To check the suitability of fine aggregate from materials of demolished concrete.

MATERIALS AND METHODOLOGY

The sample of brick aggregate concrete was collected from academic building of IEM, CSE, and ECE in KUET. Sample of stone concrete was collected from concrete of crushed cylinder of engineering material lab of civil department, Khulna. The sample of lime aggregate concrete was collected from Fazlul Haque Hall. The demolished concrete was taken to concrete laboratory for study. It was crushed manually. It was hard job to separate of fine aggregate from concrete. The concrete was broken by hammer (1.25 kg) to smaller size and then broken to aggregate (using 0.25 kg hammer).It was then screened by standard sieve. Material passing through #4 sieve and retained on #100 sieve was taken. For further test for fine aggregate similarly samples fine aggregate was obtained from stone aggregate concrete and lime concrete shown in Figure 1. For all the three samples passing through #200 sieves was also collected and study. After separation the coarse aggregate and fine aggregate the following test i.e. unit weight, specific gravity is performed in laboratory.

Fig. 1. Sample of prepared fine aggregate from A) brick aggregate concrete B) stone aggregate concrete and C) lime aggregate concrete

Cement particle is heterogeneous substance, containing tri-calcium silicate (C_3S), di-calcium silicate (C_2S), tri-calcium aluminate (C_3A), and solid solution described as tetra-calcium alumino-ferrite (C_4AF). Di-calcium silicate (C_2S) is responsible for the progressive strength of cement. The basic ingredients of cement used in this study obtained from routine laboratory test are given in Table 2. In general the potable water is also satisfactory for concrete. The basic properties of water is evident in Table 3.The used sand in this study is free from silt, clay and organic matter through performed test.

Table 2: Physical properties of cement used in this study

Physical properties	Values
Normal consistency (%)	22.40
Initial setting time	2 hours 10 minutes
Final setting time	4 hours 50 minutes
Fineness (%)	0.60

Table 3: Basic Properties of used water

Properties	Value
P^H	7.58
Cl^-	435 mg/lit
Fe	0.0 mg/lit
Color	0.31 mg/lit
TDS	650 mg/lit

In the laboratory, the specific gravity and unit weight test are performed of fine aggregate obtained from demolished brick and stone aggregate concrete that are shown in Table 3.

Table 4: Specific gravity and unit weight value of fine aggregate

Type and source of fine aggregate	Specific gravity	Unit weight (kg/m^3)
Obtained from demolished brick aggregate concrete	2.50	1274
Obtained from demolished stone aggregate concrete	2.46	1287
Fresh fine aggregate	2.59	1876

Compressive strength was performed on cubic specimens 2×2×2 inch. Mixing ratio of mortar cement: sand= 1:2.75. In this test sample preparation recycle brick/stone/lime dust and fine aggregate obtained from demolished brick aggregate concrete, demolished stone aggregate concrete and lime concrete. Brick/stone fine aggregate are used with pure sand and brick /stone dust are used with cement at different percentage (10, 20, 30 and 100%). Lime dust is used with cement at 5, 10 and 15 %. The cube and its base must be clamped together during cube making in order to prevent leakage of mortar. Before assembling the cube, its mating surfaces should be covered with mineral oil to the inside surfaces of the mould in order to prevent the development of bond between the cube and the mortar. After mixing, the cube were filled with mortar and compacted and removing the excess mortar by sawing. Remolding was realized after 24 hours and the specimens were cured under water till 7 days age. Then the specimen is tested to determine the compressive strength cube specimen.

RESULTS AND DISCUSSION

The effect of recycled brick /stone /lime fine aggregate and dust at different mixing proportion with pure sand and cement on compressive strength as well as the laboratory on the basis of 2x 2 x 2 inch block testing that was prepared in the laboratory were analyzed and discussed in hence following.

Variation of compressive strength between fresh fine aggregate and recycled brick/stone fine aggregate at different percentage with pure sand

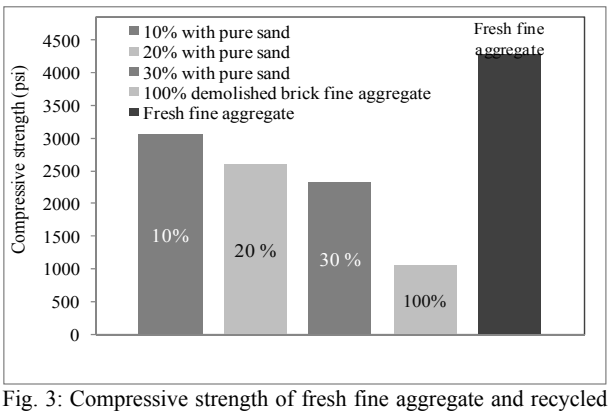

Fig. 3: Compressive strength of fresh fine aggregate and recycled brick fine aggregate at different percentage with pure sand

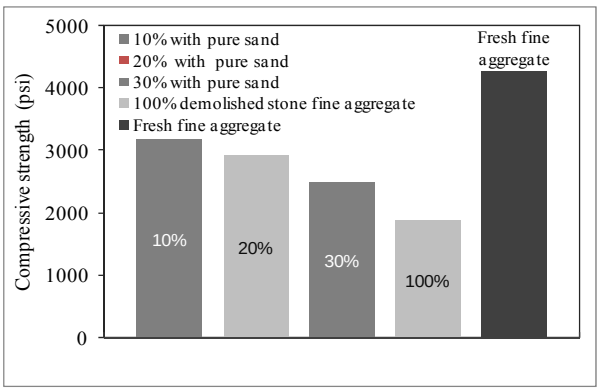

Fig. 4: Compressive strength of fresh fine aggregate and recycled stone fine aggregate at different percentage with pure sand

The Figure 3 and Figure 4 describe the compressive strength (psi) of brick /stone fine aggregate at ifferent % with pure sand and also show the compressive strength (psi) of fresh fine aggregate. Recycled brick and stone fine aggregate obtained from demolished brick aggregate concrete and stone aggregate concrete. Natural fine aggregate in concrete is replaced by 10%, 20%, 30% and 100% of crushed brick and stone aggregates demolished concrete waste. With the increasing of replacing % of recycled brick/stone fine aggregate with pure sand, the value of compressive strength decrease gradually. Figure 4 i.e. used fine aggregate obtained from stone aggregate concrete in mortar shows slightly more compressive strength (psi) then Figure 3.

Variation of compressive strength between fresh fine aggregate and recycled brick/stone/lime dust at different percentage with cement

Here, fresh cement in mortar is replaced by 10%, 20%, 30% of crushed brick and stone dust.
The Figure 5 and Figure 6 describe the compressive strength (psi) of block from brick and stone dust at different % with cement and also show the compressive strength (psi) of fresh fine aggregate .Fresh cement in mortar was replaced with 5%, 10%, and 15% of crushed lime dust that are shown in figure 7. Figure 5 to 6 shows that with the increasing of replacing percentage recycled brick/stone/lime dust with cement in mortar, the value of compressive strength (psi) decreases significantly. Figure 7 also show that cement is replaced by lime dust in mortar shows more strength then recycled brick and lime dust. Fresh fine aggregate shows more compressive strength compared brick/lime/lime dust used as replacing of cement in mortar.

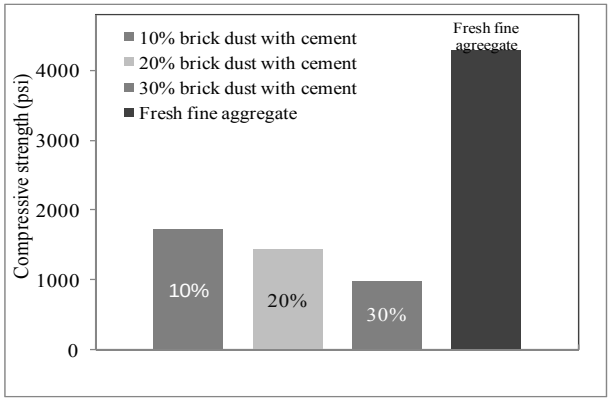

Fig. 5: Compressive strength of fresh fine aggregate and recycled brick dust at different percentage with cement

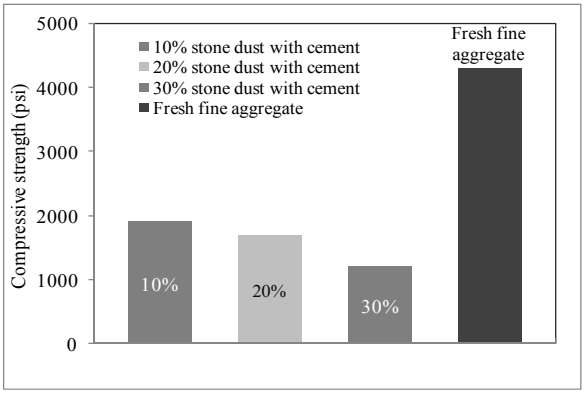

Fig. 6: Compressive strength of fresh fine aggregate and recycled stone dust at different percentage with cement

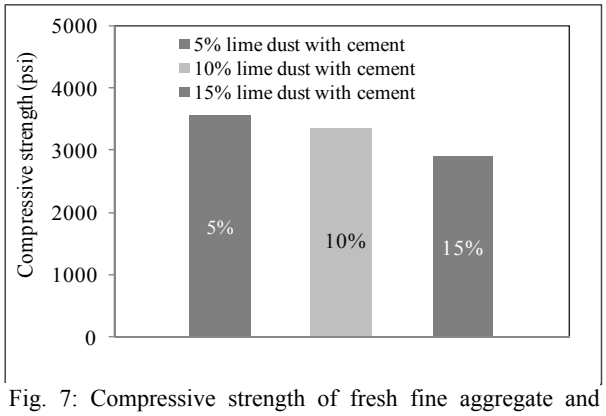

Fig. 7: Compressive strength of fresh fine aggregate and recycled lime dust at different percentage with cement

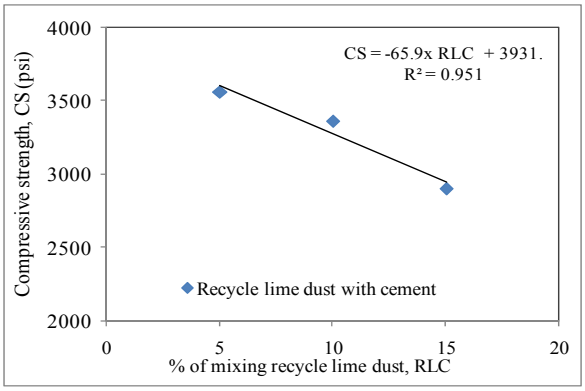

Fig. 8: Compressive strength of recycle lime dust at different percentage (%) mixing proportion with cement

Compressive strength at different percentage (%) mixing proportion of recycle brick /stone/lime dust obtained from demolished brick/stone/lime concrete

With the increasing of mixing percentage the recycle brick/stone/lime dust with cement, Figure 8 ~ 10 the value of compressive strength (psi) decreases gradually. Among the Figure 8 ~10, Figure 8 shows the compressive strength decreases rate are less than brick and stone dust. Here lime dust act as a helping material for cement that act as a binding material. On the basis of co-relation coefficient (R^2) value, lime dust (R^2=0.951), brick dust (R^2= 0.985) and stone dust (R^2=0.785) are nearly 1.

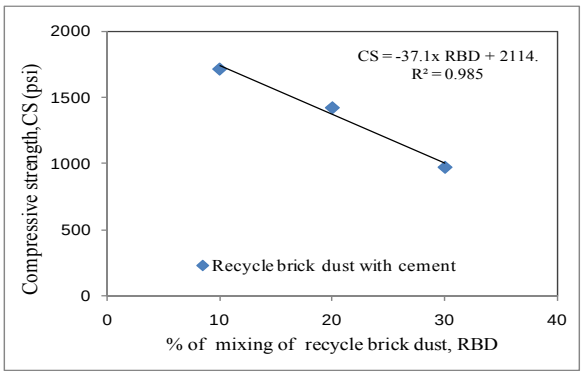

Fig. 9: Compressive strength of recycle brick dust at different percentage (%) mixing proportion with cement

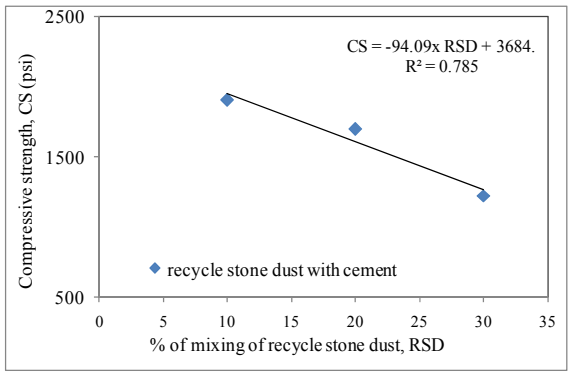

Fig.10: Compressive strength of recycle stone dust at different percentage (%) mixing proportion with cement

CONCLUSION

Through the experimental result and analysis deals with the compressive strength of mortar and Engineering properties of recycled coarse aggregate and fine aggregate obtained from demolished concrete.

- ✓ Adding recycled fine aggregate in the mortar will decrease the compressive strength of cube specimen. The quantity of recycled fine aggregate in the mortar is more effective than the water/ cement ratio in governing the percentage reduction in strength for recycled mortar.
- ✓ This is totally different from the behavior of recycled coarse aggregate in recycled concrete. The quality (unit weight, specific gravity) of the recycle fine aggregates are lower than their corresponding fresh fine aggregates.
- ✓ The less strength of recycle concrete can be used in less important work like as short slab, drainage cover etc. The recycle fine aggregate can be used in construction op to 20 % perfectly but dust is not suitable & the dust of the recycle lime can be used in construction up to 15 %.
- ✓ The recycled fine aggregate is used in the fields such as Noise protection barriers, frost protection course, hydraulic bound base course, plaster sand and shoulder stabilization, concrete kerb and gutter mix, granular base course materials, embankment fill materials, paving blocks, backfill materials and building blocks.

REFERENCES

Annual books of ASTM standards.199. *Concrete & aggregate* section 4, vol-04.02, , publication code (pcn) :01-040297-07.

Hansen, T. C. 1986. *Recycled aggregates and recycled aggregates concrete second state-of-the-art report developments 1945-1985*. Materials and Structures, V. 1, no. 111. Springer Netherlands. pp. 201-246.

Neville, A.M. (1996). *Properties of concrete*. Essex CM20, England.

U.S. Army corps of engineers. *Laboratory soils testing*. EM 1110-2-1906, Appendix V: Grain-size analysis.

Chen, H.J., Yen, T. and Chen. K.H. 2007.The use of building rubbles in concrete and mortar, *Journal of the chinese institute of engineers*, Vol. 26, No. 2, pp. 227-236.

Dosho, Y. 2007. Development of a sustainable concrete waste recycling system. *Journal of advanced concrete technology*. Vol. 5, No. 1, pp. 27-42.

Parekh,D. N. and Dr. Modhera C. D. 2011. Assessment of recycled aggregate concrete. *Journal of engineering research and studies*, Vol. II, E-ISSN 0976-7916.

Kumutha, R. and Vijai, K. 2010. Strength of concrete incorporating aggregate recycled from demolition waste. *ARPN journal of engineering and applied Sciences* ,VOL. 5, NO. 5.

Sagawa, Y,. Matsushita, H. and Kawabata, Y. 2007. Microstructure of new cement matrix phase and performance of mortar incorporating recycled fine aggregate. *International seminar on durability and lifecycle evaluation of concrete structures*, Japan.

ID : ASEE 021

1st International Conference on Advances in Civil Engineering 2012 (ICACE 2012)
12 –14 December 2012
CUET, Chittagong, Bangladesh

DEM BASED SIMULATION OF A PARTICULATE SYSTEM UNDER AXIAL EXTENSION

M. M. SAZZAD[1*]

[1] *Department of Civil Engineering, Rajshahi University of Engineering & Technology (RUET), Rajshahi-6204, Bangladesh, <mmsruet@gmail.com>*
**Corresponding Author*

ABSTRACT

The aim of current paper is to present the DEM-based simulated results of a particulate system under axial extension test condition using the three-dimensional discrete element method (DEM). Two cubical shaped numerical samples, having different porosities, were prepared to carry out the numerical simulations. Spherical shaped particles were first randomly generated in a cubical frame. The samples generated in this way were compressed isotropically to 100 kPa such that the unbalanced force at the end of isotropic compression remained fairly small. Axial extension tests were conducted under strain controlled condition keeping the stresses in lateral directions constant. The digital data were recorded at regular interval to perform post processing works. The simulated results depict that the stress-strain-dilative responses are consistent to that observed in the experimental studies qualitatively. The evolution of dilatancy index depicts no unique characteristic. Normalized work (normalized by mean stress) is also not unique for different porosities of the numerical samples tested under axial extension condition.

Keywords: Axial Extension, Simulation, DEM, Dilatancy Index.

INTRODUCTION

Granular material such as sand behaves differently when the stress path is different. For example, the internal friction angle in case of plane strain compression is larger than that of conventional triaxial compression (Conforth, 1964; Targaghi et al., 1996). The behaviour of granular material is also different when the axial extension (tension) stress path is used. Experimentally, the behaviour of soil under extension tests has been reported (e.g., Al-Husssaini, 1981; Berdie, 1991). These studies depict that the stress ratio decreases with strain in case of extension tests. These behaviours can also be studied numerically using the discrete approach. Recently, discrete element method (DEM) (Cundall and Strack, 1979) has been used widely as a discrete approach. It is a numerical tool which can be effectively utilised to simulate the behavior of granular material. The major advantage of DEM is that it offers the capability of monitoring the behaviour of granular materials at any stage of simulation. Although other stress paths such as plane strain compression, conventional triaxial compression etc. has been studied extensively in both experimental and numerical studies (e.g., Ochiai and Lade, 1983; Alshibli et al., 2003) ; however, the simulation of the behaviour of granular material under axial extension stress path using the particulate approach DEM is very rare (e.g., Ng, 2004). Consequently, axial extension stress path has been considered in the current study. Two cubical samples having different porosities have been numerically prepared and subjected to axial extension test. The

numerical simulation data are qualitatively validated with the experimental tendencies to warrant the versatility of the simulated results using DEM.

ABOUT DEM AND YADE

The current numerical simulations were carried out using the numerical method DEM proposed by Cundall and Strack (1979). The basic idea of DEM is very simple and straight forward. Each particle in the model sample is considered to be an element and each element can make and break contact with its neighbour particles. The particles in the model sample can move and rotate. It uses an explicit numerical scheme. Newton's second law of motion is used to calculate the accelerations of the particle and the double integration of the acceleration gives the displacement of the particle. The incremental displacement is then calculated and used in the force displacement law to compute the force exerted on each particle and thus the cycle continues for the next step. The details of DEM are discussed in Cundall and Strack (1979). The accelerations of the particles are calculated as follows:

$$m\ddot{x}_i = \sum F_i \qquad i = 1,3 \tag{1}$$

$$I\ddot{\theta} = \sum M \,, \tag{2}$$

where F_i are the force components on each particle, M is the moment, m is the mass, I is the moment of inertia, $\ddot{x}_i$ are the components of translational acceleration and $\ddot{\theta}$ is the rotational acceleration of the particle.

The numerical simulation was carried out using YADE; an open source code based on DEM. YADE is written in C++ with Object Oriented Programming techniques and consists of softwares, libraries and necessary plug-ins. The code is capable of modelling 3D DEM based problems. It runs on Linux platform. YADE provides a common framework for all users and increases its capability to couple different simulation algorithms. YADE has graphical user interfaces. A Coulomb type friction criterion is used to reproduce the behaviour of cohesionless geomaterials. The rolling resistance is incorporated; the major reason of which is to introduce the roughness of grains missing in spheres. For details of YADE, readers are referred to Kozicki and Donze (2008).

SAMPLE PREPATION METHOD

In DEM, preparation of sample generally consists of two phases; namely sample generation and sample preparation. In the first phase, 3896 spheres were randomly generated in a cubical frame such that the particles were not in contact with each other. The radius of randomly generated spheres varied from 2.09 to 2.83 cm. In the current study, spheres represent the particles and the roughness of the particles is ensured by applying the rolling resistance under a certain condition. Use of spheres as particles in the model sample reduces the computational cost of the simulation. In the second phase, the sample is isotropically compressed to 100 kPa using rigid boundaries all around such that the unbalanced force at the end of isotropic compression remains fairly small. This ensures the accuracy of the simulated data. Two types of samples were prepared: (i) dense sample and (ii) loose sample. To prepare the dense sample, the interparticle friction angle was set to 0.5 degree and compressed isotropically. A smaller value of the interparticle friction angle ensures the making of a dense sample. When the sample became compact enough, the isotropic compression was halted and an interparticle friction angle of 26.5 degree was assigned for the second phase of isotropic compression. By contrast, the interparticle friction angle was set to 26.5 degree to prepare the loose sample in both the phases of isotropic compression. The porosities of the isotropically compressed dense and loose samples are 0.387 and 0.436, respectively. The configurations of the isotropically compressed dense and loose samples are depicted in Fig. 1.

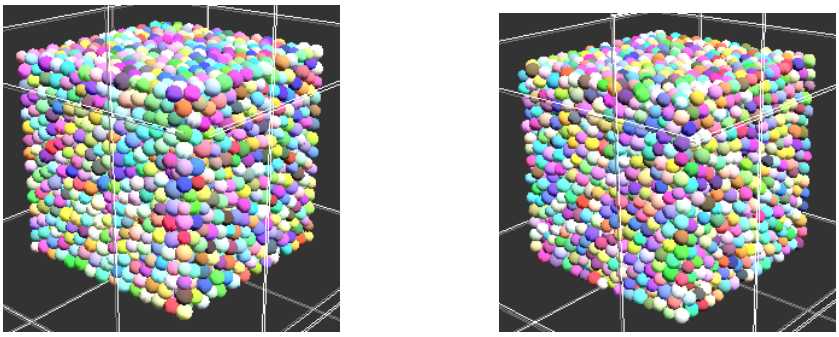

Dense sample (n =0.387) Loose sample (n =0.436)

Fig. 1 Configurations of the isotropically compressed dense and loose samples

NUMERICAL SIMULATIONS

The numerical simulations were carried out under strain controlled loading condition. Axial extension tests were conducted by moving the top and bottom platens upward and downward, respectively with a very small strain rate of 0.1 by keeping the confining pressure 100 kPa in other four boundaries. The simulation condition of the axial extension test is depicted in Fig. 2 for clarity. The DEM parameters used in both the numerical simulations are shown in Table 1. During the simulation, care has been taken so that the unbalanced force remains small.

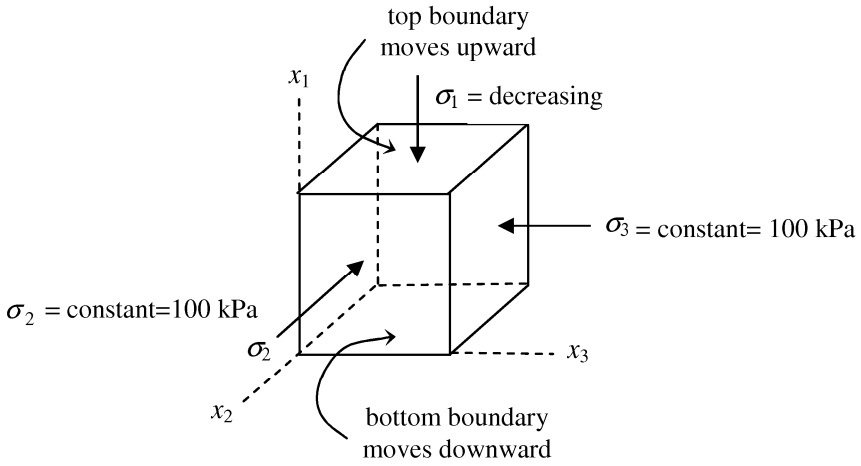

Fig. 2 Simulation condition of axial extension test

Table 1 DEM parameters used in the simulations

DEM parameters	**Value**
Young's Modulus (MPa)	60
Stiffness ratio (K_s/K_n)	0.50
Mass density (Kg/m^3)	2600
Inter particle friction angles (degree)	0.5, 26.50
Damping coefficients	0.20

RESULTS AND DISCUSSION

During the simulations, the digital data are recorded at regular interval. The digital data are then analyzed and results are reported in the following sections.

Stress-strain-dilative Responses

The stress-strain response for different porosities of the samples under axial extension test condition is depicted in Fig. 3. A negative value of strain indicates extension, while a positive value indicates compression. It is noted that the stress ratio gradually decreases as the axial strain increases. The decrease in the stress ratio is dominant for dense sample (n = 0.387). The simulated stress-strain results are qualitatively similar to that observed in experimental studies (e.g., Usmani et al., 2011). This demonstrates the versatility of the current simulated results. The relationship between the axial strain ε_1 and the lateral strain ε_3 is depicted Fig. 4. Note that the movement of the lateral boundaries in inward directions are dominant for loose sample (n = 0.436) than dense sample (n = 0.387). The evolution of volumetric strain ε_v with the axial strain ε_1 is depicted in Fig. 5. Volumetric strain is defined here as $\varepsilon_v = \varepsilon_1 + \varepsilon_2 + \varepsilon_3$, where ε_1, ε_2 and ε_3 are the strains in x_1-, x_2- and x_3- direction, respectively. A positive value of ε_v indicates compression, while a negative value indicates dilation. Note that dilation prevails in dense sample (n = 0.387), while compression prevails in loose sample (n = 0.436).

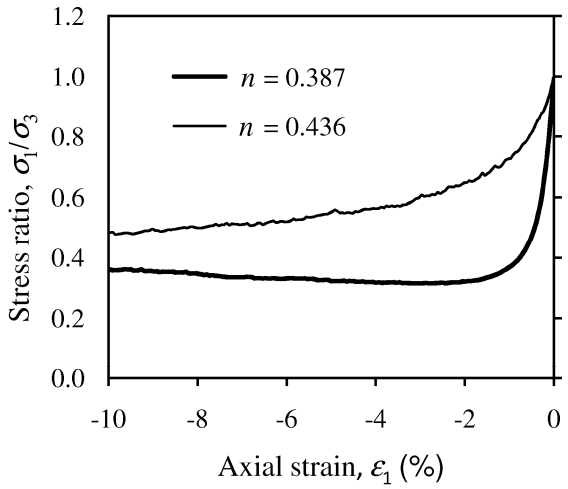

Fig. 3 Stress-strain response for different porosities of the samples under axial extension test

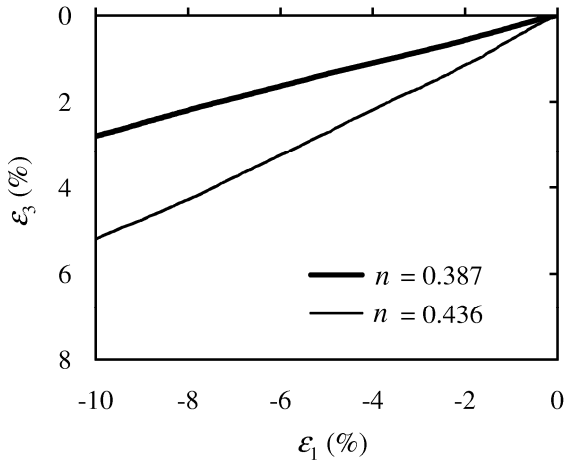

Fig. 4 Relationship between ε_1 and ε_3 for different porosities of the samples under axial extension

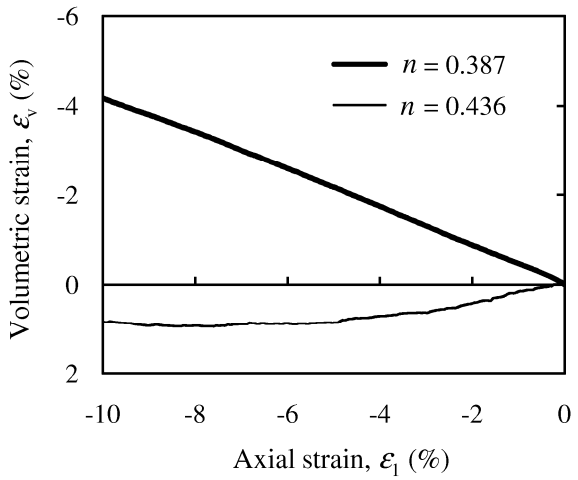

Fig. 5 Relationship between ε_1 and ε_v for different porosities of the samples under axial extension

Dilatancy Index

The evolution of dilatancy index with axial strain ε_1 is depicted in Fig. 6. Dilatancy index is defined here as $DI = -d\varepsilon_v / d\varepsilon_1$, where $d\varepsilon_v$ is the change in the volumetric strain and $d\varepsilon_1$ is the change in axial strain, respectively. A positive value of dilatancy index indicates compression, while a negative value indicates dilation. Note that the evolution of dilatancy index depicts no unique characteristic even at large strain.

Normalized Work

The evolution of normalized work with axial strain ε_1 is also examined in the current simulation and depicted in Fig. 7. Normalized work is computed by normalizing the total work by the mean stress $p\,[=(\sigma_1+\sigma_2+\sigma_3)/3]$ and defined as $W_n = W/p$, where W is the total work and defined as $W = \sigma_1 d\varepsilon_1 + \sigma_2 d\varepsilon_2 + \sigma_3 d\varepsilon_3$. It should be noted that the normalized work is not unique for different porosities of the samples simulated under axial extension condition.

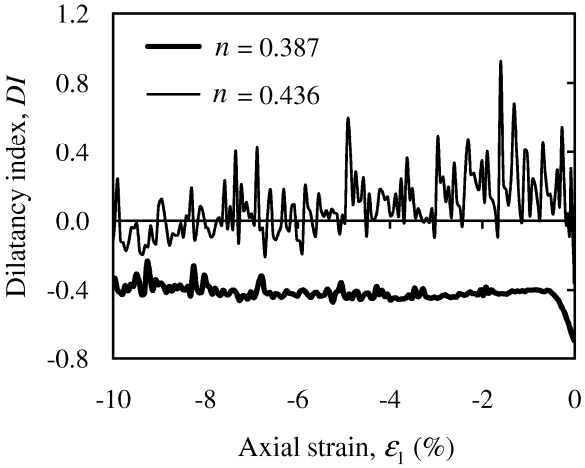

Fig. 6 Relationship between axial strain ε_1 and dilatancy index DI for different porosities of the samples under axial extension test

.

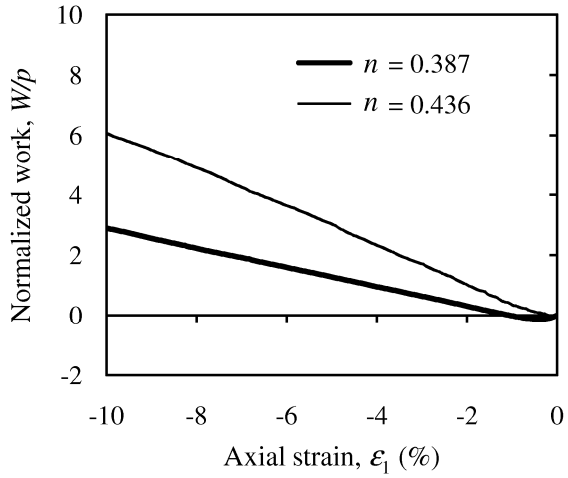

Fig. 7 Evolution of normalized work with ε_1 for different porosities of the samples under axial extension test

CONCLUSIONS

Numerical simulation was carried under axial extension test condition for different porosities of the numerical samples using DEM. It is noted that the stress-strain-dilative responses are consistent to that observed in the experimented studies. This reveals the versatility of the current simulated results using DEM. The dilatancy index depicts no uniqueness even at the large strain. The normalized work also depicts no uniqueness for different porosities of the samples simulated under axial extension test condition.

LIST OF REFERENCES

Al-Hussaini, MM. 1981. *Tensile properties of compacted soils in laboratory shear strength of soils*. ASTM STP 740, RN Yong and FC Townsend (Eds), pp. 207–225.

Alshibli, K; Batiste, S and Sture, S. 2003. Strain localization in sand: plane strain versus triaxial compression. J. *Geotech. Geoenviron. Eng*., 129(6): 483–494.

Berdie, EK. 1991. Triaxial tension tests on compacted kaolin. *J. Geotech. Engrg.*, 22: 121–141.

Cornforth, DH. 1964. Some experiments on the influence of strain conditions on the strength of sand. *Geotechnique*, 14(2): 143–167.

Cundall, PA and Strack, ODL. 1979. A discrete numerical model for granular assemblies. *Geotechnique*, 29(1): 47-65.

Koziki, J and Donze, FV. 2008. A new open-source software developed for numerical simulations using discrete modeling methods. *Computer Methods in Applied Mechanics and Engineering*, 197(49-50): 4429–4443.

Ng, T-T. 2004. Macro- and micro-behaviors of granular materials under different sample preparation methods and stress paths. *Int. J. Solids Struct.*, 41(21): 5871-5884.

Ochiai, H and Lade, P. 1983. Three-dimensional behavior of sand with anisotropic fabric. *J. Geotech. Engrg.*, 109(10): 1313–1328.

Terzaghi, K; Peck, RB and Mesri, G. 1996. *Soil mechanics in engineering practice*. New York: JohnWiley & Sons.

Usmani, A; Ramana, G and Sharma, K. 2011. Experimental evaluation of shear-strength behavior of Delhi silt under static loading conditions. *J. Mater. Civ. Eng.*, 23(5): 533–541.

ID : ASEE 024

1st International Conference on Advances in Civil Engineering 2012 (ICACE 2012)
12 –14 December 2012
CUET, Chittagong, Bangladesh

NONLINEAR DYNAMIC ANALYSIS OF RC BRIDGE RAILING SUBJECTED TO VEHICULAR IMPACT

S. SUSMITA[1*] & I. ANAM[2]

[1] *Department of Civil Engineering, University of Asia Pacific, Dhaka, Bangladesh, saiqamustari@yahoo.com*
[2] *Department of Civil Engineering, University of Asia Pacific, Dhaka, Bangladesh, iftekhar@uap-bd.edu*

ABSTRACT
The paper presents the structural response of a reinforced concrete bridge railing due to impact of a speedy vehicle. The dynamic inelastic response and failure prediction of bridge railing is performed by numerical analysis of reinforced concrete structures. The analysis of structural response is accomplished by changing the weight of the vehicle, as well as the magnitude and direction of its velocity. As the material behaviour changes with the type of load it is subjected to and the rate of loading, the changes in material property of reinforced concrete structure due to impact loading has been taken under consideration. Therefore, the paper also considers the effect of high strain rate on the stress-strain relationship of concrete and steel. The results show vulnerability of existing railings designed by conventional design methods using 'equivalent' static loads. The effects of vehicular weight, magnitude and direction of impact are also found to be significant.

Keywords: RC bridge railing, impact loading, dynamic inelastic response, high strain rate, stress-strain relationship

INTRODUCTION

Development of bridges contributes to economic growth of the society as well as change in people's lifestyle. Such structures also involve a large amount of money during construction and they are to carry traffic continuously. Failure of any part of these structures makes the system inactive and may lead to severe injury to travellers and serious economic loss as well. However, Reinforced Concrete structures are rarely designed considering the effect on their behaviour under impact load.

Vehicular collision with traffic barrier is a common case of impact. The primary function of a traffic barrier is to contain or safely redirect errant vehicles away from fixed features or to (occasionally) protect workers, pedestrians, or bicyclists from vehicular traffic. They can be installed as roadside or median barriers and are used to reduce the overall severity of collisions that occur when a vehicle leaves the travelled way. Barriers are designed so that such encounters might be less severe and not lead to secondary or tertiary collisions. However, when impacts occur, they are not guaranteed to redirect vehicles without injury to the occupants or additional collisions. Barrier performance is affected by the characteristics of the types of vehicles that collide with them. The safe design of traffic barrier is of paramount importance, since a vehicular crash involves the life and safety of several passengers, and in addition to the loss of life and property may seriously dent the morale of families and communities, if not the entire nation.

IMPACT LOADING

The term impact refers to a dynamic effect of a load applied suddenly. If a load has kinetic energy and strikes instantaneously on a body, then the load is termed as impact load. The impact or sudden load condition may occur in tension, compression, torsion or bending or combinations of these. While considering the strength of any structural element it is almost invariably assumed that the load it will be subjected to is static or applied gradually. However, sometimes the loading case can be considered to be of an instantaneous nature. The element may be subjected to cyclic or repetitive loading or it may involve impact or suddenly applied loads.

Several common and important examples of impact loading are encountered regularly in our daily lives; including running, playing popular games like football, cricket, tennis, carom, pelting of stones or terrorist attacks including blast loads, and of course various types of vehicular collision. Impact loads result in shock waves propagating through the elements with possible serious consequences.

Extreme loading conditions like impact loads occur at a high rate of speed and transfer a large amount of energy into a structure over a short period time causing extreme local deformations and damage to structure. Structures can be exposed to extreme loads in their lifetimes. The analysis of reinforced concrete structures subjected to impact loads can be made in several ways. However, it is difficult to name one commonly accepted method. In this study, determination of safety of reinforced concrete bridge railing against vehicular impact load and prediction of failure to the case of impact loads has been analysed numerically using concepts of nonlinear structural dynamics (e.g., by Severson, 2000; Daudeville & Malécot, 2011).

DESIGN OF BRIDGE RAILING

Conventional design of traffic barrier or bridge railing involves assumption of distributed static loads to account for crowded human loads. In addition, it includes concentrated static loads at selected critical locations to approximate the effect of vehicular impact. However, such design of highway bridge railing is often insufficient to sustain the dynamic impact of vehicles. The railing may not be able to absorb the horizontal loads created by the impact of a truck, which could lead to a serious damage. Conventional strengthening methods, such as increasing the area with concrete, are unsuitable because of lack of space and for aesthetical reasons. In this work, the arrangement shown in [Fig. 1] is chosen for the railing and rail post, while [Fig. 2] shows the cross-sections of railing and post obtained from RC design.

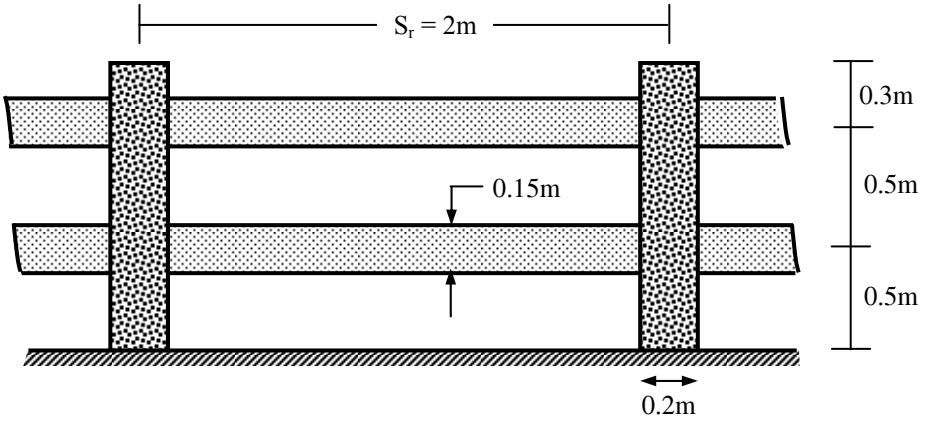

Fig. 1: Elevation of RC Railing used in the analyses (showing c/c view only)

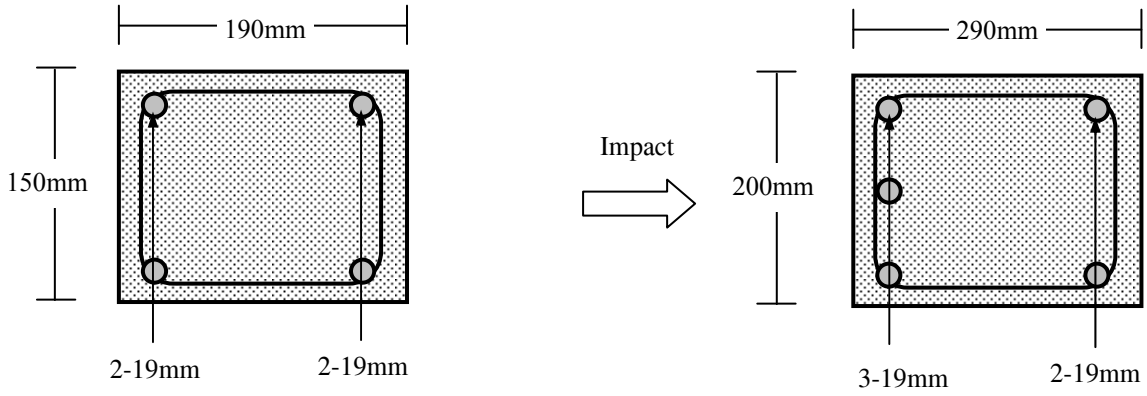

Fig. 2: Cross-sections of Railing and Rail Post

MATERIAL AND SECTIONAL BEHAVIOUR

Material Behaviour at High Strain Rate

Impact loads typically produce very high strain rates. This high loading rate would alter the dynamic mechanical properties of target structures and accordingly, the expected damage mechanisms for various structural elements. For reinforced concrete structures subjected to blast effects the strength of concrete and steel reinforcing bars can increase significantly due to strain rate effects. While ordinary static strain rate is located in the range 10^{-6}~10^{-5} per second, blast pressures normally yield loads associated with strain rates in the range 10^{0}~10^{2} per second.

Dynamic Properties of Concrete and Steel Under High-Strain Rates

The mechanical properties of concrete under dynamic loading conditions can be quite different from that under static loading. While the dynamic stiffness does not vary a great deal from the static stiffness, the stresses and strains that are sustained for a certain period of time under dynamic conditions may gain values that are remarkably higher than the static compressive strength. Strength magnification factors as high as 4 in compression and up to 6 in tension for strain rates in the range 10^{2}~10^{3}/sec have been reported (Grote et al., 2001; Abu-Lebdeh et al., 2010; Ngo et al., 2004).

The mechanical properties of concrete (at slow strain rate) used in this work are the compressive strength f_c' = 20 MPa, modulus of elasticity E_c = 20 GPa, strain at peak stress ε_c = 1.80×10^{-3} and maximum strain (at failure) ε_{max} = 3.35×10^{-3}, tensile strength f_t = 2.0 MPa. Moreover, steel of yield strength f_y = 415 MPa and maximum strain = 0.20 is also used. However, these properties change significantly at high strain rates; i.e., the ultimate strength of concrete increases to 35 MPa and 81 MPa at train rates of 100/sec and 1000/sec respectively. The corresponding yield strengths of steel are 670 and 730 MPa respectively.

Fig. 3 shows the Dynamic Increase Factor (DIF) of the strengths of concrete and steel. The more marked increase of concrete strength and less increase in steel yield strength are to be noted. This is due to the greater creep factor of concrete at slow loading compared to steel.

Nonlinear Moment (M) vs. Curvature (ϕ) Relationship

The nonlinear moment-curvature relationship of the railing and rail post sections [Fig. 2] are derived numerically and shown in [Fig. 4] for different strain rates (i.e., static load and strain rate = 100/sec). It demonstrates the strongly nonlinear properties of both the sections, which are modelled as elastic-fully plastic in this work. Also apparent is the influence of strain rate on the cross-sectional properties of both sections. Most significantly, the consideration of strain rates makes the sections stronger. Apparently, the effect on ultimate ductility of the section is not very significant because it depends on the ductility of steel, which is not much affected by strain rate.

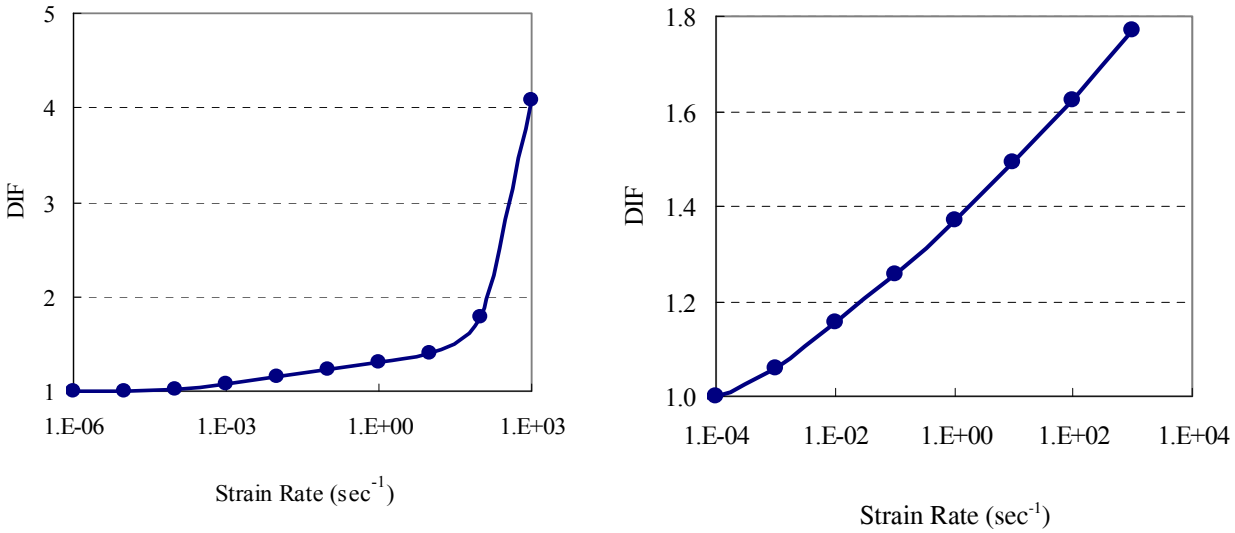

Fig. 3: Dynamic Increase Factor (DIF) vs. Strain R

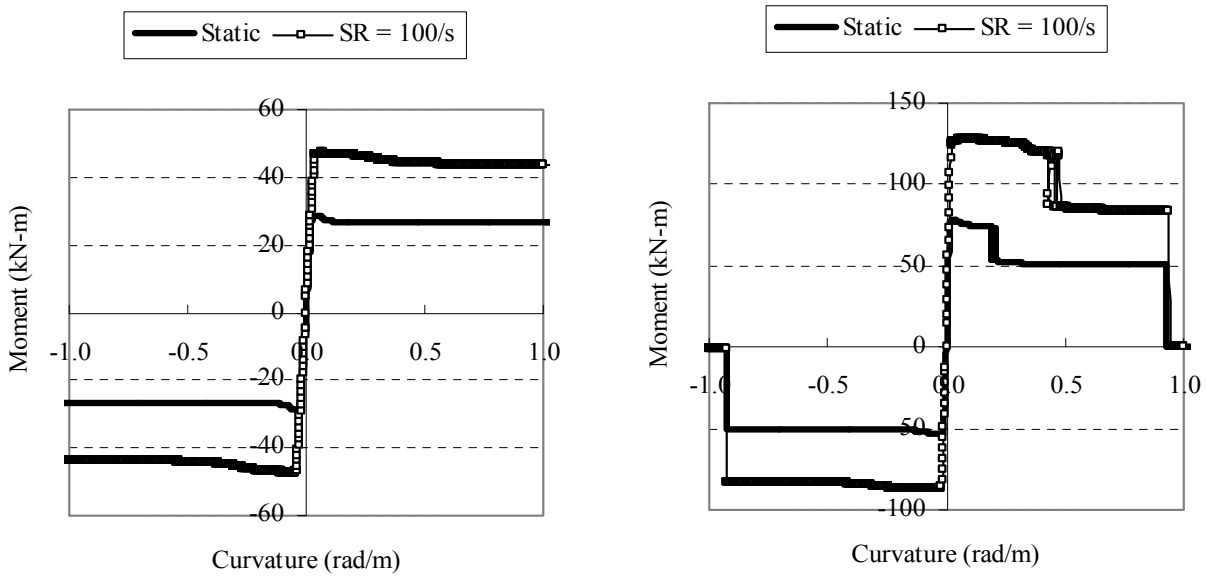

Fig. 4: Moment-curvature relationship of Railing and Rail Post for different strain rates

RESULTS FROM NUMERICAL ANALYSES

As mentioned, nonlinear structural dynamics is used to analyse the bridge railing shown in [Fig. 1]. Parametric studies are performed to demonstrate the effects of different items on the dynamic response of the structure (represented by rail post deflections) to vehicular impact. A significant component of the vehicular velocity being perpendicular to the structural plane, this is to simulate the effect of a fast moving derailed vehicle colliding with the bridge railing. A 2-ton car colliding at a velocity of 100 kmph and angle 30° is taken as reference for vehicle, while the reference damping ratio of the structure is assumed 8%. Results of the parametric studies are shown in [Fig. 5] to [Fig. 8]. It involves the variation of damping ratio from 2% to 8%, deflection of top, bottom and side posts, variation of

vehicular weight from 2 tons to 1 and 4 tons, vehicular velocity from 50 to 100 kmph and angle of impact from 30° to 90°. The results (deflection of rail post) are summarized in Table 1.

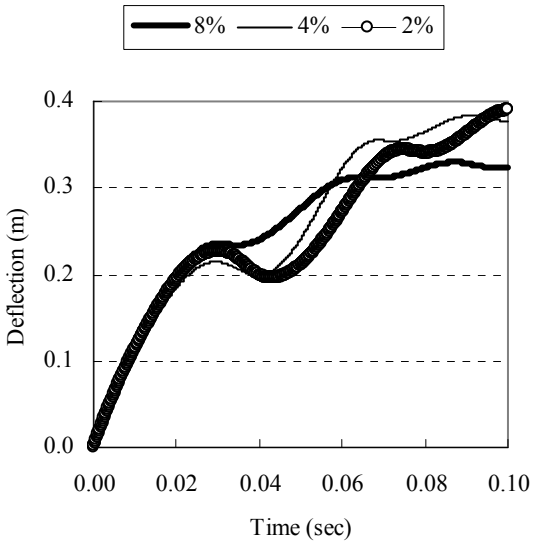

Fig. 5: Effect of Damping Ratio

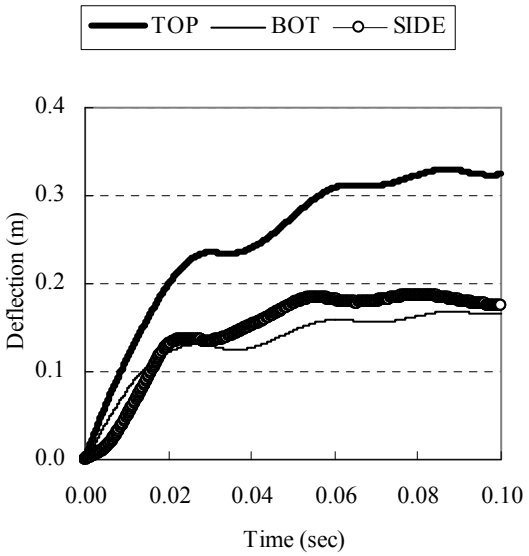

Fig. 6: Deflections at various posts

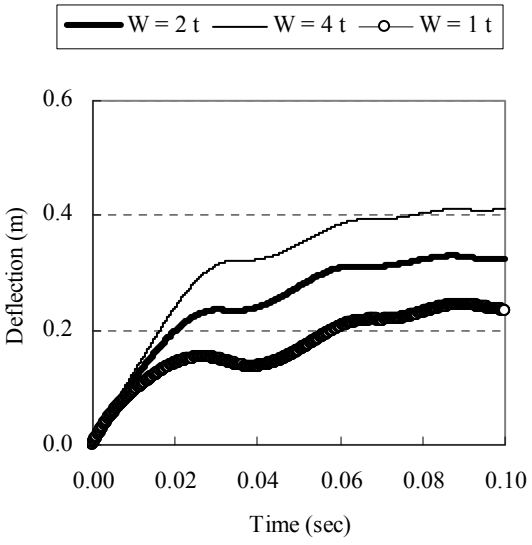

Fig. 7: Effect of Vehicular Weight

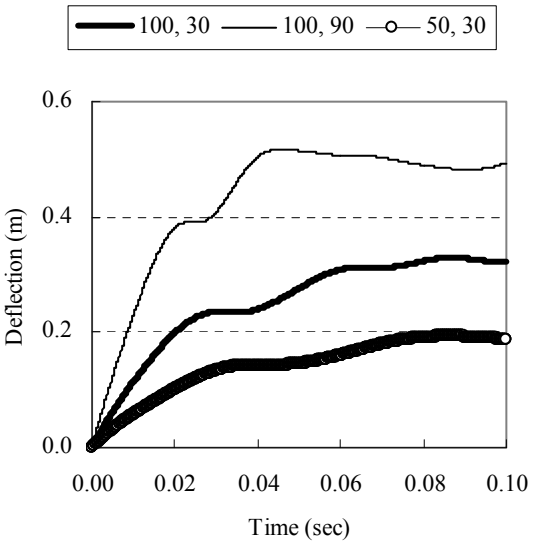

Fig. 8: Effect of Velocity and Angle

Table 1: Maximum Deflections (mm) from Parametric Studies

Δ_{ult}	Δ_{Ref} of various Posts			Damping Ratio		Weight (ton)		Velocity (kmph), Angle (θ)	
	Top	Middle	Side	4%	2%	4	1	100, 90°	50, 30°
250	330	168	187	377	390	413	244	517	193

Finally, the dynamic analyses are simplified ignoring the effect of the railings (keeping the rail posts only), as shown in Fig. 9 (resulting in much increased deflections), while Fig. 10 shows even larger deflections if the structure is simplified as a Nonlinear Single-Degree-of-Freedom (NSDF) system.

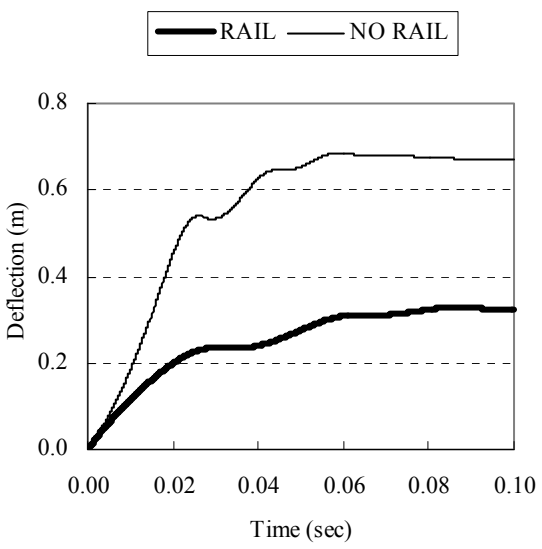

Fig. 9: Ignoring the Rail

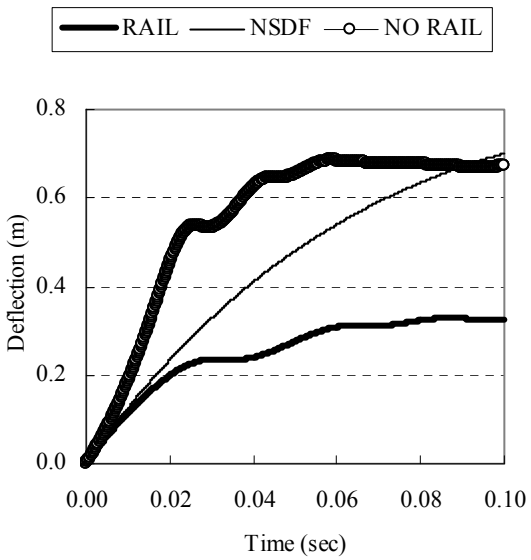

Fig. 10: Comparison with SDF Analysis

CONCLUSIONS

Numerical analyses are performed on a model RC railing designed initially for static loads only. Nonlinear structural dynamic analyses are performed, leading to parametric studies varying different parameters involved. The variation of material properties and cross-sectional moment-curvature relationships are shown to depend on the rate of loading. As impact loads involve high strain rates, the resulting higher material strengths may significantly increase the ultimate moment capacity of the sections. Results from parametric studies also demonstrate the effects of damping ratio (increasing structural deflections for lower damping), weight and velocity of colliding vehicle. They demonstrate particularly the possible catastrophic effects of heavy vehicles and high-speed cars, and more so on lightly damped structures, the resulting maximum deflections in such cases exceeding the ultimate top deflection capacity of the rail post. Moreover effects of numerical simplifications ignoring rail posts and simplifying the structure as a SDF system are found to produce unacceptably inaccurate results.

REFERENCES

Abu-Lebdeh, T.; Hamoush, S. and Zornig, B. 2010. Rate effect on pullout behaviour of steel fibers embedded in very-high strength concrete. *American Journal of Eng. Applied Science*, 3: 454-463.

Daudeville, L.; Yann Malécot, Y. 2011. Concrete structures under impact. *European Journal of Environmental and Civil Engineering*, 15: 101-140.

Grote, D.; Park, S. and Zhou, M. 2001. Dynamic behaviour of concrete at high strain rates and pressures. *Journal of Impact Engineering*, 25: 869-886.

Ngo, T.; Mendis, P.; Hongwei, M. and Mak, S. 2004. High strain rate behaviour of concrete cylinders subjected to uniaxial compressive impact loading. *Proc. of 18th Australasian Conference on the Mechanics of Structures and Materials*, Perth, Australia.

Severson, K. J. 2000. *The development of collision dynamics models to estimate the results of full-scale rail vehicle impact tests. M.Sc. Engg*. Thesis, Tufts University, USA.

ID : ASEE 025

1st International Conference on Advances in Civil Engineering 2012 (ICACE 2012)
12 –14 December 2012
CUET, Chittagong, Bangladesh

APPLICATION OF NON-DESTRUCTIVE TESTING TECHNIQUES FOR STRUCTURAL CONDITION ASSESSMENT IN BANGLADESH

R. K. MAZUMDER[1*] & M. A. ANSARY[2]

[1] Department of Structural Engineering and Geotechnics, La Sapienza University of Rome, Italy, <rk.mazumder@uniroma1.it>*
[2] Bangladesh Network Office for Urban Safety, Department of Civil Engineering, Bangladesh University of Engineering and Technology, Dhaka, Bangladesh, <ansary@ce.buet.ac.bd>

ABSTRACT
Bangladesh has recently experienced earthquakes at regular intervals that have not caused immense damage but makes us aware about the future risk. Non-Destructive Testing (NDT) is a suitable way to find out properties of structure without destroying any part of it. To evaluate the condition of existing structures against different loading patterns, several non-destructive tests have been conducted in this study. Ferroscan, Rebar detector, Ultrasonic device, Rebound hammer, Microtremor and Ground Penetrating Radar have been introduced for the first time to assess building vulnerability in different parts of Bangladesh. This paper presents a brief overview about NDT equipments and major findings obtained from the analysis of the surveyed data. The paper also presents the findings obtained from 65 buildings.

Keywords: Assessment, NDT, Structure.

INTRODUCTION

Assessment of an existing structure is a difficult task. The construction of a structure is never exactly as per a designer's specification and a number of defects and uncertainties crop up during the construction. Moreover, the quality of the materials deteriorated with time and the assessment of an existing structure becomes a time dependent problem. The problem of assessment of an existing structure involves not only the current status of the structure but also its exploration in the life of the structure with or without repairs. There are three sources of deficiency in structures: a) Defect arising from the original design, such as under estimation of loads as per old standards or practices, inadequate section or reinforcement anchorage and detailing; b) Defects arising from original construction, such as under strength of concrete, poor compaction, poor construction joints, improper placing of reinforcement and honeycombing; and c) Deterioration since the completion of the construction due to reinforcement corrosion, alkali-aggregate reaction, etc. If the design documents are available, the first type of deficiency can be assessed with a satisfactory level of confidence. A number of techniques have been developed to detect the other two types of deficiency. Almost all of them depend on indirect measurement and have a low reliability (Singh, 2011). Further the variation of test result is large and interpretation of results requires experience and skills. However, modern NDT techniques have a much more reliability to condition assessment of buildings before taking up repair and upgrading work.

In Bangladesh, most of the houses are non-engineered constructions, which are mainly load bearing buildings. In urban areas, there are many RC frame buildings which have been constructed without any consideration to resist earthquake forces or without following current code of Earthquake Resistance Design. For such type of seismically deficient buildings, a quick NDT assessment could be a good approach for safety measurement of buildings within considerable cost. This paper introduces different NDT instruments, its methodology of structural safety assessment and finally results from the NDT conducted in different parts of Bangladesh.

NON-DESTRUCTIVE TESTING TOOLS

Ferroscan

Ferroscan is portable, non-destructive steel reinforcement detection system using electromagnetic pulse. It can reduce costly effort to drill, cut or physically break concrete surface to find out the bar. Ferroscan has been used for determining the position, depth and diameter of rebar in existing structure. This is a portable, quick and simple-to-operate system carrying out structural analyses quickly and exactly in a non-destructive manner. This also determines coverage over the entire surface of a structure. The key elements of the system are the scanner and the monitor. After scanning a structure data has been transferred to the monitor. Collected data can be analyzed by monitor or in a PC using PS 200 software's. Maximum depth of scanning is 180 mm (at 36 mm rebar diameter) where rebar diameter range 6 - 36 mm. Accuracy of depth measurement for rebar is ±1 mm, depending on depth range and scan mode used. Three types of scanning can be checked out by using Ferroscan device. Line scan is simple way to detect position and depth of rebar where Image scan provides detail information (diameter of bar, concrete cover, location etc.) with scanned image (2 ft x 2 ft grid) of any structure. Block scan is a combination of a set of image scan for a comparatively large area (Rahman et. al, 2010). Fig. 1 shows monitor and scanning device produced by Hilti Corporation, 2011.

Fig. 1: Hilti PS 200 Monitor and Scanner device

Rebar Detector

Rebar Detector has been used to determine the exact location of rebar in existing structure. The Profoscope is a versatile, fully-integrated rebar detector and cover meter with a unique real-time rebar visualization allowing the user to actually see the location of the rebar beneath the concrete surface to a maximum depth of 180 mm (Proceq SA, 2011). This is coupled with rebar-proximity indicators and optical and acoustical locating aids. Rebar diameter can also be estimated within the specified testing range. The Profoscope combines these unique features in a compact, light device that allows to operate this rebar detector with one hand making the task of locating rebars a simple and efficient process. In addition, Proceq's rebar detector convinces through its intuitive user interface making rebar detection easy. Fig. 2(a) shows a Profoscope Rebar detector.

Rebound Hammer

A simple equipment known as Rebound Hammer or Schmidt Hammer is used determine a surface hardness in order to establish the theoretical relationship between the strength of concrete and the rebound number of the hammer. The details of the equipment are shown in Fig. 2b, 2c. Surface hardness measured during the test give an idea about the soundness and quality of cover concrete. Locations having very low rebound numbers indicate weak surface concrete and may be affected by corrosion.

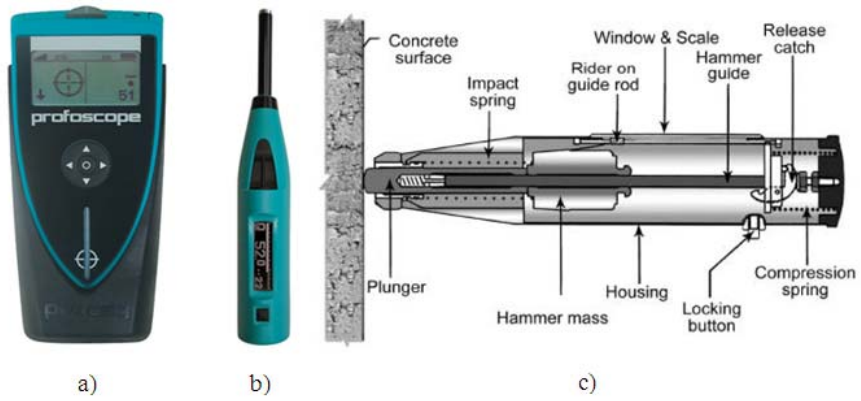

Fig. 2: a) Profoscope Rebar Detector, b) Schmidt Hammer and c) Different parts of Schmidt Hammer

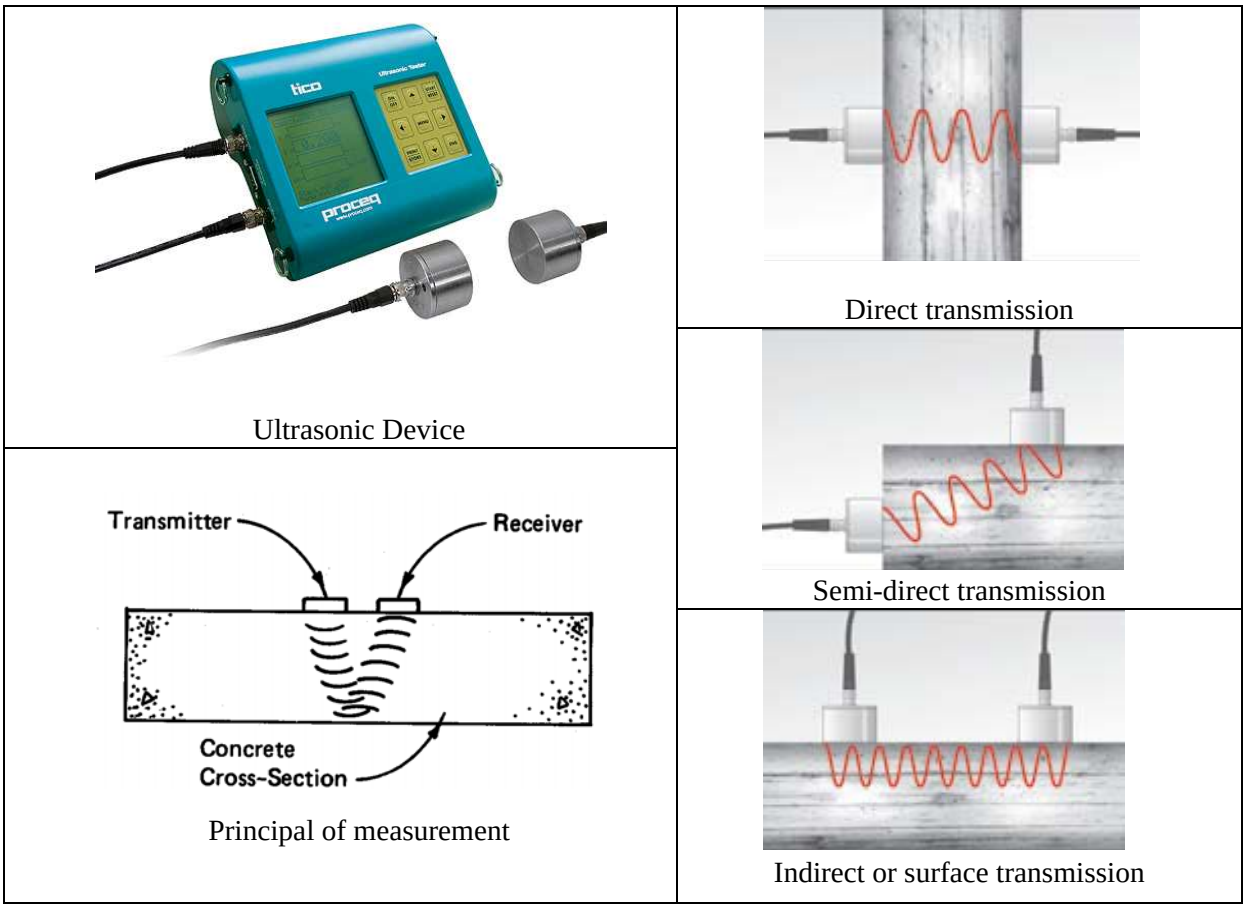

Fig. 3: Ultrasonic concrete testing instruments and its observation

Ultrasonic Pulse Velocity (UPV) Instrument

The ultrasonic pulse velocity method is used to determine material strength and quality, based on the relation-ship to material density and elasticity. The test equipment has provisions for generating ultrasonic pulse, transmitting it to concrete, receiving and amplifying the pulse and measuring and displaying the pulse travel time. Good acoustic coupling between the transducers and concrete is to be established for correct measurement of the speed (IAEA, 2002). The instrument uses transducers as transmitters and receivers to calculate pulse velocity by measuring transmission time. This flexible unit can measure via direct transmission, semi-direct transmission, indirect or surface transmission to accommodate the demands of virtually any test site. Fig. 3 shows UPV instrument and its observation.

Microtremor

Microtremor measurement has been done with five component of sensor. At each site, microtremor ground motions were measured for 15 minutes. Each accelerometer recorded data in three direction two horizontal (N-S and E-W components) and one vertical direction (up-down). For free field near to building, First Fourier Transform (FFT) has been done in order to calculate H/V spectral ratio for microtremors. At the top and ground floors of the both buildings, horizontal X- and Y-component microtremor motions, which are in longitudinal and transverse directions of the buildings, were observed. Fig. 4 shows Microtremor testing equipments.

Fig. 4: Test equipments used in microtremor measurements.

Ground Penetrating Radar

Ground Penetrating Radar (GPR) is a technique of obtaining sub-surface images using electromagnetic radiation. The energy radiated by the antenna of the system penetrates the surface, and is either absorbed or reflected back at any discontinuities. GPR is valuable for in locating defects and voids in concrete structures, determining embedded reinforcement and other subsurface details. The StructureScan Standard system provides a nondestructive means to accurately inspect concrete structures. This StructureScan Standard used to safely locate embedment within concrete structures prior to drilling, cutting or coring. Reach depths of 0-18 inches with confidence using a 1600 MHz antenna, survey cart and SIR–3000 control unit (GSSI, 2011). This is generally used to locate metallic and non-metallic targets in walls, floors. Fig. 5 shows GPR control units and a 1.6 GHz antenna for structure scan.

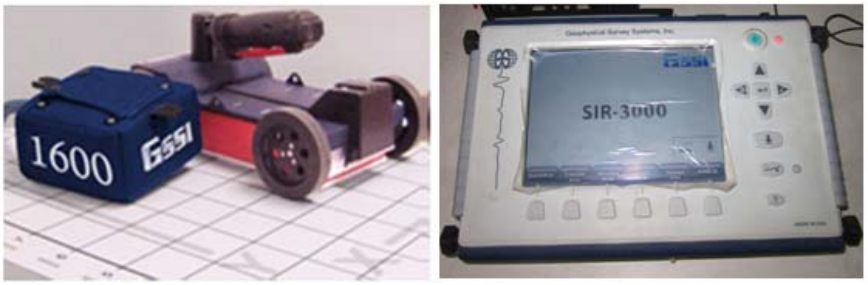

Fig. 5: 1.6 GHz Antenna and Control Unit of GPR by Geophysical Survey System Inc.

STUDY AREA

In the last two years, these Non-Destructive Testing equipments have been used in different parts of Bangladesh. Important buildings of Chittagong hill tracts region (Khagrachari, Rangamati and Bandarban districts), new and old buildings in Dhaka and an electrical power plant building in Kushtia and two school buildings in Sylhet have been covered. Basically Unreinforced Masonry (URM) and Reinforced Concrete (RC) frame structure has been tested for structural safety. Fig. 6 shows conducted NDT location in Bangladesh.

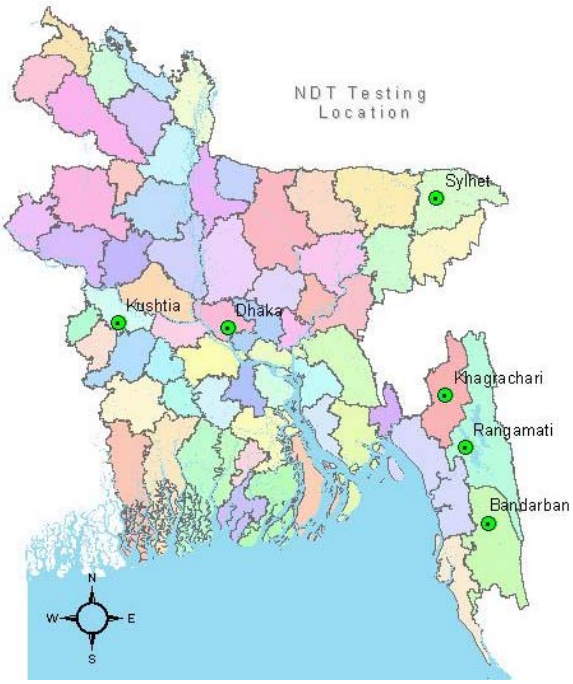

Fig. 6: Locations of NDT conducted in Bangladesh

METHODOLOGY OF EVALUATION

Location and spacing requirements of column transverse reinforcement and beam stirrup have been checked by using Ferroscan and Rebar Detector. Existing beam and column have been scanned by those two equipments. Reinforcement configuration has been compared with seismic specification provided in ACI 318. Fig. 7 and Fig. 8 give reinforcement requirement for column where Fig. 9 provides reinforcement requirement for beam (ACI, 2008). Slabs also scanned to check the existing reinforcement location as per design.

To measure the elastic properties or strength of concrete, Rebound hammer was used in all columns located at the ground floor of the surveyed building. Schmidt hammer was also used for some of the beams at ground floor. The quality of concrete may be interpreted as shown in the Table 1(GoI-UNDP, 2007).

Table 1: Average Rebound number and quality of concrete

Average Rebound number	Quality of Score
>40	Very good hard layer
30 to 40	Good layer
20 to 30	Fair
< 20	Poor concrete
0	Delaminated

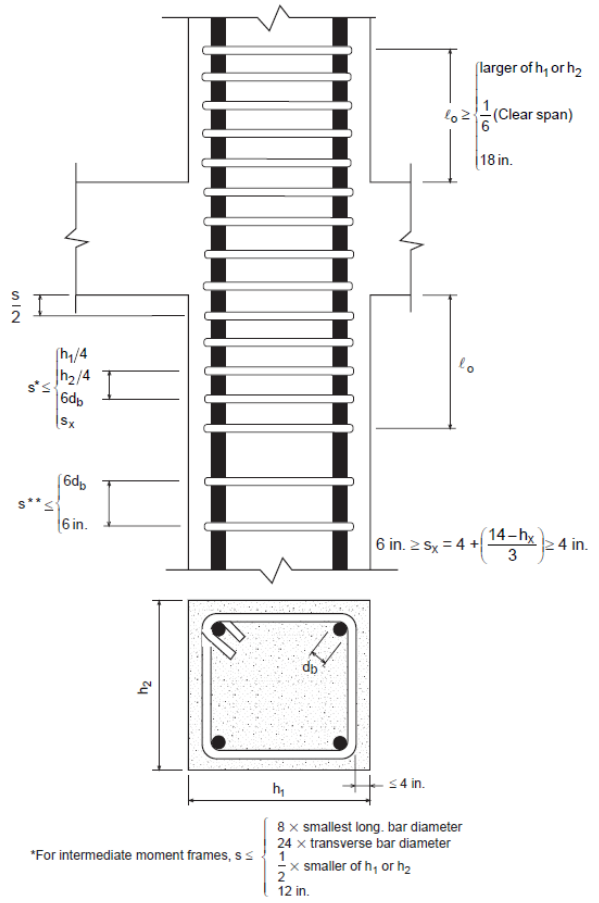

Fig. 7: Column transverse reinforcement spacing requirements.

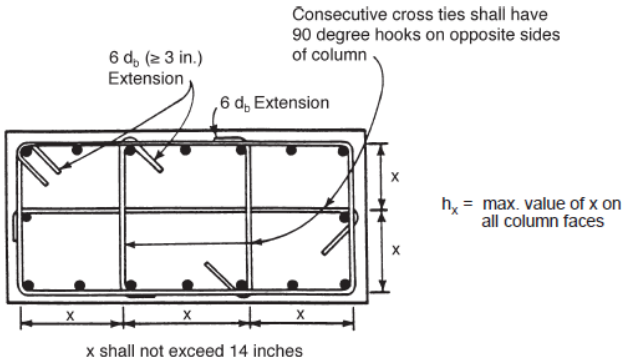

Fig. 8: Transverse Reinforcement in Columns.

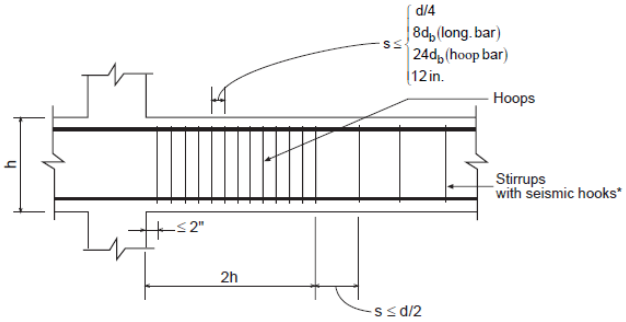

Fig. 9: Transverse Reinforcement for Beams.

Using this ultrasonic method, the ultrasonic instrument determines, indirectly, the modulus of elasticity and concrete strength. The instrument is typically used on site to assess uniformly of concrete and to locate cracks, voids, cavities, and defects due to fire and frost. The quality of concrete may be interpreted from the Table 2 (GoI-UNDP, 2007).

Table 2: UPV value and concrete quality

UPV value in m/sec (V)	Concrete quality
V > 4000.0	Very good
V = 3500 - 4000	Good, but may be porous
V = 3000 - 3500	Poor
V = 2500 - 3000	Very poor
V = 2000 - 2500	Very poor and low integrity
V < 2000 and reading fluctuating	No integrity, large voids suspected

Microtremor instruments measures predominant ambient frequency of the structures and soil. If predominant frequency of both structure and soil are close to each other, there will be more likelihood to damage during an earthquake. GPR 1.6 GHz antenna can identify the rebar position in a structure by generating radar pulse. Semi-automatic mapping of deterioration zones within concrete structures can be identify using RADAN software.

RESULTS

Among 65 buildings only 7 buildings are masonry, rest of all are reinforced concrete buildings. Considered masonry structures are situated at Dhaka and only microtremor test are performed for these masonry buildings in order to check the resonance criteria. Other NDT equipments have been used for all RC buildings.

Ferroscan and Rebar Detector have been used alternatively for RC buildings. Identified reinforcement spacings have been verified with ACI 318 guideline for seismic consideration. According to priority basis on structural configuration, at least three columns have been scanned for each building in different storey level. From 57 buildings, only 12 buildings comply with seismic provision for column middle part as per ACI 318 where 45 buildings didn't satisfy. For end portion of column, only 9 buildings are satisfied as per ACI 318. Beam reinforcement configuration also justified with ACI 318 provision. From 54 scanned cases, 19 cases have been satisfied for middle part of beam. Other hand, only 2 beams are satisfied for end portion check from 11 cases. Reinforcement identification of end portion hasn't been performed for most of the beams due to insufficient space. Scanned image of slabs have been generate using image scan mode by Ferroscan. Fig.10 and Fig.11 show typical image scan result and reinforcement position in structural elements respectively.

Schmidt hammer has been used for 55 buildings. Average of 10 impacts has been considered for each concrete surface. From the assessment it has been found that column rebound value is below 30 for 36 buildings. So, concrete conditions of those 36 buildings are fair to poor (see Table 1). Average rebound number more than 40 have been found for only 2 buildings, where 17 buildings have score greater than 30. Fig. 12 shows impact data in Hammerlink software.

Ultrasonic equipment has been used in three hill tract districts. Among 44 ultrasonic results, 2 buildings have very poor and low integrity, 4 buildings have very poor to poor condition, 21 buildings have good to very good condition (see Table 2).

Microtremor has been used for 21 buildings in Dhaka, Sylhet and Kushtia. Fourier Transform indicates that only 3 masonry buildings have likelihood to significant damage during an earthquake.

From other 14 RC buildings, 4 buildings have a high possibility to resonance during earthquake where 10 buildings have a moderate to low risk for resonance. Predominant frequency can be found from Fourier analysis (in Fig. 13). Those structure are situated at soft soil, has a high likelihood to occur resonance during earthquake.

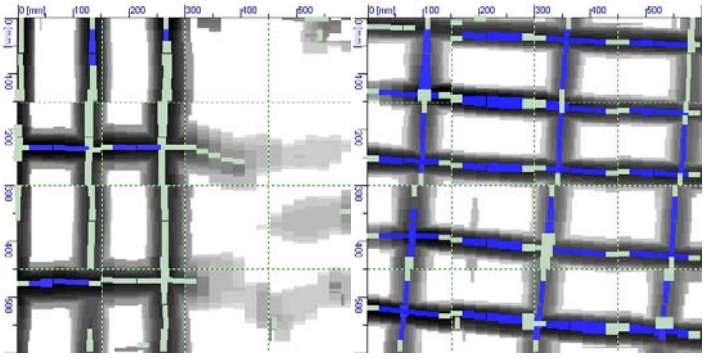

Fig. 10: Typical image scan for column (left) and slab

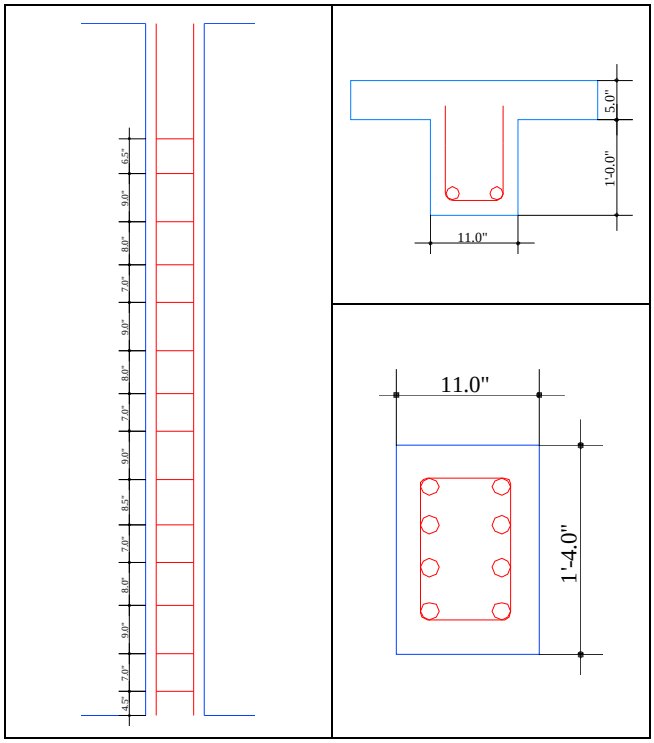

Fig. 11: Identified reinforcement position in column and beam.

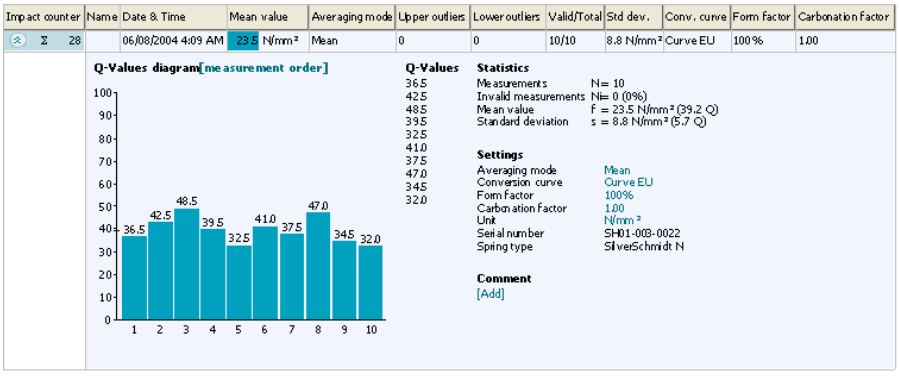

Fig. 12: Impacts data analyzed in Hammerlink software.

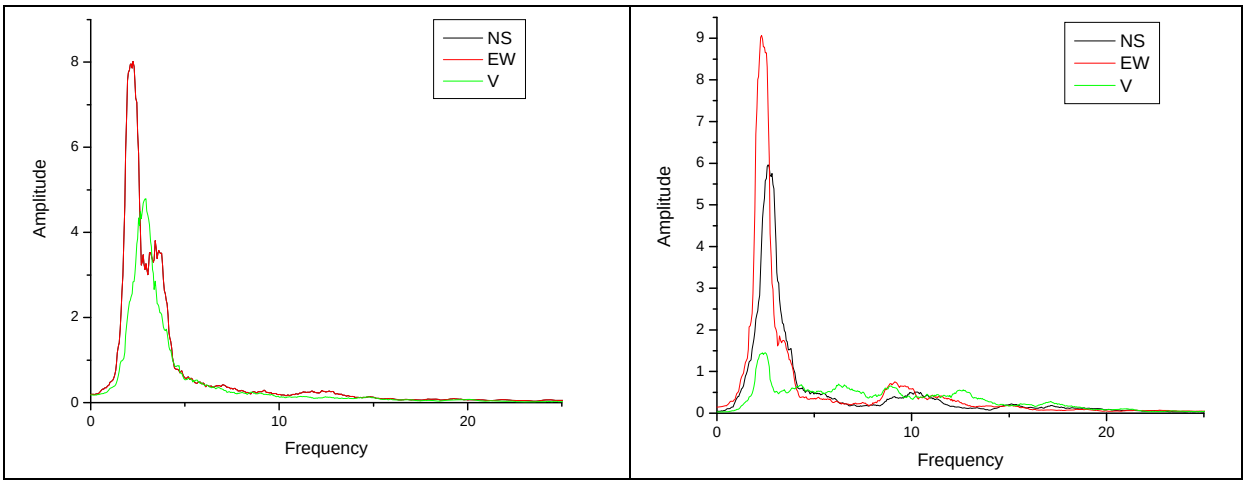

Fig. 13: Typical Fourier analysis for free field and roof of structure

A raft founded basement has been scanned by GPR. 3D data has been collected in order to investigate deterioration zones within concrete structures. After RADAN analysis, no deterioration has been found. Fig. 14 shows 3D model of raft basement.

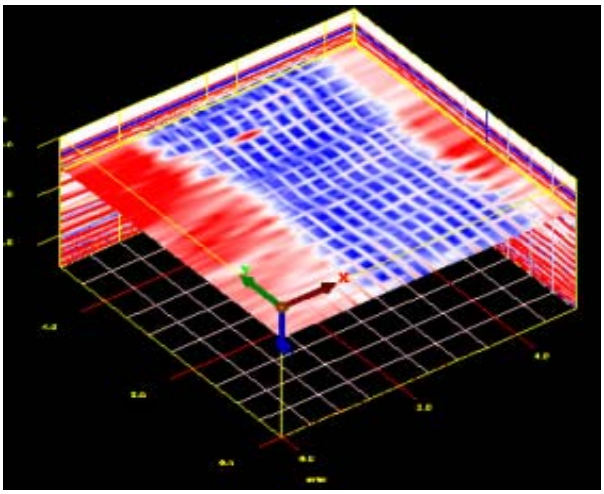

Fig. 14: 3D data set showing rebar mat.

CONCLUSIONS

The importance and need for NDT assessment and evaluation of safety of existing buildings have been highlighted in this paper. Safety evaluation forms the basis for designing and carrying out strengthening of buildings to satisfy the safety and performance standards as per the extant building codes. An overview of the procedures and different investigations including tests involved in condition assessment and evaluation of safety is presented in a simple. It can be seen that detailed visual inspection and Non Destructive Testing (NDT) plays an important role in condition assessment of existing buildings. It may be emphasized here that a great deal of expertise is required for interpretation of field observations and test results to make a proper assessment of the condition as well as for analyzing and evaluating safety.

REFERENCES

American Concrete Institute (ACI) -318. 2008. “Building Code Requirements for Structural Concrete”.

GoI-UNDP Disaster Risk Management Programme, Government of India. 2007. “Condition Assessment of Buildings for Repair and Upgrading Report”.

International Atomic Energy Agency (IAEA). 2002. “Guidebook on Non-Destructive Testing of Concrete Structures”, Training Course Series No. 17.

Rahman, M. S., Islam, B. and Ansary, M. A. 2010. “Diagnosis of the Seismic Vulnerability of Buildings at Dhaka Using Non-Destructive Testing”, 9th Proceedings of New Technologies for Urban Safety of Mega Cities in Asia, Kobe, Japan.

Singh, Y. 2011. “Seismic Vulnerability Assessment of Existing Buildings”, Earthquake Risk Mitigation Training Manual, SAARC Disaster Management Center, L-18.

Geophysical Survey Systems, Inc. (GSSI). (2011). http://www.geophysical.com/

Hilti Corporaton. (2011). “PS 200 Ferroscan system”, http://www.hilti.com.

Proceq SA. (2011). http://www.profoscope.com/

ID : ASEE 034

1st International Conference on Advances in Civil Engineering 2012 (ICACE 2012)
12 –14 December 2012
CUET, Chittagong, Bangladesh

A STUDY IN THE DEVELOPMENT OF APPROPRIATE MIX DESIGN OF CONCRETE FOR RECYCLED COARSE AGGREGATE

M. N. KHAN[1*], M. O. IMAM[1] & S. BISWAS[1]

[*1] *Department of Civil Engineering,Chittagong University of Engineering and Technology, Bangladesh,*

ABSTRACT

At present, a huge amount of coarse aggregate is required in construction of various types of concrete structure. To meet these requirements, a large amount of aggregate is extracted from natural resources. Demolished concrete may provide an alternative source of coarse aggregate. From this perspective, this study is focused on the mix design of concrete by using recycled coarse aggregate with different FM of fine aggregates. In this study, tried to find out the maximum compressive strength by using recycled coarse aggregate with different fineness modulus value of sand (FM = 1.0 - 1.4) by method of ACI mixed design. 100% recycled coarse aggregate (RCA) with different types of fine aggregate (FM = 1.4, 1.3, 1.25, 1.2, 1.1 and 1.0) are used in design of concrete structure for design strength of 21 MPa. The results shows that, the compressive strength of concrete made by recycled coarse aggregate with fine aggregate of fineness modulus value of 1.25 gives the maximum compressive strength. By using recycled coarse aggregate it could be possible to minimize the costing of recycled concrete up to around 40%.

Keywords: Recycled Concrete, Recycled Coarse Aggregate (RCA), Compressive Strength.

INTRODUCTION

At present the concrete industry requires about 11.25 billion tons of natural aggregate globally every year to produce 14.5 billion tons of concrete for making buildings, bridges, tunnels, culverts, highways, port and harbor facilities, concrete dams, and other civil engineering infrastructures(Figure 1). The aggregate consumption rate is estimated at 1.55 tons per capita per year globally (Uddin, 2006). To supply such a huge amount of aggregate, a significant portion of mountain is to be cut and also a huge amount of land is to be utilized for making clay bricks in the south Asian countries. This process is playing a vital role in the global environmental problems. These negative environmental problems can be reduced significantly by recycling of demolished concrete produced due to the demolition of deteriorated concrete structures or reconstruction of buildings, bridges, highways and other infrastructures. It is estimated that in the near future the global production of the demolished concrete will rise to 10 to 12 billion tons. If this huge amount of demolished concrete is not recycled, an area of 10 times of Bangladesh has to be filled by a depth of 3m (as per year 2006) that will create other environmental problems (Uddin, 2006). By recycling of the demolished concrete, the aforementioned environmental problems caused by the aggregate production can be greatly reduced. In addition, the disposal problems of the demolished concrete will be solved.

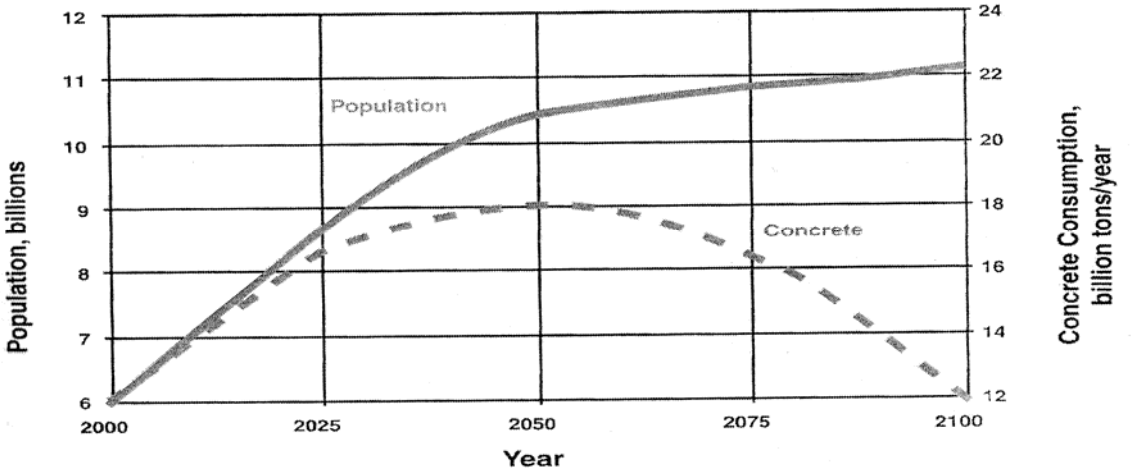

Figure 1: Concrete consumption and Population in the world. (Uddin, 2006)

MIX DESIGN

There are a number of different methods of mix design available. Although they are not directly comparable, they do give approximately the relative proportion of materials, and all are capable of yielding suitable concrete mixes. The most common method used in North America is that established by ACI Recommended Practice 211.1. It must be remembered, however, that any mix design method will provide approximation of proportions. These must be checked by trial batches in the laboratory or on the field and can then be adjusted as necessary to produce the desired concrete characteristics. With any given set of materials, it may be found that considerable deviation from the ACI recommended practice might be necessary. Once sufficient experience with local materials is acquired, the ACI method should be modified to take their properties into account. In this studies, for casting of concrete cylinder use fine aggregate of fineness modulus value 1.0 to 1.4. For mix design of concrete, estimation of coarse aggregate content use the Figure 2 instead of Table 1.

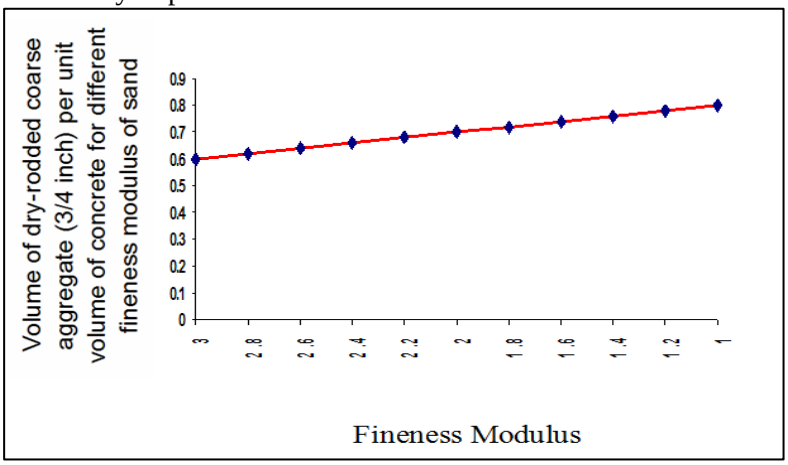

Figure 2: Volume of Coarse Aggregate per Unit of Volume of Concrete (Based on ACI 211.1).

Table 1: Volume of Coarse Aggregate per Unit of Volume of Concrete. (ACI 211.1)

Maximum size of Aggregate		Volume of Dry-Rodded Coarse Aggregate per Unit Volume of Concrete for different Fineness Moduli of sand			
in.	mm	2.4	2.6	2.8	3
3/8	10	0.5	0.48	0.46	0.44
½	12.5	0.59	0.57	0.55	0.53
¾	20	0.66	0.64	0.62	0.6
1	25	0.71	0.69	0.67	0.65
1½	40	0.76	0.74	0.72	0.7
2	50	0.78	0.76	0.74	0.72
3	75	0.82	0.8	0.78	0.76
6	150	0.87	0.85	0.83	0.81

COMPRESSIVE STRENGTH OF RECYCLED CONCRETE

The compressive strength of concrete is one of the most important and useful properties of concrete. In most structural applications concrete is employed primarily to resist compressive stresses. In those cases where strength in tension or in shear is of primary importance; the compressive strength is frequently used as a measure of these properties. Therefore, the concrete making properties of various ingredients of mix are usually measured in terms of the compressive strength. Compressive strength is also used as a qualitative measure for other properties of hardened concrete.
In this study, recycled coarse aggregate were collected as broken cylindrical specimen from strength of materials laboratory, Civil Engineering Department, CUET, and crushed into coarse aggregates manually, which are defined as recycled coarse aggregate. After grading, maximum size of aggregate is 20 mm (3/4 in) and evaluates the properties of the recycled coarse aggregate. Thorough mixing of the materials is essential for the production of uniform concrete. The mixing should ensure that the mass becomes homogenous, uniform in color and consistency. For proper mixing vibrator are used here in preparation of cylindrical specimen (6 in. dia and 12 in. long) by ACI 211.1 method of mixed design. A series of test (BS 1881: Part 110:1983 and by ASTM C 192-90a) were carried out in the laboratory, to determine the compressive strength of recycled concrete cylinder after curing of 28 days in fresh water. For preparing cylindrical specimen, here used fine aggregates FM= 1.0 – 1.4.

The compressive strength (28 Days) and type of fine aggregate used in the preparation of recycled concrete specimen are listed in the Table 2 to Table 7.

Table 2: Recycled concrete compressive strength for FM=1.0 (Design Strength 21 MPa).

Set	FM of fine aggregate	Mix Ratio	Compressive strength (MPa)	Average compressive strength (MPa)
1st			22.7	
2nd	1.0	1 : 2.28 : 4.28 : 0.54	21.9	22.2
3rd			22.1	

Table 3: Recycled concrete compressive strength for FM=1.1 (Design Strength 21 MPa).

Set	FM of fine aggregate	Mix Ratio	Compressive strength (MPa)	Average compressive strength (MPa)
1st			22.8	
2nd	1.1	1 : 1.87 : 4.24 : 0.53	22.5	22.7
3rd			22.7	

Table 4: Recycled concrete compressive strength for FM=1.2 (Design Strength 21 MPa).

Set	F.M. of fine aggregate	Mix Ratio	Compressive strength (MPa)	Average compressive strength (MPa)
1st			24.5	
2nd	1.2	1 : 1.90 : 4.18 : 0.52	24.4	24.4
3rd			24.3	

Table 5: Recycled concrete compressive strength for FM=1.25 (Design Strength 21 MPa).

Set	FM of fine aggregate	Mix Ratio	Compressive strength (MPa)	Average compressive strength (MPa)
1st			24.6	
2nd	1.25	1 : 1.70 : 4.16 : 0.51	24.5	24.5
3rd			24.4	

Table 6: Recycled concrete compressive strength for FM=1.3 (Design Strength 21 MPa).

Set	FM of fine aggregate	Mix Ratio	Compressive strength (MPa)	Average compressive strength (MPa)
1st			23.3	
2nd	1.30	1 : 1.94 : 4.13 : 0.50	23.3	23.3
3rd			23.4	

Table 7: Recycled concrete compressive strength for FM=1.4 (Design Strength 21 MPa).

Set	FM of fine aggregate	Mix Ratio	Compressive strength (MPa)	Average compressive strength (MPa)
1st			23.3	
2nd	1.40	1 : 1.98 : 4.07 : 0.49	23.2	23.1
3rd			22.8	

COST ANALYSIS

Price according to the Bangladesh Market (2012):
Cement = 450.00 Tk Per bag (50Kg)
Sand = 1050.00 Tk Per m^3.
Fresh stone chip = 4200.00 Tk Per m^3.
Recycled coarse chip = 1150.00 Tk Per m^3.

Table 8: Cost per Cubic meter (In taka) of plain concrete.

Materials	Price (TK)	Price (TK)
Coarse aggregate	3600.00 (Fresh coarse aggregate)	990.00* (RCA)
Sand	450.00	450.00
Cement (OPC)	2893.00	2893.00
Total	6943.00	4333.00

* Manually broken & transportation cost.
If we use recycled stone chips, safe 38% cost than use of fresh stone chips.

RESULTS AND DISCUSSIONS

In this study 100% recycled coarse aggregate (RCA) with different types of fine aggregate (FM = 1.4, 1.3, 1.25, 1.2, 1.1 and 1.0) are used in design of concrete structure for design strength of 21 MPa.

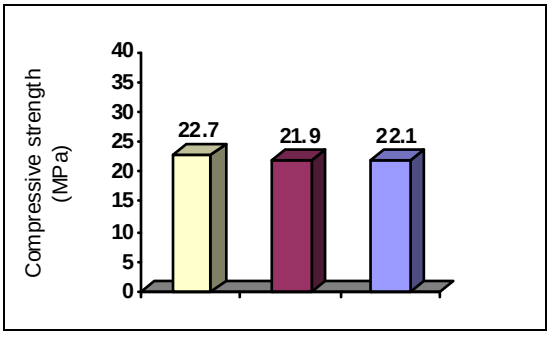

Figure 3: Variation of recycled concrete compressive strength for design strength 21 MPa (Reference-Table 2), FM=1.0.

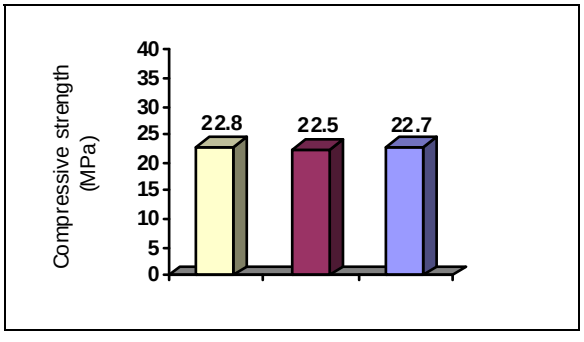

Figure 4: Variation of recycled concrete compressive strength for design strength 21 MPa (Reference-Table 3), FM=1.1.

Test result show that, (Figure 3) for design strength 21 MPa (FM = 1.00), Avg. compressive strength of recycled concrete is found 22.2 MPa. That is 5.7% higher than the design strength. For FM = 1.10,

Avg. compressive strength of recycled concrete is found 22.7 MPa (Figure 4). That is 8.9% higher than design strength.

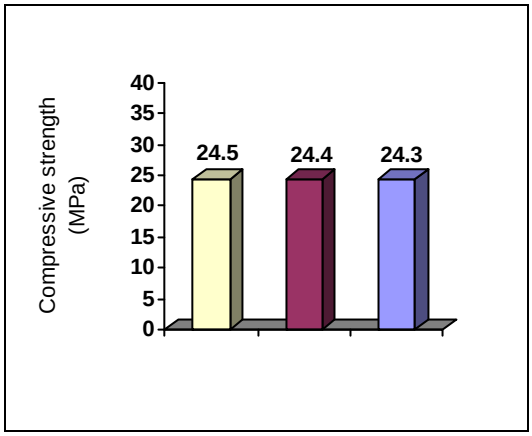

Figure 5: Variation of recycled concrete compressive strength for design strength 21 MPa (Reference-Table 4), FM=1.2.

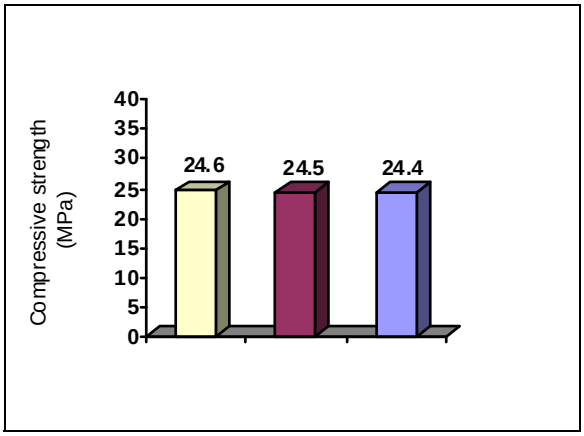

Figure 6: Variation of recycled concrete compressive strength for design strength 21 MPa (Reference-Table 5), FM=1.25.

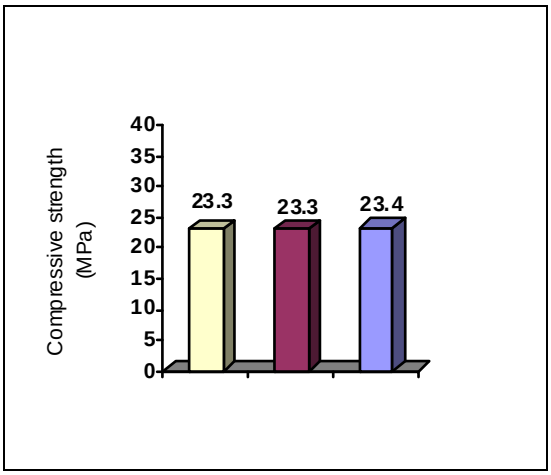

Figure 7: Variation of recycled concrete compressive strength for design strength 21 MPa (Reference-Table 6), FM=1.3.

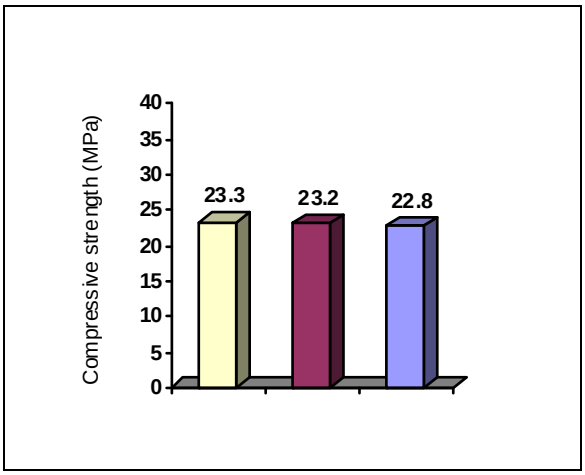

Figure 8: Variation of recycled concrete compressive strength for design strength 21 MPa (Reference-Table 7), FM=1.4.

For FM = 1.2, Avg. compressive strength of recycled concrete is found 24.4 MPa (Figure 5). That is 16.2% higher than design strength. For FM = 1.25, Avg. compressive strength of recycled concrete is found 24.5 MPa (Figure 6). That is 16.67% higher than design strength. For FM = 1.3, Avg. compressive strength of recycled concrete is found 23.3 MPa (Figure 7). That is 10.95% higher than design strength. Similarly, For FM = 1.2, Avg. compressive strength of recycled concrete is found 23.1 MPa (Figure 8). That is 10% higher than design strength.

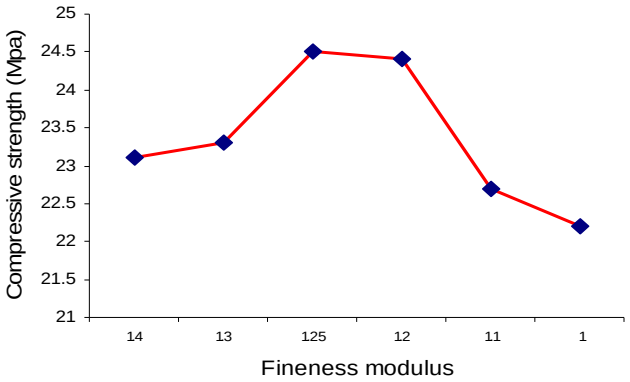

Figure 9: Variation of recycled concrete compressive strength with different value of fineness modulus

For design 21 MPa compressive strength, all the six FM Value (1.0, 1.1, 1.2, 1.25, 1.3 & 1.4) are satisfied, but among of this FM = 1.25 gives maximum compressive strength of 24.5 MPa is 16.67% higher than design strength.

CONCLUSION

The compressive strength of concrete made by recycled coarse aggregate with fine aggregate of fineness modulus value of 1.25 gives the maximum compressive strength by ACI method of mixed design. By using recycled coarse aggregate it could be possible to minimize the costing of recycled concrete up to around 40%.

REFERENCE

Shetty, M.S, “Concrete Technology”.

Neville, A.M, “Properties of Concrete (Fourth Edition)”.

Aziz M.A. Ph D, “Engineering Materials”, First edition, revised August 5, 1995.

Orchard D.F, “Concrete Technology (Vol-1) by Applied Science” UK 1973.

ACI Manual of concrete practice, part-1, Materials of general properties of concrete, 68pp. (Detroit, Michigan, 1994).

ACI 116R-90, “Cement and Concrete technology”.

ACI 211.1; BS 1881: Part 110:1983; ASTM C 192-90a.

Uddin M.T. “Recycling of Demolished Concrete as Coarse Aggregate”, (2006).

Watford, “The use of Recycled Aggregate in concrete, Information paper 4pp, (England 1994).

Lauritzen, E.K, “Demolition and reuse of concrete and masonry”, 1994.

Richardsons, “D.N Review of variables that influence measured concrete compressive strength”, Journal of Materials in civil Engineering. 3. No.2 pp.95-112 (1991).

Mcintosh, J.D., “The Siphon-can test for measuring the moisture content of aggregates”, (1955).

Popovics. S. , “The use of fineness modulus for the grading evaluation of aggregates for concrete”.

Biswas S, Lecturer, Department of Disaster & Environmental Engineering, CUET, Bangladesh, “An Investigation on Recycling of Demolished Concrete”.

Ullah M. S., Undergraduate thesis, Department of Civil Engineering, CUET, Bangladesh, “An Investigation on Recycling of Demolished Concrete”.

ID : ASEE 040

1st International Conference on Advances in Civil Engineering 2012 (ICACE 2012)
12 –14 December 2012
CUET, Chittagong, Bangladesh

SEISMIC PERFORMANCE OF STEEL AND RC FRAME BUILDINGS DESIGNED USING DIFFERENT R-VALUES

A. SAADAT [1] & M. BEGUM [2]

[1]*Lecturer, Department of Civil Engineering, Military Institute of Science and Technology, Dhaka-1216, Bangladesh, anwarsaadat@yahoo.com*
[2]*Associate Professor, Department of Civil Engineering, Bangladesh University of Engineering and Technology, Dhaka, 1000, Bangladesh, mahbuba@buet.ac.bd*

ABSTRACT
Seismic capacity of a building can be defined as the capacity of absorbing base shear coming onto it due to an earthquake. Ductile structures are more capable of absorbing earthquake base shear. In Dhaka city day-by-day the land scarcity is increasing thus the need of high rise structures is increasing too, so cautious selection of structural system is necessary. This study focuses on the seismic behaviour analysis and comparison between concrete and steel structures of three-, six-, ten-storied designed with different response modification factor *R* (8,9, 10 & 12). In this study comparison of the behavior of steel and concrete buildings of same story height was done by pushover analysis designed with same response modification factor *R*. Developed pushover curves plotted for the response shown by each kind of buildings allowed to compare the performance of different structural systems on the basis of story heights and response modification factor, *R*. The results of the study show that steel buildings are better than concrete buildings with the increasing story of buildings. Ductility of the steel building increases with the increase of story although for concrete buildings ductility decreases with the story increase. The response shown by the frames can be used on decision making procedure when comparing steel and concrete frames on the basis of seismic performances.

Keywords: Roof Displacement Angle, Seismic Behaviour, Response Modification Factor, Ductility

INTRODUCTION

Realistic evaluation of the magnitude of the maximum earthquake force at a site encounters many uncertainties and difficulties. There are different methods described in different codes to simplify the analysis of a structure for seismic load and to cope with the seismic hazard. Pushover analysis is a static, nonlinear procedure in which the magnitude of the structural loading is incrementally increased in accordance with a certain predefined pattern. In this study pushover analysis is used for the seismic behaviour analysis and comparison between concrete and steel structure. Capacity of each building on undergo deflection before collapse due to the earthquake force coming over them can be examined by observing the Roof displacement angle caused due to the pushover force coming into it. Currently, seismic design regulations for the buildings in the Bangladesh have used a simplified procedure for achieving acceptable performance. This procedure calculates the design base shear by mainly reducing linear elastic response spectra by the response modification factor *R*. Then, member forces are determined throughout the linear elastic analysis. Usually for Moment Resisting Frame Systems such as IMRF, OMRF and SMRF type of buildings values of *R* are used 5, 6, 8 and 12 in BNBC-1993. While the *R* factors prescribed in the seismic codes are intended to represent the energy-absorbing capacity, ductility capacity, and other factors, the *R* factors tabulated in the current seismic codes are

primarily based on observation of the performance of different structural systems in previous strong earthquakes (Miranda and Bertero 1994). Many researchers have also shown concern with the lack of rationality for determining the values of *R* factors prescribed in different seismic codes (Miranda and Bertero 1994; ATC 1995; Foutch and Shi 1998). In this study based on different seismic response modification factor, *R* (8, 9, 10 and 12) obtained pushover response curves can be useful for evaluating the seismic modification factor imposed upon them by examining their behaviour to a real time earthquake. This study mainly intends to compare the performance of these two kind of structural systems on the basis of their structural response on an earthquake. Similar type of study was done by Lee and Foutch (2005) on steel structures to evaluate the performance of steel frames after Northridge earthquake (1994) at Reseda, L.A., California, USA with the variation of response modification factor *R*. Objectives of the thesis can be summarized as, 1) To compare the performance of steel and concrete buildings of same story height subjected to pushover analysis designed with same response modification factor *R*. 2) To investigate the performance of steel and concrete buildings of a fixed story height due to the variation of response modification factor *R*. 3) To observe the performance of steel and concrete buildings of a fixed value of response modification factor *R* with the variation of story height.

METHODOLOGY

Three dimensional finite element analyses for typical building frames were performed using ETABS 9.6. Only the bare frames of the building structures were modelled. The numbers of stories used are 3, 6, 10 & 15. These buildings were analysed and designed with two different framing systems: RCC frames and Steel frames. The description of the building frames, loading conditions and design codes followed are included in the following sections. Seismic behaviour of RCC and Steel framed buildings were evaluated by push over analysis. The results of different frames were compared.

Description of the Structures

Two types of structures steel and concrete were used as specified before. Their story height was variant in different stages of the study. All structures are 4×3 bay building; length of each bay is 7.32m in X-direction and 9.14m in Y-direction. Floor height of each floor was 3.048m except the ground floor height was 1.8288m. For the concrete building dimensions of floor beams and grade beams and columns varied according to the story height and for different R values. Members were designed by ETABS. Figure 1 and figure 2 provided below shows the typical plan view of concrete and steel buildings.

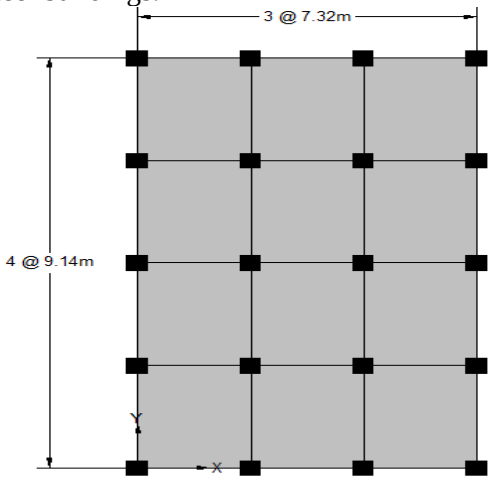

Figure: 1 Plan view of the concrete building

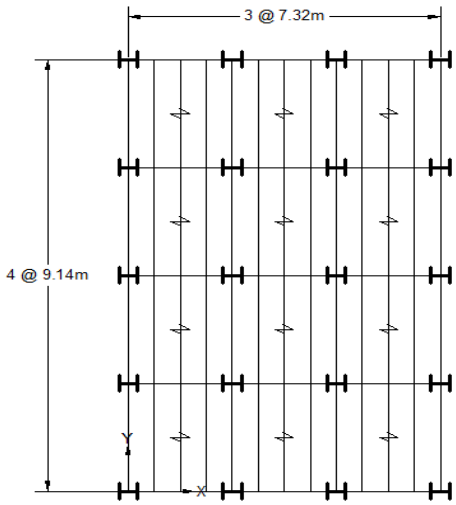

Figure: 2 Plan view of the steel building

The steel and concrete buildings were designed according to the AISC-2005 and BNBC-1993 respectively.

Loading Conditions

Self-weight was calculated automatically by the program. With self-weight, 1.4364 kN/m^2 of floor-finish and 1.4364 kN/m^2 of future partition wall were considered as dead load in typical floor level. In the typical floor Live load was considered as 2.8728 kN/m^2. Live load and dead load is given as gravity load. For seismic dead load, 25% of the live load is added to total dead load. Seismic response modification factor R=5~12 was considered. Other coefficient used as, Seismic zone coefficient, Z = 0.15 for Zone 2; Structure importance coefficient, I = 1.00 and Site coefficient, S = 1.5.

Material Properties

Concrete material used in the design of RC beam and column having the properties, Cylinder strength of concrete, f'_c= 28 MPa; Yield strength of concrete, f_y = 415 MPa; Modulus of elasticity, E_c = 24820 MPa .Standard steel bar is used as reinforcing material. Steel material used in the design of steel beams and columns having the properties, Yield strength of steel, f_y= 345 MPa; Tensile strength, f_u= 448 MPa; Modulus of elasticity, E_c = 199950 MPa.

RESULTS AND DISCUSSIONS

The force and displacement relationship were plotted in terms of the seismic base shear coefficient and top story drift angle. The seismic base shear coefficient was calculated for the ratio of lateral force to structural seismic weight. The top story drift angle was obtained for the top floor displacement divided by the total height of the structure. The comparison of the curves produced by pushover analysis was based on,

1. Comparison between steel and concrete building systems of same story for different R-values.
2. Effect of number of story for a fixed R-value.
3. Effect of R-values on a fixed number of stories.

For all structures after modeling, the structures were designed properly and then their performance under seismic condition was evaluated for the bare frame through pushover analysis.

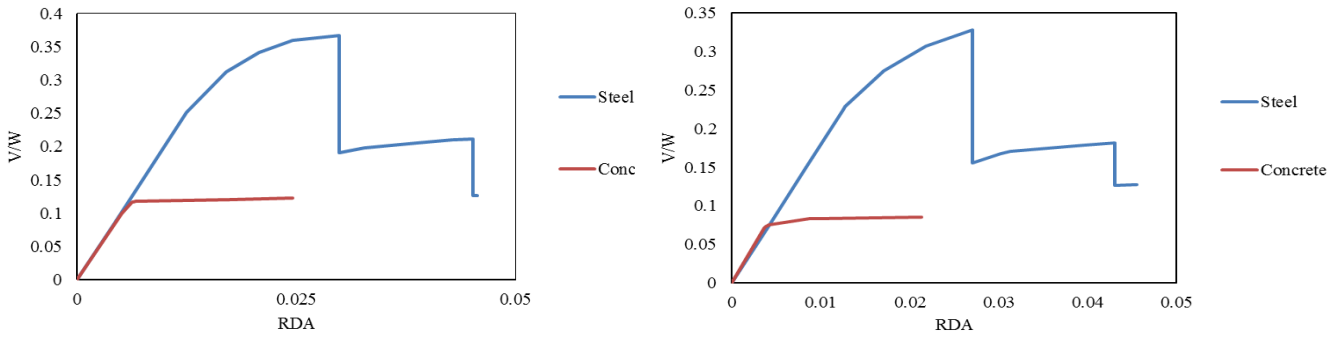

Comparison between steel and concrete building systems of same story for different R-values

For this comparison pushover curves of three-story, six-story and ten-story for R-values 5 and 12 were taken. Obtained curves are shown below,

(a) (b)

Figure 3: Comparison between three-storied buildings for (a) R=5 & (b) R=8

From the figure above it's observed that,

- Initial stiffness of both of the buildings was nearly same.
- There is large difference between the peak values of normalized base shear of the steel building and concrete building curve. For the value of R=8 the peak difference was 74%

and 66% for R=5. It means the energy absorption capacity of the steel building is higher than the concrete building.

The deflection undertaken by steel building was higher than the concrete building, the percentage difference of roof drift angle between steel and concrete building for R=8 was 21% and for R=5 it's 17%. Similar types of curves were observed for six-story and ten-story buildings.

Effect of Story height for a fixed value of R

Effect of story height on the pushover curve for a fixed value of R was investigated for steel buildings and concrete buildings separately, for three-, six-, ten- and 15-storied buildings with R-values 5, 8 and 12. For example the obtained curves for steel and concrete buildings for R= 8 are presented below,

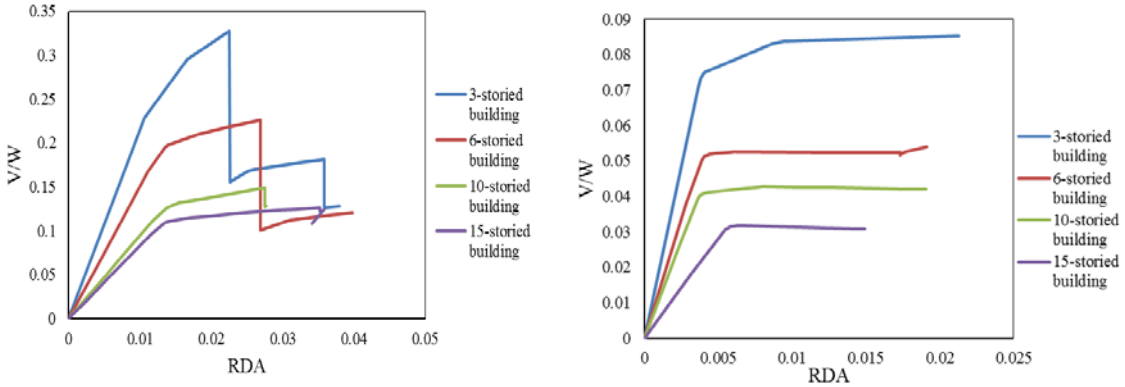

(a) (b)

Figure 4: Comparison between different storied buildings of steel and concrete for R=8

From the curves presented above the observations can be listed as,

- For a fixed value of R the capacity of absorbing base shear ascends in a descending manner with story height.
- The roof drift angle sustained by any building before initial failure was increasing with the increase of story height.
- Ductility observed before initial failure of the buildings increased with the increasing number of building height.

From the curves obtained for 3-, 6-, 10- and 15-storied concrete buildings for R=5, 8 and 12 the observations are similar to the steel buildings except that, difference in roof drift angle is not very prominent. Strength of lower storied building was always higher to with take the base shear coming on to it.

Effect of value of R for a fixed story height

Variation in pushover curve for R=5, 6, 8, 9, 10, 11 & 12 on three-story and ten-story steel and concrete buildings were compared. Obtained curves for three-storied buildings are shown in Fig-5. From the curves presented above it's observed that increasing the *R* factor from 8 to 12 leads to a decrease in the stiffness and strength. This is because the building designed with an *R* factor of 8 must have much larger member properties and joint configurations compared to the building designed with an *R* factor of 12 due to the large base shear incorporated into the design.

While comparing concrete and steel buildings of same story for different R-values it was observed that the capacity of steel buildings to withstand base shear was higher than the concrete buildings. Investigation of the performance of story height for a fixed R-value showed that structures of lower story are more capable of absorbing base shear before initial failure than the higher storied buildings. For the variation of R-values from 5~12 the characteristics of a building of fixed height shows that, the increase of R values decreases the strength of a building of fixed height.

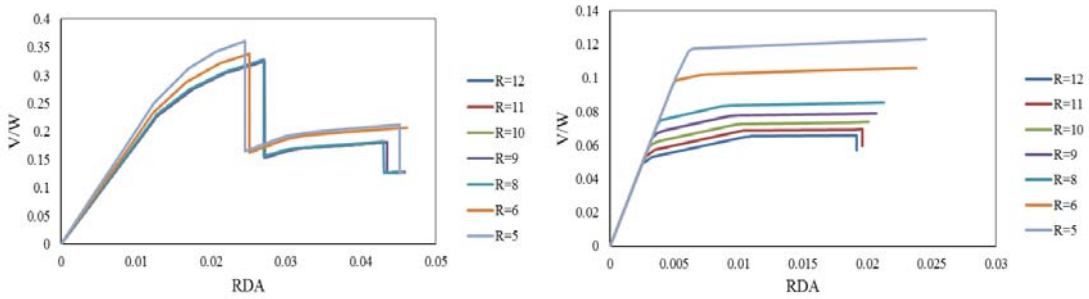

a) (b)

Figure 5: Comparison among three-storied building for different R-values (a) steel and (b) concrete

CONCLUSION

A total of 20 buildings were designed and analyzed to evaluate the results of the *R* factor variations, story variations and the variations of structural systems. These structures can be considered to be representative of regular steel and concrete structures and provide a general idea of the behavior and response to be expected when designed with larger *R* factors and the effects of the other variations. This may be more likely to occur for a building with plan or mass and/or stiffness irregularity, which are not considered in this study. In addition, a real building is a three-dimensional structure and horizontal and vertical ground motions occur simultaneously. These issues are beyond the scope of this project.

The findings of the study can be summarized as,

1. Response of steel buildings to earthquake base shear is better than concrete buildings in case of an earthquake.
2. Decreasing the *R* factor value leads to greater strength and stiffness as larger base shear incorporated in the design.
3. Performance of a steel building gets better when comparing with a concrete building when the story height increases.
4. Ductility and stiffness of the steel structure was seen in an increasing manner with the increase of story height but for concrete structures it was decreasing with the increase of story height.

REFERENCES

Applied Technology Council (ATC). 1995b. ‘‘A critical review of current approaches to earthquake-resistant design.’’ *Rep. No. ATC-34*, Redwood City, Calif.

Bangladesh National Building Code (BNBC) 1993. “Response Modification Coefficient for Structural Systems, *R.*”*House Building and Research Institute*, Mirpur, Dhaka, Bangladesh.

Foutch, D. A., and Shi, S. (1998). “Effects of hysteresis types on the seismic effects of buildings.” *Proc., 6th U.S. National Conf. on Earthquake Engineering*, Seattle, Earthquake Engineering Research Institute, Oakland, Calif.

Lee, K. and Foutch, D.A., 2006. “Seismic Evaluation of Steel Moment Frame Buildings Designed Using Different *R*-Values” *J. Struct. Eng.*, 132(9).

Miranda, E., and Bertero, V. V. _1994_. “Evaluation of strength reduction factors for earthquake-resistant design.” *Earthquake Spectra*, 10(2), 357–379.

DESIGN OF STEEL-CONCRETE COMPOSITE DECK SLAB

R.T.NAZMUL[1] & M.BEGUM[2]

[1]*Lecturer, Department of Civil Engineering, Stamford University, Dhaka-1000, Bangladesh,tasnuva.nazmul@gmail.com*

[2]*Associate Professor, Department of Civil Engineering, Bangladesh University of Engineering and Technology, Dhaka-1000, Bangladesh, mahbuba@ce.buet.ac.bd*

ABSTRACT

The composite construction with steel and concrete is a relatively new concept in Bangladesh. The demands for steel and composite construction for medium to high rise buildings in Bangladesh are increasing now days. To meet the demand of the construction industry the designers are required to have fair knowledge about the construction of steel concrete composite deck slab which is primarily the gravity load resisting system for steel as well as composite buildings. An attempt has been made in this study to present a brief description of the components of steel concrete composite slab followed by a step by step design procedure of composite slab according to the AISC code. Finally a simplified analytical tool for the design of composite slab is developed using Microsoft Excel and the programming language C++. The spreadsheet in MS Excel accepts information about the applied loads, the dimensions of the floor, member sizes and material strengths and strength factors from the user. Given the above information, the spreadsheet then calculates cross-sectional properties such as the location of neutral axis, the section's transformed moment of inertia and section modulus, as well as its bending moment and shear capacity in a step-by-step procedure according to established codes and standards. The programming language C++ was used for the rapid evaluation of the optimum cross-section for the structural components of the deck slab through several iterations..

INTRODUCTION

One of the recent developments in the structural system is the innovation of composite structure. Design of composite steel and concrete structures has become an essential component of engineering due to the widely popular use of the two materials in construction. The high tensile resistance of steel and the compression strength of concrete complement each other in construction and their combination makes for highly efficient design. However, the full development of composite beam system began with the invention of shear connectors which are located at the top flange of a steel section and embedded into the concrete slab. Shear connectors ensure the composite action between the steel and concrete and ensure the best use of the properties of the individual materials. They have an ideal combination of strength with concrete efficient in compression and steel in tension. Additionally, a composite beam has greater stiffness and usually a higher load resistance than its separate components. As a result, there is a reduction not only in the size of the steel section but also in the concrete slab depth required when compared with a non-composite design. Hence this new floor system has many advantages in construction such as reduced construction time, lighter weight of structure and cost savings because the sheeting acts as both permanent formwork and tensile reinforcement. Therefore some of the disadvantages of composite section design can be the extra cost of shear connector and their presence as a tripping hazard during construction. Also, during service, the vibration of the floor/deck may sometimes be an issue due to the shallow depth of the sections. Finally, design of composite sections requires more engineering time and effort. The objective of this thesis is to develop simple and easy to use tools to allow rapid engineering calculation and documentation. Previously Azimkor N.(2010) worked on steel-composite deck slab and developed a program on visual basic programming language. As such, a spreadsheet has been developed that takes user input information with regards to loads and dimensions of the section and performs step-by-step analysis to aid with design. For the purposes of very quick analysis another code has also been developed using C++ programming language. This paper also provides a general overview of the theory behind

composite design and construction. The approach taken to develop the above design tools is discussed. Thereafter, an overview of the step-by-step design procedure outlined in the spreadsheet according to AISC (2005) guidelines is provided. The directions for use and the limitations of the developed design tool are also discussed.

METHODOLOGY

Composite section design can be a time consuming process with many steps involved in calculating shear transfer between the materials and full and partial moment resistance for a given section. Therefore a well-laid-out spreadsheet or a computer program would be an asset to any engineer who completes composite section design on a regular basis. Although limit state design requires checks for both ultimate limit state and serviceability limit state, the focus of this paper has been on ultimate limit states. The paper presented here discusses and provides a flow chart of the program code developed in excel or in the C++ programming language. Both the Excel worksheet and C++ programming language code accept user input for material properties and geometric data. The Excel spreadsheet also works for specified loads and calculates factored applied bending moment and shear. The main goal was to obtain:

1. Effective width of concrete slab, b_{eff}
2. Moment resistance of composite section, M_r
3. The number of required shear connectors in longitudinal and transverse direction.

In addition to the above outputs, the Excel spreadsheet performs checks to ensure conditions during construction are satisfactory and the allowable dead load and live load deflections and allowable limit of spacing of shear connectors. Major outputs of this worksheet are highlighted for clarity. The following section after the material limitations explains in detail each analysis step as laid out in this worksheet.

Material limitation

Concrete and steel reinforcing bars in composite systems shall be subject to the following limitations.

1. For the determination of available strength, concrete shall have a compressive strength (f'_c) of not less than 3 ksi (21 MPa) nor more than 10 ksi (70 MPa) for nominal weight concrete and not less than 3 ksi (21 MPa) for light weight concrete.
2. The specified minimum yield strength of steel and reinforcing bars used in calculating the strength of a composite column shall not exceed 75 ksi (525 Mpa).

Preliminary section

For the preliminary selection of section first it is necessary to calculate the specified loads. The construction of composite section consists of the following three major steps such as:

Stage 1: Steel beams/ girders are installed. Here, the steel member must have enough capacity to withstand its own weight.

Stage 2: Decking and/or formwork is laid above the steel beams and wet concrete is poured. At this stage, the steel member and the concrete slab are still in non-composite action since concrete has not yet hardened. As such, the steel member must hold up its own weight as well as the live loads during construction due to the placement of decking/formwork and pouring of the concrete slab.

Stage 3: Concrete has hardened and acts together with steel. Finally, once concrete has hardened at the third stage, steel member and the concrete slab must resist all specified loads in composite action.

During stage 1 and 2, the steel beam is treated like a temporary structure and so must be strong enough to withstand its own weight as well as the weight of the wet concrete. Work Safe boundary conditions require that all temporary structures have capacity to resist a minimum of 2 kPa construction live load. This construction live load may require the selection of deeper steel section for construction purposes even though a shallower member would suffice once composite action is achieved. This may be a source of inefficiency in design where shallower members are crucial.

After calculating the specified loads, the factored applied moment and shear are calculated according to the provisions of American Institute of Steel Construction, Inc. and using the live and dead load factors as appropriate. These factored applied moment and shear are used in the analysis section to assess the strength of the section in composite action. Moments due to specified loads (factored) during phases 1, 2 and 3 of construction as previously discussed are calculated in this section. These factored applied moments are then used in combination with the transformed section modulus to determine stresses during each construction phases. It is then ensured that the sum of these stresses does not exceed the yield strength of steel.

Calculation of Effective width

For practical purposes, an equivalent width may be defined over which the stresses are assumed to be uniformly distributed. According to AISC (2005) specification, the effective width of concrete slab is the sum of the effective width for each side of the beam centerline, each of which shall not exceed:

(1) $\frac{1}{8}$ th of the beam span, center to center of supports;
(2) $\frac{1}{2}$ the distance to the centerline of the adjacent beam; or
(3) The distance to the edge of the slab.

Composite beam selection table

The table 3-19 of AISC manual (AISC 2005) can be used to design composite beams by entering with required flexural strength and determine the required $\sum Q_n$. With the effective width of the concrete flange determined, the appropriate value of the distance from concrete flange to beam top flange Y_2 can be determined as

$$Y_2 = Y_{conc} - \frac{a}{2} \qquad (1)$$

Where Y_{conc} = distance from top of the steel beam to top of concrete, in.

$$a = \frac{\sum Q_n}{0.85 f'_c b} \qquad (2)$$

The available flexural strength $\emptyset_b M_n$ can be determined from the AISC manual table 3-19, value for the distance from PNA to the top beam flange are also tabulated. The parameters are illustrated in the following figure.

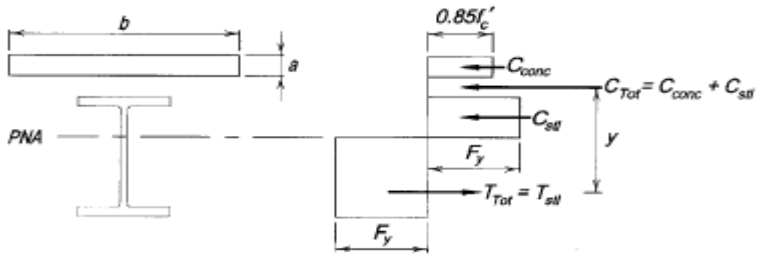

Fig. 1 Mechanics of forces in composite deck slab

Check for selected section

Check for deflection

AISC (2005) specifies allowable deflection for construction dead load is less than or equal to 2.5 in. To limit the deflection to maximum 2.5 in, the I_{req} can be calculated as follows

$$I_{req} = \frac{5W_{DL}l^4}{384E\Delta} \quad (3)$$

Now from AISC manual Table 3-20, for the selected section determine the moment of inertia, I of the section and check whether the section satisfies the required criteria. If this section does not satisfy the deflection criteria under construction then choose the required section.

Check for construction and service loading

During stage 1 and 2, the steel beam is treated like a temporary structure. To check whether this section is ok for stage 1 or not, calculate the factored load and moment using the following equations

$$Wu = 1.2DL + 1.6LL \quad (4)$$

$$M_u = \frac{wl^2}{8} \quad (5)$$

Where, l is the length of the span.

Now the stresses at the top and bottom flange are calculated by using equations

$$\sigma = \frac{Mc}{I} \quad (6)$$

Where, c = distance of top/bottom flange from the neutral axis

In stage 2, the decking and formwork is laid above the steel beam and wet concrete is poured. So the steel beam has to take

- Its self-weight
- The deck slab weight
- The weight of wet concrete
- The construction live load

The moment and shear are calculated as the previous section and the stresses of top and bottom flange of steel section are calculated as earlier and checked whether the section is ok or not at stage 2.

Check 'a'

At first when selecting the section, a reasonable value of 'a' was assumed, the fictitious depth of compressive stress in the concrete flange for computation of Y2, distance from top of steel beam to the concrete flange force. From the calculated value of Y_2 and the moment on the composite section on stage 3, select the section for appropriate PNA location. Now for that PNA location and the value of Y_2 previously calculated, determine the value of $\sum Q_n$ from table 3-20. With the value of $\sum Q_n$, calculate the 'a' with the following formula,

$$a = \frac{\sum Qn}{.85f'_c b} \qquad (7)$$

and check whether it complies with the assumed value.

Check for live load deflection

Allowable live load deflection specified by AISC (2005) is $\Delta_{LL} = \frac{\text{Span}}{360}$

Determine the Lower Bound Elastic Moment of Inertia, I_{LB}, for plastic composite section from table 3-20 (AISC 2005) for the selected PNA location and calculated value of Y_2. Now calculate the actual live load deflection on the slab by using the following equation,

$$\Delta = \frac{5W_{LL}l^4}{384EI} \qquad (8)$$

And check whether this deflection value comply with the allowable limit or not.

Determination of number of shear connectors

The entire horizontal shear at the interface between the steel beam and the concrete slab shall be assumed to be transferred by the shear connectors. For composite action with concrete subject to flexural compression, the total horizontal shear force V', between the point of maximum positive moment and the point of zero moment shall be taken as the lowest value according to the limit states of concrete crushing, tensile yielding of the steel section, or the strength of shear connectors:

a) concrete crushing $V' = 0.85f'_cA_c$
b) tensile yielding of steel section $V' = F_yA_s$
c) Strength of shear connectors $V' = \sum Q_n$
   Where, $\sum Q_n$ =sum of nominal strength of shear connectors between the point of maximum positive moment and point of zero moment, kips

In continuous composite beams where longitudinal reinforcing steel in the negative moment regions is considered to act compositely with the steel beam, the total horizontal shear force between the point of maximum negative moment and the point of zero moment shall be taken as the lower value according to the limit states of yielding of the steel reinforcement in the slab, or strength of the shear connectors:

a) Tensile yielding of the slab reinforcement $V' = A_rF_{yr}$
   Where, A_r = area of adequately developed longitudinal reinforcing steel within the effective width of the concrete slab, in^2
   F_{yr} =specified minimum yield stress of the reinforcing steel, ksi
b) Strength of shear connectors
   $V' = \sum Q_n$

Shear connector placement and spacing

Shear connectors required on each side of the point of maximum bending moment, positive or negative, shall be distributed uniformly between that point and the adjacent points of zero moment, unless otherwise specified. AISC (2005) specifies that

1) Shear connectors shall have at least 1 in (25 mm) of lateral concrete cover, except for connectors installed in the ribs of formed steel decks.
2) The diameter of the studs shall not be greater than 2.5 times the thickness of the flange to which they are welded, unless located over the web.

3) The minimum center to center spacing of stud connectors shall be six diameters along the longitudinal axis of supporting composite beam and four diameters transverse to the longitudinal axis of supporting composite beam.
4) The maximum center to center spacing of shear connectors shall not exceed eight times the total slab thickness nor 36 in.

From the above specifications determine the appropriate number of shear studs to comply with the specification.

Check for serviceability

Cracking of concrete

The profiled deck sheeting protects the lower surface of the slab. Cracking will occur in the top surface where the slab is continuous over a supporting beam in the hogging moment regions. Crack width will be wider over the supports if each span of the slab is designed as simply supported, rather than continuous, and if the spans are propped during construction. To counter cracking, longitudinal reinforcement should be provided above internal supports according to the code provision (EN 1994).

Strength of the composite beam with formed steel deck

The available flexural strength of composite construction consisting of concrete slabs on formed steel decks connected to steel beams has the following requirements:

- the deck normal rib height must not be greater than 3 in(75mm). the average width of concrete rib shall not be less than 2 in.(50 mm), but shall not be more than the clear width near the top of the steel deck.
- The concrete slab shall be connected to the steel beam with welded stud shear connectors ¾ in(19 mm). Studs shall be welded directed through the deck or directly to the steel cross section. Stud shear connectors, after installation, shall extend not less than 1.5 in(38mm) above the top of the steel deck and there shall be at least ½ in(13 mm) of concrete cover above the top of the installed studs.
- The slab thickness above the steel deck shall not be less than 2 in(50 mm).
- Steel deck shall be anchored to all supporting members at a spacing not to exceed 18 in(460 mm)
- For deck ribs oriented perpendicular to steel beam Concrete below top of the steel deck shall be neglected in determining composite section properties.
- For deck ribs oriented parallel to the steel beam concrete below top of the steel deck may be included in determining the section properties and shall be included in calculating A_c.

FLOW CHART

In this section the developed process for the excel program and the C++ program is presented through flow charts as given below,

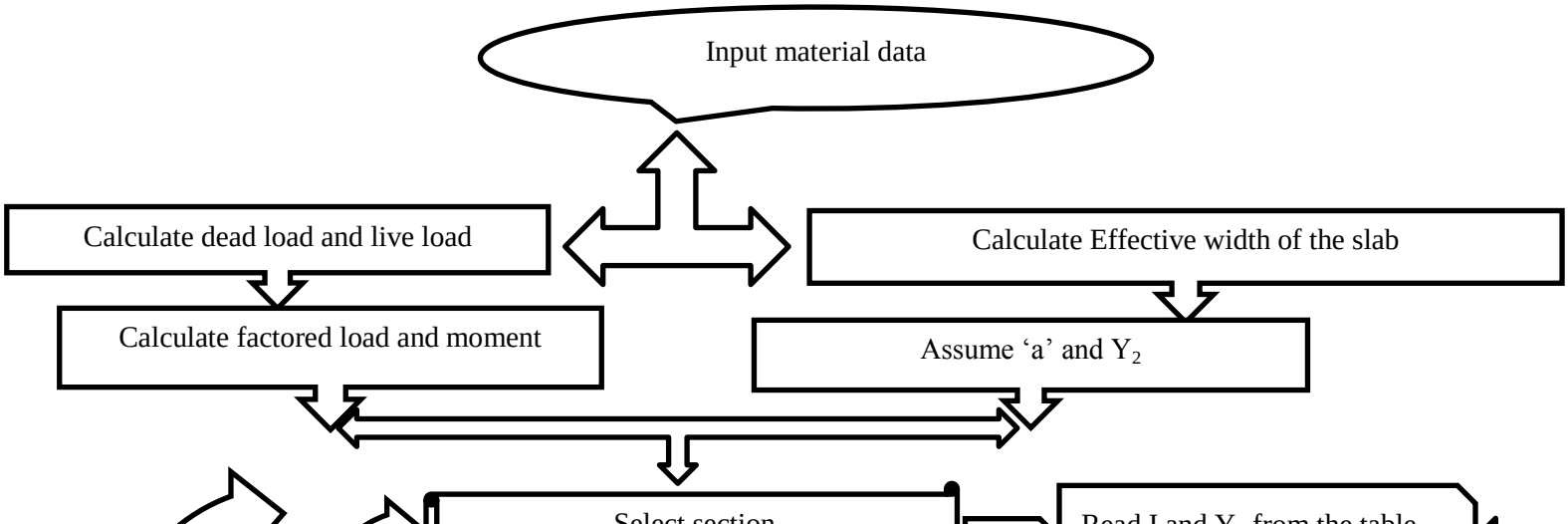

if ok

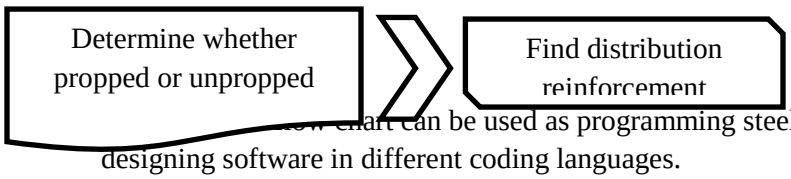

low chart can be used as programming steel-concrete composite deck slab system designing software in different coding languages.

DESIGN EXAMPLE

The problem presented below has been solved by the developed methodology and the solution and the detailing are given below.

A series of 20-ft. span composite beams at 5 ft. c/c are carrying the loads shown below. The concrete has f'_c = 4 ksi. Secondary beams are perpendicular to the rib. A typical floor beam with a deck rib height of 3 in and 4½ in. normal weight concrete above the deck, is designed here following the developed methodology. The appropriate beam section and the required number of shear studs are also determined. Here the primary beams are connected with the composite columns by fixed connection. And the secondary beams are connected with the primary beams by moment resisting connection. A diagrammatic representation of the problem is given in the following figure.

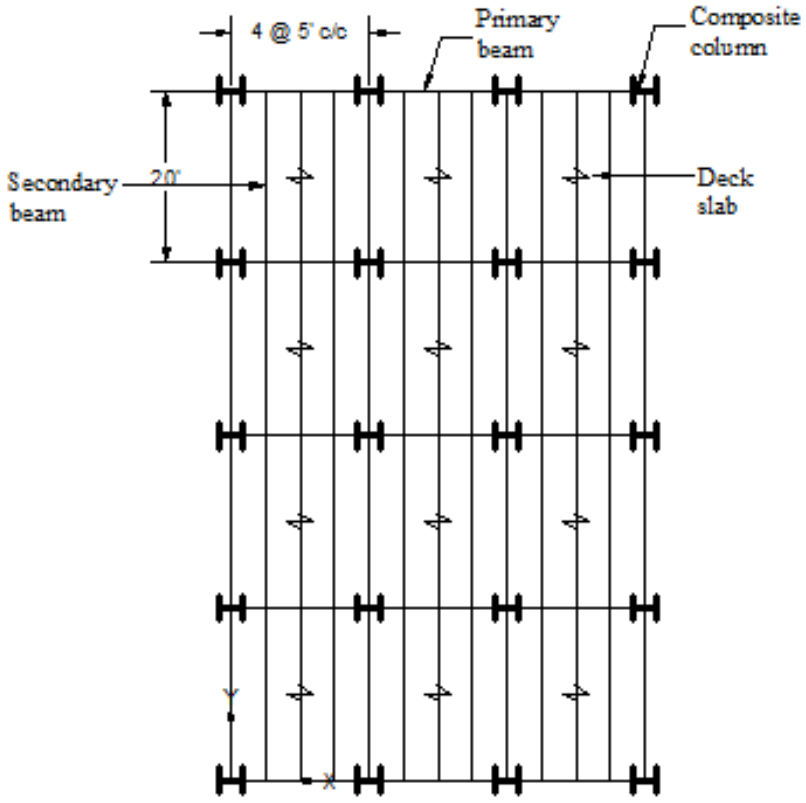

Fig 1. Plan view

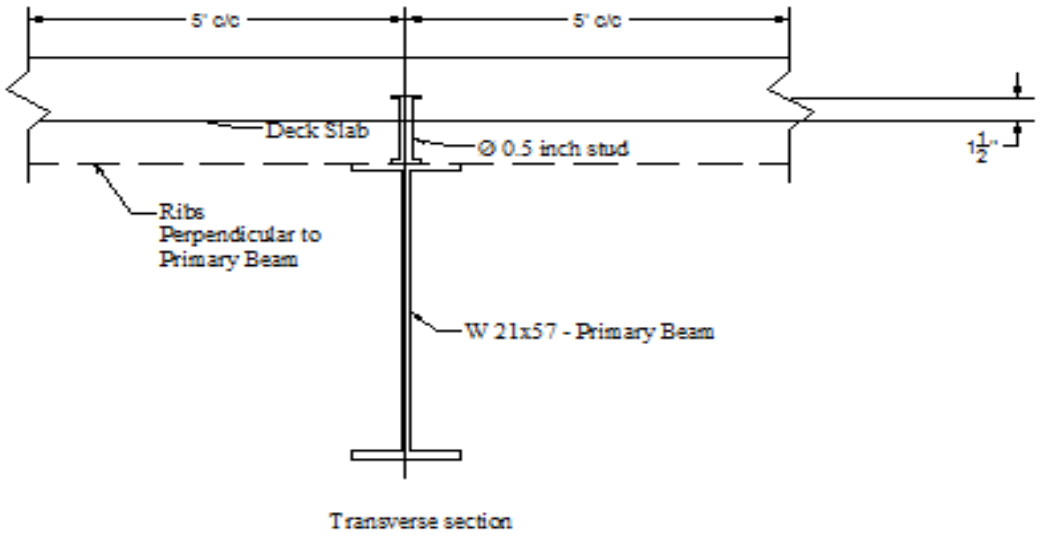

Fig 2. Transverse section of secondary beam

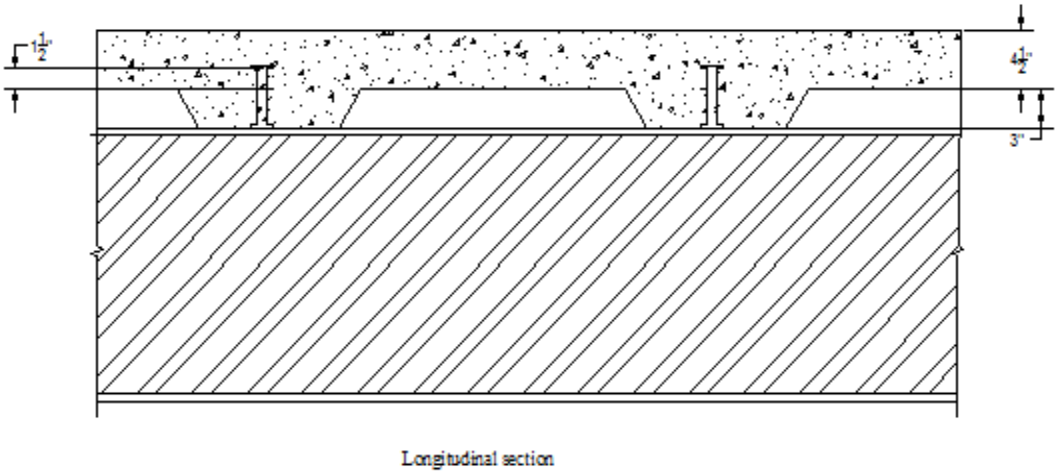

Fig 3. Longitudinal section of secondary beam

CONCLUSIONS

This paper presents a general overview of the theory behind composite deck slab design. The approach taken to develop the above design tools is discussed. These tools provide quick and accurate solutions to calculations that would normally be tedious to complete by hand. However, with all engineering software, the user must be familiar with the fundamental concepts underlying the design of composite sections and

utilize the output of the spreadsheet and the software judiciously. Developed flow chart can be used to develop any kind of programming codes in future for the ease of design of steel-concrete composite deck slab. The limitation of the developed method such as, manual data reading from the charts can be mitigated by more efficient coding which will efficiently find the values on its own. The composite slab design method developed here is for gravity load only.

References

American Institute of Steel Construction, Inc. (AISC) 2005. "Code of Standard Practice for Steel Buildings and Bridges", One East Wacker Drive, Suite 3100, Chicago, Illinois 60601-2000.

American Institute of Steel Construction, Inc. (AISC) 2005. "Design Example Version 13.0", One East Wacker Drive, Suite 3100, Chicago, Illinois 60601-2000.

Azimikor, N. 2010. "Design of Steel-Concrete Composite Decks", *University of British Columbia*, British Columbia, Ca.

EN 1994 - Eurocode 4 1994 "Design of composite steel and concrete structures".

ID : ASEE 043

1st International Conference on Advances in Civil Engineering 2012 (ICACE 2012)
12 –14 December 2012
CUET, Chittagong, Bangladesh

EARTHQUAKE VULNERABILITY OF DHAKA CITY: A CASE OF WARD NO. 36 OF OLD DHAKA CITY CORPORATION (DCC) AREA

N. MORSHED[1*], M. S. SHARIF[2] & A. J. ESA[3]

[1*]*Urban Planner, BETS Consulting Services Ltd., Gulshan-1, Dhaka, Bangladesh.*
<e-mail: nahid_urp06@yahoo.com>
[2]*Lecturer, Khulna University of Engineering and Technology, Khulna, Bangladesh*
<e-mail: sabbir_069@yahoo.com>
[3]*Student, Masters of Urban & Regional Planning, BUET, Dhaka, Bangladesh*
<e-mail: esa_urp844@yahoo.com>

ABSTRACT

Nearly 15 million people of Bangladesh live in capital Dhaka. The development growth trend of Dhaka city is far more faster than other urban areas. Despite this fact there has been little or no awareness about reducing the earthquake associated risks. Because of poor quality of construction and no quality control measures, most of the buildings in Dhaka city are thought to be vulnerable to earthquake. The recently measured plate motions clearly demonstrate that Dhaka is moving 30.6 mm/year in the direction northeast. Further, the rate of strain accumulation is relatively high in and around Dhaka. Dhaka city falls under the zone II of earthquake zones of Bangladesh, where the shocks of intensity of 8.0 are possible. The shallow subsurface of Dhaka is also characterized by number of faults of variable dimensions. These faults are vulnerable to motion where these coincide with the zones of high particle velocity. Several studies shows that nearly 70% structures of Dhaka city will be collapsed with an earthquake of nearly 8.0 intensity with mass number of human loss. Earthquake cannot be prevented. But certainly it is necessary to be concerned about the probable forthcoming of earthquake in order to minimize the loss of lives and property in national interest. The current study tries to analyse the earthquake vulnerability of Ward no. 36 of old Dhaka City Corporation (DCC).

Keywords: Earthquake Vulnerability, Dhaka city.

INTRODUCTION

A sudden, transient motion or trembling in the earth's crust, resulting from the propagation of seismic waves caused by faulting of the rocks either at shallow and/or deeper depths is known as earthquake. The motion is caused by the quick release of slowly accumulated energy in the form of seismic waves. Any physical phenomenon associated with an earthquake that may produce adverse effects on human activities is termed as earthquake hazard. This includes surface faulting, ground shaking, landslides, liquefaction, tectonic deformation, tsunami, and their effects on land use, man-made structures, and socio-economic systems. A commonly used restricted definition of earthquake hazard is the probability of occurrence of a specified level of ground shaking in a specified period of time. Similarly, earthquake risk is the expected (or probable) life loss, injury, or building damage that will

happen, given the probability of earthquake hazard. Earthquake risk and earthquake hazard are occasionally used interchangeably (Khan, 2004).

Bangladesh, by and large, is seismically active. The occurrence of earthquakes with magnitude averaging around 5 in Richter scale is quite frequent especially in its eastern region. Although, Dhaka has not been experienced with any moderate to large earthquake in historical past. In addition, micro-seismicity data also supports the existence of at least four earthquake source points in and around Dhaka. The earthquake disaster risk index has placed Dhaka among the 20 most vulnerable cities in the world. Dhaka with its population of around 15 million and enormous poorly constructed and dilapidated structures signifies extremely vulnerable conditions for massive loss of lives and property in the event of a moderately large earthquake (Khan, 2004). The recently measured plate motions clearly demonstrate that Dhaka is moving 30.6 mm/year in the direction northeast. Further, the rate of strain accumulation is relatively high in and around Dhaka. Dhaka city falls under the zone II of earthquake zones of Bangladesh, where the shocks of intensity of 8.0 are possible. The shallow subsurface of Dhaka is also characterized by number of faults of variable dimensions. These faults are vulnerable to motion where these coincide with the zones of high particle velocity. Several studies shows that nearly 70% structures of Dhaka city will be collapsed with an earthquake of nearly 8.0 intensity with mass number of human loss.

Ward no. 36 of Old Dhaka City Corporation (DCC) contains the areas of Rajarbag Police Line, Chameli Bag, Shanti Nagar, Shanti Nagar Bazar, Purana Paltan, Naya Paltan, Bijoy Nagar and Sayed Nazrul Islam Shoroni. Among the notable establishment, Bangabandhu Stadium and Baitul Mukarrum Masjid are situated within this ward. This study tries to find out the earthquake vulnerability of Ward no. 36 of old Dhaka City Corporation (DCC).

MATERIALS AND METHODS

Related database and information about Ward No. 36 is collected from the Old DCC, currently named as Dhaka South City Corporation (DSCC).

In this study, ‘Likert Scale’ is used to calculate vulnerability of Ward no. 36 of old DCC. Likert Scale is a method of attributing quantitative value to qualitative data. A numerical value is assigned to each potential choice and a mean figure for all the responses is computed at the end of the evaluation or survey. In this study only three variables are used to calculate vulnerability, those are: building type, building condition and building age. All of these three variables are given same weightage and the responses of the variables are given separate point. Then index matrix is generated with the variables and points of each building of Ward no. 36. The final average score represents overall level of vulnerability of each building.

RESULTS

There are 1868 structures are found in the Ward No. 36 area. Most of the structures (37.47%) of Ward No. 36 are one storied. Highest 24 storied structure found in this ward, which is used as Mixed use. Most of these structures are pucca (67.88%) and semi-pucca (25.54%). There are few Katcha (4.28%) and under construction (2.30%) building too. Most of the structures are found in the Santinagar

(21.09%) area. Most of the Katcha (24 nos.) and under construction building (14 nos.) are also situated in Santinagar area. The different locations and types of building structures are shown in Table 1.

Table 1: Location and Types of Structures

Building Type / Area	Pucca	Semi-Pucca	Katcha	Under Construction	Grand Total	Percentage
Bangabandhu Avenue	3	1	-	-	4	0.21
Bijoy Nagar	35	9	5	-	49	2.62
Chamelibag	132	23	11	3	169	9.05
Naya Paltan	112	48	5	2	167	8.94
Naya Paltan Line	143	44	6	5	198	10.60
Purana Paltan Line	246	51	18	7	322	17.24
Purana Paltan Road	195	78	6	8	287	15.36
Rajarbag Police Line	61	5	-	1	67	3.59
Santinagar	282	74	24	14	394	21.09
Santinagar Bazar	28	137	2	2	169	9.05
Sayed Nazrul Islam Soroni	31	7	3	1	42	2.25
Grand Total	**1268**	**477**	**80**	**43**	**1868**	**100.00**
Percentage	67.88	25.54	4.28	2.30	100.00	-

(Source: DCC 2010)

56.10% of the structures are used as Residential purpose. The number of commercial structures (27.73%) and mixed use structures (7.82%) is also very high. Different used of the structure are shown in the Table 2.

Table 2: Different use of the Structures.

Building Use	Total	Percentage
Bank, Insurance	3	0.16
Car House	1	0.05
Commercial	518	27.73
Community Center	3	0.16
Educational	18	0.96
Govt. Organization	34	1.82
Medical & Health Care	11	0.59
Mixed	146	7.82
Non Govt. Organization	1	0.05
Police	16	0.86
Recreational	6	0.32
Religious	18	0.96
Residential	1048	56.10
Social	1	0.05
Stadium	1	0.05
Under Construction	43	2.30
Total	**1868**	**100.00**

(Source: DCC 2010)

Buildings with poor conditions are more vulnerable to earthquake damage. For example buildings that already show visible cracks in the walls probably don't need a large ground shacking to collapse. Likewise the presence of floor cracks differential settlements, dampness on walls are also contributing factor to make a building more vulnerable (Jimee, 2006). Most of the structures are found in good condition (53.48%). But, 4.3% are found Bad condition and 9.31% structures are found in average condition.

Every building has its own natural frequency and swings accordingly during an earthquake. So the building attachment and the floor height coincide will have significant role for damage of buildings during an earthquake. If two buildings have not enough space between them, then they can not swing freely and create pounding effect, which cause local crushing of the structures and failure of structural and non-structural elements located in the zone of impact (Jimee, 2006).

Age of the building also decides the posibility of earthquake. In the study area, it is found that 58.94% structures are constructured within 15 years. 10.2% buildings are found constructued in 30-50 years ago and nearly 2% structures are found constructed before 50 years, which are very old and very much vulnerable for earthquake. Figure 1 shows structure use map of Ward No. 36.

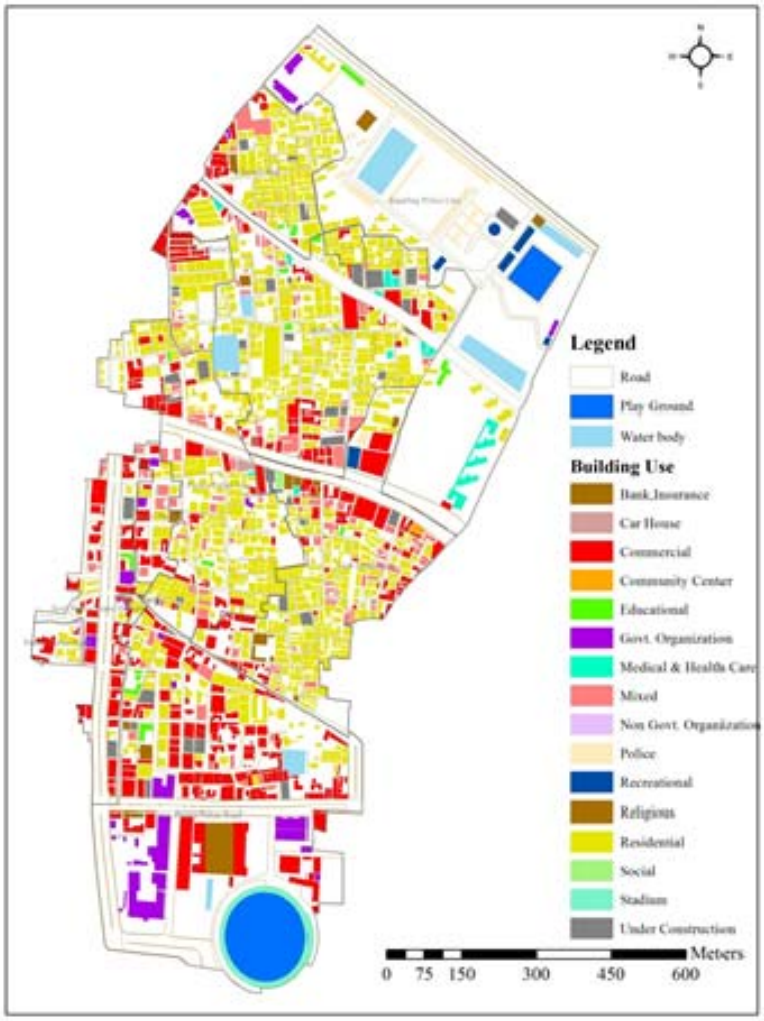

Figure 1: Different use of Buildings in Ward no. 36.

DISCUSSIONS

Building vulnerability to earthquake highly depends on the building characteristics, such as age, construction materials, height, structural elements and existing condition in addition of earthquake intensity and the geology of the site (Jimee, 2006). For this study, building type, condition and age is considered for vulnerability calculation in 'Likert scale'.

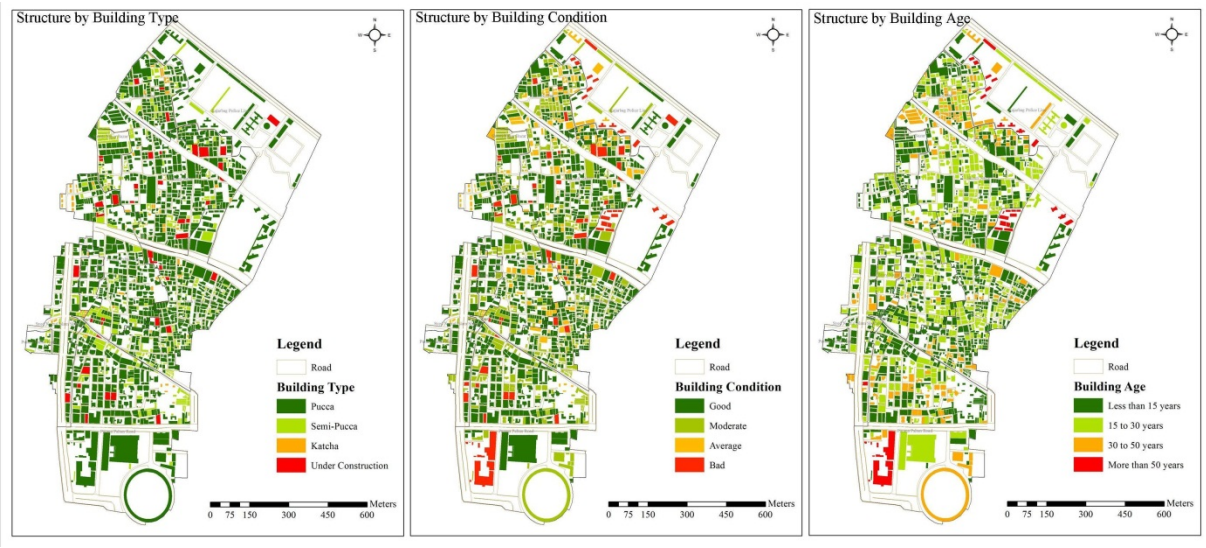

Figure 2: Structures of Ward No. 36 by different category.

Figure 2 shows 3 different maps of Ward No. 3 according to three different variables; i.e. building type, condition and age. The vulnerability matrix is generated by Likerd scale using these three indexes. The probabilities of building damage were calculated taking into account the vulnerability levels calculated from the building characteristics and conditions.

From the index matrix is found that, 4.28% buildings of the study area are vulnerable to earthquake, 44.49% buildings are medium vulnerable and 51.23% buildings vulnerability are Low. Most of the high risked buildings (1.34%) are found in Rajarbag Police Line area, where number of Police colony with bad condition is found. 0.91% building of Purana Paltan Road and 0.8% buildings of Santinagar are found highly vulnerable to earthquake. Vulnerability map is shown in Figure 3.

Table 3: Building Vulnerability of Ward No. 36.

Row Labels	Low	Medium	High	Grand Total
Bangabandhu Avenue	-	1	3	4
Bijoy Nagar	29	20	-	49
Chamelibag	74	92	3	169
Naya Paltan	93	72	2	167
Naya Paltan Line	122	71	5	198
Purana Paltan Line	206	109	7	322
Purana Paltan Road	140	130	17	287
Rajarbag Police Line	24	18	25	67
Santinagar	220	159	15	394
Santinagar Bazar	23	144	2	169
Sayed Nazrul Islam Soroni	26	15	1	42
Grand Total	**957**	**831**	**80**	**1868**
Percentage	51.23	44.49	4.28	100

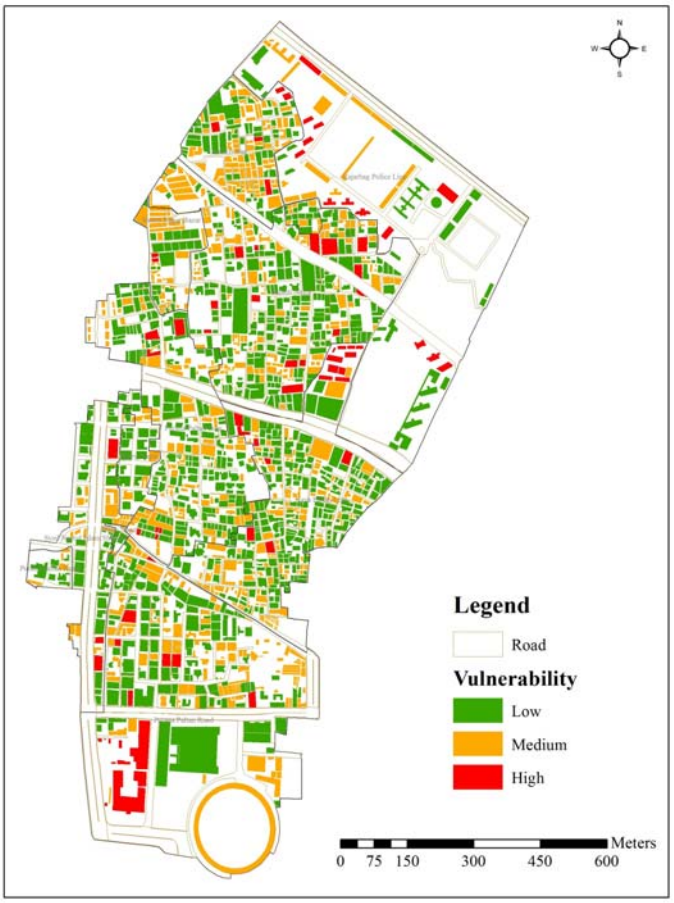

Figure 3: Structure Vulnerability of Ward No. 36.

CONCLUSION

This study was an effort to estimate the vulnerability of individual buildings. The vulnerability of a building highly depends on its condition and other building components in addition to floor height and types. It is important to state here that the approach which was followed is only an assumption, and has clear drawbacks. The behavior of individual buildings under an earthquake is a highly complicated matter, which is the domain of earthquake engineers.

Earthquake cannot be prevented. But certainly it is necessary to be concerned about the probable forthcoming of earthquake in order to minimize the loss of lives and property in national interest. The current study found that, buildings of Dhaka city is highly vulnerable to earthquake. It is of prime importance to practice of earthquake research to develop high skilled manpower that can perform the task for earthquake risk assessment and management.

REFERENCES

Dhaka City Corporation (DCC). 2010. *GIS database of Ward no. 36*. Dhaka.

Jimee G. K. 2006. *Seismic Vulnerability and Capacity Assessment at Ward Level: A Case Study of Ward No. 20, Lalitpur Sub - Metropolitan City, Nepal, Master's* Thesis, International Institute for Geo-Information Science And Earth Observation, Enschede, The Netherlands.

Khan, Dr. A. A. 2004. Earthquake hazard: Dhaka city perspective. *The Daily Star.* Vol. 5 Num 40.

ID : ASEE 044

1st International Conference on Advances in Civil Engineering 2012 (ICACE 2012)
12 –14 December 2012
CUET, Chittagong, Bangladesh

DRIFT MINIMIZATION BY PLACEMENT OF SHEAR WALL

MD. ASSADUZZAMAN[1*], T. RABBEE[1], S. MASUD[1] & MD. N. ISLAM[2]

[1]*Department of Civil Engineering, America Bangladesh University (ABU), Dhaka, Bangladesh*
asad_kuet06@yahoo.com, purnarabbee@yahoo.com, Shadia_masud@yahoo.com,
[2]*Department of Civil Engineering, Rajshahi University of Enginnering &Technology (RUET), Rajshahi, Bangladesh*

ABSTRACT

This paper depict the relation between drift and story number at different position and thickness of shear wall at 10 story residential Building. Due to lateral load, it causes drift (displacement of on level relative to the level above are below). As a huge amount of damage of structure is occur due to excessive drift , hear the structural analysis m of shear wall is performed to minimize the drift by changing the placement and thickness of shear wall. To minimize the drift the beams and columns of the structure have to be of large thickness, which is not economical. So in this case, a shear wall of required thickness and proper placement may reduce the excessive drift caused lateral load. The main objectives of this research is to reduce the excessive drift by proper placement and providing required thickness of shear wall and also to represent the comparison of drift between the structure with or without shear wall. Shear wall resist varies types of forces like as translation shears, rotational shears, horizontal forces on shear wall with opening and uplift forces. In this study the analysis of shear wall has been perform in package program. In this study the software Staad Pro-2004 has been used to analyzed shear wall. Firstly a 10 storied building having a lift core has been selected to carry out the comparative story of height 3.0 m. Two type modeling are performed in this study, one is without shear wall and another wall is with shear wall. Total dimension of the plan is 12.95 m x 10.62m. Thickness of wall is 250 mm and dimension of beam and column are 250 x 375 mm and 450 x 450 mm. At loading condition Environmental load are calculated according to BNBC code. After analysis the both modeling story drift are found out from the analysis output of varying position of shear wall and thickness in modeling. Then plot the graph drift vs. story number without shear wall and with shear wall of varying thickness (6”, 8” and 10”). From graph analyses and mathematical calculation of drift we can find out that a huge amount of drift caused by lateral load can be reduced by providing shear wall at appropriate position and lift core. On the basis of economical consideration 6” thickness shear wall is recommended to control the drift within limit.

Keywords: Drift, Earthquake, Shear, Stiffness, Structure, Mathematical, Modeling

INTRODUCTION

Drift are minimized by providing various structural system. One of them shear wall. In recent years, various drift control methods have been developed for sizing members of lateral load resisting system in tall building to satisfy stiffness criteria. In resizing techniques using energy methods presented v by Baker (1990), Charney (1991) and Wada (1991) the active members which have a relatively high influence on the magnitude of the target displacement to be controlled, are selected and the cross sectional properties of the actives member are modified. Park and park (1997) presented the drift control tool for high rise buildings subjected to lateral forces based on the unit load method. Shear wall have been the most common structural system used in the past for stabilizing building structure

against lateral forces causes by wind or earthquake. With the advent of reinforced concrete, shear wall system are now widely accepted as a rational and economical part of construction. Shear walls may be part of a service core or a stair wall, or they may serves as partitions between accommodations. They are usually continuous down to the base to which they are rigidly attached to form vertical cantilevers. When shear walls are designed and constructed properly, they will have the strength and stiffness to resist the horizontal forces. Their high stiffness and strength makes them well suited for bracing building, while simultaneously carrying gravity loading. It is usual to locate the walls on plan so that they attract an amount of gravity dead loading sufficient to suppress the maximum tensile bending stress in the wall caused by lateral loading. Shear wall resist varies type of forces or shear like as translation shear, Rotational shear, Horizontal forces on shear wall with opening and uplift forces. Connection to the structure above transfer lateral forces to the shear wall. This transfer creates shear forces throughout the height of the wall between the top and bottom shear wall connection. Figure 1 shows a building with wind or seismic force represented by arrows acting on the edge of each floor or roof. The horizontal surface acts as a deep beams to transmit loads to vertical resisting elements A and B. These shear wall, in turn, act as cantilever beams fixed at their base carry loads down to the foundation. They are subjected to

- A variable shear, which reaches a maximum at the base
- A bending moment, which tends to cause vertical tension near the loaded edge and compression at far edge, and
- A vertical compression due to ordinary gravity loading from the structure.

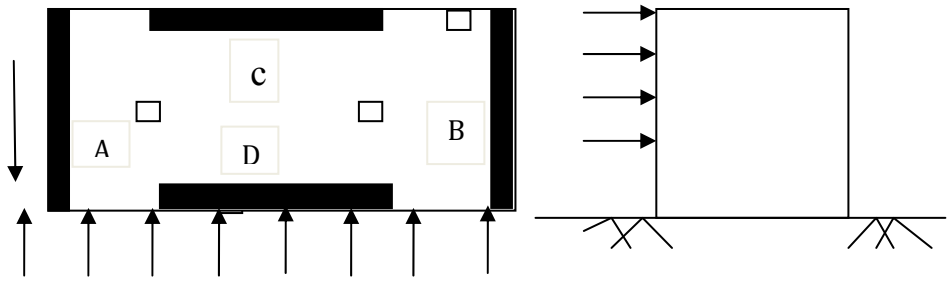

Fig. 1: Building with shear walls subjected to horizontal loads

Shear walls should be located on each level of the structure including the crawl space. To from an effective box structure, equal length shear wall should be placed symmetrically on all floor exterior walls of the building. Shear walls should be added to the building interior when the exterior walls cannot provide sufficient strength and stiffness or when the allowable span –width ratio for the floor or roof diagrams exceeded.

A. Shear walls may be constructed between columns lines, or may be incorporated into stairwells, elevator shaft or utility shafts
B. Shafts walls often are placed in elevator or stair way areas so that both structural and user need are satisfied.
C. The structural engineer must locate shear walls so that they will be the least detrimental to the use and aesthetics of the building.

Within every building, there are multiple elements that are used to transmit and resisting lateral force. Shear walls are vertical seismic elements that resist lateral loads in their plane. They are like vertical dividing boards extending upward from the foundation. The earthquake force act horizontally in the plane of this vertical cantilever. After the diaphragm shear forces has been transmitted into the shear wall behaves like an almost rigid diaphragm to resist these forces. Shear walls develop bending forces as well as shear and all forces, which resist the tendency of the seismic forces to push the wall over its own plane. The effect of opening on the ability of shear wall to resist lateral forces must be considered. If opening are very small, their effect on the overall state of stress in a shear wall will be minor. Large openings will have a more pronounced effect. When the opening in a shear wall become so large that the resulting wall approaches an assembly similar to a rigid frame or a series of element linked by connecting beams, the wall will be analyzed accordingly. In most cases, a rigorous

analysis of a wall with opening is not required. When designing a wall with opening, the deformation must be visualized in order to establish some approximate method to analyze the stress distribution of the wall. The major points that must be considered are, the lengthening and shorting of extreme sides due to beam action , the stress concentration at the corner junctions of the horizontal and vertical components, between openings, and the shear and diagonal tension in both the horizontal and vertical components. There are very modes of failures shear wall, such as steel yielding /fracture of steel and concrete crushing /shear crack. These failure patterns of the wall are greatly influenced by its tallness relative to its width. For high rise wall shows several possible failure modes shear walls with large height to length ratio such as a wall with a very low vertical reinforcement ratio, a wall that fails in shear after a large number a flexure cracks formed and the most common failure mode. Again, on the basis of low rise wall, the wall with small height to width ratio failure generally involves development of inclined crack. Displacements of one level relative to the level above or below known as drift. Due to lateral load causes drift. As a huge amount of damage of structure is occur due to excessive drift, hear the structural analysis shear wall is performed to minimize the drift the beams and columns of the structure have to be of large thickness, which is not economical. So in this case, a shear wall of required thickness and proper placement may reduce the excessive drift caused lateral load. The main objective of this study is given below.

- ✓ To reduce the excessive drift by proper placement of shear wall.
- ✓ To reduce the excessive drift by providing required thickness of shear wall.
- ✓ To represent the comparison of drift between the structure with or without shear wall.

MATERIALS AND METHODOLOGY

To these attempts a 10 storied shear wall building at Dhaka city of the Bangladesh having a lift core has been selected to carry out the comparative story. Story height of the building is 3.0 m. The structure is 10.42 m by 16.15 m in plan dimension. The shear wall thickness is 250 mm, beam are 250 x 375 mm and the column are 450 mm x 450 mm in dimension. Plan area selected for modeling and analysis has been shown in figure below. The total dimension of the plan is 12.95 x 10.62 m.The methodology followed for the laboratory investigations as presented in Figure 3.

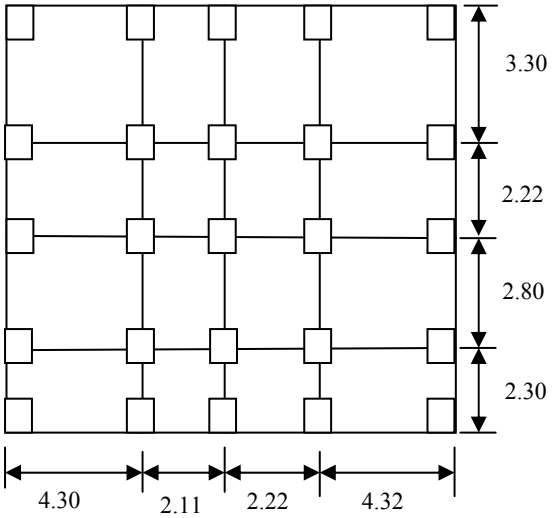

Fig. 2: Plan of example problem

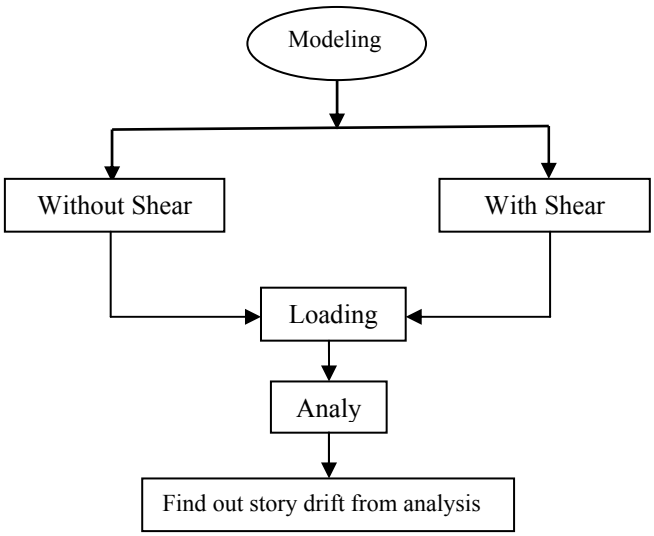

Fig. 3: Flow chart of working methodology

A suitable modeling technique for a particular structure can reduce the analysis time ensuring sufficient accuracy of result. Modeling technique are available in different text and manual of computer package. In this study the software Stadd-Pro has been used to analyze which is widely used at present. In the prototype model lift core has been idealized by plate or shell finite element. In this study wind load and earthquake load calculation are done according to BNBC and all coefficient and factor take into calculation on the basis of Dhaka City. Building shall be investigated for adequate strength to resist the most unfavorable effect resulting from the various combinations of loads. The

most unfavorable effect of loads may also occur when one or more of the contributing loads are absent, or act on the reverse direction. The most unfavorable effects from both wind and earthquake loads shall be considered where appropriate, but they need not be assumed to act simultaneously.

RESULT AND DISCUSSION

The effect of number of story, shear wall, shear wall position and shear wall thickness on drift as well as the software based experiment on the 10 story residential building were analyzed and discussed in hence following.

The effect of shear wall and shear wall thickness on drift minimization at lift core – A

On the basis of drift analysis for the shear wall at different thickness and without shear wall at position A the following drift value are found that are shown in Table 1.

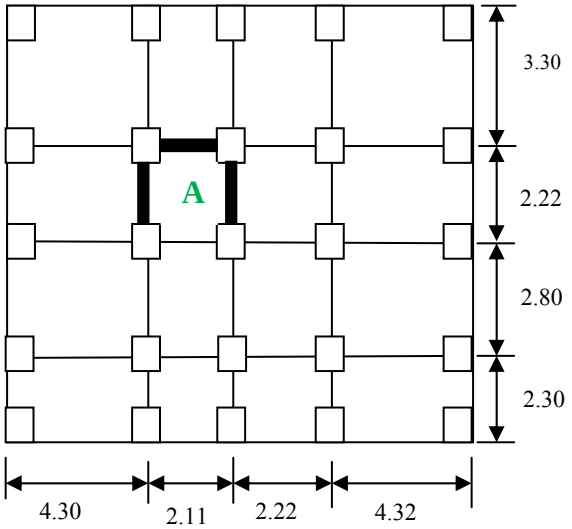

Table 1: Drift value for lift core- A

Number of story	Story drift (inch) without shear wall	Story drift (inch) With shear wall		
Shear wall	thickness =	6”	8”	10”
0	0	0	0	0
1	0.64	0.21	0.19	0.18
2	1.85	0.63	0.58	0.54
3	3.19	1.14	1.05	0.98
4	4.49	1.68	1.55	1.45
5	5.67	2.24	2.07	1.94
6	6.70	2.78	2.58	2.41
7	7.56	3.30	3.06	2.87
8	8.25	3.76	3.53	3.30
9	8.76	4.20	3.92	3.68
10	9.11	4.58	4.27	4.02

The change of drift value of different shear wall thickness and without shear wall with the increases number of building story was shown in Figure 4. a presentation of drift (inch) versus number of story diagram. Moreover, Figure 4 shows that with the increasing of story height the drift value increasing at different condition such as without shear wall and with different shear wall thickness. Again, different shear wall thickness shows different drift value for same story height. Figure 4 shows that with the increasing of shear wall thickness the drift values are decreased for same story height. Figure 4 show that 10 inch thickness shear wall can minimize more drift than 6 inch and 8 inch thickness shear wall. It is very interesting hear is that 6 inch thickness shear wall minimize 56%, 8 inch thickness shear wall minimize 59% and 10 inch thickness shear wall minimize 62% drift value of without shear wall created drift value.

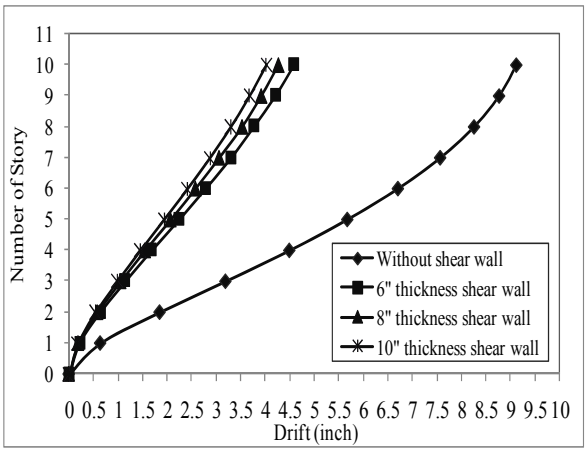

Fig. 4: Graphical representation of drift v_s number story at varying thickness shear wall at lift core -A

The effect of shear wall and shear wall thickness on drift minimization at lift core – B

Now consider the shear wall at lift core position –B. On the basis of drift analysis output through Stadd Pro software the Figure 6 are drawn that are given below. Figure 4 show that with the increasing of number of story the drift value are increased. Again Figure 5 shows that 10 inch thickness shear wall can minimize more drift than 6 inch and 8 inch thickness shear wall. Hear 6 inch thickness shear wall minimize 59%, 8 inch thickness shear wall minimize 60% and 10 inch thickness shear wall minimize 64% drift value of without shear wall created drift value.

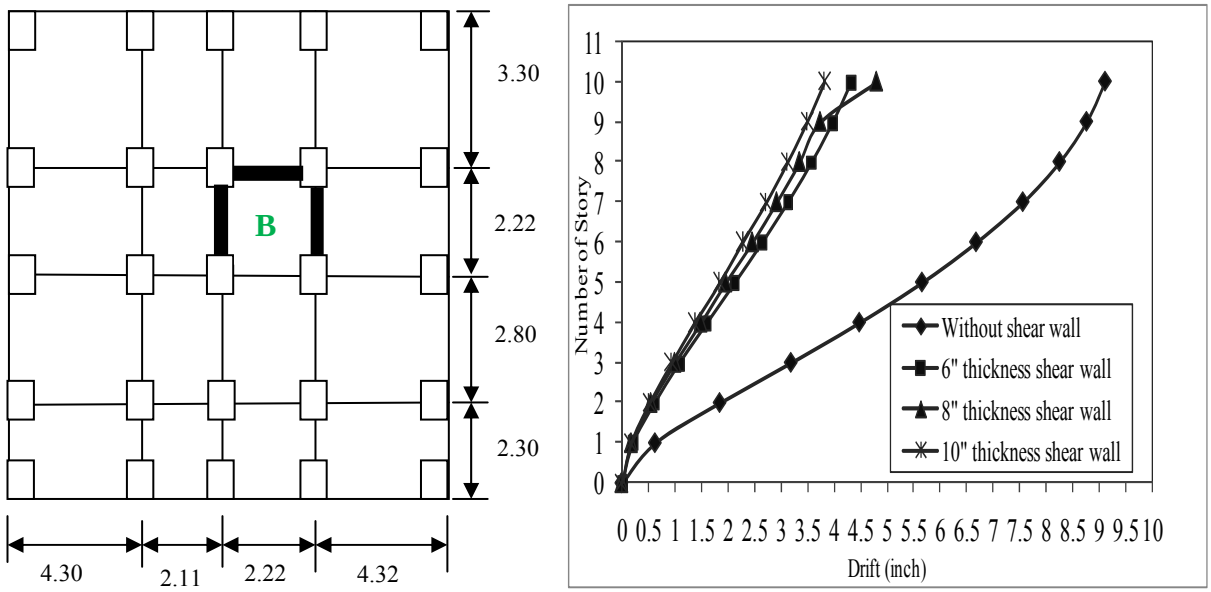

Fig. 5: Graphical representation of drift v_s number story at varying thickness shear wall at lift core-B

The effect of shear wall and shear wall thickness on drift minimization at lift core – C

Now consider the shear wall at lift core position –B. On the basis of drift analysis output through Stadd Pro software the Figure 6 are drawn that are given below. Figure 4 show that with the increasing of number of story the drift value are increased. At lift core-C, 6 inch thickness shear wall minimize 62%, 8 inch thickness shear wall minimize 66% and 10 inch thickness shear wall minimize 69% drift value of without shear wall created drift value.

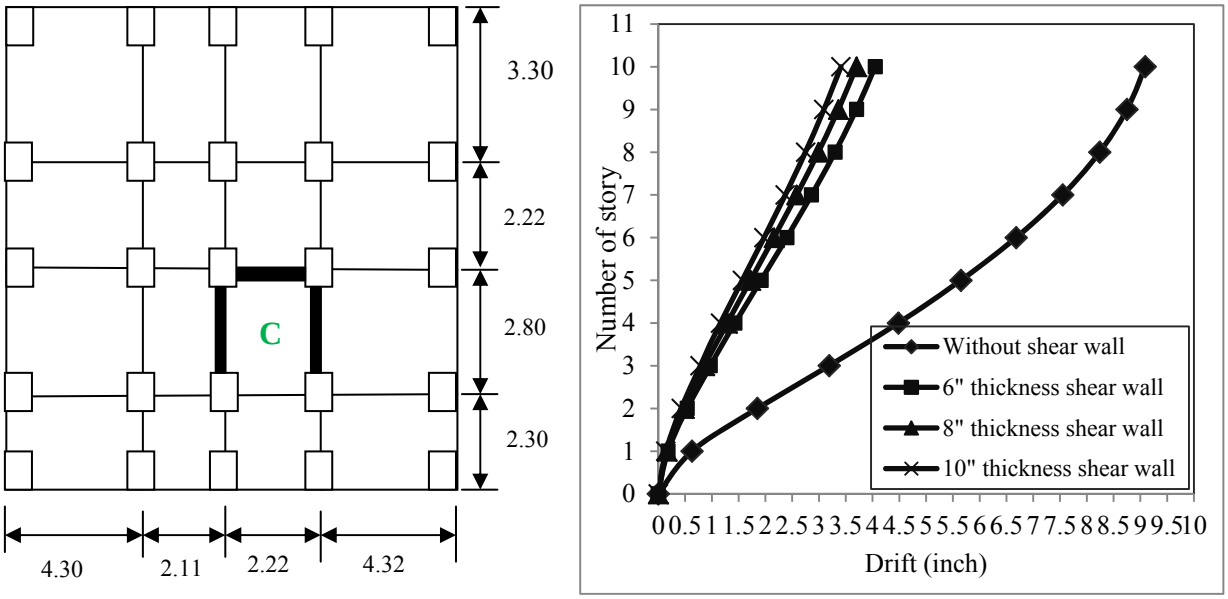

Fig. 6: Graphical representation of drift v_s number story at varying thickness shear wall at lift core -C

On the basis of mathematical calculation, story drift shall be confirm to the following requirement
a) Story drift, $\triangle$ shall be limited as follows

1) $\triangle \leq 0.04\ h/R \leq 0.005h$ For $T \leq 0.7$ second

2) $\triangle \leq 0.03h/R \leq 0.004h$ For $T \geq 0.7$ second, Where h= height of the building

The period T used in this calculation shall be the same as that used for determining the base shear after calculation. The limits involving R in (1) and (2) above shall be applied only when earthquake forces are presents b)The drift limits set out in (a) above may be exceed where it can be demonstrated that greater drift can be tolerated by both structural and non structural elements without affecting life safety. To avoid an excessive drift that causes damage both to structural elements and to non-structural elements, the calculated at the final stage of design must be checked not to checked specified limits for the drift.

As T = 1.06 Seconds ≥ 0.7 Second, Story drift, $\Delta \leq 0.03h/R \leq 0.004h$

$\Delta \leq 0.03x98.43x\ 12/8 \leq 0.004x98.43x12, \quad \Delta \leq 4.43" \leq 0.004x98.43x12, \ \Delta \leq 4.43" \leq 4.72"$

Table 2: Drift limit for lift core- A, B & C

Without and with shear wall	Max^{m} drift (inch)			Calculated drift limit (inch)
	Lift core-A	Lift core-B	Lift core-C	
Without shear wall	9.11	9.11	9.09	4.43
Shear wall of thickness 6 inch	4.58	4.33	4.05	4.43
Shear wall of thickness 8 inch	4.27	4.80	3.70	4.43
Shear wall of thickness 10 inch	4.02	3.83	3.41	4.43

CONCLUSION

From the limited study of drift minimization by shear wall, shear wall thickness and shear wall position analysis the following output can be drawn tentatively such as a huge amount of drift caused by lateral load can be reduced by providing shear wall at lift core. After checking the minimum drift obtained by placing the shear wall of various thickness at different palace of lift core with respect to the drift limit, it is clear that the maximum drift is minimized by providing shear walls for placement of lift core-C. Among the three thickness of 6 inch, 8 inch and 10 inch shear wall, the 10 inch minimize the excessive drift. But it is not appropriate from the point of economical consideration. On the other hand, if the shear wall of thickness 6 is is provided, the obtained drift is within the limit. So it can be recommended to provide the shear wall of thickness 6 inch.

REFERENCES

Bangladesh national Building code, 1993

Ferguson P.H et al. 1998. *Reinforced concrte Fundamental*. Fifth eddition, Jhon wiley & Sons

Robert D. Cock, *Concepts and applications of finite element analysis*, 2nd edition, Jhon wiley & Sons

Stafford smith B. and coul A, 1991. *Tall building structure: Analysis and design*, Jhon Wiley & Sons

Taranath , B.S 1998. *Structural analusis and design of tall building*. Mc Graw Hill

User manual, 1996. *STAAD-III, Research engineers Inc*. Calfornia, America

Stafford smith B and Giris A. 1984, Simple analogous frames for shear wall analysis, *ASCE Journal of structural Engineering*. vol.110

ID : ASEE 045

1st International Conference on Advances in Civil Engineering 2012 (ICACE 2012)
12 –14 December 2012
CUET, Chittagong, Bangladesh

MEASUREMENT OF THERMAL DIFFUSIVITY OF NORMAL STRENGTH CONCRETE

MD. ASSADUZZAMAN[1*], D. MALLICK[1], M. H. RASHID[2] & MD. M. HOSSAIN[2]

[1]Department of Civil Engineering, America Bangladesh University (ABU), Dhaka, Bangladesh*
asad_kuet06@yahoo.com
[1]Shamsuddin Mia & Associates Ltd, Dhaka-1000, Bangladesh
debashis.ce@gmail.com,
[2]Department of Civil Engineering, Khulna University of Engineering &Technology (KUET), Khulna, Bangladesh
hafin02@yahoo.com,drmonjur@yahoo.com

ABSTRACT

This paper depicts the investigation of the thermal diffusivity of concrete manufactured from burned clay brick khoa and stone chips as coarse aggregate. Thermal diffusivity measures the index of the facility with which concrete can undergo temperature changes. So measurement of thermal diffusivity of concrete is very necessary. The thermal diffusivity of concrete is affected by the type & moisture content of aggregate, the original water content of the mix, degree of hydration of cement and exposure to drying. To these attempts two types instrument setup are used in this study, one is boiling part and another is cooling part. Sample is prepared by bricks chips and stone chips at different mixing ratio of 1:1.2:2 and 1:2:3 separately. Size of cylindrical sample is 4" dia. and 8" height. Each (at 28 days) specimen should be heated to the same temperature by continuous immersion in boiling water until the temperature of the center is 100^0c. In this study the CRD C 36-73 methods are adopted. The specimen is then transferred to a chamber of running cold water. The temperature difference in degrees is plotted against the time in minutes on a semi-logarithmic scale. The time elapsed between the two temperature select from graph and then thermal diffusivity (δ) value are find out by the using equation . Two different mixing ratios (1:2:3 and 1:1.2:2) were tested to find out the differences in thermal diffusivity of the different concrete. The thermal diffusivity of concrete manufactured by brick khoa of looser mixing ratios(1:2:3) was 54.5% less than the thermal diffusivity of concrete manufactured by brick khoa of denser mixing ratios(1:1.2:2).The thermal diffusivity of concrete manufactured from brick khoa as coarse aggregate is less than the thermal diffusivity of concrete manufactured from stone chips as coarse aggregate.

Key words: Concrete; Hydration; Diffusivity; Temperature; Aggregate

INTRODUCTION

Now-a-days temperature change is becoming a burning issue. For various reasons such as global warming, temperature increases rapidly. Due to urbanization, high production of carbon di oxide (co_2) causes global warming. For this reason various civil engineering structures undergo temperature changes. With the increase of temperature concrete goes in elongation and with the decrease of temperature it goes in contraction which may fail structures in bonding etc. Thermal diffusivity measures the index of the facility with which concrete can undergo temperature changes. Thermal diffusivity is also related to thermal conductivity and specific heat. So measurement of thermal diffusivity of concrete is very necessary. The thermal diffusivity is defined as the rate at which temperature changes within a mass taking place and thus is an index of the facility with which

concrete can undergo temperature changes. The thermal diffusivity is denoted by "δ". Its unit is ft^2/ hr, m^2/hr. The range of typical values of diffusivity is between 0.002 and 0.006 m^2/hr (0.02 to 0.06 ft^2/ hr) [1]. Diffusivity, δ is simply related to the conductivity by the following equation

$$\delta = \frac{k}{c\rho} \qquad (1)$$

Where, c is the specific heat, ρ is the density of concrete and k is the conductivity .From this expression, it can be seen that conductivity and diffusivity vary in linear way. The thermal diffusivity of concrete is affected by the following factors such as the type of aggregate, the moisture content of aggregate, the original water content of the mix, degree of hydration of cement and exposure to drying. Concrete is an artificial stone like material which is a mixture of coarse aggregate, fine aggregate, and binding material with water. Concrete has relatively high compressive strength, but much lower tensile strength, and for this reason is usually reinforced with materials that are strong in tension (often steel). The elasticity of concrete is relatively constant at low stress levels but starts decreasing at higher stress levels as matrix cracking develops. Concrete has a very low coefficient of thermal expansion, and shrinks as it matures. All concrete structures will crack to some extent, due to shrinkage and tension. Concrete that is subjected to long-duration forces is prone to creep.

Concrete is one of the most durable building materials. It provides superior fire resistance compared with wooden construction, can gain strength over time. Structures made of concrete can have a long service life. Concrete is the most widely used construction material in the world. There are different method of measuring of thermal diffusivity like as the laser flash method, the TWI method, the thermo graphic method 1 (spatially resolved method), the thermo graphic method 2 (lateral thermal method), the thermo graphic method 3 (one side flush method) and the CRD C36-73 method. Above all the methods, the CRD C36-73 methods are adopted in this study. The CRD C 36-73 Method consist of 4 apparatus, like as bath, Diffusion chamber, temperature indicating or recording chamber and timer. A heating bath in which concrete cylinders can be raised to uniform high temperature (212F, 100C), Diffusion chamber containing running cold water. The procedure of measuring thermal diffusivity through CRD C 36-73 method are given below.

1. Preparation of Specimen: The test specimen shall be a 4 inch by 8 inch cylinder. If prepared from a hardened concrete core, shall contain a similarly placed thermocouple inserted in an axially drilled hole 3/8 inch (9.5 mm) in diameter which has been subsequently grouted. Molded specimens shall be moist-cured for 28 days prior to testing.
2. Heating: Each specimen shall be heated to the same temperature by continuous immersion in boiling water until the temperature of the center is 212 F (100 C). The specimen shall then be transferred to a bath of running cold water.
3. Cooling: The cooling history of the specimen shall be obtained from readings of the temperature of the interior of the specimen at 1-min intervals from the time the temperature difference between the center and the water is 120 F (67 C) until the temperature difference between the center and water is 8 F (4 C). The data shall be recorded.
4. Calculations: The temperature difference in degrees F shall be plotted against the time in minutes. The time elapsed between the temperature difference of 80^0 F (44^0C) and 20^0 F (11^0 C) shall be read from the graph, and this value inserted in equation (3) below, from which the thermal diffusivity shall be calculated:

$$\delta = \frac{M}{(t2-t1)} \qquad (2)$$

where, δ= Thermal diffusivity, ft^2/hr, (t_2-t_1) = The time elapsed between the temperature of 44^0c and 11^0c, min

$$M = \frac{60 \ln\left(\frac{T1}{T2}\right)}{\left(\frac{5.783}{r^2} + \frac{\pi^2}{l^2}\right)} \qquad (3)$$

Where,

T_1, T_2= Temperature differences at times t_1 & t_2, r= Radius of cylinder, l= Length of cylinder.

This project involves the development an instrumental arrangement for measuring thermal diffusivity of concrete and the comparison of the diffusivities with two different types of concrete.
The objectives of this study such as

- To make an instrumental arrangement for measuring thermal diffusivity of concrete.
- To measure the thermal diffusivity of concrete.
- To compare the diffusivities with different types of concrete manufactured from different coarse aggregate and different mixing ratios.

MATERIALS AND METHODOLOGY

In this study, to attempt the goal ordinary portland cement , sylyet sand (coarse sand) , brick chips and stone chips are collected from the local market, Before making test sample by the coarse aggregate, unit weight(loose and compact), void, moisture content, specific gravity and sieve analysis test of the coarse aggregate are done in the laboratory. Basic properties coarse aggregate that are used in this study are given in Table 1 according to ASTM testing procedure.

Table 1: Basic properties of coarse aggregate

Name of Test	Bricks chips	Stone chips
Moisture content	9.4%	2.4%
Voids	50.56%	56.8%
Unit weight	898 kg/m^3	1138 kg/m^3
Specific gravity	1.82	2.64
Fineness modulus	7.51	7.42

At mixing ratio 1:2:3 and 1:1.2:2 (ordinary portland cement: fine aggregate: coarse aggregate) with 50% water of cement (w/c=0.5) make the sample of 4 inch dia. and 8 inch height. For sample identification in the laboratory the following nomenclature IDs are used. IDs are: B48R3, B48R2, S48R3, S48R2

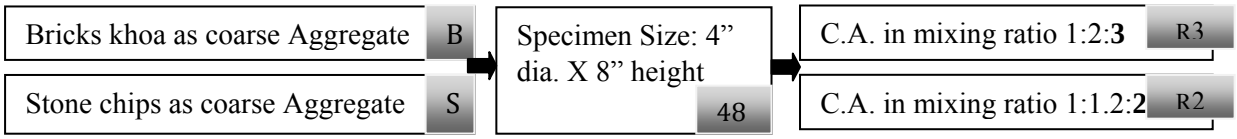

The test specimens are 4 inch X 8 inch cylindrical shape which contains a thermocouple placed at the center of mass. The thermocouple is inserted in an axially drilled hole 3/8 inch diameter. Specimens should be moist-cured for 28 days prior to testing. In this study instrument setup has two parts, one is boiling part which capacity is 2000 watt and voltage is 220-250 volt and another is cooling part which has 2 nos. of PVC containers of 140 liter capacity and pump - 1 nos. which has a capacity of 0.8 hp. Line diagram of boiling instrument and cooling instrument are given in Figure 1.

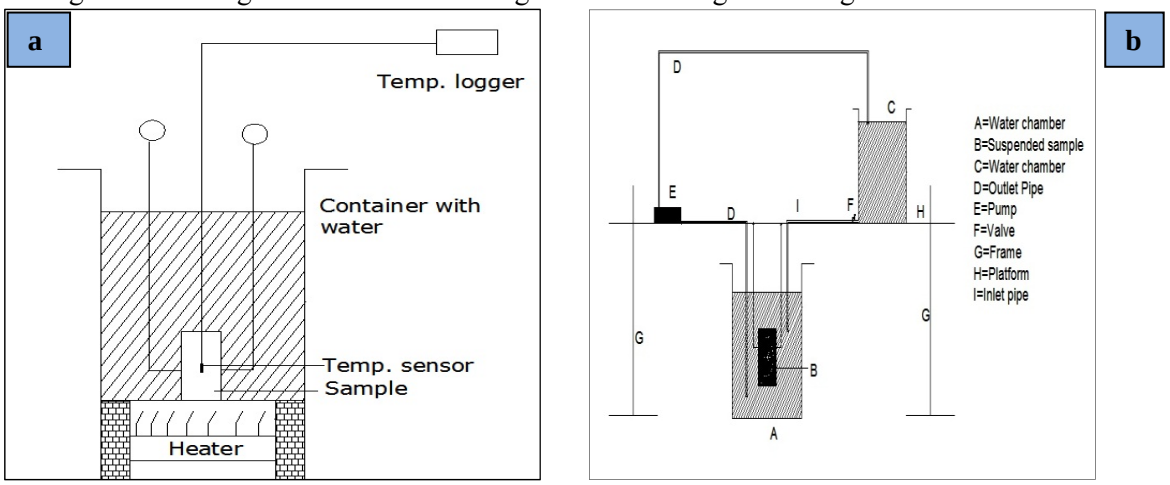

Fig. 1: Line diagram of a) boiling instrument b) cooling instrument

Fig. 2: Pictorial view of heating part (left) cooling part (Right)

Each specimen should be heated to the same temperature by continuous immersion in boiling water until the temperature of the center is 100^0c. The specimen is then transferred to a chamber of running cold water. The temperature of the cold water remains constant by adding ice. The cooling history should be obtained from readings of the temperature of the interior of the specimen at 1 minute interval from the time the temperature difference between the center and water is 67^0c to 4^0c. The data should be recorded. The temperature difference in degrees F shall be plotted against the time in minutes on a semi-logarithmic scale. The best possible straight line is drawn through the points so obtained. The time elapsed between the temperature of 44^0c and 11^0c is read from graph, and this value put in the Equation 4.

$$\delta = \frac{M}{(t2 - t1)} \qquad (4)$$

RESULT AND DISCUSSION

The different coarse aggregate and mixing ratio of concrete mold effect on thermal diffusivity as well as the laboratory on the basis of 2x 2 x 2 inch block testing that was prepared in the laboratory were analyzed and discussed in hence following.

The thermal diffusivity of different sample

From the collected data based in the laboratory test, Figure 3 to 6 is a presentation of time (minute) versus temperature difference (^{0}c) diagram as measured for various coarse aggregate and mixing proportion. Based on the Figure 3 to 6, the value of temperature difference are decreased with the increasing of elapsed time.

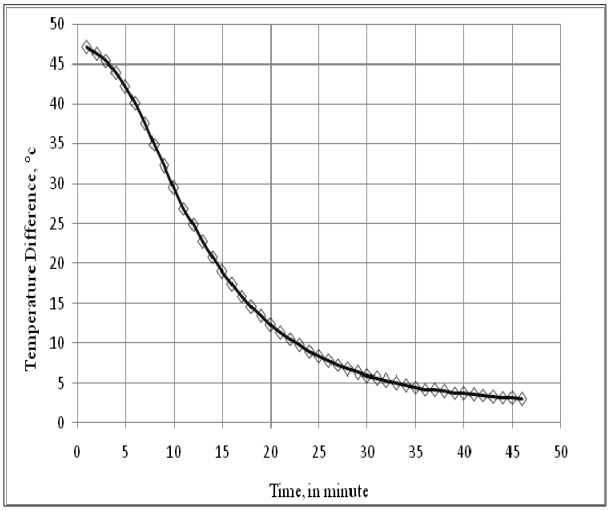

Fig. 3: Graph for temperature differences versus elapsed time during cooling of sample- B48R3

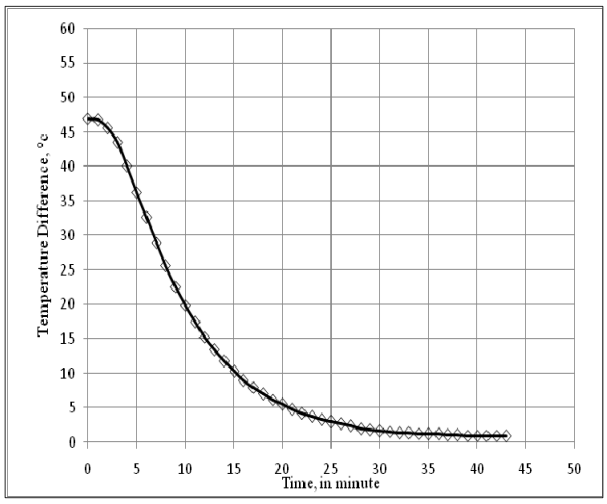

Fig. 4: Graph for temperature differences versus elapsed time during cooling of sample- B48R2.

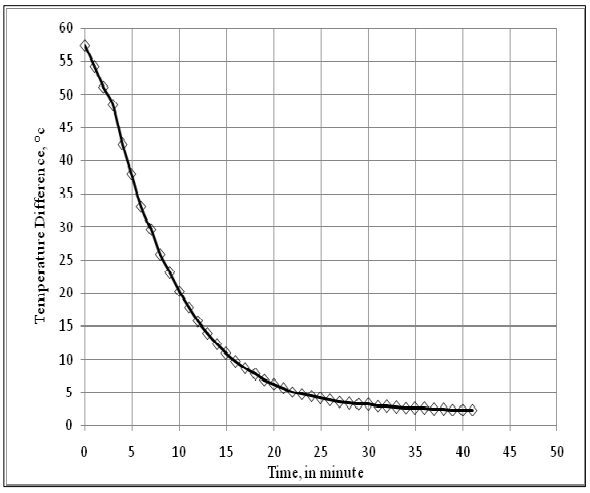

Fig. 6: Graph for temperature differences v_s elapsed time during cooling of sample- S48R2

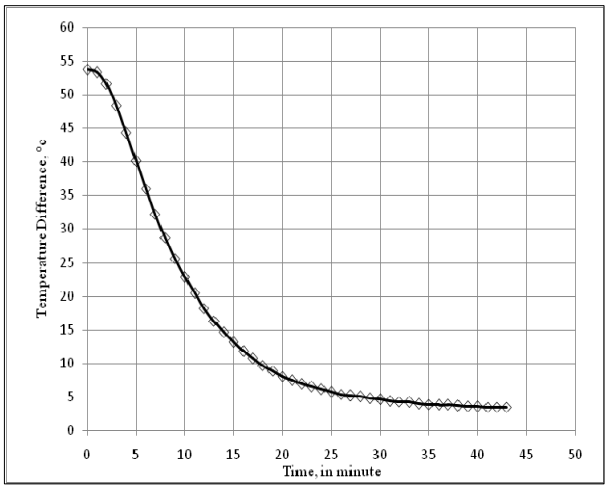

Fig. 5: Graph for temperature differences v_s elapsed time during cooling of sample- S48R3

Now thermal diffusivity at temperature 44°c and 11 °c from Figure 3.

$$\text{So,} \qquad M = \frac{60 \ln\left(\frac{44}{11}\right)}{\left(\frac{5.783}{(2/12)^2} + \frac{\pi^2}{(8/12)^2}\right)} = 0.3864$$

$$\text{So, the thermal diffusivity, } \alpha = \frac{0.3864}{(21.4-4)} = 0.022 \text{ ft}^2\text{/ hr.}$$

The thermal diffusivity calibrated Sample ID: B48R3= 0.022 ft^2/ hr.

Similarly, the thermal diffusivity of sample ID: B48R2, α = 0.034 ft^2/ hr., sample ID**:** S48R3, α = 0.034 ft^2/ hr. and sample ID**:** S48R2, α = 0.035 ft^2/ hr.

Different sample gives different thermal diffusivity for different cooling temperature of water and for different heating peak temperature of sample, so, the thermal diffusivity of normal strength concrete does not depend on cooling temperature and peak heating temperature. But the temperature of cooling water should remain constant during the whole cooling period. In this study, the temperature of cooling water was kept constant. According to the reference, the typical range of thermal diffusivity of normal concrete is 0.02 ft^2/hr to 0.06 ft^2/hr. In this study, the thermal diffusivity of normal concrete lies between the typical range.

The thermal diffusivities of all sample mentioned Table 2 lies between the typical range of thermal diffusivity of normal strength concrete

Table 2: Diffusivity of different sample

Sample No.	Sample ID	Mixing Ratio (Cement: Fine aggregate: Coarse aggregate)	Coarse Aggregate	Diffusivity, ft^2/hr
1	B48R3	1:2:3	Brick khoa	0.022
2	B48R2	1:1.2:2	Brick khoa	0.034
3	S48R3	1:2:3	Stone chips	0.034
4	S48R2	1:1.2:2	Stone chips	0.035

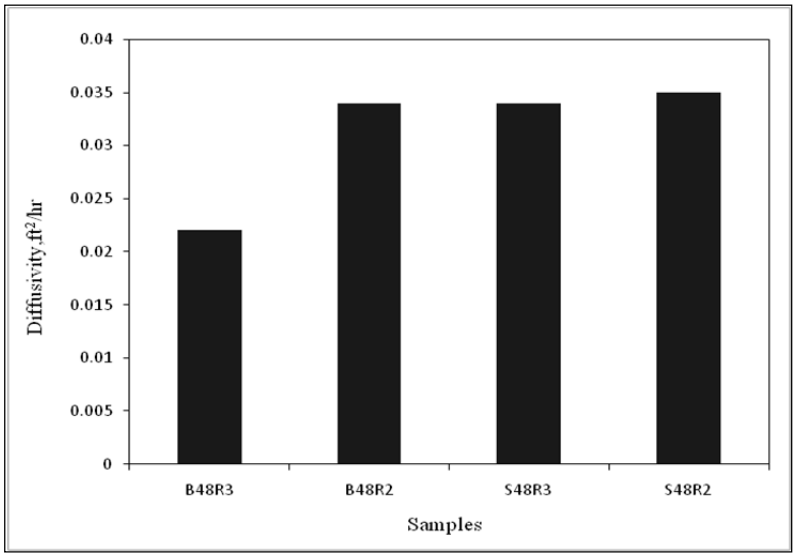

Fig. 7: Bar diagram showing diffusivities of different samples

As shown in Figure 7, it has been concluded that, the diffusivity varies with the aggregate types used in concrete specimens. The diffusivity of concrete is less when bricks khoa used as coarse aggregate than the diffusivity of concrete when stone chips used as coarse aggregate. Again, When all parameters are constant, the diffusivity of concrete varies with the mixing ratios, as shown in Figure 7, Here, it has been seen that the diffusivity of concrete specimen containing denser mixing ratio (cement: sand: coarse aggregate) is greater than the diffusivity of concrete specimen containing looser mixing ratio.

CONCLUSION

The following conclusions are drawn on the basis of results obtained from this study, The thermal diffusivity of concrete is different for different coarse aggregates. The thermal diffusivity of concrete having bricks khoa as coarse aggregate is 54.5% less than the diffusivity of concrete having stone chips as coarse aggregate for mixing ratio 1:2:3 and the thermal diffusivity of concrete having bricks khoa as coarse aggregate is 2.9% less than the diffusivity of concrete having stone chips as coarse aggregate for mixing ratio 1:1.2:2. The thermal diffusivity of concrete varies with the mixing ratios of ingredients of concrete. The thermal diffusivity of concrete with denser mixing ratio is greater than concrete having concrete with looser mixing ratio.

REFERENCES

Adam M. Neville, July 1996. *Properties of concrete: fourth and final edition.* America*:* John Wiley & Sons.

CRD-C 36-73. 1973. *Method of test for thermal diffusivity of Concrete*, Issued 1.

D.P. Almond, P.M. Patel. 1996. *Photothermal science and techniques,* Chapman & Hall, London.

F. Cernuschi, L. Lorenzoni.2001. CESI Report n° A1/033124.

T. Mollbog, H. Wang, H.E. Littleton, AFS Transactions Paper No: 00-167, pp.471-478.

H.S. Carslaw and J.C. Jaeger.1959. *Conduction of Heat in Solids*, Oxford University Press, London.

ID : ASEE 046

1st International Conference on Advances in Civil Engineering 2012 (ICACE 2012)
12 –14 December 2012
CUET, Chittagong, Bangladesh

ESTIMATION OF BASE ROCK VIBRATION CHARACTERISTICS FROM SURFACE GROUND MOTION

MD. RAQUIBUL HASSAN[1*]

[1*] *Graduate Student, Department of Civil Engineering, BUET, Dhaka, Bangladesh, <shyamol_88@yahoo.com>*

ABSTRACT

A computer program is developed assuming underlying soil as horizontally layered and one-dimensional. Soil material non-linearity is considered in this problem. One dimensional shear wave equation is solved. Space is discretized by Finite Element method and time is discretized by Central Difference method. Two Parameter Hyperbolic model and Masing rule are used to obtain the dynamic stress-strain behaviour. The number of soil layers, the properties of different soil layers such as density, initial shear modulus, reference strain and the properties of rigid base rock such as density and shear modulus are used as input data. Record of the earthquake which occurred at El-Centro in 1940, is used here as surface acceleration data. The output of the program is dynamic stress-strain behaviour in different soil layers, variation of secant shear modulus with time in different soil layers, deformation in different soil layers and base rock acceleration of the soil layer. The soil properties data assumed here is soft layer in the upper portion and comparatively stiffer layer in the bottom layer. The base rock layer is the stiffest layer. The peak base rock acceleration is found greater than the peak surface acceleration. Hysteresis loop is maintained in each layer of the soil column for obtaining dynamic stress-strain behaviour. Variation of secant shear modulus with time is fluctuating. The surface deformation is found greater than the base rock deformation.

Keywords: Finite Element Method, Central Difference method, Hyperbolic Model, Secant Shear Modulus.

INTRODUCTION

One of the most important applications of the theory of structural dynamics is in analyzing the response of structures to ground shaking caused by an earthquake. Earthquakes may be defined as the vibration of earth produced by the rapid release of energy. The energy radiates in form of waves in all directions from its source (focus). Another definition is trembling or shaking of the ground caused by the sudden release of energy stored in the rocks beneath the earth surface. The actual cause for earthquake occurance is the great forces acting deep in the earth, these forces put a stress on the rock which may bend or change in volume (strain). The rock can deform until it reaches the ultimate capacity of the rock and a rupture (rock break) occurs. Most earthquakes are also produced from active faults. Surface ground motion can be measured by different instruments. But it is important to know the base rock vibration for determining different soil properties.

RESEARCH OBJECTIVES

The main objective of the study is to develop a computer program for determining base rock vibration from surface earthquake response data. The program requires several input data. The length of each

soil layer, the number of soil layer, the properties of soil layer, the properties of rigid bed rock and the time step of input acceleration are required as input data. The properties of soil layer is characterized by density, initial shear modulus & reference strain. The properties of rigid bed rock are characterized by density and shear modulus. The output of the program are several soil parameters such as deformations with time, variations of secant modulus of each layer with time and the stress-strain history of each layer. The output are in graphical form. The specific objectives are-

- To determine the base-rock vibration from surface vibration.
- To determine different soil parameters such as dynamic stress-strain behaviour, variations of secant modulus with time at different soil layers.

MATERIALS AND METHODS

A Matlab (MATLAB 7.5.0(R 2007b)) based computer program was modified to estimate the rigid base rock acceleration from surface acceleration. For this reason, global mass matrix and global stiffness matrix and force matrix were modified according to the formulation. The soil column was assumed as one-dimensional and one dimensional shear wave equation was solved. The space was discretized by finite element method and time was discretized by central difference method. The soil material non-linearity was considered and hyperbolic model and Masing's rule were used. The input data was several soil properties such as density, initial shear modulus and shear strain. The earthquake which was occurred at El-Centro, 1940 was used as the surface acceleration data. The rigid bedrock property which is governed by density and initial shear modulus was also required as input. The output of the program was dynamic stress-strain behaviour, variation of secant modulus with time in each layer, displacement history at each layer and base rock acceleration.

RESULTS

The input surface acceleration and surface deformation are presented below in graphical form –

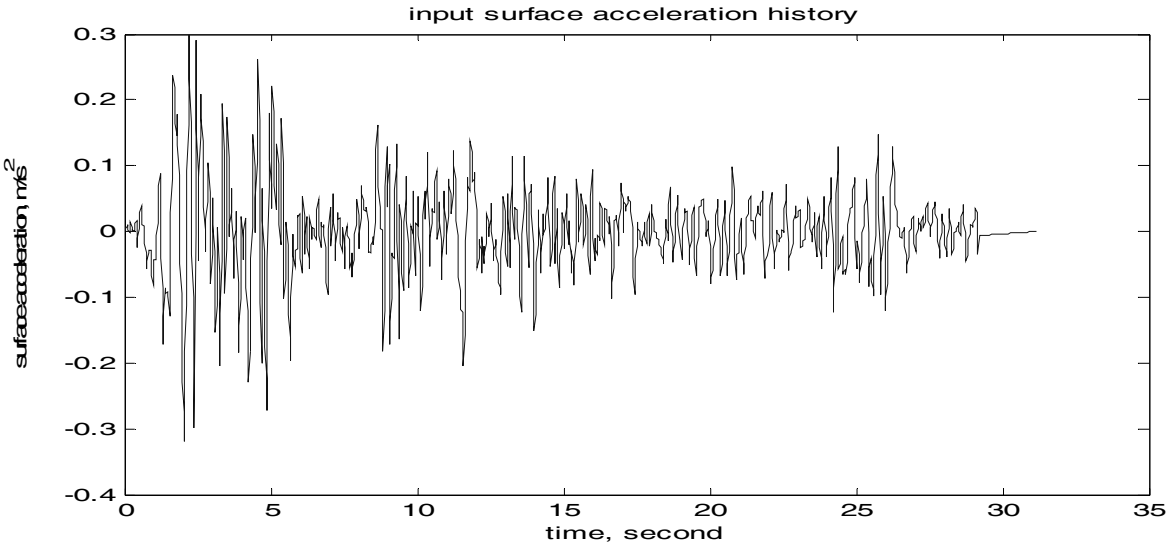

Fig. 1 Input surface acceleration with time.

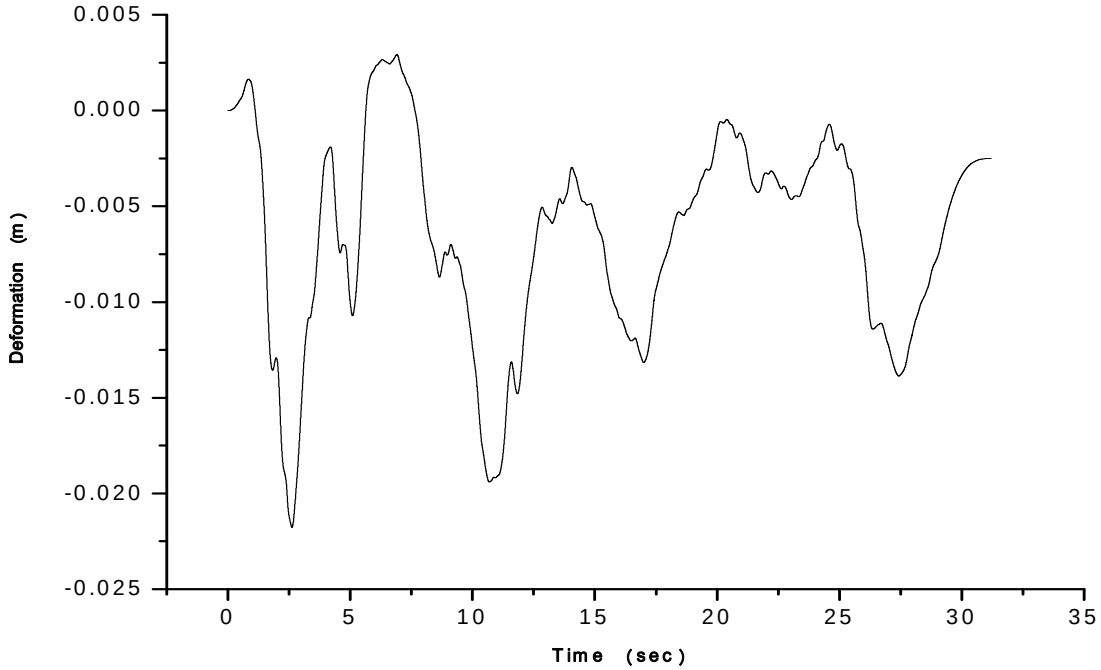

Fig. 2 Input surface deformation with time.

The output base rock acceleration and base rock deformation is presented below in graphical form –

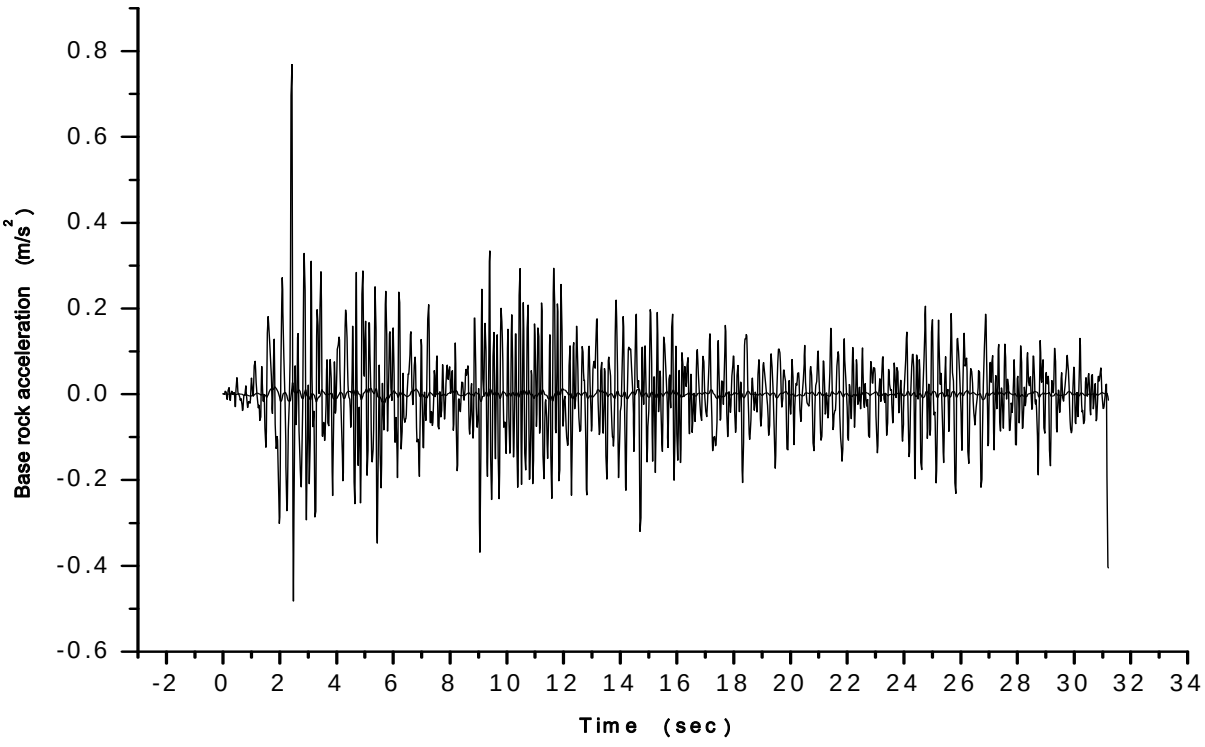

Fig. 3 Base rock acceleration with time.

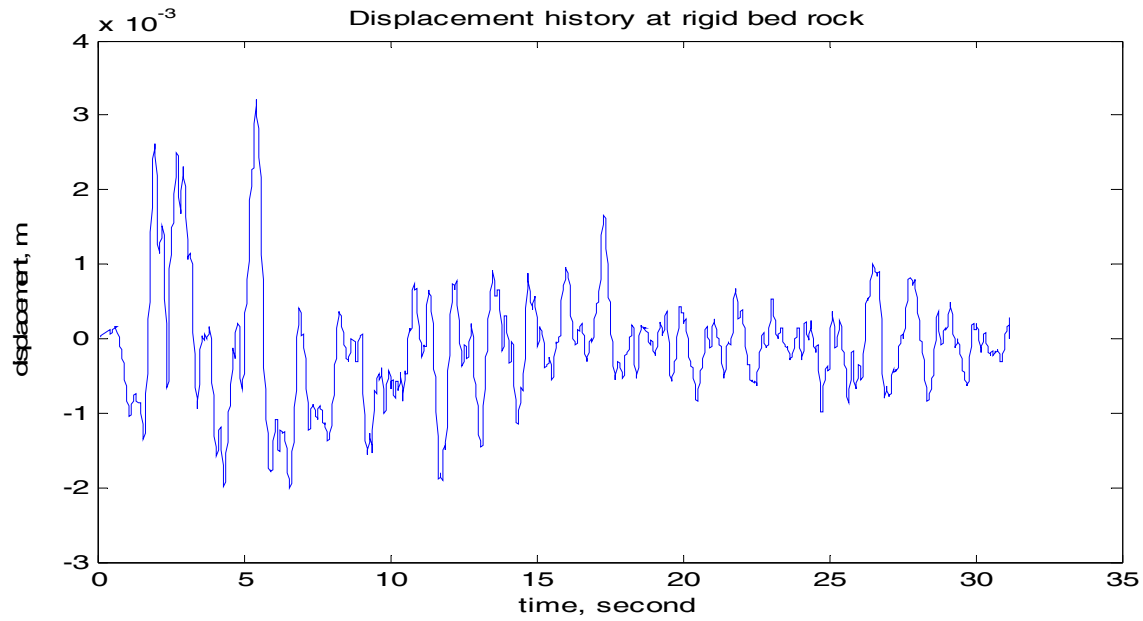

Fig. 4 Displacement at rigid bed rock with time.

The output stress-strain history and change of secant modulus with time of different layers of soil column are presented below in graphical form –

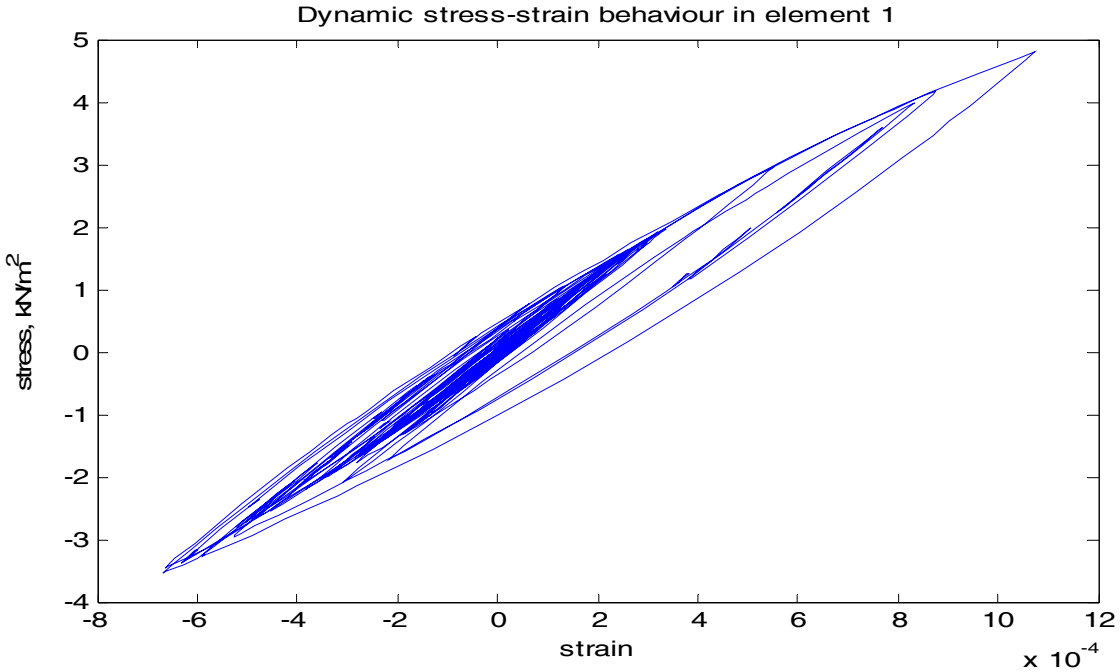

Fig. 5 Dynamic stress-strain behaviour in a layer just below the surface layer.

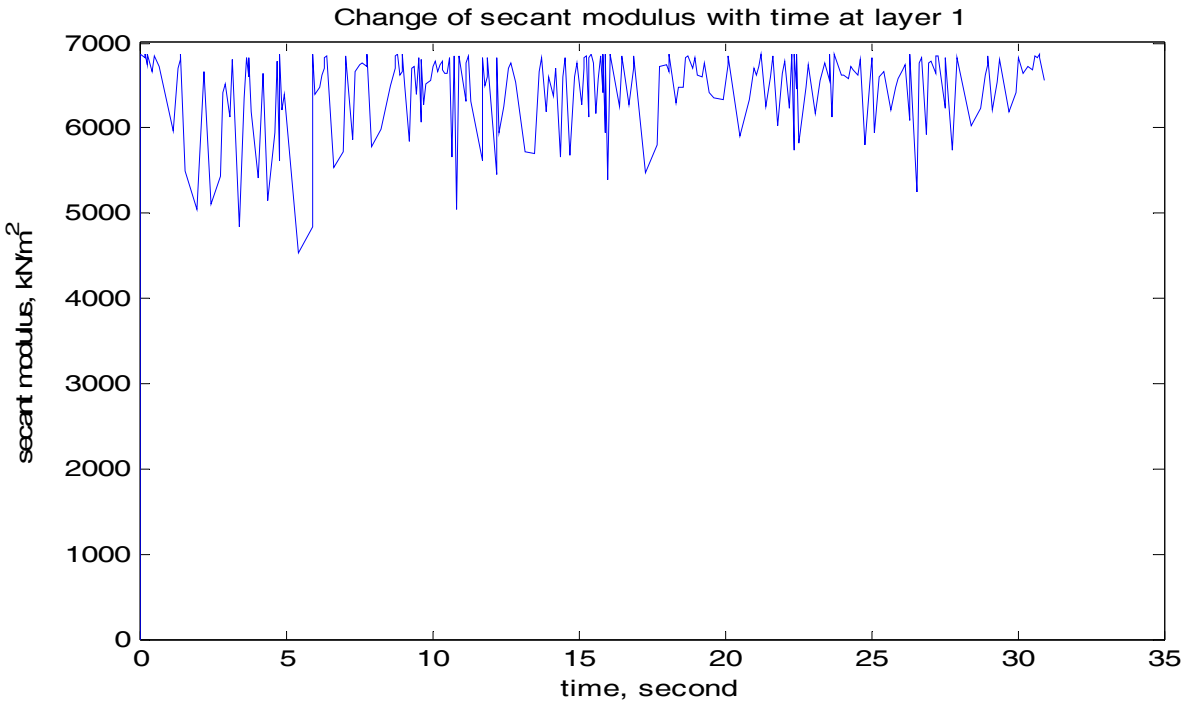

Fig. 6 Change of secant modulus with time in a layer just below the surface layer.

DISCUSSIONS

- From the results we have found that surface acceleration and base rock acceleration varies with time in a very highly irregular manner.
- The soil properties data implies that if we calculate the shear wave velocity then we find that the upper surface layer is soft and the bottom layer is comparatively stiff than the upper layer.
- For the soil condition and the results we have found we can say that the rigid base rock acceleration is higher than the surface acceleration. The displacement is higher at the surface and lower at the rigid base rock.
- The dynamic stress-strain maintains a hysteresis loop.
- The variation of secant modulus shows high frequency fluctuation. High value of secant modulus represents smaller loops, where smaller value of secant modulus represents smaller loops.
- At each reversal point of the stress-strain history, the corresponding secant shear modulus was determined as the slope of the line joining the present and previous reversal points.
- Due to the high frequency reversal of loading, the variations of the secant modulus show high frequency fluctuations. It is evident that the high values of the secant shear modulus are mainly due to the smaller loops or rapid reversals of the stress-strain history; whereas the smaller values correspond to the bigger loops. Hence the variations of the minima of the history of the change of secant shear modulus are more representative of the material property.
- The dynamic stress-strain behaviour was plotted for each element of the soil column. We have found that for each element of the soil layer it maintains a hysteresis loop. The hysteresis loop represents energy dissipation characteristics which are non-linear. Because of the non-linearity the hysteresis loop does not have rounded corners.

CONCLUSION

In most of the case, we can measure surface acceleration by the instruments which are set on the ground. From the program, we can easily find different soil properties from rigid base rock to surface layer due to an earthquake. The output is very useful in earthquake resistant structure design.

ACKNOWLEDGMENTS

The writer would like to show his gratitude and thankful acknowledgement to Professor Dr. Raquib Ahsan, Civil Engineering Department, BUET for suggesting all the necessary steps through the progress of the work.

REFERENCES

Chopra, A.K. (2006), "*Dynamics of Structures*", Prentice-Hall of India, New Delhi-110 001, ISBN-81-203-2139-1.

Clough, R.W and Penzien, J.(1993), "*Dynamics of Structures*" , Second Edition, McGraw-Hill, Inc, ISBN 0-07-113241-4.

Ishihara, K. (1996) ," *Soil Behaviour in Earthquake Geotechnics*", Clarendon Press, Oxford, ISBN 019 856224.

Lou, L and Zerva, A.(2004), "Effects of spatially variable ground motions on the seismic response of a skewed , multi-span , RC highway bridge, "*Soil Dynamics and Earthquake Engineering"*, August-October, pp. 729-740 , 11th International Conference on Soil Dynamics and Earthquake Engineering (ICSDEE) : Part 1 .

Raheem,S.E.A, Hayashikawa,T., Hashimoto, I. (2003), "Effect of soil-foundation-superstructure interaction on seismic response of cable stayed bridges tower with spread footing foundation", Journal of Structural Engineering Vol.49A.

Hassan, Md. Raquibul 2011. *Estimation of base rock vibration characteristics from surface ground motion. BSc* Thesis, Department of Civil Engineering, Bangladesh University of Engineering and Technology, BUET.

ID: ASEE 048

1st International Conference on Advances in Civil Engineering 2012 (ICACE 2012)
12 –14 December 2012
CUET, Chittagong, Bangladesh

OPTIMAL BRACING SYSTEM FOR MULTI-STORY STEEL BUILDINGS

S. R. CHOWDHURY[1*], F. ALI[1] , F.A. HAQUE[1] & S. B. KABIR[1]

[1]*Ahsanullah University of Science & Technology, Dhaka, 1208, Bangladesh (*srchowy@yahoo.com)*

ABSTRACT

The major concern in the design of the multi-storied buildings is the structure to have enough lateral stability to resist wind and earthquake forces. Bracing methods are normally used for steel structures to resist the lateral forces as well as to achieve control drift. There are different ways to limit the lateral drift. The method which is concerned for this study is to use braced frame with moment resisting connections. In this study, steel structures with 20, 30 and 40 floors using cross bracing of different lengths, configurations and x-section are studied by Finite Element software, ETABS in order to find the best suited configuration of bracing. For this purpose various forms of bracing system are studied under earthquake and wind loads in equivalent static analysis. In this study, also the concept of mega bracing and their properties as a new approach of bracing method is investigated. Main parameters of interests in the study of bracings effects are storey drift. Results show that using of mega bracings reduce displacements significantly with compare to other bracing arrangements. Mega bracing system is also found an economic solution among all other bracing systems considering the material consumption.

Keywords: Bracing, Mega-Bracing, Drift, Finite Element Analysis.

INTRODUCTION

Bracing is a highly efficient and economical method of resisting horizontal forces in a frame structure (Smith and Coull, 1991). The most efficient, but also most obstructive types of bracings are those that form fully triangulated vertical truss. These include the single-diagonal, double-diagonal, and K-braced types. The full-diagonal types of braced bent are usually located where passage is not required and which are unlikely to be relocated in the lifetime of the building. Other types of braced bent allow window and door openings, but those arrangements cause bending in the girder. Recently, new type of bracing system called mega bracings is introduced. Adding these bracings to the structural system is associated with increasing lateral stiffness and decreasing shear lag. Bracings in these structures cover several stories and spans as a single bracing. Azar BB and Karimi MRB ,2012 reviewed and discussed about this mega bracing in details. Since it crosses several stories, it sometimes causes obstruction for some stories. An attempt is made in this study to check the mega bracing systems whether it is economic over other cross bracing systems available in the literature considering material consumption and total lateral displacement. Steel structures with 20, 30 and 40 floors using cross bracing method are studied by Finite Element software, ETABS in order to find the best suited configuration of bracing under earthquake and wind loads in equivalent static analysis.

PROBLEM STATEMENT AND MODELING OF STRUCTURE

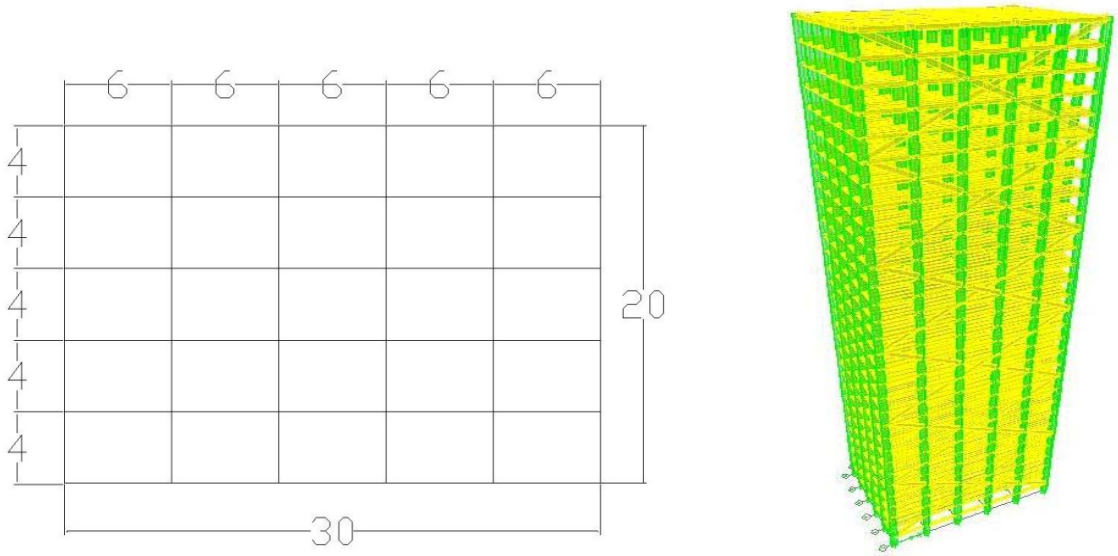

(a) Plan view of the building (dimension in meter) (b) View from ETABS

Figure 1: 30 storied steel building with mega bracing

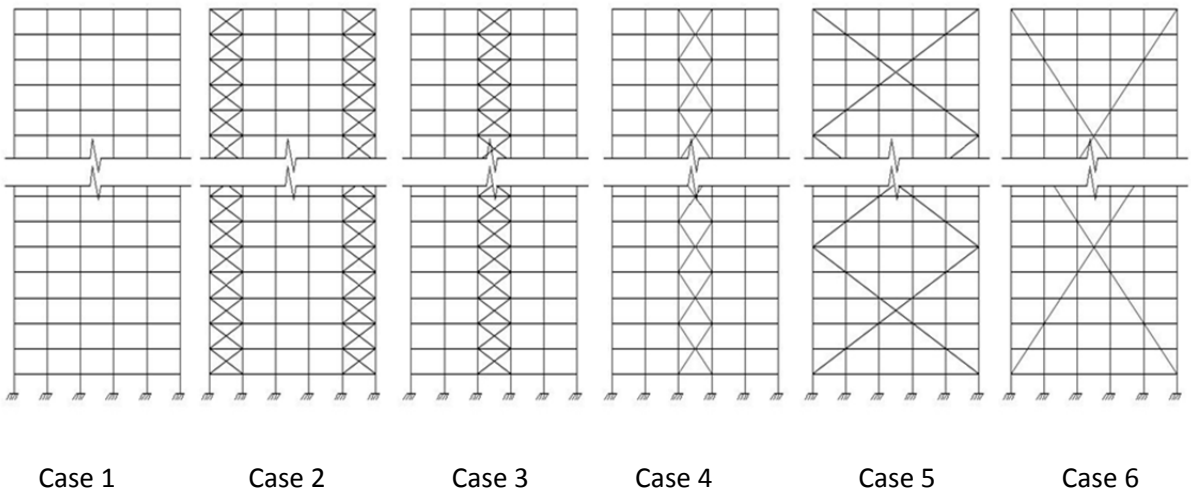

Figure 2: Different types of bracing system

The typical building plan layout of 3D reinforced concrete moment resisting building frame is studied as shown as Figure 1. The building is kept symmetric in both orthogonal directions in plan to avoid torsional response under pure lateral forces. Number of storey is varied from 20, 30 and 40 but the plan is unaltered. Floor height of 3 meters is maintained throughout the full height of the building.Linear elastic analysis is performed with the help of finite element software ETABS under earthquake loads in equivalent static method. In the present study, earthquake and wind load is preferred as a source of lateral loading on the building frame as set forth by the provision of Bangladesh National Building Code (BNBC, 1993). The frame members are modeled with rigid end zones and the floors are modeled as diaphrams riigid in-plane. Thicknesses of slab and deck are maintained for all buildings as 88.9 mm and 76.2 mm respectively. Although, bracings (only cross-bracing) are placed around the periphery of the building, bracings placed in plane of loading will take

most of the stresses. Buildings are modeled with different bracing systems available in leterature which are denoted by different cases (from case 1 to case 6) as shown in Figure 2. Case 1 represents the building model where there will be no bracing, case 2 stands for bracing placed at two exterior span, case 3 represents the building model where bracings are placed only at middle span. In casese 1, 2 and 3 one cross-bracing covers only one floor. Case 4 is exactly like case 3 with the exception of each one cross-bracing covers two storys. Case 5 stands for the building models where one mega cross bracing is placed for the whole 5 spans and covers 5 storeys at a time. Case 6 represents the building models where one mega cross bracing is placed for the whole 5 spans and covers 10 storeys at a time. Due to space limitation, half of each mega bracings (each half mega bracing covers 5 story means one full mega bracing will cover 10 storeys) is possible to show in the Figure 2 for case 6. Generally for columns, beams and bracings, wide flange (I) section is chosen in this study.

Table 1: Sizing of the members

	Column	Beam	Bracing (Wide Flange)	
20 story	W 33x291	W24X76	W 21x101	Case 2
				Case 3
				Case 4
				Case 5
				Case 6
30 story	W 40x503	W 24x76	W 30x148	Case 2
				Case 3
				Case 4
				Case 5
				Case 6
40 story	W 40x593	W 24x76	W 21x201	Case 2
				Case 3
				Case 4
				Case 5
				Case 6

The sizes of beams, columns and bracings for different cases and different storied building are described in Table 1. The wind load is applied as per BNBC, 1993 considering exposure condition A and wind velocity 210 km/hr. Earthquake load is applied as per BNBC, 1993 considering Seismic Zone Factor 0.15, Site Coefficient 1.5, and Importance Factor 1. Live load, floor finish load, partition wall load are taken as, 1 KN/m^2 , 1.5 KN/m^2 and 2 KN/m^2 respectively. Modulus of Elasticity of Steel and Concrete are taken as 200000 MPa and 24820 MPa respectively.

RESULTS AND DISCUSSION

Choice of Mega Bracing over Other Bracing:

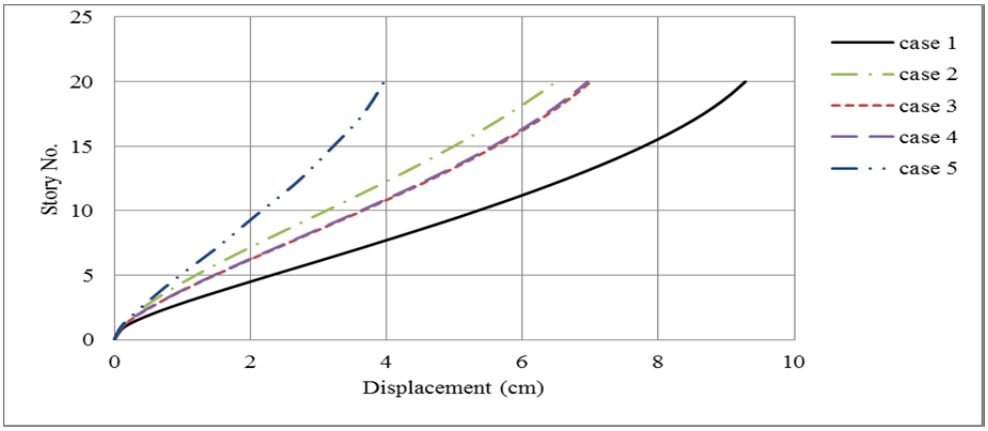

Figure 3: Variation of displacements with number of story for different bracing system for 20 storied building

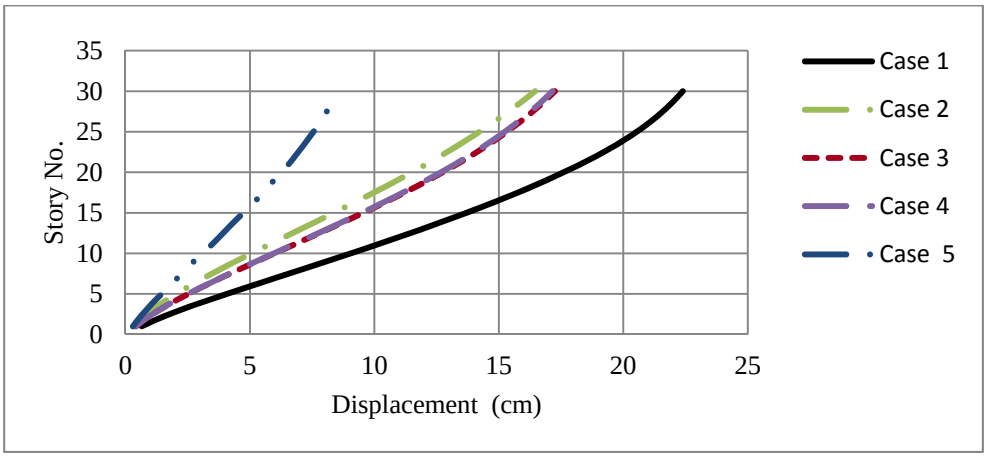

Figure 4: Variation of displacements with number of story for different bracing system for 30 storied building

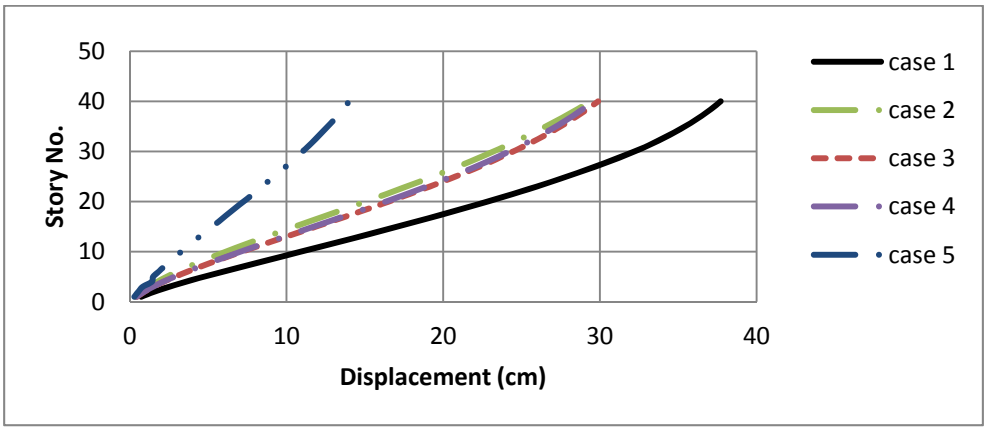

Figure 5: Variation of displacements with number of story for different bracing system for 40 storied building

Figures 3, 4 and 5 shows the influence of different cross-bracing systems on displacement of the building at different story levels for 20, 30 and 40 storied steel building. Mega bracing of case 5 produces the least displacement at all story levels of all three types of buildings and rate of decreasing displacement increases with increasing story height for all three types of buildings. For this reason it is advisable to use mega bracings as far as material consumption and drift control is concerned.

Mega Bracing of Different Types:

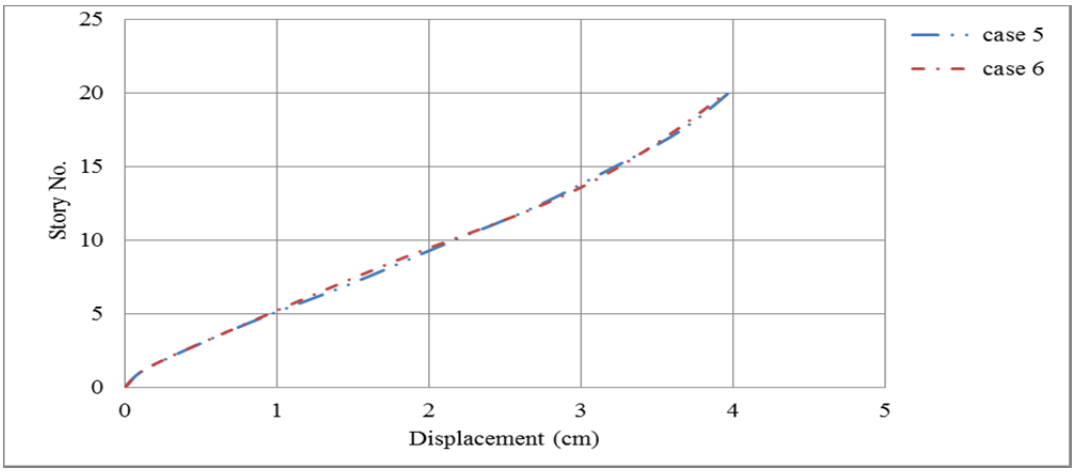

Figure 6: Variation of displacements with number of story for different mega bracing system for 20 storied building

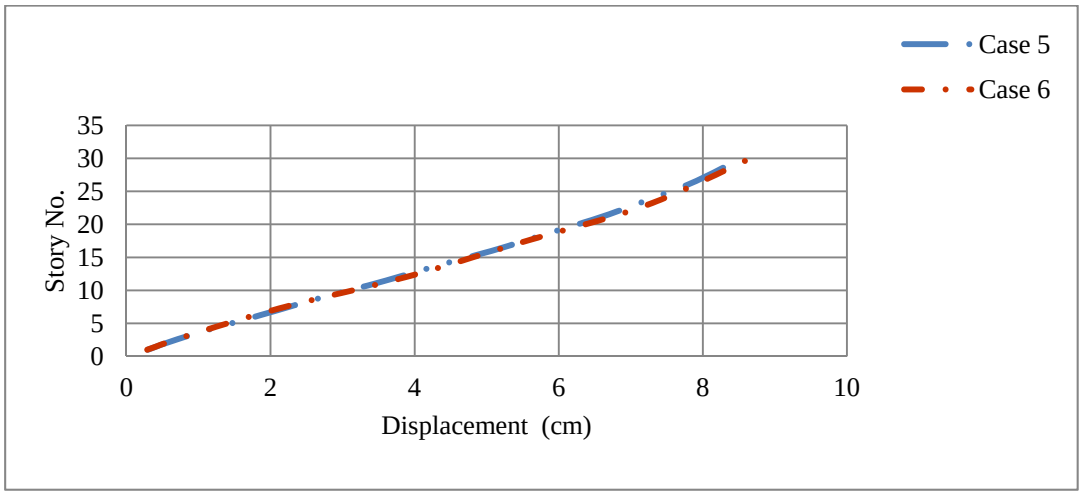

Figure 7: Variation of displacements with number of story for different mega bracing system for 30 storied building

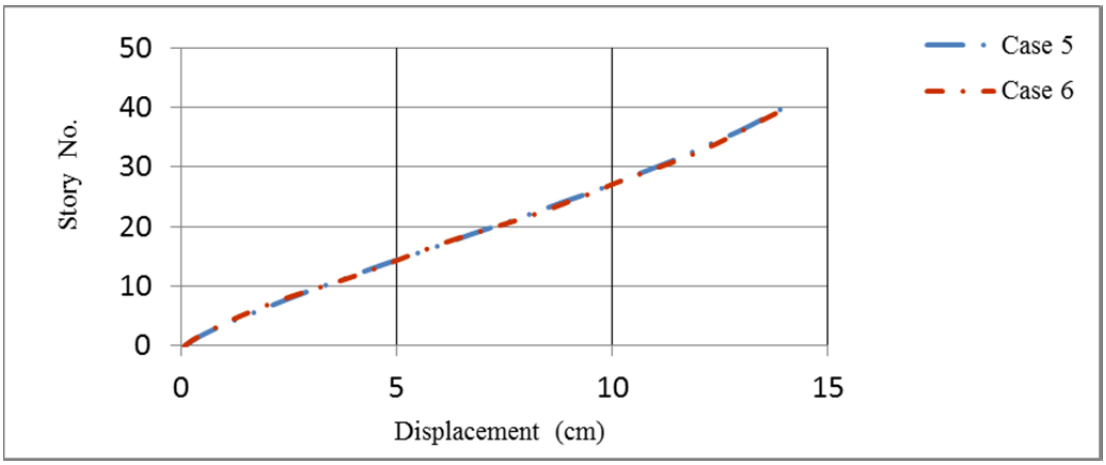

Figure 8: Variation of displacements with number of story for different mega bracing system for 40 storied building

Figures 6, 7 and 8 shows the impact of different mega bracing systems on displacement of the building at different story levels for 20, 30 and 40 storied steel buildings respectively. Mega bracings of case 5 and case 6 are concerned in these analyses. For all types of buildings, mega bracings of both cases 5 and 6 yield same displacements at all story levels. W30x148 and W30x99 sections are required for case 5 and case 6 respectively for 30 storied building to satisfy the design criteria of bracing. So, it is concluded here that mega bracing of case 6 should be used in this case as less amount of material is needed for case 6.

Variations of Stresses in Different Bracing Systems:

Bracing systems may have influence on the stresses (axial force, shear force and bending moment) of coulmns which can be shown from Table 2. Table 2 shows the maximum Axial Force, Shear Force and Bending Moment (mostly in the middle columns) at the bottom of 1st story for diferent bracing systems (cases) of 30 storied building. There is no significant differences in Axial Forces and Shear Forces in columns of different bracing systems (cases 2 to 6), even in columns of building without any bracing (case 1). Whereas after introducing bracings, bending moments of columns of all bracing systems have been reduced significantly and for mega bracing (cases 5 and 6), it (bending moment) reaches the least values among the bracing systems considered in this study.

Table 2: Axial Force, Shear Force and Bending Moment at the bottom of the First Storey for 30-Story Building

Different Cases	Maximum Axial Force (kN)	Maximum Shear Force (kN)	Maximum Bending Moment (kN-m)
Case 1	9450	275	1800
Case 2	9400	300	1100
Case 3	9450	275	1300
Case 4	9400	275	1300
Case 5	9400	275	1000
Case 6	9400	275	1000

Selecting the Shape of Cross-Section of Bracing:

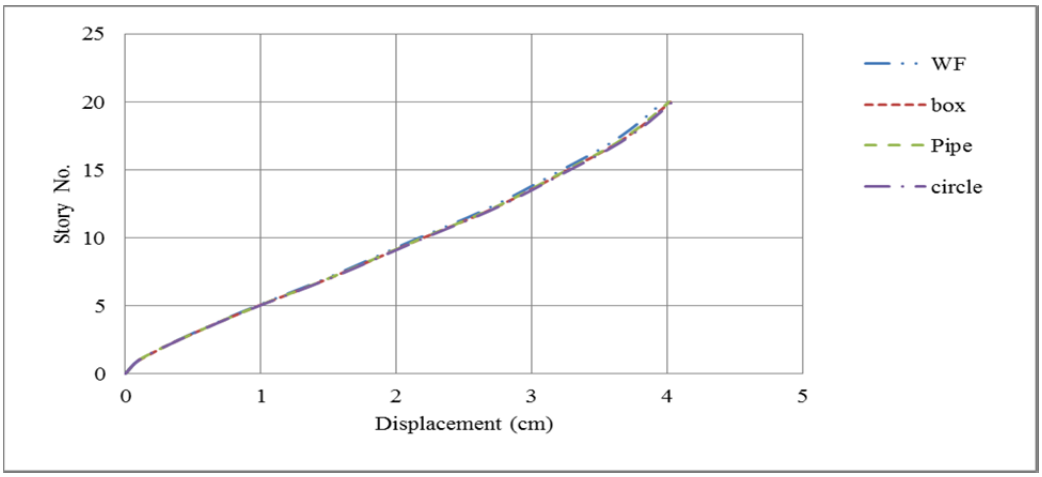

Figure 9: Variation of displacements with number of story for different X-sections of mega bracing for 20 storied building

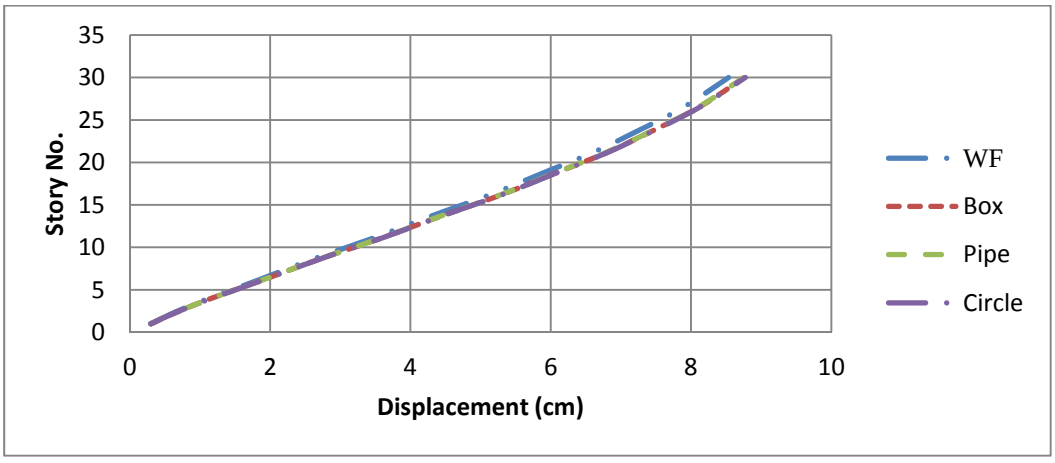

Figure 10: Variation of displacements with number of story for different X-sections of mega bracing for 30 storied building

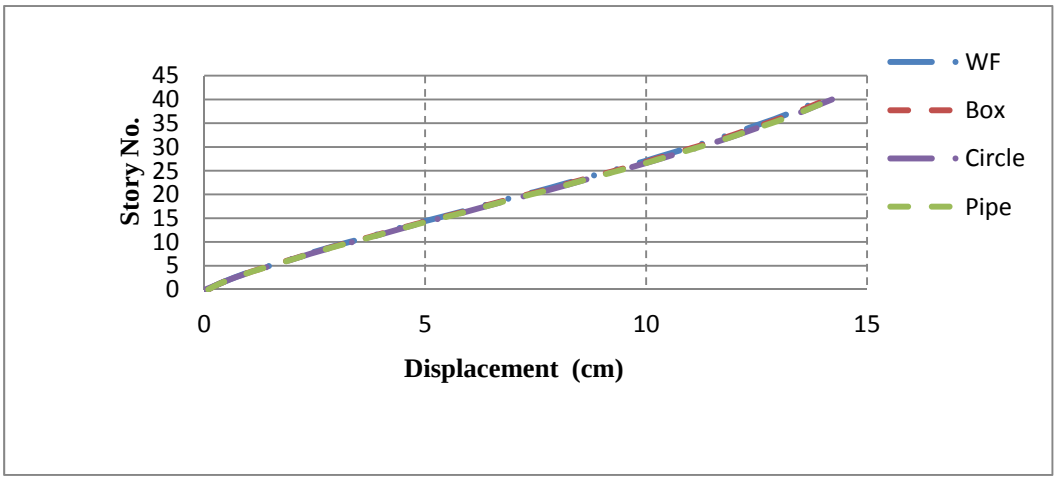

Figure 11: Variation of displacements with number of story for different X-sections of mega bracing for 40 storied building

Figures 6, 7 and 8 shows the impact of the shape of the cross-section of mega bracing on displacement of the building at different story levels for 20, 30 and 40 storied building respectively. Mega bracing of case 5 is concerned in these analyses.

For 20 storied building wide flange (W21x101), pipe (inner dia 38mm, outer dia 200mm), box (inner dimension 172mmx172mm and outer dimension 200mmx200mm) and circular section (dia 156mm) are used as different sections of mega bracings.

For 30 storied building wide flange (W30x148), pipe (inner dia 233mm, outer dia 300mm), box (inner dimension 180mmx150mm and outer dimension250mmx220mm) and circular section (dia 189mm) are used as different sections of mega bracings.

For 40 storied building wide flange (W21x201), pipe (inner dia 60mm, outer dia 228mm), box (inner dimension 254mmx249mm and outer dimension 457mmx305mm) and circular section (dia 220.5mm) are used as different sections of mega bracings. Sections are chosen in that way so that almost same amount of equivalent area is required for each section. From all types of buildings, wide flange proves the best section of mega bracing as far as lateral displacement is concerned.

CONCLUSIONS

It is wise to use mega bracings compare to other types of bracings as far as material consumption, drift control and stresses in column is concerned. For high rise steel building wide flange proves the best cross-section section of mega bracing as far as total lateral displacement is concerned. Only linear elastic analysis is made in this study. To make comprehensive and complete comment, nonlinear dynamic analysis is highly recommended.

REFERENCES

Smith, BS and Coull, A, 1991.Tall Building Structures, John Wiley and Sons, Inc.

Azar BB and Karimi MRB, 2012. Study the Effect of using Different Kind of Bracing System in Tall Steel Structures, American Journal of Scientific Research, ISSN 1450-233X, Issue 53, pp. 24-34

Bangladesh National Building Code (BNBC), 1993.

ID : ASEE 049

1st International Conference on Advances in Civil Engineering 2012 (ICACE 2012)
12 –14 December 2012
CUET, Chittagong, Bangladesh

FRAGILITY OF ELECTRICAL EQUIPMENT ITEMS IN SWITCHYARDS

M. ASHIQUZZAMAN[1], D. W. NA[2], M. K. HA[3] & K. J. HONG[4*]

[1,2,3,4] Department of Civil and Environmental Engineering, Kookmin University, Seoul, Korea
[1]nahid_ce8@yahoo.com, [2]ekdhk7146@naver.com, [3]minkooklove@kookmin.ac.kr. [4]kjhong@kookmin.ac.kr*

ABSTRACT

The main focus of this study is to evaluate the fragility of electrical equipment items in switchyard to support the seismic design. The probability of seismic damage during the ground motion can be determined by the developed fragility curve. The methodology of developing this curve is based on the design standards of FEMA 450, FEMA 451 and ACI 318.

Keywords: Fragility Curve, Electrical Equipment item, Switchyard, Probabilistic Risk Assessment.

INTRODUCTION

Failure probability of electrical equipment is the convolution of the hazard and the fragility curves. The seismic hazard is the probability of occurrence of the potential destruction in a defined area and a given time interval due to expected earthquake ground motions. Seismic fragility of a structure illustrates the probability to reach or exceed different degrees of distortion, including possible failure. Based on the total probability, the probability of failure of the circuit breaker can be expressed by the following equation:

$$P_F = \int_0^{+\infty} H(a)\left(\frac{dP_{F/a}}{da}\right)da \qquad (1)$$

where, $P_{F/a}$ is the conditional probability of failure given the ground motion level a, which is also called as the mean fragility curve, $H(a)$ is the mean hazard frequency exceeding the ground motion level, a.

Fig. 1. Circuit breaker in Switchyard

Fig. 2. Base of circuit breaker anchored by bolts

Regarding the possibility of collapse, damage etc. to electrical facilities such as switchyards at nuclear power plants demand the seismic fragility analysis. Circuit breaker is one of important item in the switchyard. A circuit breaker is protective equipment which is designed to automatically open an electrical circuit thus preventing the damages due to over load, short circuits and sometimes earth faults. Normally high voltage circuit breakers are used in the switchyards. The Fig. 1 and Fig. 2 show the circuit breaker and its base respectively. This paper focuses on the seismic fragility analysis of the bolt anchorage used in the base of the circuit breaker. In order to develop fragility curve, it is required to estimate the median acceleration, logarithmic standard deviation for aleatory (irreducible) randomness and logarithmic standard deviation for epistemic uncertainty.

METHODOLOGY OF FRAGILITY ANALYSIS

Overview of the Methodology

To develop the fragility curve, we need to follow the steps which are given below:

Step 1: Determining the demand spectral acceleration and variables.
Step 2: Frequency sampling to get median spectral acceleration and logarithmic standard deviation for epistemic uncertainty.
Step 3: Determining the demand force and capacity of the bolts.
Step 5: Establishing the earthquake scale factor.
Step 6: Determining the logarithmic standard deviation.
Step 7: Development of the fragility curve.

Spectral Acceleration Demand

The horizontal spectral acceleration demand of circuit breaker is shown in Fig. 3 (Reed, J. W.; Kennedy, R. P., 1994). The data is assumed to be same in both horizontal directions.

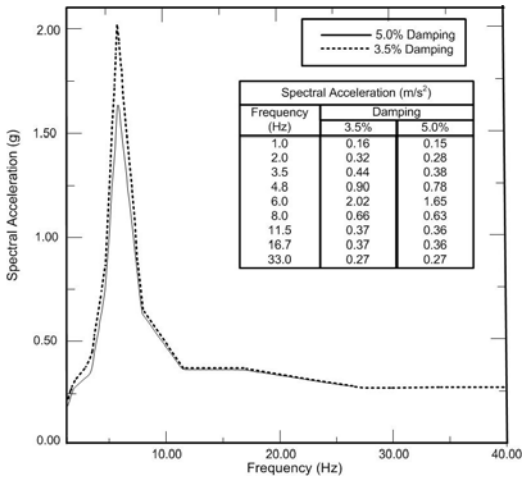

Fig. 3. Horizontal spectral acceleration demand at circuit breaker.

Demand Variables

The base of the circuit breaker has a rigid and stiff frame in which the bolts are attached. In the fragility analysis, the response and the strength variables of equipment items affect the capacity of the anchored bolts. It is required to define the demand variables of equipment for the fragility analysis (Reed, J. W.; Kennedy, R. P., 1994). The demand variables are shown in Table 1.

Table 1: Demand variables for fragility analysis of anchor bolts

Variable	Median Demand Factor	Logarithmic Standard Deviation	
		β_r	β_u
Equipment			
Frequency	1.0	-	0.10
Damping	0.05 (median)	-	0.035(-1 σ)
Mode shape	1.0	-	0.05
Mode Combination	1.0	0.05	-

Frequency Sampling

The initial work in the fragility analysis is to estimate the median demand in the anchor bolt based on the reference earthquake input. A reasonable attempt is to probabilistically vary the frequency about the median value with 5% damped response spectrum to obtain a distribution of spectral acceleration and fit a lognormal to this distribution. Monte Carlo simulation represents an effective procedure to vary the frequency probabilistically. One simple method for performing Monte Carlo analysis is called Latin hypercube simulation.

The left sided box of the simulation process where the range of probability values 0 to 1 is divided up into N equal slices. A random value is sampled within each slice and the corresponding dynamic frequency value, f_i ,

$$f_i = \breve{f}.e^{\beta.\Phi^{-1}(P_i)} \tag{2}$$

where,

$\breve{f}$ = median frequency

β = logarithmic standard deviation for frequency

P_i = corresponding probability value with each frequency = $\frac{i-1+rnd\,(1)}{N}$

i =1 to N

Φ^{-1} =inverse normal (Gaussian) distribution function

rnd_i =random number between 0 and 1 (different for each i)

Demand Median Spectral Acceleration, Epistemic Uncertainty and Load

The best fit lognormal distribution is found by linear regression analysis on a transformation of the spectral acceleration data. For the median spectral acceleration, $\breve{S}_a$, assuming that the spectral acceleration, S_a is lognormal distribution, probability, P_i is

$$P_i = \Phi\left[\frac{\ln\left(S_{a_i}/\breve{S}_a\right)}{\beta_u}\right] \tag{3}$$

The above equation can be rearranged for S_{a_i} as below.

$$\ln\left(S_{a_i}\right) = \ln\left(\breve{S}_a\right) + \beta_u \Phi^{-1}[P_i] \tag{4}$$

Therefore, it is clear that the lognormal demand data are linearized into a straight line when plotted. From the combined plotting of spectral acceleration sample distribution and best fit lognormal distribution, slope of the regression line is the logarithmic standard deviation for epistemic uncertainty, β_u and the exponential of the intercept of the line is median spectral acceleration, $\breve{S}_a$.

For estimating the demand tensile force and shear force of the bolt, the NEHRP recommended provisions for electrical component design requirements of FEMA 451(Building Seismic Safety Council, 2006) is followed.

Capacity of anchor bolts

In this study, based on the Appendix D of ACI 318-11(ACI Committee 318, 2011), the shear and tensile capacity of the bolt of circuit breaker is determined.

Earthquake scale factor

For determining logarithmic standard deviation, it is required to define the scale factor. Usually the scale factor analysis is determined for the first time by using the median values for all the input parameters. Then the analysis is repeatedly done by changing each of the subjected variables and then the logarithmic standard deviation is obtained by using the equation (6). As per ACI 318-11, scale factor can be defined by,

$$FS = \frac{1.2}{\frac{P_S}{\phi P_C} + \frac{V_S}{\phi V_C}} \geq 1.0 \qquad (5)$$

Where, P_S & V_S =demand tension and shear force in bolt respectively and ϕP_C & ϕV_C = capacity in bolt for tension and shear respectively.

Determining Logarithmic standard deviation

Basing on basic fragility analysis demand variables of equipment and its characteristics, the logarithmic standard deviations (β) for aleatory randomness and epistemic uncertainty are determined. The β -value can be calculated by the following equation,

$$\beta = \frac{1}{|\phi|} \ln\left[\frac{\left(\breve{F}S\right)}{\left(FS\right)_{\phi\sigma}}\right] \qquad (6)$$

where, $\breve{F}S$ is the median scale factor and $FS_{\phi\sigma}$ is the scale factor at ϕ standard deviation. The parameter ϕ is generally set at 1 in case of median that leads to the lowest capacity.

The $HCLPF_{50}$ is defined by the following equations,

$$HCLPF_{50} = \breve{S}_a . e^{-1.65\left(\beta_r + \beta_u\right)} \qquad (7)$$

Where, β_r & β_u = logarithmic standard deviation for aleatory randomness and epistemic uncertainty respectively.

NUMERICAL APPLICATION

After following the above mentioned procedure, the best fit lognormal distribution can be obtained from the simulation data based on the equation (2) to (4). The observed data from the simulation is given in the Table 2. Based on the simulation data, frequency sampling process and the best lognormal distribution are shown in Fig. 4 and Fig. 5 respectively.

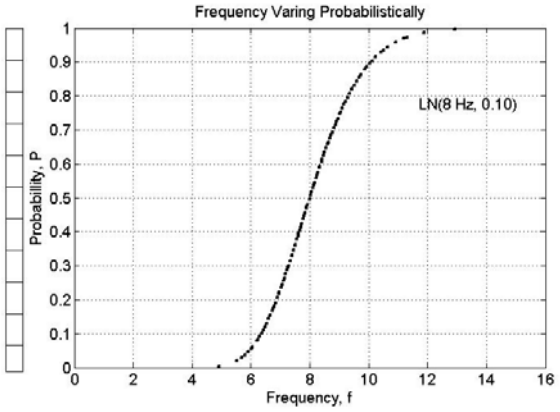

Fig. 4. Frequency sampling process

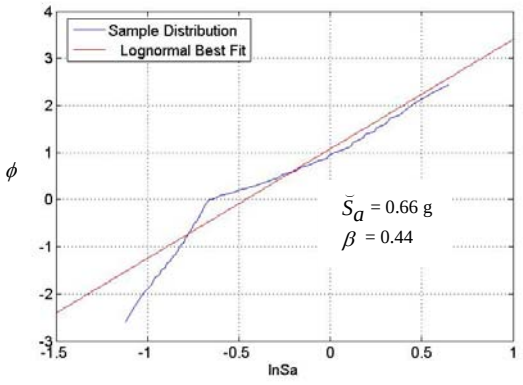

Fig. 5. Best fit lognormal distribution for demand

Table 2: Result of Simulation

Sample	Probability, P_i	$\phi = \Phi^{-1}(P_i)$	Dynamic Frequency, f_i (Hz)	Spectral Acceleration Sa(f , 0.05) (g)	$\ln Sa_i$
1	0.0023	-2.8407	6.0217	1.6389	0.7128
2	0.0129	-2.2301	6.4009	1.4456	0.5316
.	.	.	.	.	.
99	0.9806	2.0654	9.8354	0.4884	-1.0338
100	0.9953	2.5964	10.3717	0.4470	-1.1615

If the total weight on the base is 35KN. Considering the base of a circuit breaker is anchored by 0.013m diameter L-bolts and the circuit breaker's vertical spectral acceleration demand is assumed to be 0.6g. The peak ground acceleration is 0.13g. Others data are given in the Fig. 6.

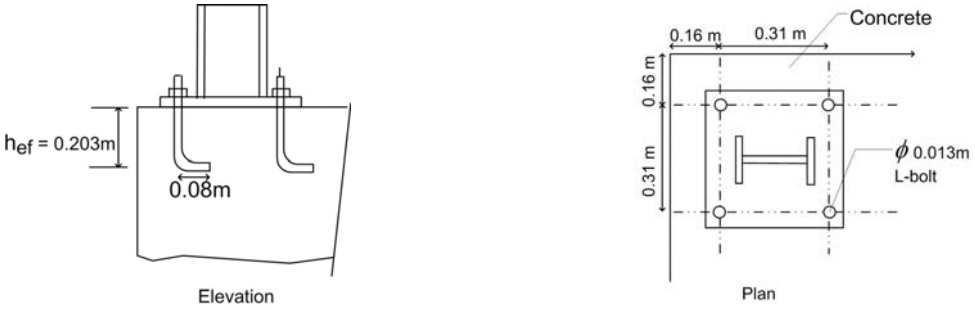

Fig. 6. Anchorage details of circuit breaker

The derived parametric values of fragility curve from the calculation can be summarized as per the following way:

Median spectral acceleration,	$\breve{s}_a$	:	$0.33\,g$
Logarithmic standard deviation for aleatory randomness,	β_r	:	0.06
Logarithmic standard deviation for epistemic uncertainty,	β_u	:	0.63
$HCLPF_{50}$		:	$0.11\,g$

Basing on the calculated parametric values, we can develop the fragility curve for the base anchorage system of the circuit breaker in a switchyard. The Fig. 7 illustrates the developed fragility curve of the circuit breaker for the base anchorage system.

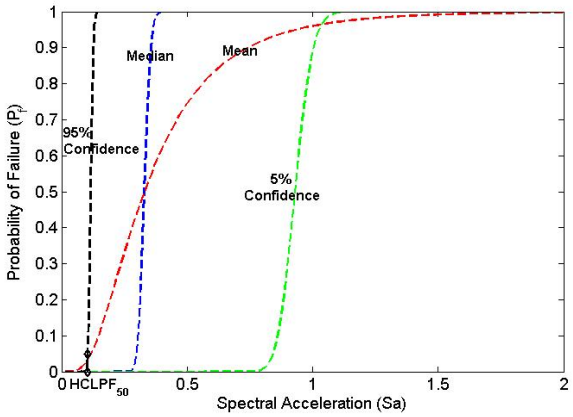

Fig. 7. Fragility curve of circuit breaker of a switchyard

CONCLUSION

This study demonstrated the feasibility of determining the parametric values of the fragility curve of circuit breaker in case of switchyard. The failure analysis, source of uncertainties and probabilities are expressed in a specific way so that the fragility curve can be developed easily based on the determined parametric values.

ACKNOWLEDGMENTS

This research was supported by grants (2011T100100111) from the Ministry of Knowledge and Economy of Korea.

REFERENCES

Reed, J. W.; Kennedy, R. P.; Buttemer, D. R.; Idriss, I. M.; Moore, D. P.; Barr, T.; Wooten, K. D.;

Smith, J. E., 1991. A methodology for Assessment of Nuclear Power Plant Seismic Margin. NP-6041, Revision 1, Electric Power Research Institute, Jack R. Benjamin and Associates, Inc., Mountain View, California.

Reed, J. W.; Kennedy, R. P., 1994. Methodology for Developing Seismic Fragilities. NP-6041, Revision 1, TR-103959, Final Report. Electric Power Research Institute, Jack R. Benjamin and Associates, Inc., Mountain View, California.

Building Seismic Safety Council, 2003. NEHRP Recommended Provisions for Seismic Regulations for New Buildings and Other Structures (FEMA 450-1).

Building Seismic Safety Council, 2006. NEHRP Recommended Provisions for Seismic Regulations for New Buildings and Other Structures: Design Examples, (FEMA-451).

ACI Committee 318, 2011. Building Code Requirements for Structural Concrete (ACI 318-11).

ID : ASEE051

1st International Conference on Advances in Civil Engineering 2012 (ICACE 2012)
12 –14 December 2012
CUET, Chittagong, Bangladesh

STRENGTH BEHAVIOR OF MORTAR USING SLAG AS PARTIAL REPLACEMENT OF SAND

MD. A. HASAN[1], MD. M. ISLAM[2*], MD. H. KABIR[1] & MD.S. ISLAM[2]

[1]*Graduate, Department of Civil Engineering, CUET, Chittagong, Bangladesh,<hasanrazu0601056@gmail.com>*
[2] *Department of Civil Engineering, CUET, Chittagong-4349, Bangladesh, <mislam@cuet.ac.bd>*
**Corresponding Author*

ABSTRACT
This paper presents the results of an experimental investigation carried out to study the mechanical properties of mortar in which fine aggregate i.e. sand was partially replaced with ground granulated blast furnace slag (GGBFS). Sand was partially replaced with seven percentages (10%, 20%, 30%, 40%, 50%, 60% and 70%) of slag by weight. Ordinary Portland cement (OPC) mortar was also prepared as reference mortar. Three different mortars with cement sand ratios of 1:2.25, 1:2.75 and 1:3.5 have been used in the study. A total of 800 nos of cube and briquette mortar specimens were cast and compressive as well as tensile strength of the mortar specimens were determined at curing age of 7, 14, 28, 60 and 90 days. Test results show that strength increases with the increase of slag up to an optimum value, beyond which, strength start decreasing with further addition of slag. Among the seven slag mortars, the optimum level of cement replacement is found at 30%, which provides 22% higher compressive and 18% higher tensile strength as compared to OPC mortar.

Keywords: Slag, Cement, Mortar, Compressive Strength, Tensile Strength, Hydration.

INTRODUCTION
Blast furnace slag is a by-product obtained during the manufacture of pig iron in the blast furnace and is formed by combination of earthy constituents of iron ore with limestone flux. When the molten slag is swiftly quenched with water in a pond or cooled with powerful water jets, it is transformed into a fine, granular, almost fully non crystalline, glassy form known as granulated slag having latent hydraulic properties. Such granulated slag when finely ground and combined with Portland cement, has been found to exhibit excellent cementitious properties (Hwang, 1986). The reactivity of ground granulated blast furnace slag (GGBFS) is considered to be an important parameter to assess its effectiveness in concrete composites (Smolczyk, 1978).

Slag is generally used in construction work to achieve energy conservation, economic, ecological and technical benefits. It is used as pozzolanic mineral admixture in mortar and concrete and also has the hydraulic properties. According to ASTM C125, Pozzolan is a siliceous or siliceous and aluminous material which itself possesses little or no cementitious value but in finely divided form and in the presence of moisture, chemically reacts with calcium hydroxide at ordinary temperatures to form compounds possessing cementitious properties. According to ASTM C125, blast furnace slag is defined as the non-metallic product consisting essentially of silicates and aluminosilicates of calcium and other bases that is developed in a molted condition simultaneously with iron in a blast furnace.

When GGBF slag is mixed with water, initial hydration is much slower as compared with Portland cement. In the hydration process, GGBF slag produces calcium silicate hydrate cement paste. This valuable contribution of GGBF slag improves the paste-to-aggregate bond in concrete. GGBF slag mixtures with Portland cement typically result in greater strength and reduced permeability. The principle constituents of blast furnace slag are silica, alumina, calcium and magnesia (reported as oxide), which comprise 95% of slags total makeup. Minor elements include manganese, iron and sulfur compounds as well as trace quantities of several others. Like Portland cement, most of the calcium oxide (CaO) found in GGBFS is tied up as calcium silicate, calcium aluminates and calcium aluminosilicate. Although these compounds are not identical to those found in Portland cement (i.e., tricalcium silicate, tricalcium aluminate, etc.), they hydrate when activated by calcium hydroxide (lime) which is one of the by-product of Portland cement hydration. When Portland cement reacts with water, it forms calcium silicate hydrate (CSH) and calcium hydroxide ($Ca(OH)_2$). CSH is the glue that provides strength and holds concrete together while $Ca(OH)_2$ is a byproduct of Portland cement hydration that does not contribute to strength. When slag is used as partial replacement of sand in a mortar or concrete mix, it reacts with water and $Ca(OH)_2$ to form more CSH. The additional CSH increase the density of the mortar or concrete matrix thereby enhancing strength. Using of Slag as partial replacement of sand increases the compressive and tensile strength of conventional mortar and concrete and is often a vital component in producing high strength concrete. 28-days concrete strengths generally increase as the percentage of slag content increases up to about 50 percent of cementitious material.

The reactivity of slag, to a great extent, depends on its composition. In general, the more basic the slag, the greater its hydraulic reactivity in the presence of alkaline activators; the higher the glassy phase, the lime, alumina and magnesia contents, the higher the hydraulic reactivity. In many specifications basicity is quantitatively defined as a mass ratio between the sum of ($CaO+Al_2O_3+MgO$) and SiO_2, which is known as the basicity factor. For instance, a basicity factor of ≥ 1 is used in Germany to evaluate slags for use in blended cements. A high MgO content in some North American slags may sometimes be of concern for the formation of expansive particles. However, Stutterheim (1960) investigated concretes made from blended cements containing 50% slag having up to 20% MgO and found that these cements were as sound as comparable Portland cements, although he recommended that high MgO slags to be checked for soundness before use. According to ACI Committee 226 (1994), the greater solid volume and higher fineness of slag allow more coarse aggregate to be used without a loss of workability. This often reduces the stickiness of the mix. Meusel and Rose (1983) investigated highly active slag at contents of 30%-50% in concrete and found that the slag improved the workability in all cases, but greater improvement was obtained with higher slag contents. In the present study, mortar specimens were made with different replacement levels of sand with slag and cured up to 90 days. Compressive as well as tensile strength tests were carried out at different period to observe the performance of slag mortar.

EXPERIMENTAL PROGRAM

The experimental program was planed to predict the compressive and tensile strength of mortars using slag as replacement of sand. Sand replacement at various percentage levels were used in this investigation to observe the effects of different slag levels in mortar in contributing the compressive and tensile strength at various ages of curing.

Materials Used:

(a) Cement: ASTM Type I Portland Cement conforming to ASTM C-150 was used as binding material. Chemical compositions of OPC are given in **Table 1.**

(b) Slag: Ground granulated blast furnace slag (GGBFS) was used for this investigation. Chemical compositions of slag are given in **Table 1.**

(c) Sand: Locally available natural sand passing through 4.75 mm sieve and retained on 0.015 mm sieve was used for this program. Gradation of the sand is given in **Table 2.**

Table 1 : Chemical Composition of Ordinary Portland Cement and Slag

Chemical Composition	ASTM Type-I Cement (%)	Slag (%)
Calcium Oxide, CaO	64.5	38.7
Silicon Dioxide, SiO_2	20.6	34.9
Aluminum Oxide, Al_2O_3	6.4	16.8
Ferric Oxide, Fe_2O_3	4.5	0.8
Magnesium Oxide, MgO	1.2	7.3
Sulfur Trioxide, SO_3	1.7	0.81
Insoluble Residue	0.5	0.65

Table 2 : Grading of Sand

Sieve size	Cumulative % Passing (for Compressive Strength)	Cumulative % Passing (for Tensile Strength)
1.18 mm (No. 16)	100	100
850 µm (No. 20)	--	88
600 µm (No. 30)	95	0
425 µm (No. 40)	75	--
300 µm (No. 50)	29	--
150 µm (No. 100)	2	--

Variables studied

(a) Mortar quality: Seven different replacement level of sand as sand : slag (90:10, 80:20, 70:30, 60:40, 50:50, 40:60, 30:70) were used in this experimental program. Sand slag mix ratio of 100:0 i.e. pure cement mortar specimens were also cast as reference mortar for comparing the properties of slag mortars.

(b) Exposure period: Specimens were tested periodically after the specified curing periods of 7, 14, 28, 60 and 90 days.

(c) Size of specimens: 50 mm x 50 mm x 50 mm cube specimens for compressive strength and briquette specimens of standard size for tensile strength tests were prepared as per ASTM standard.

(d) Mortar mix ratios: The mix ratio of cement and sand was 1:2.25, 1:2.75 and 1:3.5 for compressive as well as tensile strength test specimens. Details of mix proportion and materials are shown in **Table 3.** Cement sand mix ratio 1:2.25 is designated as M1 grade, 1:2.75 as M2 and 1:3.5 as M3 grade. Also S is used to indicate the replacement level of sand with slag. Thus M2S40 indicates cement sand mix ratio 1:2.75 and 40% sand replacement by slag.

Table 3: Mix Proportions of Various Ingredients of Mortar

Sl. No	Specimen Type/ Materials	For Compressive strength test		For Tensile strength test	Remarks
1.	Specimen	50 mm Cube*		25 mm Briquette**	Materials required for 6 specimens
Mix Ratio		**1:2.25**	**1:2.75**	**1:3.5**	
2.	Cement	500 gm	500 gm	500 gm	
3.	Sand	1125 gm	1375 gm	1750 gm	
4.	Water	242 ml		132 ml***	

* ASTM C190-85 ** ASTM C190-87 *** Normal Consistency = 27%

(e) Curing environment and testing: A total of 800 mortar specimens were cast in the laboratory. After casting, the specimens were kept at 27°C temperature and 90% relative humidity for 24 hours. After demoulding, all the specimens were cured in water in a curing tank at room temperature. After

specific exposure period, specimen was tested for compressive and tensile strength in accordance with test procedure **ASTM C190-85 and ASTM C190-87**.

RESULTS AND DISCUSSION

Compressive Strength:

Compressive strength of various types of mortars made with different sand replacement level by slag has been graphically presented in **Fig.1 to Fig.4.** Test results showed that the 7 days compressive strength for M1S10, M1S20, M1S30, M1S40, M1S50 mortar is 1%, 4%, 17%, 8%, 2% higher as compared to reference mortar; whereas the same strength values are increased by 5%, 9%, 22%, 15%, 13% for M2S10, M2S20, M2S30, M2S40, M2S50 mortar. After 28 days of curing, compressive strength is increased to 4%, 8%, 22%, 18%, 15%, 10%, 8% for M1S10, M1S20, M1S30, M1S40, M1S50, M1S60, M1S70 mortar as compared to reference mortar; whereas the same strength values are increased of 6%, 10%, 27%, 20%, 15%, 10%, 8% for M2S10, M2S20, M2S30, M2S40, M2S50, M2S60, M2S70 mortar. So it is clear from the test results that after 28 days of curing for all grade of mortar compressive strength of mortar are increased for all replacement level of sand. 60 and 90 days compressive strength data shows almost similar trend. In all cases 20%, 30% and 40% sand replaced mortar shows better strength result as compared to other types for mortar for all mixes. Cement normally gains its maximum strength within 28 days. During that period, lime produced from cement hydration remains within the hydration product. Generally, this lime reacts with slag used as partial replacement of sand and imparts more strength. For this reason, mortars made with slag will have almost same strength at the early ages of curing as that of reference mortar and higher strength at the later ages of curing.

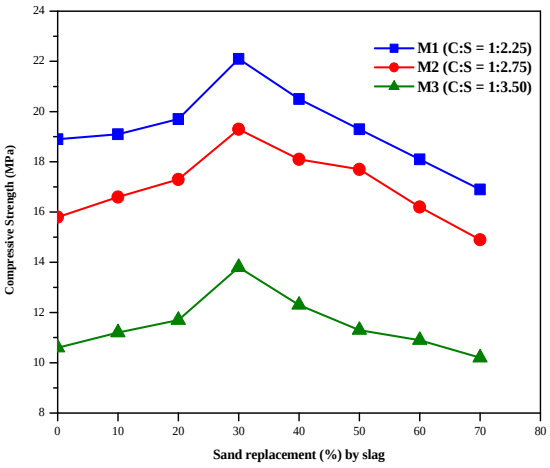

Fig.1: Compressive Strength vs Sand Replaement(%) by Slag for Various Types of Mortar (Curing age 7 days)

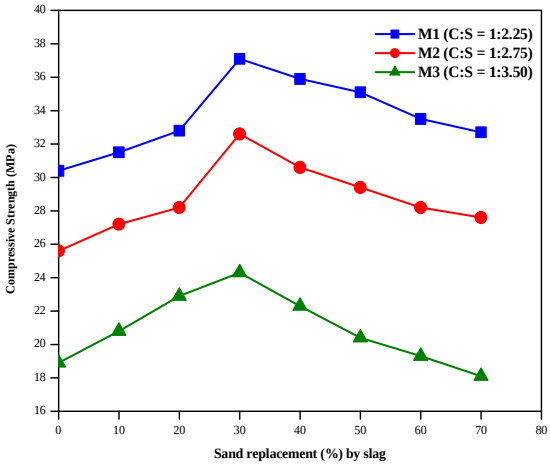

Fig.2: Compressive Strength vs Sand Replaement(%) by Slag for Various Types of Mortar (Curing age 28 days)

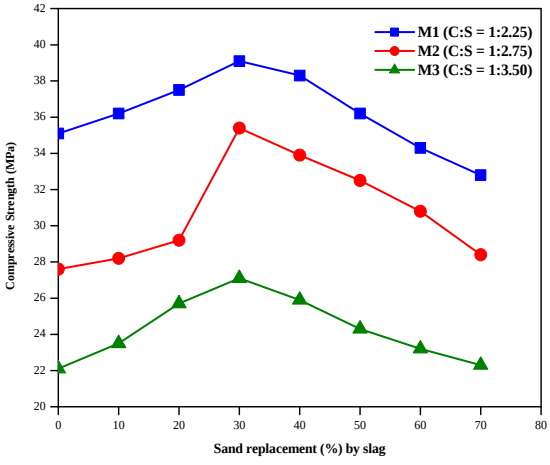

Fig.3: Compressive Strength vs Sand Replaement(%) by Slag for Various Types of Mortar (Curing age 60 days)

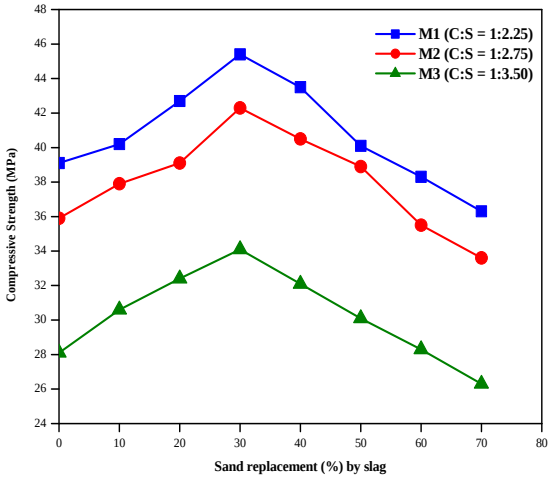

Fig.4: Compressive Strength vs Sand Replaement(%) by Slag for Various Types of Mortar (Curing age 90 days)

Rate of strength gaining for different types of mortar is observed to vary with the grade of mortar. Among all the mortar studied, 60 days compressive strength is increased by about 4%, 8%, 14%, 11% and 4% for M1S10, M1S20, M1S30, M1S40 and M1S50 mortar respectively as compared to 28 days compressive strength of reference mortar; whereas the same strength value is increased by around 7%, 19%, 26%, 20% and 12% for M3S10, M3S20, M3S30, M3S40 and M3S50 mortar respectively. After 90 days of curing, the compressive strength as compared to 28 days of curing of similar mortar was observed as 5%, 11%, 20%, 14% higher for M1S10, M1S20, M1SA30, M1S40 mortar; 8%, 13%, 25%, 18% higher for M2S10, M2S20, M2S30, M2S40 mortar and 13%, 22%, 31%, 21% higher for M3S10, M3S20, M3S30, M3S40 mortar respectively. So it can be concluded that strength gaining rate is lower for the higher grade of mortar.

Tensile strength

The tensile strength of mortar mixes made with and without slag as partial replacement of sand was determined at the ages of 7, 14, 28, 60 and 90 days. **Fig.5 to Fig.8** shows the variation of tensile strength of different grades of mortar with different slag content as partial replacement of sand for various curing ages.

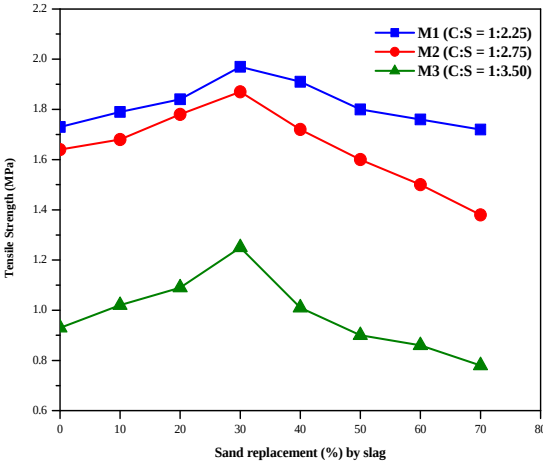

Fig.5: Tensile Strength vs Sand Replaement(%) by Slag for Various Types of Mortar (Curing age 7 days)

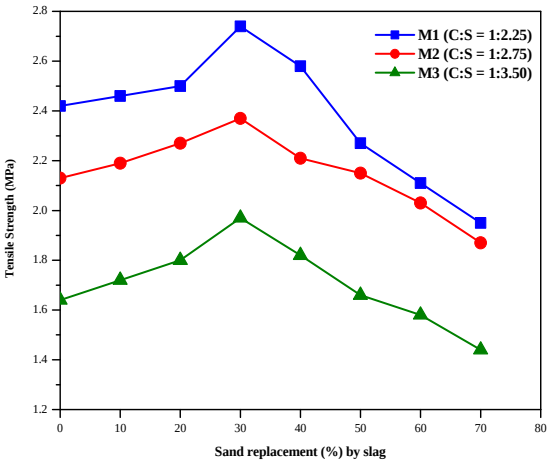

Fig.6: Tensile Strength vs Sand Replaement(%) by Slag for Various Types of Mortar (Curing age 28 days)

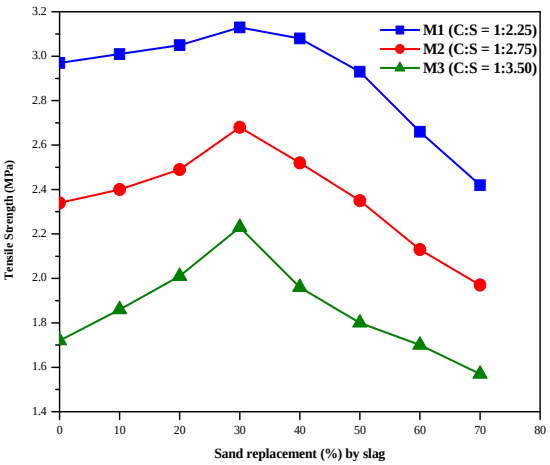

Fig.7: Tensile Strength vs Sand Replaement(%) by Slag for Various Types of Mortar (Curing age 60 days)

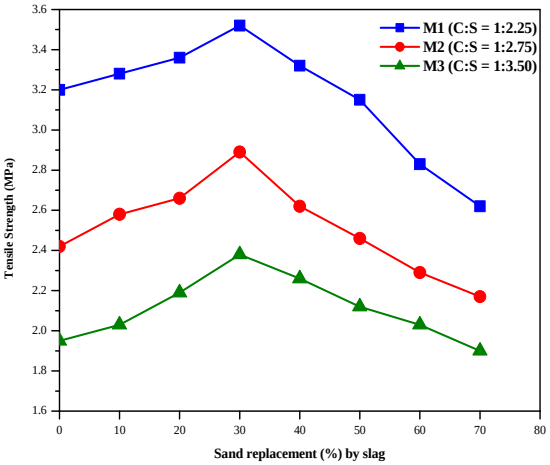

Fig.8: Tensile Strength vs Sand Replaement(%) by Slag for Various Types of Mortar (Curing age 90 days)

At early age of curing tensile strength of mortar made by replacing sand with slag are almost same as that of reference mortar. Test results showed that the 7 days tensile strength for M1S10, M1S20, M1S30, M1S40 mortar is 3%, 6%, 14%, 10% higher as compared to reference mortar; whereas the same value is increased by 2%, 9%, 14%, 5% for M2S10, M2S20, M2S30, M2S40 mortar. After 28

days of curing, tensile strength is increased to 2%, 3%, 13%, 7% for M1S10, M1S20, M1S30, M1S40 mortar as compared to reference mortar; whereas the same value is increased 3%, 7%, 11%, 4% for M2S10, M2S20, M2S30, M2S40 mortar. The mortar specimens made by replacing sand with slag shows almost identical tensile strength results as that of reference mortar up to sand replacement level of 40% and upto curing age of 28 days. Tensile strength values for mortar having sand replacement of 50%, 60% and 70% achieve lower strength as compared to reference mortar.

Again, the rate of strength gaining for different types of mortar is observed to vary with their grade. Relative tensile strength is higher for the lower grade mortar. Among all the mortar mix studied, 60 days tensile strength is observed to be increased by about 1%, 3%, 6% and 4% for M1S10, M1S20, M1S30 and M1S40 respectively as compared to 28 days strength of M1 grade mortar; whereas the same value is seen to be increased by around 3%, 7%, 16% and 8% for M2S10, M2S20, M2S30, M2S40 mortar and 8%, 18%, 31%, 15% for M3S10, M3S20, M3S30, M3S40 mortar respectively as compared to 28 days strength of reference mortar. In case of 90 days of curing, compressive strength compared to 28 days of curing of similar mortar was observed that 4%, 7%, 13% and 5% higher for M1S10, M1S20, M1SA30 and M1S40 mortar, 7%, 11%, 12% and 9% higher for M2S10, M2S20, M2S30 and M2S40 mortar, 5%, 15%, 26% and 29% higher for M3S10, M3S20, M3S30 and M3S40 mortar. Thus it is seen that tensile strength gaining is relatively faster for lower grade mortar as compared to higher grade.

CONCLUSION

Based on the results of the investigation conducted on different grades of mortars made with various level of sand replacement with slag and cured for various curing period up to 180 days, the following conclusions can be drawn:

(1) Slag mortar mix having various sand replacement level up to 50% exhibited satisfactory results for both compressive and tensile strength.

(2) The optimum use of slag as partial replacement of sand in the mortar is observed to be 30% of sand. Mortars made with 30% sand replacement shows around 22% higher compressive strength than reference mortar after 90 days curing. The corresponding increase in tensile strength is reported to be 18%.

(3) Higher grade mortar showed lower rate of strength gaining as compared to lower grades of mortar for various replacement level of sand.

(4) Use of high volume slag as a partial replacement of sand, in any construction work, provides judicious use of by-products otherwise being dumped making environmental hazard.

REFERENCES

Hwang, C.L., Lin, C.Y., 1986, Strength development of blended furnace slag cement mortars, SP 91-65, Proceedings of the *2nd International Conference on Fly Ash, Silica Fume, Slag and Natural Pozzolans in concrete*, Vol. 2, American Concrete Institute, USA, pp. 1323-1340.

Smolczyk, H.G., 1978, The effect of chemistry of slag on the strength of blast furnace cements, *Zem-Kalk-Gips* 31 (6), pp.294-296.

Stutterheim, N., 1960, Properties and Uses of High Magnesia Portland Slag Cement Concretes, Journal of the *American Concrete Institute*, Proceedings V:56, Vol.31, No.10, pp.1027-1045.

Meusel, J. W. and Rose, J. H., 1983, Production of Granulated Blast Furnace Slag at Sparrows Point, and the Workability and Strength Potential of Concrete Incorporation the Slag, Fly Ash, Silica Fume, Slag & Other Mineral By- Products in Concrete, Journal of the *American Concrete Institute*, SP-79, pp.867-890.

ID : ASEE 054

1st International Conference on Advances in Civil Engineering 2012 (ICACE 2012)

12 –14 December 2012

CUET, Chittagong, Bangladesh

WAVE-STRUCTURE INTERACTION PROBLEMS USING NEWLY IMPROVED THREE-DIMENSIONAL PARTICLE METHOD

M. M. RAHMAN[1*], T. IRIBE[2], E. NAKAZA[3] & M. A. ROUF[4]

[1]MS, Dept. of Civil Eng. and Architecture, University of The Ryukyus

Senbaru 1, Nisihara, Nakagami, Okinawa 903-0213, Japan, e-mail: rahman_ku@yahoo.com

[2] Assist. Professor, Dept. of Civil Eng. and Architecture, University of The Ryukyus

Senbaru 1, Nisihara, Nakagami, Okinawa 903-0213, Japan, email: iribe@tec.u-ryukyu.ac.jp

[3] Professor, Dept. of Civil Eng. and Architecture, University of The Ryukyus

Senbaru 1, Nisihara, Nakagami, Okinawa 903-0213, Japan, email: enakaza@tec.u-ryukyu.ac.jp

[4] Professor, FMRT Discipline, Khulna University

Khulna-9208, Bangladesh, email: roufku@yahoo.com

**Corresponding Author*

ABSTRACT

A newly improved three-dimensional (3D) particle method is used to simulate the wave-structure interaction problems. Two types of different existing experiment are considered to verify the numerical simulation method. Both qualitative and quantitative verifications between experimental and numerical simulations results are shown here. Wave height and pressure distributions at different positions on the box model experiment are numerically simulated. Forces and vertical velocity for tall structure model experiment are also calculated by using newly improved 3D-particle method. The 3D-particle method shows good agreement with both experimental results.

Keywords: 3D-particle method, wave-structure interaction, experiment, numerical simulation

INTRODUCTION

Wave-structure interaction problem is a complex phenomenon and it is difficult to study only by analytical means. Experimental and numerical simulation studies have been conducted on wave-

structure interaction problems (Gomez-Gesteria and Dalrymple, 2004; Kleefsman et al., 2005; Rahman et al., 2012). However, it is urgent to develop the accurate numerical simulation method to understand this interaction. A newly improved three-dimensional (3D) particle method (Iribe and Nakaza, 2011), using Navier-Stokes equation as governing equation, is applied in a wave-structure interaction problem to assess the potentiality of this method. This study presents the consistency of the newly improved 3D particle method by assigning in two different existing wave-structure interaction experimental problems (Gomez-Gesteria and Dalrymple, 2004; Kleefsman et al., 2005). It shows consistent agreement with both experimental results.

DESCRIPTION OF EXPERIMENTS

Dam break experiments with box model were performed at the Maritime Research Institute Netherlands (MARIN) (Kleefsman et al., 2005). The complete schematic diagram of the experiment is shown in Fig. 1 (details in Kleefsman et al., 2005). Experimental diagram (Gomez-Gesteria and Dalrymple, 2004), conducted by Yeh and Petroff, on the wave-tall structure model interaction also shown in Fig. 2. A layer of water is considered on the bottom of the tank for the tall structure model case.

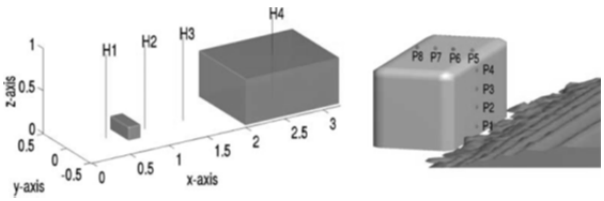

Fig. 1: Experimental diagram wave impact on box model (H = Water height, P = Pressure Sensor) (Kleefsman et al., 2005).

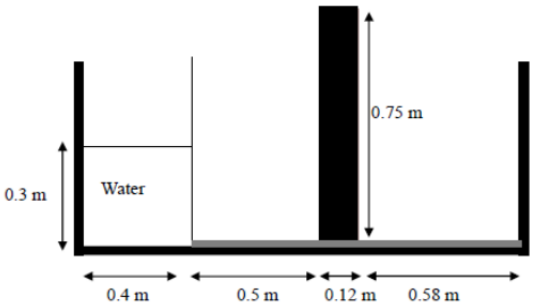

Fig. 2: Experimental diagram of wave impact on tall structure model.

NUMERICAL SIMULATION

Newly improved 3D-particle method (Iribe and Nakaza, 2011) is applied to simulate the wave-structure interaction. This particle method, moving particle semi-implicit (MPS) developed by Koshizuka and

Oka, 1996, has frequently been used to solve incompressible flow having free surface and complex flow with wave breaking (Iribe et al., 2012; Nakaza et al., 2012). The newly improved 3D-MPS method can be briefly described as follows:

Weight Function

For the calculation of interaction between particle *i* and its neighboring particles *j*, a weight function *w*, representing in Eq.(1), has been introduced.

$$w(r)=\begin{cases}\dfrac{r_e}{r}-1 & r \le r_e \\ 0 & r_e < r\end{cases} \qquad (1)$$

Where, r is the distance between particles *i* and *j*, the radius of the interaction area is represented by parameter r_e. As shown in Eq.(2), The particle number density with respect to particle *i* is given by the summation of the weight function of neighboring particles *j*. The initial particle number density n^0 is calculated for the initial particle positions.

$$\langle n \rangle_i = \sum_{j \neq i} w\left(\left|\vec{r}_j - \vec{r}_i\right|\right) \qquad (2)$$

Gradient Model

In the original MPS method, the pressure gradient for the particle *i* was defined based on the arrangement of neighboring particles *j*. In the original method, particles must be arranged at regular lattice points. However, in actual numerical process, the arrangement of neighboring particles *j* is generally irregular so that the accuracy based on original gradient method is not well enough.

The newly improved MPS method uses the following formula which does not depend on the particle arrangement and it shows higher accuracy than the original MPS method.

$$\nabla \phi|_{ij} = \left[\frac{1}{n^0}\sum_{j \neq i} w\left(\left|\vec{r}_j - \vec{r}_i\right|\right)\frac{\left(\vec{r}_j - \vec{r}_i\right)}{\left|\vec{r}_j - \vec{r}_i\right|} \otimes \frac{\left(\vec{r}_j - \vec{r}_i\right)}{\left|\vec{r}_j - \vec{r}_i\right|}\right]^{-1} \left(\frac{1}{n^0}\sum_{j \neq i} w\left(\left|\vec{r}_j - \vec{r}_i\right|\right)\frac{\phi_j - \phi_i}{\left|\vec{r}_j - \vec{r}_j\right|}\frac{\left(\vec{r}_j - \vec{r}_i\right)}{\left|\vec{r}_j - \vec{r}_i\right|}\right) \qquad (3)$$

Where, ϕ is a physical quantity, *w* is the weight function.

Poisson Equation of Pressure

The following improved Poisson equation of pressure was proposed by Tanaka and Masunaga, 2008 to get the better accuracy than the original MPS method.

$$\nabla^2 p_i = \frac{\rho}{\Delta t}\nabla \cdot \vec{u}_i^{\,*} + \gamma \frac{\rho}{\Delta t^2}\frac{n^0 - n_i^{\,k}}{n^0} \qquad (4)$$

Where, ∇^2 is the Laplacian, p is the pressure, ρ is the density, Δt is the time increment, u^* as speed between time steps, n^k is the particle number density of the previous time step. In this equation, second term in the right hand side must be zero as to keep the incompressibility of flow.

Simulation Algorithm

A semi-implicit algorithm is applied to the Navier-Stokes equation of an incompressible fluid.

$$\frac{\partial \vec{u}}{\partial t} = -\frac{1}{\rho}\nabla p + \nu \nabla^2 \vec{u} + \vec{F} \qquad (5)$$

Where, ρ is the fluid density and ν is the kinematic viscosity coefficient. In a time step, external force terms, viscosity terms and pressure gradient terms are calculated explicitly. The Poisson equation of pressure is calculated implicitly using an iteration solver. First, external terms and viscosity terms of the Navier-Stokes equation are calculated explicitly, and the temporary velocity $\vec{u}_i^{\,*}$ is obtained.

$$\vec{u}_i^{\,*} = \vec{u}_i^{\,k} + \nu \nabla^2 \vec{u}_i^{\,k} \Delta t + \vec{F} \Delta t \qquad (6)$$

Where, Δt is the time increment.

The temporary particle position $\vec{r}_i^{\,*}$ is calculated as

$$\vec{r}_i^{\,*} = \vec{r}_i^{\,k} + \vec{u}_i^{\,*} \Delta t \qquad (7)$$

The temporary particle number density n^*, which is evaluated from the temporary position, generally deviates from the initial particle number density n^0. In this case, the fluid density is not constant. Therefore, pressures at the particles are calculated by using Eq.(4).

The pressure at the time $t + \Delta t$, p_i^{k+1} is obtained by solving the Poisson Eq.(4). Substituting p_i^{k+1} into Eq.(8), we obtain the correction velocity $\vec{u}_i^{\,'}$.

$$\vec{u}_i^{\,'} = -\frac{1}{\rho}\nabla p_i^{k+1} \Delta t \qquad (8)$$

Adding the correction velocity to the temporary velocity, we have the new velocity of particle *i*

$$\vec{u}_i^{\,k+1} = \vec{u}_i^{\,*} + \vec{u}_i^{\,'} \qquad (9)$$

After adding the correction displacement to the temporal position, the new position of particle *i* is

$$\vec{r}_i^{\,k+1} = \vec{r}_i^{\,*} + \vec{u}_i^{\,'} \Delta t \qquad (10)$$

Numerical Conditions

The same geometry as the experimental model is applied to numerical simulation. The initial distance between particles is 0.02 m (box model) and 0.01 m (tall structure model). The time increment for both calculations is 0.05 s. The total particle numbers are 241434 and 277384 for box model and tall structure model condition respectively.

RESULTS AND DISCUSSIONS

Fig. 3 shows the qualitative agreement between 3D-particle method and box model experiment. Wave impacts on the box model with splash. In the mean time, water goes around the model. Time instant of wave impact on the box model is same for both simulation cases. Numerical simulation shows similar phenomena as in the experiment.

Experiment Numerical Simulation

Fig. 3: Snapshot of wave impact on box model (at 0.56 s).

Figs. 4 and 5 show the good validation of the newly improved 3D-particle method with the box model experimental results. Fig. 4 exhibits that the water in reservoir goes downward and then returns to the reservoir from the back wall. The pressure distribution patterns exhibits same magnitude both in the experimental and numerical simulation results for front section (P1 and P3) and on the roof of box model (P7). P1 shows the highest pressure impact peak on the box model.

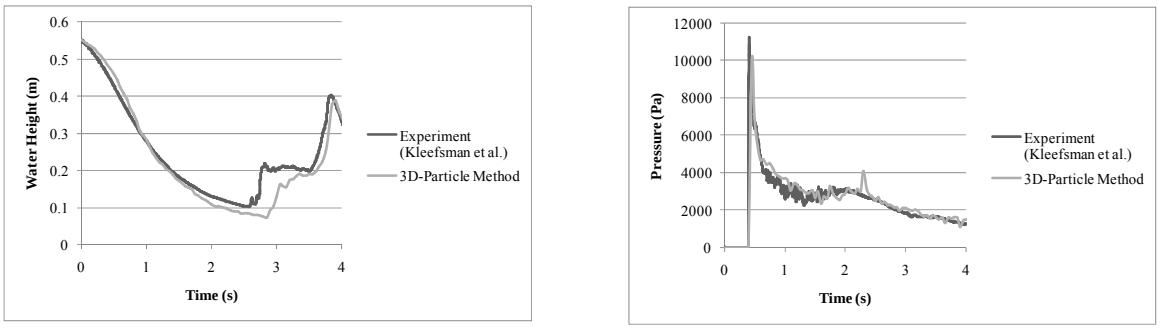

Fig. 4: Vertical water heights in the reservoir H4 (left) and Pressure time histories at P1 (right) for wave impact on box model.

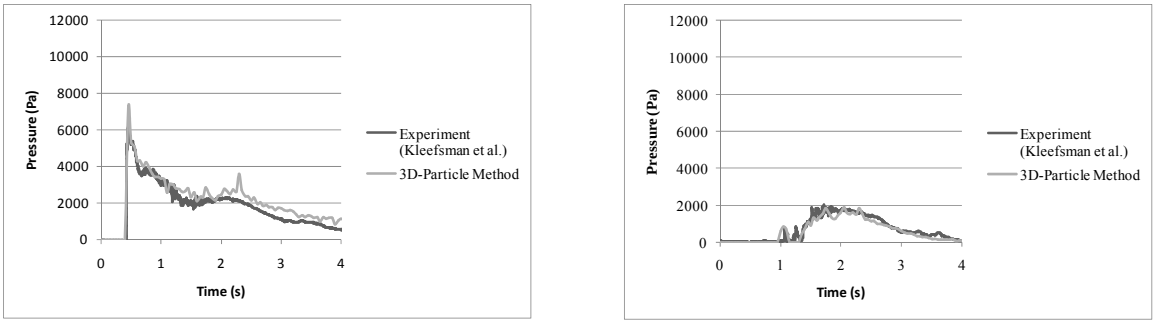

Fig. 5: Pressure time histories at P3 (left) and P7 (right) for wave impact on box model.

Fig. 6 shows the forces exerted on the tall structure model and horizontal velocity in front of the structure. It also shows good agreement between experimental and numerical simulation results. Net forcers are exerted on the tall structure model and the horizontal velocity is calculated in front of the tall structure model (14.6 cm upstream at the center of the tall structure model). The gaps in case of horizontal velocity graph for the physical experiment are due to the presence of bubbles in the water.

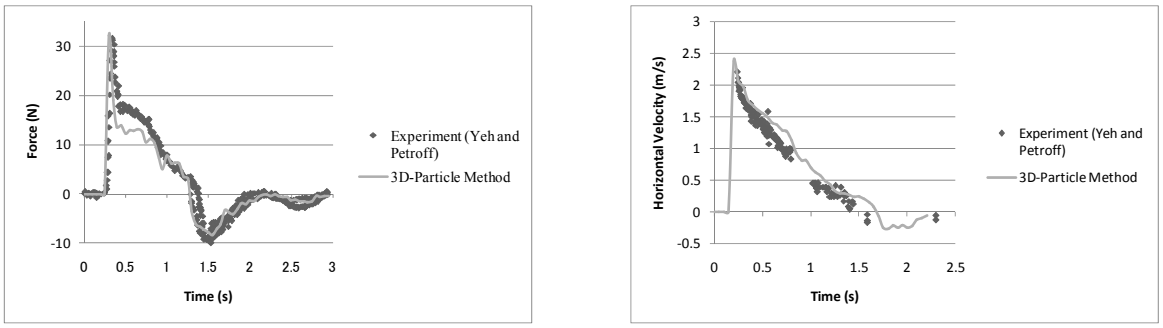

Fig. 6: Force and horizontal velocity for wave impact on tall structure model.

CONCLUSION

Verified numerical simulation method is urgent to develop the information of wave-structure complex interaction problems. This study shows a newly improved 3D-particle method with the verification results against two varied existing wave-structure interaction experiments. Present numerical method shows good agreement with the experimental results. This study exhibits that wave-structure interaction problems can be numerically simulated with this newly improved 3D-particle method.

REFERENCES

Gomez-Gesteira, M and Dalrymple, RA. 2004. Using a three-dimensional smoothed particle hydrodynamic method for wave impact on a tall structure. *J. of Waterway, Port, Coast. and Ocean Eng.*, 130 (2): 63-69.

Iribe, T and Nakaza, E. 2011. A study to improve accuracy of MPS method by a new gradient computation method. *Coast. Eng. J.*, JSCE, 6 (1): 36-48 (*in Japanese*).

Iribe, T; Nakaza, E; Rusila, S; Rahman MM and Seiya I. 2012. Estimations of impact wave force of tsunami acting on a vertical sea wall with MPS method. *33rd International Conference on Coastal Engineering,* Santander, Spain, ICCE, 33.

Kleefsman, KMT; Fekken, G; Veldman, AEP; Iwanowski, B and Buchner, B. 2005. A volume-of-fluid based simulation method for wave impact problems. *J. Comp. Phys.*, 206: 363–393.

Koshizuka, S and Oka, Y. 1996. Moving particle semi-implicit method for fragmentation of incompressible fluid. *Nucl. Sci. and Eng.,* 123: 421-434.

Nakaza, E; Iribe, T; Rusila, S; Rahman MM and Watanabe T. 2012. Numerical simulation of the runup of solitary waves with the improved MPS method. *33rd International Conference on Coastal Engineering,* Santander, Spain, ICCE, 33.

Rahman, MM; Iribe, T and Nakaza, E. 2012. Experimental study of the pressure acting on structures due to tsunami bore impact. *Proceedings of International Sessions in Coastal Engineering,* JSCE, 4, Article in Press.

Tanaka, M and Masunaga, T. 2008. Stabilization and smoothing of pressure on mps method by quasi-compressibility. *Transactions of JSCES* (*in Japanese*).

ID: ASEE 055

1st International Conference on Advances in Civil Engineering 2012 (ICACE 2012)
12 –14 December 2012
CUET, Chittagong, Bangladesh

CIVIL ENGINEERING APPLICATION OF SHAPE MEMORY ALLOYS

M. G. RASHED[1*], R. AHSAN[2] AND B. ISLAM[3]

[1]AUST, Dhaka, 1208, Bangladesh, <rashed.golam@gmail.com>
[2]BUET, Dhaka, 1000, Bangladesh, <raquibahsan@ce.buet.ac.bd>
[3]BUET-JIDPUS, BUET, Dhaka, 1000, Bangladesh, <bushrabuet@gmail.com>

ABSTRACT
Shape Memory Alloy (SMA) materials are widely used in different disciplines and it has substantial potential for civil engineering applications. The unique properties of SMA result in high damping, combined with repeatable re-centering capabilities which can be used in civil infrastructures, especially in vibration control devices. An overview of the Shape Memory Effect (SME) and Pseudo-Elasticity (PE) characteristics of SMA due to thermal or/and stress variation controlled reversible hysteretic phase transformation between Martensite & Austenite is presented in this paper. This paper also reviews the constitutive modeling of SMA's, current research using SMA-based devices for civil structures along with established examples while focusing on the disadvantages that may arise.

Keywords: Smart materials, Shape memory alloy, Pseudo elasticity, Shape memory effect.

INTRODUCTION

The name shape memory implies that it remembers its original formed shape. The super-elastic behavior exhibited by shape-memory alloys help material to totally recover from large cyclic deformations, while developing a hysteretic loop. Due to its hysteretic behavior and excellent re-centering capability, SMA can be used in a wide variety of civil engineering applications. The other key features of SMA's include high strength, good fatigue and corrosion resistance, high damping capacity, temperature-dependent Young's modulus, ability to undergo large deformations, and availability in many possible shapes and configurations.
SMA's have two main phases which have different crystal structures. One is called martensite that is stable at low temperatures and/or high stresses and the other austenite, which is stable at high temperatures and/or low stresses. Austenite, also named as the parent phase, generally has a cubic crystal structure while martensite has a less-ordered crystal structure (Song et al., 2006). Austenite phase provides more stiffness than that of Martensite and civil engineers can leverage the variation in stiffness depending upon temperature & stress.

Table 1: Typical properties of NiTi SMA with comparison to Structural steel (Santos, 2011).

Property	NiTi SMA		Structural Steel
	Austenite	Martensite	
Density (g/cm^3)	6.45		7.85
Recoverable elongation (%)	up to 8		0.20
Young's modulus (GPa)	30–83	21–41	200
Yield strength (MPa)	195–690	70–140	248 − 517
Ultimate tensile strength (MPa)	895–1900		448 − 827
Elongation at failure (%)	5–50 (typically 25)		20
Poisson's ratio	0.33		0.27 − 0.30
Corrosion performance	Excellent (similar to stainless steel)		Poor

A comparison between structural steel and Nickel-Titanium (NiTi) SMA in its martensitic and austenitic phases is presented in Table 1. It is seen that structural steel is much stiffer than NiTi and that the martensitic yield strength of NiTi is lower than its austenitic counterpart. However, the most important characteristic of NiTi is its outstanding ability to recover from strains up to about 8%, without residual deformations, while showing a mechanical hysteresis. This provides the material with unique energy dissipation and re-centering capabilities (Santos, 2011).
Over the past two decades, SMA's have been widely investigated for their possible application in civil engineering structures. This paper tries to cover some latest applications of SMA's in civil engineering along with established examples while also focusing on the limitations in application.

BASIC CHARACTERISTICS OF SMA'S

SMA's have two unique properties, The Shape Memory Effect (SME) which is the phenomenon that the material returns back to their original shape upon heating and the Pseudo-Elasticity (PE) which is the phenomenon that the material can undergo a large amount of inelastic deformation and recover after unloading. These properties are the result of reversible phase transformations between the austenite phase and the martensite phase.
In the stress-free state, an SMA is characterized by four transition temperatures such as martensite start temperature M_s, martensite finish temperature M_f, austenite start temperature A_s and austenite finish temperature A_f. At a temperature below M_f, the SMA exhibits the SME and at a temperature above A_f, the SMA exhibits the PE.

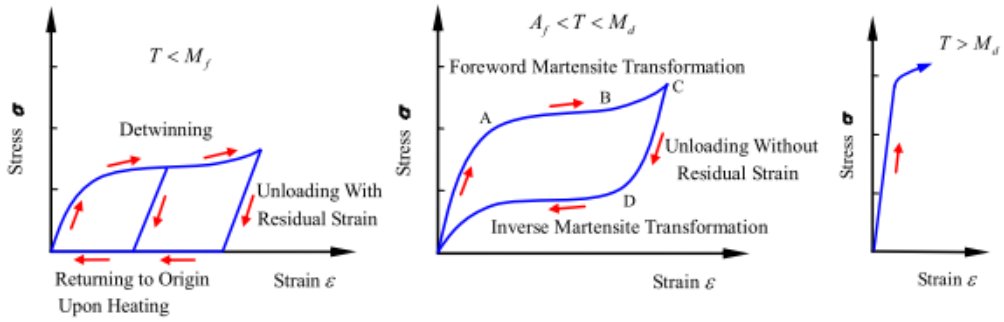

(a) (b) (c)

Figure 1: Stress-strain diagrams of NiTi SMA, (a) SME; (b) PE; (c) Ordinary plastic deformation (Qian et al., 2010).

SHAPE MEMORY EFFECT

Shape memory effect (SME) is a unique characteristic of SMA that exhibits thermo-elastic martensitic phase transformation. It is the ability of SMA material to recover its original shape after being deformed through a thermal cycling. Through training, the material has the ability to memorize a very specific physical configuration or shape in either the martensite or austenite phase, which is called one-way shape memory (Fig. 1a). Also it is possible to train the material, such that it memorizes two different configurations or shapes in martensite and austenite phases, which is called two-way shape memory.
The key to the SME is the build-up of residual stress fields within the SMA, by deforming the material plastically, and then these stress fields control the phase transformation (Saadat et al., 2002).

PSEUDO-ELASTICITY

Pseudo-Elasticity (PE), also known as super-elasticity, is described as the recovery of large strain as a result of the stress-induced martensitic phase transformations under constant temperature. When $T>A_f$, SMA is in its austenite phase. If a sufficiently high stress is applied to the material in the austenite phase, the SMA transforms into the detwinned martensite. When the load is released, a reverse transformation to the austenite state takes place, which results in complete shape recovery and a substantial hysteretic loop (Fig. 1b). However, if the temperature is below A_f but above A_s, there

will be only a partial shape recovery. Also, if the temperature in the austenite phase exceeds the maximum temperature at which martensite occurs, M_d, the material is stabilized in the austenite phase and the martensitic transformations cannot be induced by an applied load, thus the PE of SMA is completely lost (Fig. 1c).

DAMPING PROPERTIES

SMA used for damping can be both martensitic as well as austenitic. The damping comes from either martensite variations reorientation in the martensitic material or from stress-induced martensite in austenitic material. When an SMA specimen is subjected to a cycle of deformation within its superelastic strain range, it dissipates a certain amount of energy without permanent deformation (Fig. 2a). This results from the phase transformation from austenite to martensite during loading and the reverse transformation during unloading, ensuring a net release of energy. When an SMA is loaded in the martensite phase, it yields at a nearly constant stress after initial elastic deformation and displays strain hardening at larger strains. When unloaded, there remains some residual strain at zero stress. This martensitic composition of SMA's generates a full hysteresis loop around the origin (Fig. 2b). Thus, martensite SMA dissipates a much higher amount of energy compared with that of austenite SMA because of its larger hysteresis loop. But it has no re-centering capability like the austenitic SMA. In the martensite phase under tension–compression cycles, the maximum stress attained in compression has been found to be approximately twice that in tension (Fig. 2b). Although superelastic SMA dissipates less energy than martensitic SMA, its advantage is that it can still dissipate a considerable amount of energy under repeated load cycles with negligible residual strain (Alam et al., 2007).

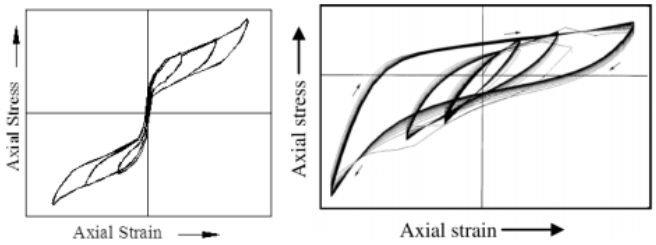

(a) (b)

Figure 2: Typical stress–strain curve of SMA under cyclic axial stresses: (a) superelastic SMA; (b) martensite SMA (Alam et al., 2007).

MODELING OF SHAPE MEMORY ALLOYS

The modeling of SMA behavior such as SME and PE has been an active area of research. The modeling approaches can be categorized into phenomenological and thermo-dynamical approaches.

PHENOMENOLOGICAL MODELING

The phenomenological modeling is essentially a macroscopic approach which attempts to capture the SMA response at the macroscopic level using phenomenology. These models are based on setting up material constants of a model to match the experimental data. A large number of phenomenological models had been proposed to capture response of SMA, both mechanical and thermomechanical, due to their relative simplicity and accuracy. In the field of civil engineering, SMA's are mostly used as bars and wires. For this reason it is convenient to use one-dimensional phenomenological model. Phenomenological model of SMA have been implemented in several finite element software packages such as Ansys, Abaqus, SeismoStruct, MSC Marc; where the material models are included from Auricchio et al. (1997), Auricchio and Taylor (1996), Auricchio and Sacco (1997), and Saeedvafa and Asaro (1995) respectively. Only the Saeedvafa and Asaro model takes both SME and PE into consideration while the rest only replicates PE (Saeedvafa & Asaro, 1995).

THERMODYNAMICS-BASED MODELING

The thermodynamics-based modeling is essentiality a microscopic approach which is built on the laws of thermodynamics and energy considerations by pursuing closely crystallographic phenomena within

the material. Several Thermodynamics-based models have been proposed, some of which are Patoor et al. (1994), Goo and Lexcellent (1997), Huang and Brinson (1998). Thermodynamics-based models are more complicated and computationally expensive than phenomenological models because they present a highly sensible technique to derive accurate three-dimensional constitutive law (Alam et al., 2007).

STRUCTURAL APPLICATIONS OF SMA IN CIVIL ENGINEERING

The vibration suppression of civil structures to external dynamic loading can be pursued by using active control, semi-active control, and passive control. The applications of SMA in civil engineering structures are described below in two broad categories, Building and Bridge structures.

SMA IN BUILDING STRUCTURES

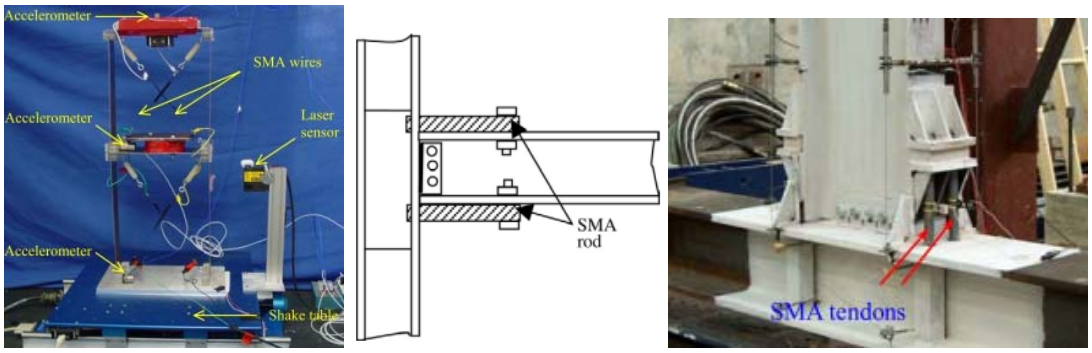

(a) (b) (c)

Figure 3: (a) SMA braced frame (Tarefder et al., 2006); (b) Schematic of SMA connector for steel structures (Song et al., 2006); (c) Steel beam-column connection using SMA tendons (Qian et al., 2010).

Several studies have considered the use of SMA's as diagonal braces in frame structures (Saadat et al., 2001; Tarefder et al., 2006). The frame structures deform under excitation, SMA braces dissipate energy through stress-induced martensite transformation (in the superelastic SMA case) or martensite reorientation (in the martensite SMA case) as shown in Fig. 3a. Auricchio et al. (2006) investigated the effectiveness of using large diameter NiTi bars as a bracing system for steel structures and compared the SMA braces with buckling-restrained steel braces. The outcome of numerical studies showed that SMA bracing systems can satisfactorily limit the inter-story drifts in steel buildings and significantly reduce the residual drifts (McCormick et al., 2007).

Several studies have been conducted on SMA beam-column connectors (Qian et al., 2010). SMA connectors have been designed to provide damping and tolerate relatively large deformations and found to be most effective in controlling structural response under high levels of seismic intensity. Ocel et al. (2004) experimentally evaluated the performance of partially restrained steel beam-column (Fig. 3b & c) connections using martensitic SMA's. It was observed that the SMA connections were able to recover 76% of the beam tip displacement.

Several studies have been made on SMA based isolation devices for seismic protection of building structures by performing shake table tests (Song et al., 2006). But majority of them are superelastic SMA due to its zero residual strain after unloading. Martensite SMA's can be used to help dissipate more energy and further improving the damping effect of the superelastic SMA isolation devices. The re-centering device by Dolce et al. (2001) is a good example of combining the superelastic and martensitic SMA's (Fig. 4a).

Figure 4: (a) Schematic of the SMA isolation system for buildings (Qian et al., 2010); (b) Schematic of the SMA spring isolation device (Song et al., 2006); (c) Schematic of a bell tower using SMA anchorage retrofitting (Song et al., 2006).

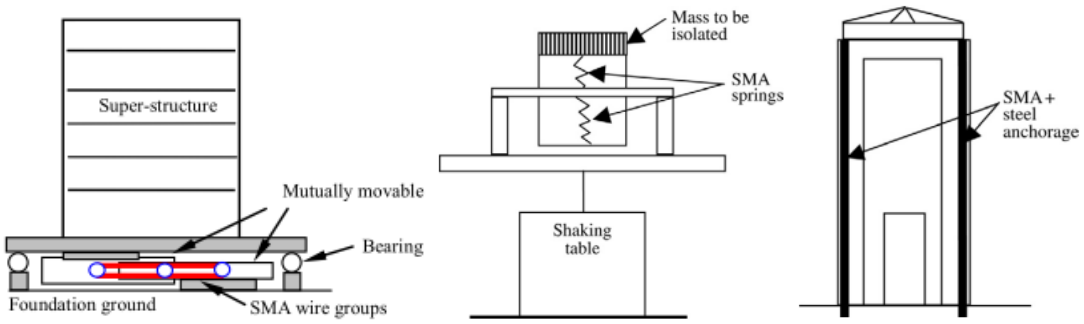

(a) (b) (c)

SMA's have been used to retrofit existing or damaged structures (Islam et al., 2012). The San Giorgio Church Bell-Tower, which was damaged in 1996 by earthquake, was retrofitted using SMA tie bars. As shown in Fig. 4c, the SMA tie bars, which run through the height of the tower and are anchored at its foundation, reinforce the structure and increase its modal frequencies. That tower stood intact after a similar earthquake in 2000 (Qian et al., 2010).

SMA IN BRIDGE STRUCTURES

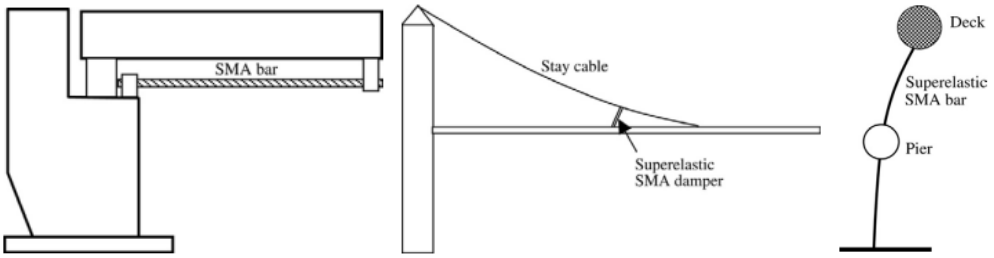

(a) (b) (c)

Figure 5: (a) Schematic of the setup of SMA restrainer for a simple-supported bridge; (b) Schematic of the SMA damper for a stay-cable bridge; (c) Schematic of the SMA isolation device for elevated highway bridges; (Song et al., 2006).

Several studies have been carried out to investigate the possibility of using SMA as unseating prevention devices on multiple span bridges to overcome some of the limitations of traditional devices such as steel cable restrainers, steel rods, and shock transmission units (Qian et al., 2010). The schematic of SMA restrainer setup for simple supported bridge is shown in Fig. 5a.

Both superelastic and martensite SMA's can be used as damper elements for bridges. Li et al. (2004) theoretically studied the vibration mitigation of a combined cable-SMA damper system which can be used on a stay-cable bridge (shown in Fig. 5b). The dynamic responses of the SMA damped cable were simulated as it vibrated at its first mode or at its first few modes respectively. They stated that the proposed superelastic SMA damper can suppress the cable's vibration in both cases (Song et al., 2006).

For highway bridges, Comparative simulations of the SMA isolation system (shown in Fig. 5c) and a conventional isolation system were conducted with three excitation levels. For small excitation level, the SMA isolation system firmly links the pier and the deck, while the relative motion emerges in the case of the conventional system. For a medium excitation level, the SMA bar undergoes a stress-induced martensitic transformation so that the soft stiffness allows a relative displacement comparable to that of the conventional isolation system. At severe loading, the SMA bar enters an elastic range of martensite and the maximum displacement is one-fifth as much as that of the conventional isolation system. The comparison shows that the damage energy of the bridge with the SMA isolation system is smaller than with the conventional system (Song et al., 2006).

LIMITATIONS

The price of the SMA's is high in comparison to the conventional civil engineering construction materials. However, a significant reduction in the price of SMA has occurred over the last decade, recently developed Iron based SMA's are quite cheaper than traditional NiTi, sometimes by ten folds (Alam et al., 2007). Fe-Mn-Si-X alloys are an example of a potentially low cost SMA.

SMA's can be heated by using electric current for actuation. But short activation times in the range of seconds are not possible for large cross sections. A high capacity power supply with a current of several hundred Ampere can reduce activation times considerably. This may incur greater costs when setting up the actuator and keeping up the high temperature state for long time (Janke et al., 2005).

Another difficulty regarding the application of SMA is the machining of large diameter bars using conventional equipment, due to its hardness. The welding of SMA's is often difficult (Desroches & Smith, 2003).

CONCLUSIONS

This paper presents a review of the basic properties of SMA such as the SME and the PE. The ability to change shape by application of heat can be used to move objects. If recovery is resisted, the SMA generates force that is useful as an actuator which can be activated by electrical Joule heating. Thus many applications are possible. Numerous analytical and experimental studies point toward the feasibility and superiority of SMA based devices over conventional methods for seismic protection. The main characteristics of such devices are high energy dissipation and re-centering capabilities.

This paper also reviews the constitutive models developed to carry out numerical simulation of SMA devices. These constitutive characteristics of SMA's greatly depend on variations in the alloy's component and manufacturing method to begin with. From discussion it is observed that phenomenological models are more adequate for civil engineering applications because they are simple and easy to incorporate in finite element programs and are not computationally demanding.

REFERENCES

Alam, MS; Youssef, MA and Nehdi, M. 2007. Utilizing shape memory alloys to enhance the performance and safety of civil infrastructure: a review. *Canadian Journal of Civil Engineering,* 34(9): 1075-1086.

Auricchio, F; Fugazza, D and Desroches, R. 2006. Earthquake Performance of Steel Frames With Nitinol Braces. *Journal of Earthquake Engineering,* 10(Special 1): 45–66.

Auricchio, F and Lubliner, J. 1997. Shape-memory-alloys: macromodelling and numerical simulations of the super-elastic behaviour. *Computer Methods in Applied Mechanics and Engineering,* 146: 281–312.

Auricchio, F and Sacco, E. 1997. Superelastic shape-memory-alloy beam model. *Journal of Intelligent Material Systems and Structures,* 8: 489–501.

Auricchio, F and Taylor, R. 1996. Shape memory alloy super-elastic behavior: 3D finite-element simulations. In P. Gobin, & J. Tatibouet (Ed.), *Proceedings of the 3rd International Conference on Intelligent Materials and the 3rd European Conference on Smart Structures and Materials,* 2779: 487–492. Lyon, France: SPIE.

Desroches, R and Smith, B. 2003. Shape memory alloys in seismic resistant design and retrofit: a critical review of their potential and limitations. *Journal of Earthquake Engineering,* 7(3): 1-15.

Dolce, M; Cardone, D and Marnetto, R. 2001. SMA re-centering devices for seismic isolation of civil structures. *Proceedings of SPIE 2001.* 4330: 238–249. Newport Beach, CA: SPIE.

Goo, B and Lexcellent, C. 1997. Micromechanics-based modeling of two-way memory-effect of a single crystalline shape-memory-alloy. *Acta Materialia,* 45: 727–737.

Huang, M and Brinson, L. 1998. Multivariant model for single crystal shape-memory-alloy behaviour. *Journal of the Mechanics and Physics of Solids,* 46: 1379–1409.

Islam B.; Ahsan R. and Rashed M.G. 2012, Retrofit Techniques of Structures Associated With Soft Story, *Proceedings of the 1st International Conference on Advances in Civil Engineering*, Chittagong, Bangladesh.

Janke, L; Czaderski, C; Motavalli, M and Ruth, J. 2005. Applications of shape memory alloys in civil engineering structures—Overview, limits and new ideas. *Materials and Structures,* 38(5): 578-592.

Li, H; Liu, M and Ou, J. 2004. Vibration mitigation of a stay cable with one shape memory alloy damper. *Structural Control and Health Monitoring,* 11: 1–36.

McCormick, J; DesRoches, R; Fugazza, D and Auricchio, F. 2007. Seismic Assessment of Concentrically Braced Steel Frames with Shape Memory Alloy Braces. *Journal of Structural Engineering,* 133(6): 862-870.

Ocel, J; DesRoches, R; Leon, R; Hess, W; Krumme, R; Hayes, J and Sweeney, S. 2004. Steel Beam-Column Connections using Shape Memory Alloys. *Journal of Structural Engineering,* 130(5): 732-740.

Patoor, E; Eberhardt, A and Berveiller, M. 1994. Micromechanical modelling of the shape memory behaviour. In L. Brinson, & B. Moran (Ed.), *Mechanics of Phase Transformations and Shape Memory Alloys: Proceedings of the ASME International Congress and Exposition.* 189: 23–37. Chicago, Ill.: American Society of Mechanical Engineers (ASME).

Qian, H; Li, H. N; Song, G; Chen, H; Ren, W. J and Zhang, S. 2010. Seismic Vibration Control of Civil Structures Using Shape Memory Alloys: A Review. *Earth and Space 2010: Engineering, Science, Construction, and Operations in Challenging Environments.* 3377-3395. Honolulu, Hawaii: American Society of Civil Engineers (ASCE).

Saadat, S; Noori, M; Davoodi, H; Hou, Z; Suzuki, Y and Masuda, A. 2001. Using NiTi SMA tendons for vibration control of coastal structures. *Smart Materials and Structures,* 10(4): 695.

Saadat, S; Salichs, J; Noori, M; Hou, Z; Davoodi, H; Bar-on, I; Suzuki, Y and Masuda, A. 2002. An overview of vibration and seismic applications of NiTi shape memory alloy. *Smart Materials and Structures,* 11(2): 218–229.

Saeedvafa, M and Asaro, R. 1995. *A numerical investigation of transformation induced plasticity.* Los Alamos, USA: Los Alamos National Laboratory.

Santos, F. 2011. *Vibration control with shape-memory alloys in civil engineering structures. PhD* Thesis, Faculdade de Ciências e Tecnologia, Universidade Nova de Lisboa, Monte de Caparica, Portugal.

Song, G; Ma, N and Li, H.-N. 2006. Applications of shape memory alloys in civil structures. *Engineering Structures,* 28(9): 1266–1274.

Tarefder, RA; Ma, N and Song, G. 2006. Dynamic Behavior of a Two-Story Building Frame Braced with SMA for Vibration Control. *Earth & Space 2006 : Engineering, Construction, and Operations in Challenging Environment*. 1-9. Houston, Texas: American Society of Civil Engineers (ASCE).

ID: ASEE 056

1st InternationalConference on Advances in Civil Engineering 2012 (ICACE 2012)
12 –14 December 2012
CUET, Chittagong, Bangladesh

RETROFIT TECHNIQUES OF STRUCTURES ASSOCIATED WITH SOFT STORY

B. ISLAM[1*], R. AHSAN[2] & M. G. RASHED[3]

[1]*BUET-Japan Institute of Disaster Prevention and Urban Safety, Bangladesh University of Engineering and Technology, Dhaka, Bangladesh, <bushrabuet@gmail.com>*
[2] *Department of Civil Engineering, Bangladesh University of Engineering and Technology, Dhaka, Bangladesh,<raquibahsan@ce.buet.ac.bd>*
[3] *Department of Civil Engineering, Ahsanullah University of Science and Technology, Dhaka, Bangladesh, <rashed.ce@aust.edu>*
**Corresponding Author*

ABSTRACT
To build a proper earthquake resistant structure, it is of fundamental importance to strictly follow the design and construction practice according to code requirements. Choosing an appropriate structural configuration is one of the considerable issues to ensure adequate safety against seismic risk. A common and worldwide practice is to construct buildings with soft story generally at ground level or in other levels to provide an open space for different purposes. In seismic point of view these structures associated with soft story are highly vulnerable to earthquake hazard. To enhance the seismic performance of existing structures to desired level, retrofit of the structure is an accepted solution in the field of civil engineering. The selection, among available seismic retrofit strategies, needs a wide consideration of existing condition, economy, preserving building occupancy, maintaining historical appearances, available facility for implementation etc. An overall balance between these factors and desired performance level can lead to an effective decision prior to structural rehabilitation. In Bangladesh, a conventional practice of constructing structures with soft story is extensively seen in urban areas, which has undoubtedly increased the potential risk during earthquake. Moreover concerns regarding seismic risk mitigation and rehabilitation of existing buildings have risen in Bangladesh because of its geological location on seismicallyactive region. In this review paper some of the common and emerging techniques of structural retrofit which have been adopted in different countries are presented along with their efficiencies in improving seismic performance of the existing structures. Finally comments on feasibility of applying these techniques considering necessary factors are made in the context of Bangladesh.

Keywords: Soft story, Retrofit, Earthquake, Bangladesh

INTRODUCTION

Proper earthquake resistant design along with its implementation in construction practice and monitoring through the service life of structure are the prerequisite of ensuring adequate safety against earthquake induced disaster. If any structure is not designed or constructed following appropriate seismic provision or already has experienced hazard in its life time then the seismic performance of the existing structure is likely to be unsatisfactory during upcoming hazardous situation.Moreover structural damage and unexpected collapse can occur due to the presence of deficient capacity

forresisting seismic loadin existing structural condition.Prior to taking necessary steps to enhance the performance of this type of structures, effective seismic evaluation is required. If it is found through the assessment that the structure will fail during earthquake or will not remain functional then it is obvious that the existing structure needs further improvement. The decision,whether the structure is required to be repaired, retrofitted or demolishedgreatly dependson the extent of deficiency of structure, economic feasibility, desirable service life of the upgraded structure, availability of materials and technology.In case of structural retrofit an optimum strategy needs to be selected to achieve the maximum desirable response by satisfying other influencing factors as well.

From the earthquake histories and observations,certain factorsare identified asthe causes behind structural damage, presence of which in a building increases the vulnerability of the structure and hence the entire risk while subjected to lateral excitation. Among them irregularity in elevation and plan is one of the major factor proven as the reason of earthquake damage.This sort of structural design concept which contains plan and/or vertical irregularities may work efficiently in non-seismic zone while very poor performance is observed under lateral ground shaking. The practice of avoiding infill in order to facilitate parking, allow open shop front or serve other purposes usually in ground floor or some other floor of building results into stiffness irregularity in different stories. This vertical stiffness irregularity leads into extreme soft and weak storydue to which building is likely to lean or fall over during earthquake. Pictures of building associated with soft story and failure pattern of this type of building while subjected to lateral excitation are shown in Figure 1 and Figure 2 respectively.

Fig. 1 Buildings associated with soft story (From Google image)

Fig. 2 Failure of structures associated with soft story under earthquake (From Google image)

In Bangladesh rapid growth in population and urbanization has lead into an increasing tendency of constructing multistorey apartment and commercial building. Majority of these buildings tend to leave

open space at ground level usually to accommodate car parking or in few cases to serve other purposes. This common practice of constructing buildings without any infill or with partial infill at ground level due to lack of knowledge on dynamic responseis leading into creating structures associated with soft story and has created a huge risk of structural damage and collapse during an earthquake event. Since Bangladesh is located in seismically active region, this present design and construction practice of soft story building has worsened the overall scenario of earthquake preparedness in this country. The practice of strengthening structures with irregularities through structural retrofithas been studied by researchers worldwide and has been found very effective in reducing existing risk(Hjelmstad et al. 1988, Miyamotto and Scholl 1996, Fukuyama et al. 2004, Mezzi and Parducci 2005, Yamakawa and Rahman 2007, Samant et al. 2009, Chandra et al. 2011). Thereforeretrofittingthe soft story buildings of Bangladesh can be an effective solution to improve the current situation. Different retrofit strategies which have been adopted globallyto enhance structural performance are presented in the present review paper and remarks have been made on their feasibility of application in the context of Bangladesh.

RETROFIT TECHNIQUES

Till now numerous retrofit strategies have been developed for the performance enhancement of structures vulnerable to earthquake.These strategies include methods of improving resistanceto horizontal ground motion by increasing capacity of local structural elements orthe wholestructure. Conventional local retrofit strategies available are strengthening of structural elements like column, beam and wall, joint strengthening and foundation strengthening while global strategies include structural stiffening by addition of infill walls, shear walls or steel bracings, reduction of irregularities and installation of energy dissipation devices and base isolation techniques. A brief description of some common and novel retrofit techniques is stated in the following sections.

Addition of infill wall

Addition of RC structural wall into existing frame is one of the common approaches which effectively can control global lateral drift. Application of this technique into soft story of a structure helps to stiffen the frame in that level and reduces the soft story effect accordingly. In this methodconsequent foundation strengthening is also necessary since overturning moment and base shear concentrates at the stiffer infill location.Lateral load resistance capacity of a soft story frame can be improved with the addition of masonry infill as well. This approach will increase the stiffness of the frame and reduce the demand on the existing frame. However this option may not contribute to the improvement ofductility.

Addition of bracing

Incorporation of bracing is another common effective approach which can be designed to provide stiffness, strength, ductility and energy dissipation. In this approach connection between bracing and frame is very important to act integrally with the structure without any failure at connection during earthquake. In the past years number of researches has been performed on structures associated with steel bracing showing the improved performance of the RC structure (Badoux and Jirsa 1990, Bush et al. 1991). This technique can effectively reduce the risk of soft story frame by providing adequate stiffness to the frame. Different types of bracing which have been proposed and applied include concentric bracing, eccentric bracing, post tensioned steel bracing and buckling restrained bracing.

High Performance Fiber Reinforced Cementitious Composite (HPFRCC) device

Behaviour of RC structure containing soft storycan be controlled using HPFRCC devices (Fukuyama et al. 2004). In this method ductile short column made of HPFRCC placed beside existing columns at soft story level act as control devices. It shows high resistance against axial force and can effectively control structural drift.

Base isolation

Base isolation of the structure is one of the novel approaches of structural retrofit. In this approach the response of the building is reduced through decoupling from the ground motion. Installation of bearings between superstructure and substructure allows the energy to dissipate in significant manner.Studies on the mechanism of base isolation have been performed by several researchers (Gates et al. 1990, Kawamura et al. 2000, Tena-Colunga et al. 1997).

Energy dissipation device

The vibration of the structure and hence lateral displacement and drift can be effectively reduced by dissipating energy with the implantation of frictional, hysteretic and viscoelastic damper within the building. Installation of energy dissipating devices provides damping to the primary structure along with increasing stiffness of the structure.In a study fluid viscous damper was usedfor the rehabilitation of a historical non ductile soft story concrete structure and the strategy was found as cost effective method and helpful in the preservation of historical appearances (Miyamotto and Scholl 1996).

Retrofit using smart materials

Application of smart materials is a cutting edge technologyapplied in the field of structural retrofit. Material specification, construction details and verification along with application of some of these techniques have been described in a report on “Recent development of seismic retrofit methods in Japan” prepared by Japan Building Disaster Prevention Association (JBDPA) in 2005.

One of these approaches is to confineexisting reinforced concrete or concrete-encased steel composite columns or reinforced concrete beams with carbon fiber reinforced plastic (CFRP) sheet or strand to improve the shear strength, lateral deformability and axial capacity of thestructural members.A figure of CFRP confined column and normal RC column tested on shake table is shown in Figure 3.

(a) RC column (b) CFRP confined column

Fig. 3Column after shake table test (JBDPA report, 2005)

Another method of retrofitting existing concrete structures is to reinforce it with FRP(fiber-reinforced plastic) sheets.Wrapping concrete surface with this strong, lightweight, and superior anti-corrosive sheet can increase the durabilityand the ductility of structural members which will allow the structure to perform well under seismic action.

Seismic retrofit of existing concrete structure using Aramid fiber (AF) was certified by JBDPA. Confining column of RC structure with Aramid fiber can improve the overall deformability of the structural element.An application of confining column with AF sheetis shown in Figure 4.

Fig. 4 Confining column with Aramid Fiber sheet (JBDPA report, 2005)

Again, the re-centering capability of shape memory alloy (SMA)resulting from its super elastic behavior can be effectively used in structural retrofit purpose to control relative displacement of the structure (Rashed et al., 2012).

Other approaches

Some other latest retrofit techniques include precast retrofit shear wall system, In precast retrofit shear wall system a precast wall is installed into existing frame system with special type of connection. Acrypair system is another advance system in whichcarbon fiber sheets and methyl methacrylate (MMA) resin are used for retrofit purpose.In Aoki seismic retrofit method external braces consisting of steel pipes and friction damper installed on the external walls of structure to be retrofitted,works as energy dissipation measure and helps to improve structural performance.

A study proposed the use of extremely thick hybrid wall for seismic retrofit of soft story frame (Yamakawa and Rahman, 2007). In thismethodcast-in-situ extremely thick hybrid walleither of opening type wing-wall or non-opening type panel wallwas constructed in the first story frame.It was based on column encasement with channel-shaped steel plate and grouting of cementing material to remove the gap between column surface and this steel channel and to achieve integrity. Additional steel plates and PC bars worked as form work for wing-wall or panel wall and formed tie during additional concrete casting. This technique contributes to enhance lateral strength, stiffness and ductility of the soft story frames.

In another study a compound arrangement of retrofit solution was suggestedfor a practical application (Mezzi and Parducci, 2005). The technique was based on the synergic dissipating behaviour of damping elements, which acts to dissipate input energy and hysteretic plastic hinges at column ends improved through confining with FRP, which acts as dissipating units.

The concept of selective weakening (SW) technique was proposed in a study which at first allows weakening of selected region of structure to prevent brittle failure then followed by subsequent improvement of strength, stiffness, ductility based on necessity (Kam and Pampanin, 2008).

BANGLADESH PERSPECTIVE

In Bangladesh the most common type of structural configuration practiced in design and constructionsector is to keep the ground floor without any infill or with partial infill for having open space to allowmainly the parking arrangement. Presence of this type of configuration has undoubtedly amplified the existing seismic risk in this region.In addition, occurrence of frequent earthquake in recent years has made stakeholders to feel theimportance of seismic performance enhancement of existing structures.At present some conventional approaches of local retrofit strategies are available in Bangladesh like concrete jacketing, steel jacketing and use of steel bracing. FRP jacketing is used in

few practical casesof structural strengthening in our country.In this context application of FRP in Bashundhara City shopping mall andDhaka Gausia market can be mentioned here. In spite of the limitations still present regarding expenses and local expertise level of this retrofit technique in this country, huge potential of this material is already accepted for its application in critical infrastructures. Other latest advancements those have been applied in developed countries like base isolation techniques, utilization of energy dissipation devices and application of smart materials to improve existing condition of structures are still not economically and technologically feasible to be practiced in this country.However application of conventional techniqueswith proper knowledge and effective construction can provide a desirable solution to the existing soft story problem.Also at present several projects are running or going to start to build up expertise on several retrofit techniques as a result of government initiative.One of these projectsisCapacity Development on Natural Disaster Resistance Techniques on Construction and Retrofitting for Public Buildings (CNCRP)conducted by Japan International Cooperation Agency (JICA) and Public WorksDepartment (PWD). This project is going to contribute in developing capacity on some retrofitting methods which include RC jacketing, RC shear wall, RC wing wall, Steel framed bracing, Carbon fiber sheets wrapping and silt on brick standing wall. After developing proper skill in design concept and construction knowledge of retrofit approaches it is required to implement them in practical cases to improve existing performance of deficient structures.

CONCLUSION

In conclusion it can be inferred that in Bangladeshthe structures those are identified as extremely vulnerable to earthquake and may collapse or undergo severe damage requireimmediate treatment. Structural retrofit as a target solution involves adjusting features of the elements or whole building to eliminate or reduce existing risk of damage.Considering Bangladesh perspective an optimum retrofit technique needs to be adoptedas solution which willensuredesirableperformanceof structure along with satisfyingtechnical, economical, social and historical aspects of the issue. Also appropriate knowledge, expertise, guidelines and research on retrofit methods, both in understanding design concept and construction mechanism are required to attempt successful applications in necessary circumstances. Accumulation of all these phenomena accompanied by well planned government policy and support can offer a saferstructural system with improved earthquake resistance. From the realization of factsinvolve with seismic risk reduction using retrofit strategy,measureshave already been taken to overcome the challenges and thusto make amendments of existing structural condition of Bangladesh.

REFERENCES

Badoux, M. and Jirsa, J.O. 1990, Steel Bracing of RC Frame for Seismic Retrofitting,*Journal of Structural Engineering*, Vol. 116, No. 1, pp. 55-74.

Bush, T.D.; Jones, E.A., and Jirsa, J.O. 1991, Behavior of RC Frame StrengthenedUsing Structural Steel Bracing,*Journal of Structural Engineering*, Vol. 117, No. 4,pp. 1115-1126.

Chandra, J.; Warnitchai, P.; Rayamajhi, D.; Anwar, N. and Ahmad, S. 2011, Performance Based Seismic Evaluation and Retrofitting of Unsymmetrical Medium Rise Buildings- A Case Study, *Pakistan Engineering Congress, 71st Annual Session,* Paper no-682, pp. 79-91.

Fukuyama, H.;Iwabuchi, K. and Suwada, H. 2004, HPFRCC device for structural control of RC Buildings with soft story, *6th RILEM Symposium on Fiber-Reinforced Concretes (FRC) - BEFIB*, Varenna, Italy, pp1163-1172.

Gates, W.E.; Hart, G.C. and Crouse, C.B. 1990, Vibration Studies of an ExistingBuilding for Base Isolation Retrofit,*4th U.S. National Conference on Earthquake Engineering, Proceedings,* Vol. 3, pp. 559-568.

Hjelmstad, K. D.; Foutch, D. A.; Del Valle, E. and Downs, R. E. 1988, Forced Vibration Studies of an RC Building Retrofit with Steel Bracing, *Ninth World Conference on Earthquake Engineering, Tokyo, Japan,* Vol. VII, pp. 469-474.

Japan Building Disaster Prevention Association (JBDPA), 2005, Recent development of seismic retrofit methods in Japan.

Kam, W. Y. and Pampanin, S. 2008, Selective weakening techniques for retrofit of existing Reinforced concrete structures, *14th World Conference on Earthquake Engineering*, Beijing, China.

Kawamura, S.; Sugisaki, R.; Ogura, K.; Maezawa, S.; Tanaka, S. and Yajima, A. 2000,Seismic Isolation Retrofit in Japan,*12th World Conference on Earthquake Engineering,* Paper No. 2523.

Mezzi, M. and Parducci, A. 2005. Preservation of existing soft-first story configurations by improving the seismic performance, *3rd International special conference on the conceptual approach to structural design*, Singapore.

Miyamoto, H. K. and Scholl, R. E. 1996, Seismic rehabilitation of a historic non-ductile soft story concerete structuresusing fluid viscous dampers, *Eleventh World Conference on Earthquake Engineering,* Paper no-315.

Rashed M.G.; Ahsan R. and Islam B. 2012, Civil Engineering Application of Shape Memory Alloys, *Proceedings of the 1st International Conference on Advances in Civil Engineering,* Chittagong, Bangladesh.

Samant, L. D.;Porter, K.;Cobeen, K.;Tobin, L. T.;Kornfield, L.;Seligson, H.;Alejandrino, S. and Kidd, J. 2009, Mitigating San Francisco's Soft-Story Building Problem, *ATC & SEI 2009 Conference on Improving the Seismic Performance of Existing Buildings and Other Structures,* pp. 1163-1174.

Tena-Colunga, A.; Gomez-Soberon, C. and Munoz-Loustaunau, A. 1997, SeismicIsolation of Buildings Subjected to Typical Subduction Earthquake Motions for theMexican Pacific Coast,*Earthquake Spectra,* Vol. 13, No. 3, pp. 505-532.

Yamakawa, T. and Rahman, M. N. 2007, A Seismic Retrofit Technique for Soft Story Frames Utilizing Extremely Thick Hybrid Walls, *The 9th International Conference, "Modern Building Materials, Structures and Techniques". Vilnius, Lithuania,* pp.362-363, 2007-5.

ID : ASEE 057

1st International Conference on Advances in Civil Engineering 2012 (ICACE 2012)
12 –14 December 2012
CUET, Chittagong, Bangladesh

RICE HUSK ASH AS A SUSTAINABLE CONSTRUCTION MATERIAL FOR BANGLADESH

G. M. SADIQUL ISLAM[1]* & AYSHA AKTER[2]

[1] Department of Civil Engineering, Chittagong University of Engineering and Technology (CUET), Chittagong, Bangladesh. <e-mail: gmsislam@cuet.ac.bd, gmsislam@yahoo.com>*
[2] Department of Civil Engineering, Chittagong University of Engineering and Technology (CUET), Chittagong, Bangladesh. <e-mail: aysha_akter@cuet.ac.bd>

ABSTRACT

Rice is the staple food in Bangladesh and its production was 32.4 million ton in the year 2009-10. To make this marketable, a significant quantity of husk is being produced and it contains approximately 20% silica. This material is not easily biodegradable which is an environmental nuisance and usually incinerated to reduce the volume before disposal to landfill. Therefore, as an alternative option, it has also been used as a fuel for power generation in many countries. The incineration product consists of minerals, mainly silica (amorphous or crystalline). On the other hand, from sustainability prospect, numerous researches are trying to explore supplementary cementitious materials to reduce carbon footprint in construction industry and use of virgin raw materials. In this study, rice husk ash (RHA) was obtained from traditional incinerators associated with rice mill in Bangladesh. The physical and chemical properties of the materials has been analysed and compared with other common pozzolanic materials under consideration. The key physical properties considered include loss-on-ignition, 45µm sieve residue and particle size distribution (using a LASER PSD analyser). Oxide composition was determined using X-Ray Florescence Spectroscopy (XRF) technology. The properties of the material also cross compared with current international standard specifications (viz. ASTM, EN) for their suitability as a Pozzolana. It was found that RHA could be a potential supplementary cementitious construction material and thereby can contribute towards sustainable environmental and economic benefits of Bangladesh.

Keywords: Rice Husk Ash (RHA), Pozzolana, Construction materials, Cement, Sustainability

INTRODUCTION

Rice production in Bangladesh has been increased by 50% during last one decade (BRRI, 2011). This massive production leaves considerable level of husk. To reduce volume before landfilling incineration is a popular option. There exists example for producing power from the heat produced from this incineration (Mehta, 1979). However, the ash produced from rice husk is rich in silica and are not easily biodegradable while used as landfill.

On the other hand construction industry is reaching its limiting value in terms of sustainability. Concerns have been raised regarding use of virgin materials for cement production and associated emission. Cement scientists are exploring alternative sources of cementitious materials for future construction considering sustainability. Being rich in silica, RHA could be an option for concrete construction. This is expected to add pozzolanic values in cement hydration and consequently enhance durability and strength in longer term. As a by-product from rice industry this could also reduce the cost of construction materials. The current study explored the possibility of using the RHA in concrete construction as a Pozzolana. In this regard, several key physical and chemical properties of rice husk ash obtained from incinerators associated with traditional rice mills in Bangladesh has been tested and examined in light of current international standards for Pozzolana.

MATERIALS AND METHODS

Rice Husk Ash (RHA)
RHA has been obtained from incinerators associated with traditional rice mills in Bangladesh. The ash was tested without further processing.

Physical Properties Test
Fineness of RHA was determined using wet 45 μm sieve analysis following BS EN 451-2 (BSI, 1995). A dry ash sample (1.0 g, weighed to the nearest 0.001 g) was sieved under a water pressure of (80 ± 5) kPa for (60 ± 10) seconds by swirling the sieve horizontally at about 1 rotation per second. The material remaining (on the sieve) was then oven dried (at 105 ± 5)°C and the proportion retained (by mass) was calculated and expressed as a percentage of the original material. The mean value from two consecutive tests (to one decimal place) was reported as the fineness.

The particle size distribution (PSD) of RHA was determined using a Malvern Mastersizer2000 LASER particle size analyser. Approximately 1.0 g of material was dispersed in water using an ultrasonic attachment in the sample vessel of the equipment. In the case of Portland Cement (PC) and this was dispersed in propanol (in a smaller dispersion unit to prevent reaction). Commercial software was used to create particle size distributions from the degree of scattering of a collimated, monochromatic, dual laser beam (red and blue) passing through the mixture of sample and solvent (de-ionized water for testing fly ash). This is based on the principle that the angle of deflection decreases proportionally with particle size. At least three measurements were carried out for each sample. Although repeated distributions were found to be similar for a given material, an average distribution result of these, created by the computer software, was reported.

For the Loss-on-ignition (LOI) test, approximately 1.0 ± 0.5 g (but accurately recorded) dry samples were ignited in an electric furnace at 975°C for 60 minutes following BS EN 196-2 (BSI, 2005b) and BS EN 450-1 (BSI, 2005c). After ignition, the samples were removed from the furnace and left in a desiccator until cooling to room temperature before recording the weight. The LOI value was calculated by expressing the loss in mass as a percentage of the original mass of material and the mean of three results reported.

Chemical Properties Test
A Philips PW2424 sequential X-ray Fluorescence Spectrometer with RhK□ source was used to determine the oxide composition of the test material. A few drops of a 2.0% Movoil water solution (organic type binder) was mixed with the fly ash sample using an agate mortar and pestle before placing in a Ø27 mm pellet mould. The pellet filled with sample was compacted under 75 kN load for the first 5 minutes and then at 150 kN for a further 10 minutes. Prepared samples were left overnight to dry out prior to testing. Certified standard materials were used to calibrate the instrument before testing the samples.

RESULTS AND DISCUSSIONS

Physical properties

LOI is a measure of the level of unburnt carbon presents in rich husk ash. In general the unburnt carbon does not contribute in pozzolanic reaction and is considered as a hindrance to air-entrainment in concrete. The key physical properties of the test RHA are shown in Table 1. Result shows presence of unburnt carbon in the material, however, the quantity was found well below (half of the ASTM and one third of EN limit) the limit specified by ASTM and EN. The fineness in terms of 45 µm sieve residue gives general indication of the reactivity of the material. As found, RHA satisfied the fineness requirements specified in both ASTM and EN.

Table 1: Physical properties of RHA with respect to current standards

Properties	RHA	ASTM C618 limit	EN 450 limit
LOI, %	3.4	6.0[a]	9.0[b]
45 µm sieve residue, %	32.8	34.0	40.0[c]

[a]*Class F and C;* [b]*Category C; and* [c]*Category N*

The 45 µm sieve residue test generally indicate fineness of the material. Particle Size Distribution (PSD) using LASER PSD analyser gives wider picture of the material's fineness. Study by Paya *et al.* (1995) found that sub-10 µm particles made a significant contribution to compressive and flexural strength development of mortars containing fly ashes. Recent study (Islam *et al.*, 2011) by this author examined the feasibility of the use of fly ash sourced from Bangladeshi power plant in concrete construction. Fig. 1 shows comparison between PSDs of Bangladeshi fly ash, RHA and a typical 42.5 N PC. It was found that the PC was finer than both fly ash and RHA. The d_{50} of RHA, fly ash and PC was 33.7, 22.1 and16.9 µm respectively, while the d_{90} of RHA (74.6 µm) was smaller than that of fly ash (82.6 µm).

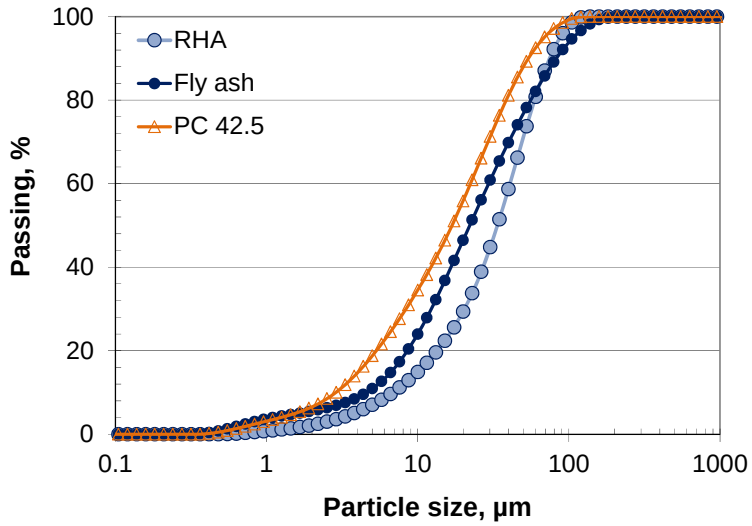

Fig 1. Comparison of laser PSDs of pozzolanic materials and PC

Chemical properties

Oxide analysis of RHA indicates that the material is mainly composed of silica. Presence of other oxides is minor and all satisfied requirements specified in ASTM and EN. Studies indicate that the amorphous alumina-silicate compounds present in pozzolanic materials are mainly responsible for the secondary cement hydration reaction (Swamy, 1986). As per ASTM and EN the sum of major oxides ($SiO_2 + Al_2O_3 + Fe_2O_3$) should be at least 70% to qualify the materials as Pozzolana. As given in Table 2 the tested RHA gives value well above the requirement by the above two international standards.

Table 2. Comparison between chemical composition of pozzolanic materials and PC

Oxides	RHA	Fly ash	PC 42.5
CaO	1.0	0.7	65.2
SiO_2	89.3	51.5	18.8
Al_2O_3	0.9	31.6	4.7
Fe_2O_3	0.7	2.8	2.8
MgO	2.4	0.3	1.1
MnO	0.1	0.0	0.0
TiO_2	0.1	3.1	0.4
K_2O	1.9	0.9	0.7
Na_2O	0.2	0.2	0.3
P_2O_5	0.9	0.6	0.2
Cl	0.0	0.0	0.1
SO_3	0.1	0.2	3.2

It is to mention that the proportion of amorphous material gives indication of its reactivity in the cementitious system. It therefore requires further analysis with X-ray Diffraction (XRD) to identify the available glassy materials to react with the released lime during cement hydration. The formation of amorphous materials depends on combustion condition of rice husk. Pre-grinding of feed materials was considered to enhance efficient burning. In addition, furnace residence time, air circulation can also influence the formation of pozzolanic materials.

The morphology of the material can be determined from scanning electron microscope. The specific surface area also needs to determine to identify admixture compatibility verification. Morphology of mineral part as well as unburnt carbon could greatly influence the workability and air-entrainment in concrete. The material needs to be tested in mortar to confirm its reactivity requirements in terms of (strength) activity index as specified by ASTM and EN.

CONCLUSION

The materials under consideration for this study indicated its potential for using as a supplementary cementitious material in concrete. It satisfied physical and chemical requirements from various international standards.

The material has been collected from the traditional incinerator associated with rice mills in Bangladesh, the burning condition of which is not totally available. Therefore, with further study the feasibility of using the material in concrete construction could be concluded. Performance of the materials could be improved (i.e. production of greater level of glassy silica) by adopting controlled burning condition.

ACKNOWLEDGMENTS

The laboratory support by University of Dundee, UK is gratefully acknowledged. Sincere thanks extended to colleague in Chittagong University of Engineering & Technology (CUET) for arranging the material for test.

REFERENCES

Bangladesh Rice Research Institute (BRRI) (2011). Rice Production (Thousand Metric Ton) in Bangladesh. [online]. Available at: http://www.brri.gov.bd/info_services/rice_database/Rice%20Production%20in%20Bangladesh.pdf [Accessed 10 May 2012].

Basak J K. 2012. Climate change impacts on rice production in Bangladesh: Results from a model. ***Unnayan Onneshan***. [online]. Available at: www.bdresearch.org.bd/home/climate_knowledge/cd1/pdf/Bangladesh%20and%20climate%20change/Agriculture/Climate_Change_Impacts_on_Rice_Production_in_Bangladesh_Report.pdf [Accessed 25 May 2012].

BS EN 196-2 (2005b). Methods of testing cement: Chemical analysis of cement. BSI, London, UK.

BS EN 450-1 (2005c). Fly ash for concrete: Definition, specifications and conformity criteria. BSI, London, UK.

BS EN 451-2 (1995). Method of testing fly ash: Determination of fineness by wet sieving. BSI, London, UK.

Ferraro, R M and Nanni A. 2012. Effect of off-white rice husk ash on strength, porosity, conductivity and corrosion resistance of white concrete. *Construction and Building Materials,* 31(): 220–225.

Helmuth, R. (1987). *Fly ash in cement and concrete*. Portland Cement Association, Skokie, IL, USA, 203 pp.

Islam, G M S. 2012. *Evaluating reactivity and sorptivity of fly ash for use in concrete construction. PhD* Thesis, Department of Civil Engineering, University of Dundee, UK.

Islam G M S, Islam M M, Akter A and Islam M S (2011). Green Construction Materials – Bangladesh Perspective. In *International Conference on Mechanical Engineering and Renewable Energy (ICMERE2011)*, 22-24 December 2011, Chittagong, Bangladesh (Electronic proceedings).

Mehta K P (1979). The chemistry and technology of cements made from rice husk ash. Proceedings of UNIDO/ESCAP/RCTT workshop on rice husk ash cement, Peshawar, Pakistan, pp. 113-122.

Paya J, Monzo J, Peris-Mora E, Borrachero M V, Tercero R and Pinillos C (1995). Early strength development of portland cement mortars containing air classified fly ashes. *Cement and Concrete Research*, Vol. 25, No. 2, pp. 449-456.

Swamy, R N. (Eds.) (1986). *Cement replacement materials*. Concrete technology and design: Volume 3, ISBN: 0-903384-52-3, Surrey University Press, London, UK, 255p.

ID : ASEE 066

1st International Conference on Advances in Civil Engineering 2012 (ICACE 2012)
12 –14 December 2012
CUET, Chittagong, Bangladesh

SEISMIC RESPONSE ANALYSIS OF BASE ISOLATED TALL BUILDINGS: EFFECT OF SUPERSTRUCTURE STIFFENING

M. N. HAQUE[1*], A. R. BHUIYAN[2] & M. J. ALAM[3]

[1*] *Department of Civil Engineering, Yokohama National, Yokohama, Japan,*
e-mail: naimulce@gmail.com
[2] *Department of Civil Engineering, Chittagong University of Engineering &Technology, Chittagong-4349, e-mail: arbhuiynace@cuet.ac.bd*
[3] *Department of Civil Engineering, Chittagong University of Engineering &Technology, Chittagong-4349, e-mail:* mjalam1232003@yahoo.com

ABSTRACT

A numerical investigation on feasibility of using base isolation mechanism in tall buildings with stiffened superstructures is carried out. This study is conducted for two reinforced concrete framed buildings of 8 and 12 stories. In order to enhance the effectiveness of base isolation in tall buildings, different stiffening features in superstructures are explored. The isolation system considered in this study comprised high damping rubber bearings at isolation level of the buildings. As the mechanical behaviour of the bearing is dominated mainly by nonlinear elasto-plastic and strain hardening features along with strain-rate dependence, a strain-rate dependent model of the isolation bearings should be used to properly evaluate the mechanical behaviour of the bearings during the seismic ground motion. However, as the first step of the work the bilinear model of hysteresis as proposed in several guides and specifications is used in the current study. Nonlinear behaviour of the building is restricted at the level of bearings and the superstructure is considered to be elastic at all times and hence the superstructure is modelled using elastic beam-column elements. In order to evaluate the seismic responses of the buildings, a representative earthquake ground motion compatible with design response spectra is employed in the study. Finally, it is observed that base isolation is feasible for the buildings considered in this study; however, the tall building needs to be stiffened for getting better performance of base isolation.

Keywords: Base isolation, high damping rubber bearings, lead rubber bearings, stiffened tall buildings

INTRODUCTION

Base isolation is a promising design approach, which provides decoupling of a structure or part of it or even of equipment placed in the structure from the damaging effects of ground accelerations. One of the goals of the base isolation is to shift the fundamental frequency of a structure away from the dominant frequencies of earthquake ground motion and fundamental frequency of the fixed base superstructure. The other purpose of an isolation system is to provide an additional means of energy dissipation, thereby reducing the transmitted acceleration into the superstructure. This innovative design approach aims mainly at the isolation of a structure from the supporting ground, generally in the horizontal direction, in order to reduce the transmission of the earthquake motion to the structure. The typical period of isolated

buildings is generally kept around 2.0 second (Constantinou, 1985). Therefore, the significant benefits from base isolation appreciate in structures for which the fundamental period of vibration without base isolation is short, i.e., less than 1.0 second. Buildings with comparatively higher natural period attract low earthquake forces even without base isolation. In the early stage of development of base isolation, prevention of collapse of the structure from earthquake effects was the main target. Therefore, seismic isolation has mostly been applied in low-rise buildings (Kelly, 1990). However, more recently considerations, like comfort of occupants, functionality of important buildings during and after earthquakes, preventing damage to non-structural elements and contents etc., have attracted the structural engineers to apply base isolation also for the buildings with more than 10-storey height. There have been applications of base isolation to newly-constructed tall buildings (Okoshi et al. 1993) and to retrofit buildings with relatively long fixed-base periods, which are deficient in seismic resistance (Honeck et al. 1993; Qamaruddin et al. 1996).

The effectiveness of base isolation can be enhanced for relatively tall buildings by employing some strategies, for example, increasing the stiffness of the superstructure, increasing damping in the superstructures and increasing the flexibility of base isolation system. However, the strategy leading to have a stiffened superstructure have appreciated wide application in the engineering community due to its simplicity in implication. The stiffening in the superstructure may result in reduced fixed base period and such buildings, if base isolated, may develop smaller seismic response. In this case, the tall flexible buildings is to be first stiffened by using bracing to reduce the fundamental period of the buildings so that the benefits of base isolation can be achieved. The purpose of this study is to investigate the effectiveness of base isolation for tall buildings subjected to ground motions of different characteristics and to observe the effect of increase in superstructure stiffness on their seismic response.

CHARACTERISTICS OF THE BUILDINGS

The buildings considered for this study are an eight storey, a twelve storey building. These are reinforced concrete ordinary moment resisting frame structures. Typical plan and elevation of these buildings is shown in Fig. 1. Equivalent viscous damping of the superstructure of the base-isolated building, in general, is assumed as 2 percent of critical; however, for fixed base buildings, it is considered as 5% of critical. In order to study the effect of superstructure stiffening, buildings with bare moment resisting frame only and the same buildings with stiffening elements like cross bracings at their end bays are analyzed. The bottom of buildings is considered as fixed restraining conditions at the foundation level. In case of stiffened building, the RC braces of 400 mm x 400 mm are provided throughout the building's height at the end bays only.

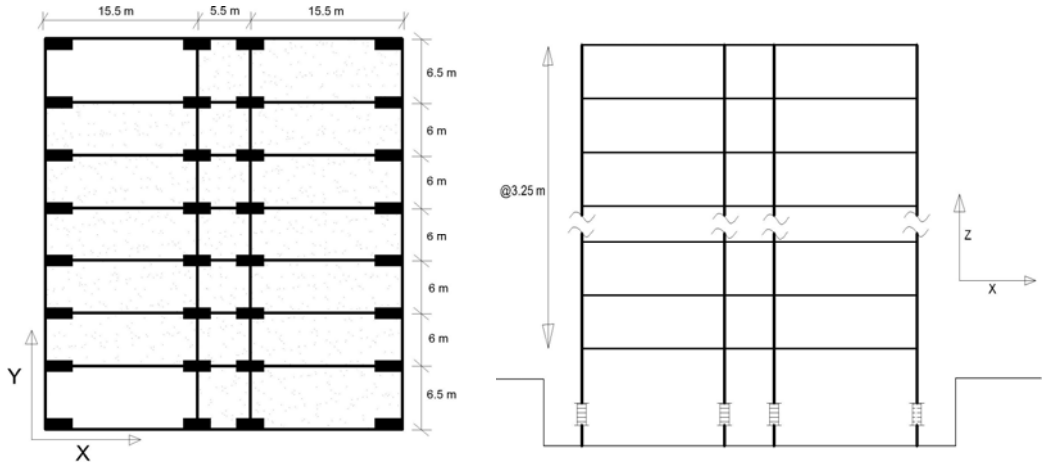

(a) (b)

Fig. 1. Typical plan and elevation of the buildings considered in the study

BASE ISOLATION OF THE BUILDINGS

High damping rubber bearing (HDRB) is used in as isolation bearings in the buildings. The HDRB is manufactured by vulcanizing rubber layers with alternate steel shims (Kelly, 1997). A schematic diagram of the bearing is shown in Fig. 2(a). Generally, the HDRB exhibits high-damping capacity, horizontal flexibility and high vertical stiffness. The damping capacity of the bearing varies considerably with the strain rates and strain levels (Bhuiyan, 2009, Bhuiyan and Okui, 2012). The bearing operates by decoupling the structure from the horizontal component of earthquake ground motion. The isolation effects in this type of system are produced not by absorbing the earthquake energy but by deflecting through the dynamics of the system (Kelly, 1997). These devices can be manufactured easily and are quite resistant to environmental effects. The base isolated building is mounted on HDRB placed at the bottom of each column.

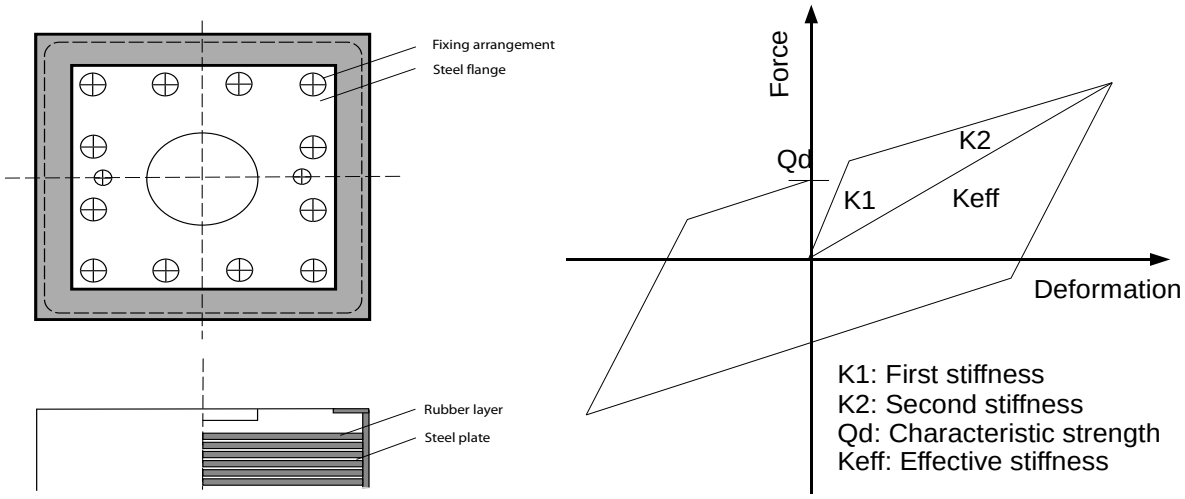

(a) (b)

Fig. 2. (a) Typical arrangement of HDRB and (b) Typical bilinear model for describing the hysteretic property of HDRB

Fig.2 (b) shows a typical bilinear model of the bearing which is widely used in different design codes and specifications (AASHTO, 2000, JRA, 2002). In order to specify the model, three parameters as stated in Fig.2 (b) are required: pre yield stiffness (K_1), post yield stiffness (K_2) and the characteristic strength (Q_d) of the bearing. The parameters of the bilinear model are given in Table 1.

Table 1: Model parameters of HDRB

HDRB	8 Story	12 Story
Pre yield stiffness K_1 (kN/m)	453	2088
Hardening ratio (K_2/K_1)	0.10	0.10

EARTHQUAKE GROUND MOTIONS

In order to study the effect of earthquake characteristics, two real earthquake motions are considered in this study, namely, the Tohoku earthquake (Tohoku, 2011) and the Kobe earthquake (Kobe, 1995). The selected records have a variety of peak ground acceleration (PGA) values as shown in Fig.3. The two earthquake records are characteristically different from each other, especially, in terms of PGA values, peak ground velocity (PGV), duration and dominant frequency range of the earthquakes. Both earthquake records correspond to near field earthquakes. The acceleration response spectra of the earthquake ground motion records are given in Fig. 4.

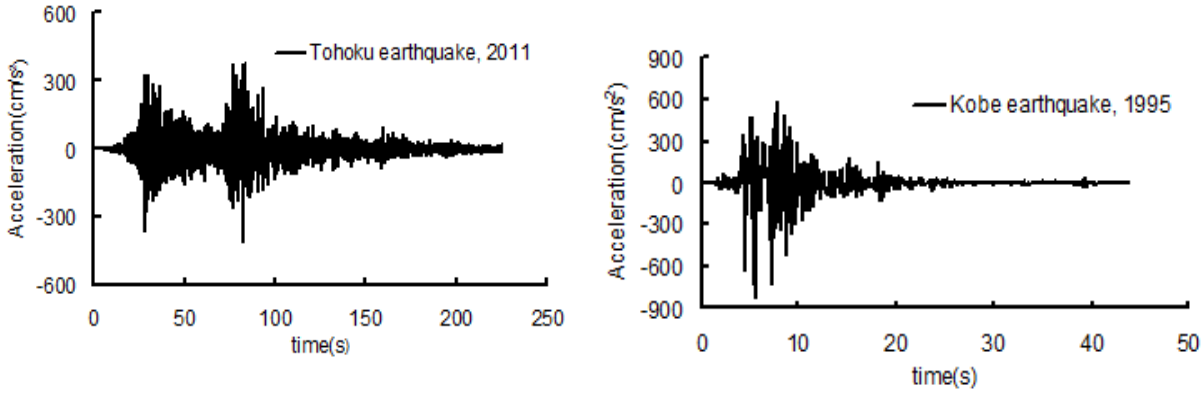

(a) (b)

Fig.3. Earthquake acceleration records used in the analysis of the buildings (a) Tohoku earthquake and (b) Kobe earthquake

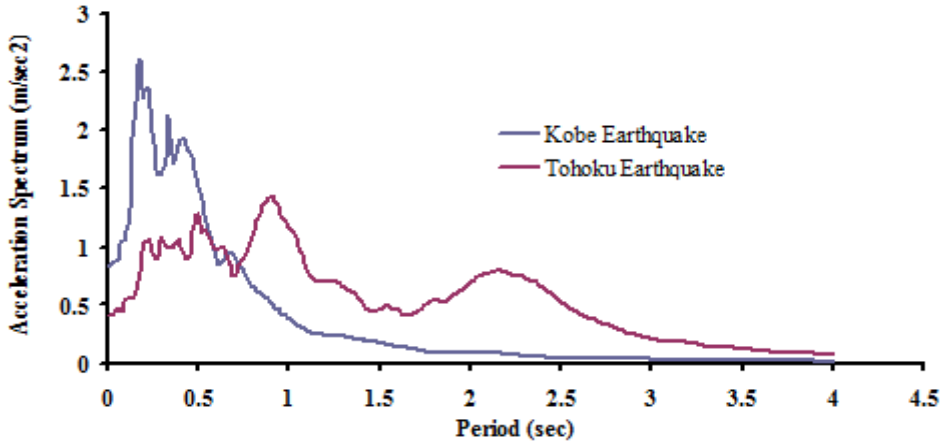

Fig.4. Acceleration response spectra of the earthquake ground motion records

SEISMIC ANALYSIS OF THE BUILDINGS

3-D static analysis of the buildings has been performed using ETABS professional software in order to evaluate the seismic responses of the buildings. The building frame is modeled by 3-D beam column elements and the bearing is modeled by link element, which is characterized by bilinear model. The linear elastic model is considered to characterize the beam-column element. The bottom of the building is considered to restrained in all directions. The analysis is based on following assumptions: The superstructure is elastic at all time and the non-linear behavior is restricted in the bearing only. The

isolation bearings are rigid in the vertical direction and have negligible torsion resistance. An eignvalue analysis is conducted to evaluate the fundamental dynamic properties of the buildings. Natural time periods of the buildings are given in Table 2.

Table 2: Fundamental time periods of the buildings

Mode number/ No of stories	Fixed		Isolated		Stiffened		Isolated stiffened	
	8 storey	12 storey	8 storey	12 storey	8 storey	12 storey	8 storey	12 storey
1	1.65	2.53	3.27	3.36	0.83	1.49	3.18	2.71
2	1.57	2.36	3.19	3.15	0.47	0.83	2.91	2.09
3	1.35	2.04	2.72	2.71	0.32	0.57	2.65	1.79
4	0.53	0.79	0.81	1.01	0.20	0.37	0.67	0.79
5	0.52	0.78	0.73	0.97	0.15	0.24	0.44	0.51

NUMERICAL RESULTS AND DSCUSSION

Time history analysis of two multi storied buildings is carried out for two earthquake records. Three responses of the buildings are considered in this analysis: absolute base shear, deck acceleration and drift of the buildings. However, the effectiveness of using isolation bearings can be interpreted in terms of effectiveness ratio (ER). The effectiveness ratio (ER) can be identified as the ratio of response of fixed base building to that of base isolated buildings. Moreover, the effect superstructure stiffening is also investigated. Tables 3 to 5 present the seismic responses of the buildings subjected to two earthquake ground motion records, i.e. the Kobe earthquake (Kobe, 1995) and the Tohoku earthquake (Tohoku, 2011) (Figs. 3 and 4). Table 3 demonstrates the absolute values of base shear of the buildings indicating that the base shears of the fixed buildings due to both earthquake ground motion records are reasonably higher than those for isolated buildings. The similar trend of the results is also obtained for deck acceleration and drift of the buildings (Tables 4 and 5).

Table 3: Absolute base shear (kN) of the buildings

Ground Motion	Fixed Building		Isolated Building		Fixed Stiffened Building		Isolated Stiffened Building	
	8 storey	12 storey	8 storey	12 storey	8 storey	12 storey	8 storey	12 storey
Kobe	12420	8775	2264	5009	45840	48050	4405	12870
Tohoku	85420	13960	3164	5067	23040	37290	5886	30540

Table 4: Absolute deck acceleration (m/sec^2) of the buildings

Ground Motion	Fixed Building		Isolated Building		Fixed Stiffened Building		Isolated Stiffened Building	
	8 storey	12 storey	8 storey	12 storey	8 storey	12 storey	8 storey	12 storey
Kobe	16870	13600	10170	8938	30860	30810	9823	10690
Tohoku	9077	12400	7468	6732	13860	17390	6503	10580

Table 5: Absolute drift (%) of the buildings

Ground Motion	Fixed Building		Isolated Building		Fixed Stiffened Building		Isolated Stiffened Building	
	8 storey	12 storey	8 storey	12 storey	8 storey	12 storey	8 storey	12 storey
Kobe	1.61	1.84	0.72	1.08	0.79	1.59	0.18	0.41
Tohoku	1.24	1.38	0.89	0.26	0.38	0.88	0.31	0.97

The rate of decrease of the responses due to isolated effect of the buildings appears to be higher in 8-story buildings than in 12-story buildings. From the results shown in Tables 3 to 5 it can be observed that the values of ER of the 8-story buildings subjected to the Kobe earthquake are larger than that for 12-story buildings. However, an exception in the results is observed in case of Tohoku earthquake due to its own characteristic properties. The similar trend of the results is also clarified for the Tohoku earthquake. The effect of earthquake characteristics is also demonstrated in the seismic responses shown Tables 3 to 5.

CONCLUSIONS

Two reinforced concrete framed buildings of 8 and 12 stories are used in the study to investigate the effectiveness of base isolated and stiffening effect on the base isolation of the buildings. The stiffening of the buildings is provided by using RC bracings in the end bents of the buildings. High damping rubber bearings characterised by bilinear model is employed. Nonlinear behaviour of the building is restricted at the level of bearings and the superstructure is considered to be elastic at all times and hence the superstructure is modelled using elastic beam-column elements. Two types of earthquake ground motion records are used in the analysis. The numerical results of the buildings have shown that the isolation effect of the 12-story building is more significant than the 8-story building. The similar trend of the results is also appreciated in the case of stiffening effect of the buildings. Moreover, the effect of earthquake characteristics noticeably appeared in the seismic responses of the building.

REFERENCES

American Association of State Highways and Transportation Officials. 2000. Guide specification for seismic isolation design, 2nd edn. Washington DC, USA

A. R. Bhuiyan and Y.Okui. 2012. *Mechanical Characterization of Laminated Rubber Bearings and Their Modeling Approach,* Earthquake Engineering, edited by Halil Sezen, ISBN 978-953-51-0694-4, InTech.

Bhuiyan AR, Okui Y, Mitamura H, Imai T. 2009. A rheology model of high damping rubber bearings for seismic analysis: identification of nonlinear viscosity. Int J Solids Struct 6:1778–1792
Constantinou MC, Tadjbakhsh IG. 1985. Optimum characteristics of isolated structures. *J. Struct. Eng.*, ASCE, 111(12): 2733-2750.

Honeck W, Walters M, Sattary V, Roeder P. 1993. The seismic isolation of the Oakland city hall, Proc. of ATC-17-1 Seminar on Seismic Isolation, Passive Energy Dissipation and Active Control, San Francisco, California, ATC-17-1, I: 221-232.

Japan Road Association. 2002. Specifications for highway bridges-partV: seismic design. Tokyo, Japan
Kelly JM. 1997. *Earthquake resistant design with rubber*, Second Edition, Springer-Verlag London Ltd., Great Britain.

Kelly JM, Chalhoub MS. 1990. Earthquake simulator testing of a combined sliding bearing and rubber bearing isolation system. Report No. UCB/EERC-87/04, Earthquake Engineering Research Center, University of California at Berkeley.

Okoshi TS, Nakagawa, Kawamura M. 1993. Aseismic design of C-1 Building: the biggest base-isolated building in the world, Proc. of Seminar on Seismic Isolation, Passive Energy Dissipation and Active Control, San Francisco, California, ATC-17-1, I: 413-423.

Qamaruddin M, Al-Jabri KS, Al-Oraimi SK. 1996. Earthquake response of multistory masonry buildings with friction base isolation, Bulletin of Indian Society of Earthquake Technology, 33(5): 215-227.